

 UANTUM FIELD THEORY
AND THE
ANALYTIC  -MATRIX

JACOB LEWIS BOURJAILY

A DISSERTATION PRESENTED
TO THE FACULTY OF
PRINCETON UNIVERSITY IN
CANDIDACY FOR THE DEGREE
OF DOCTOR OF PHILOSOPHY

RECOMMENDED FOR ACCEPTANCE
BY THE DEPARTMENT OF PHYSICS
ADVISOR: NIMA ARKANI-HAMED

MAY 2011

© Copyright by Jacob Lewis Bourjaily, 2011.
All Rights Reserved.

ABSTRACT

Quantum field theory is as ubiquitous and important in modern theoretical physics today as the calculus was shortly after Newton. And like the calculus during the eighteenth century, quantum field theory is still considered very difficult by many, and is still surprising to us all. Although the ultimate foundations of quantum field theory have changed very little in the decades since its creation, we continue to find ourselves ill-prepared for the remarkable simplicity of the predictions it makes. Among the most striking examples of this failed intuition has been from the computation of scattering amplitudes (the ‘S-Matrix’) in theories with maximal supersymmetry ($\mathcal{N} = 4$), which are notoriously difficult to compute using familiar Feynman diagrams and yet turn out to be extremely simple and elegant. Recently, this underlying simplicity has been made more manifest through powerful alternative approaches to quantum field theory, including a recursive on-shell definition of the S-Matrix of planar $\mathcal{N} = 4$ to all orders of perturbation theory described in this dissertation. These new developments increasingly suggest the existence of a fundamentally different and more powerful understanding of quantum field theory, with broad theoretical implications as well as practical applications.

als hommage an die Graßmannian.

Contents

Abstract	iii
Acknowledgements	x
Spiritus Movens: Foreshadowing Recent Advances in the S-Matrix	1
1 Grassmannian Contour Deformation and CSW Recursion	6
1.1 $\mathcal{N} = 4$ SYM and the Grassmannian	6
1.2 Brief Review of CSW and Risager	11
1.3 Relaxing δ -Functions	13
1.4 NMHV and CSW from δ -Relaxation	15
I. Preliminaries	15
II. Localization Properties of the Grassmannian	17
III. Establishing the CSW Equivalence	21
1.5 Risager from δ -Relaxation	23
1.6 Concluding Remarks	25
2 The Unification of Residues and Grassmannian Dualities	27
2.1 Scattering Amplitudes and the Grassmannian	27
2.2 Unification of Residues	30
I. Local Residues	30
II. Tree-Amplitude Contours as Algebraic Varieties	32
III. Manifest Soft-Limits and the Particle Interpretation	34
IV. Connection to CSW Localization	35
2.3 Veronese Particle Interpretation	38
I. Twistor String Theory	40
II. Veronese Operators for Conics	43
III. General Veronese Operators	45
2.4 Deformation and Duality	47

2.5	NMHV Amplitudes	51
	I. Recursive Construction	53
	II. The $n = 7, 8$ Amplitudes	54
	III. General Proof For All n	59
	IV. “Inverse-Soft” Interpretation	61
	V. Connection to the Twistor String	62
2.6	Generalization to N^2 MHV	63
	I. The Geometry of Residues in the Grassmannian	66
	II. The 8-Particle N^2 MHV Amplitude	70
	III. Connection to the Twistor String	76
2.7	Discussion	78
3	The Grassmannian and Twistor String: Unifying All Trees in $\mathcal{N} = 4$	80
3.1	Introduction	80
3.2	All Tree Amplitudes in $\mathcal{N} = 4$ superYang-Mills	83
3.3	Building the Contour one Particle at a Time	86
	I. NMHV amplitudes	87
	II. N^2 MHV Amplitudes	88
	III. N^3 MHV Amplitudes and Beyond	90
	IV. General Properties of the Result	92
3.4	Transformation to the Twistor String	94
	I. Transforming the $\delta(F_\ell^j)$'s	95
	II. Collecting Prefactors	97
4	The All-Loop Extension of BCFW Recursion	99
4.1	The Loop <i>Integrand</i> for $\mathcal{N} = 4$ SYM Amplitudes	99
	I. Grassmannian Duality for Leading Singularities	100
	II. The Planar Integrand	102
	III. Recursion Relations for All Loop Amplitudes	102
4.2	Canonical Operations on Yangian Invariants	105
	I. Adding Particles	106
	II. Removing Particles	107
	III. Fusing Invariants	108

IV.	Leading Singularities are Yangian Invariant	109
V.	The BCFW Bridge	110
4.3	Loops From Hidden Entanglement	113
4.4	Recursion Relations For All Loop Amplitudes	116
I.	Single-Cuts and the Forward-Limit	118
II.	BCFW For All Loop Amplitudes	120
III.	Simple Examples	120
IV.	Unitarity as a Residue Theorem	123
4.5	The Loop Integrand in Local Form	125
4.6	Multi-Loop Examples	130
I.	All 2-Loop MHV Amplitudes	131
II.	All 2-Loop NMHV Amplitudes	133
III.	All 3-Loop MHV Amplitudes	135
4.7	Outlook	136
I.	The Origin of Loops	136
II.	Simplicity of Integrals and IR-Anomalies	139
III.	Other Planar Theories	141
5	Local Integrals for Planar Scattering Amplitudes	143
5.1	Invitation to Local Loop Integrals and Integrands	143
5.2	Foundations	148
I.	Loop Integrals	151
II.	The Loop <i>Integrand</i>	159
III.	Leading Singularities	161
5.3	Chiral Integrals with Unit Leading Singularities	177
I.	Integrals with Unit Leading Singularities, or <i>Pure</i> Integrals	178
II.	Chiral Integrals	182
III.	Evaluation of Pure Integrals	184
IV.	Example: 1-Loop MHV Amplitudes	185
5.4	Finite Integrals	186
5.5	1-Loop Integrands, Integrals, and Amplitudes	191
I.	The Chiral Octagon: A Basis of 1-Loop Integrands	192

II.	Integration of Manifestly-Finite Octagons	194
III.	Application: the NMHV 1-Loop Ratio Function	197
5.6	Multiloop Amplitudes	200
I.	A New Form for the MHV 1-Loop Integrand	200
II.	The 1-Loop NMHV Integrand, Revisited	203
III.	The 2-Loop MHV Amplitude and Its Logarithm	207
IV.	All 2-Loop NMHV Amplitudes	210
V.	All 3-Loop MHV Amplitudes	213
6	Scattering Amplitudes and the Geometry of Polytopes	215
6.1	Towards a Geometry of Scattering Amplitudes	215
6.2	Warm-Up: The Area of Polygons in \mathbb{CP}^2	219
6.3	1-Loop MHV Amplitude Integrands	225
6.4	NMHV Tree Amplitudes	228
6.5	Discussion	236
A	The Vernacular of the S-Matrix: Kinematics & Computational Tools	238
A.1	Introduction	238
A.2	Kinematics: Momenta to Momentum-Twistors (and Back)	242
A.3	Trees as Contour Integrals in the Grassmannian	246
I.	Generalized BCFW Recursion Schemes	249
II.	Extracting Helicity Component-Amplitudes from Tree-Contours	252
A.4	The <code>bcfw</code> MATHEMATICA Package	254
I.	Setup and Initialization	254
II.	Getting Started with Analytic Tree Amplitudes	254
III.	Referencing, Generating, or Specifying Kinematical Data	256
IV.	Numerical Evaluation of Tree Amplitudes	259
V.	Example Applications	260
A.5	Conclusions	262
B	The Nine-Point N^2MHV Tree Amplitude	264
C	The BCFW Form of the 1-Loop 6-Point NMHV Integrand	265

D The Local 7-Point 2-Loop NMHV Amplitude	266
E Residue Computations in Momentum-Twistor Space	271
F All 2-Loop NMHV Amplitude Integrands	273
G All 3-Loop MHV Amplitude Integrands	275
Bibliography	279

ACKNOWLEDGEMENTS

Although there are many people to whom I am deeply indebted for my education as a theoretical physicist, it is not possible to overstate the role played by my advisor and frequent collaborator Nima Arkani-Hamed. His broad and deep knowledge of quantum field theory, penetrating insight, charismatic curiosity, and inimitable work ethic have been a constant source of inspiration for me; and I have learned more from him between the hours of two and five in the morning than during all my years of coursework and problem sets. And it is with enormous pride that I acknowledge not only the impact he has had on my personal education, but also his enormous contributions to this dissertation in particular.

In many ways, Freddy Cachazo has been a second advisor to me, and it is my humble honor to consider myself his student. Like Nima, Freddy has been extremely influential in my development and education as a theoretical physicist. Freddy's insatiable appetite for discovery, indefatigable spirit, and vast knowledge of quantum field theory generally—and scattering amplitudes in particular—has been not only an invaluable resource for this research, but also a constant, uplifting source of optimism in the face of uncertain progress.

This dissertation is largely composed of results obtained in collaboration with Nima, Freddy, and several others with whom it has been a joy to work. In particular, I am grateful to Simon Caron-Huot, Andrew Hodges, Anastasia Volovich, Congkao Wen, and especially Jaroslav Trnka for their important contributions to the results described in this dissertation. I am also grateful for ongoing work in collaboration with Mark Spradlin and Johannes Henn, each of whom have made very important contributions to my understanding of scattering amplitudes, and with whom it has been a pleasure to work.

It is not possible to do justice to all the people from whom I have learned so much during my time at Princeton, but I am especially indebted to many fruitful conversations about scattering amplitudes with Fernando Alday, James Bedford, Matthew Bullimore, James Drummond, Anatoly Dymarsky, Johannes Henn, Davide Gaiotto, Juan Maldacena, Lionel Mason, Amit Sever,

David Skinner, Cristian Vergu, Herman Verlinde, Pedro Vieira, and Edward Witten; and for conversations about physics more generally with Daniel Baumann, Steve Gubser, Igor Klebanov, Katie Mack, Nathan Seiberg, Paul Steinhardt, Neal Weiner, and Itay Yavin.

Thanks to Matthew Baumgart, Jared Kaplan, Clifford Cheung, and Josh Ruderman, who have been great friends and fellow students. I have learned much from each of them, and they have made my time at Princeton extremely enjoyable and not unproductive.

Thanks to Paul Langacker, Paul Steinhardt, Herman Verlinde, Liantao Wang, and Edward Witten for the wisdom they've shared with me, the advice they've given, and the friendly welcome they made when I first arrived at Princeton. Thanks also to my TASI roommate James Bedford, who made my transition through Cambridge to Princeton productive, enjoyable and filled with music.

Thanks to Ben Allanach, Frederik Denef, Michael Douglas, Dragan Huterer, Shamit Kachru, Eva Silverstein, Andy Strominger, and David Tong for many fruitful conversations, and for sharing their passionate curiosity and vast knowledge and experience with me.

Thanks to Bobby Acharya, Konstantin Bobkov, Joe Conlon, Gordy Kane, Eric Kuflik, Piyush Kumar, Paul Langacker, Brent Nelson, Malcolm Perry, Fernando Quevedo, Herman Verlinde, and Cumrun Vafa for teaching me so much about local model building in string theory.

I am extremely grateful for the time I spent as an undergraduate student of Gordy Kane, who shared with me both his passion for science—and life generally—his vast experience, and his broad outlook on life and physics. Thanks also to Michael Duff, Finn Larsen, Timothy McKay, and James Wells for everything they taught me about physics while an undergraduate.

Thanks to Jean Krisch and Homer Neal, who courageously gave a freshman nuclear engineering student the chance to devote himself to learning physics. I do not know where I would be if it were not for their investment and continued

support—from a time when my only asset was an insatiable curiosity and a passion to learn.

Thanks to Brenden Blanco and Chris Curecka, and to Porscha McRobbie and Steven Reed for their invaluable friendship during my years in Ann Arbor.

Thanks to my parents, Elsbeth and Kenneth, my sister Lora, and my brothers Eric, Nicholas, and Matthew for all their support, and to my grandparents for the inspiration they gave me.

And finally, thanks to the Institute for Advanced Study, to the Aspen Public Library, and to Small World Coffee for their hospitality. This dissertation was supported by a Graduate Research Fellowship from the National Science Foundation, and funded in part by National Science Foundation Grant PHY-0756966.

Spiritus Movens: *Foreshadowing Recent Progress in Scattering Amplitudes*

In 1985, Parke and Taylor pushed the boundaries of theoretical and computational tools known at the time and succeeded in determining the ‘leading contribution’ to the scattering amplitude for two incoming gluons to produce four outgoing gluons in quantum chromodynamics (QCD) [1]. In order to accomplish this Herculean computation, they first translated the problem into a simpler one by exploiting an artificially-introduced ‘ $\mathcal{N} = 2$ supersymmetry’—an extremely convenient trick, and one which is still used widely today—and they employed a supercomputer to combine all of the several hundred Feynman diagrams which contribute to the amplitude. Their final answer spanned eight dense pages, but—as they apologized to their readers—the ‘details of the calculation’ would have to wait for a future, more lengthy work. And yet, somewhat whimsically, they chose to close their report with the seemingly fantastical hope that they may somehow “obtain a simple analytic form of the answer, making [the] result not only an experimentalist’s, but also a theorist’s delight.”

Six months later, they stumbled upon exactly what they had hoped for: they arrived at “an educated guess” for the same leading part of the scattering amplitude painfully computed earlier, but not merely for the amplitude involving six gluons, but for amplitudes involving *any number of gluons* whatsoever [2]. And the answer they proposed was spectacularly simple: in modern notation, they suggested,

$$A_{\text{MHV}}(1^+, 2^+, \dots, i^-, \dots, j^-, \dots, n^+) = \frac{\langle i j \rangle^4}{\langle 1 2 \rangle \langle 2 3 \rangle \langle 3 4 \rangle \dots \langle n 1 \rangle}. \quad (0.1)$$

This formula was meticulously checked against their previous calculation, and found to agree perfectly.

Perhaps the single most astonishing thing about the now-famous Parke-Taylor formula (0.1) is the stark contrast between its simplicity—and vast generality—and the eight dense pages of tabulated contributions they had presented for the six-gluon scattering

amplitude six months earlier (both formulae, of course being ultimately different ways of writing the same polynomial). Clearly, the final answer betrays a deep, underlying simplicity which was completely obfuscated by the way it had been calculated.

In the quarter-century since Parke and Taylor’s discovery, there have been many leaps forward in our understanding of perturbative quantum field theory; this is especially the case for theories with maximal supersymmetry ($\mathcal{N} = 4$ and $\mathcal{N} = 8$), but it is also true for the more banal, non-supersymmetric quantum field theories such as quantum chromodynamics (QCD) (which constitutes much of the background which must be understood at today’s particle accelerators). It is worth mentioning that to the leading-order of perturbation theory (referred to as ‘tree-level’) supersymmetry serves only as a powerful book-keeping device: ultimately, tree-level scattering amplitudes for gluons are the same whether or not a theory is supersymmetric. At higher orders in perturbation theory—those involving loops of virtual processes—however, $\mathcal{N} = 4$ is quite different from its non-supersymmetric cousins. Nonetheless, largely because of the important advantages gained by using supersymmetry at tree-level, amplitudes in $\mathcal{N} = 4$ play a central role in virtually all gauge-theory scattering amplitude computations, both in supersymmetric and non-supersymmetric theories alike. Indeed, it could be said that $\mathcal{N} = 4$ has played an important role in almost all the major breakthroughs in our broad understanding of quantum field theory over the past two decades.

Much of this new understanding has been facilitated by the development of a number of rich, alternative formulations of perturbative quantum field theory which have very little resemblance to their Feynman-diagram ancestral origins. These ‘dual’ descriptions have made it possible to easily calculate scattering amplitudes of ever-expanding complexity, dramatically increasing the amount of ‘theoretical data’ available for formulating (and testing) new hypotheses to explain the surprising simplicity discovered at the end of almost every scattering amplitude computation. Among these new formulations are the Berends-Giele recursion relations [3]; Witten’s twistor string theory [4]; the CSW [5] and Risager [6] recursion relations; and the BCFW recursion relations [7]. These frameworks are all quite distinct from one another, each making quite different properties of scattering amplitudes manifest. And for the most part—until very recently—there has been very little understanding of whether, or how these strikingly different descriptions of quantum field theory could be related to one another, let alone how they could fit

into any larger structure. One salient feature shared by all, however, was the *lack* of any intrinsic justification for its existence—any new picture for what scattering amplitudes were computing or why they were so simple.

The conflict between the manifest simplicity of scattering amplitudes and the traditional tool-box given to us by Feynman became extremely sharp in 2008, when it was discovered that scattering amplitudes (at tree-level, and—in a qualified sense—to all loop-orders) were not merely invariant under the defining superconformal symmetries of $\mathcal{N} = 4$, but they are *also* invariant under an entirely-new set of *dual* superconformal transformations [8,9]. And because arbitrary combinations of the two superconformal symmetries are also symmetries, these two in fact generate an infinite-tower of successively-dual symmetries under which scattering amplitudes are invariant; this infinite-dimensional symmetry algebra is known as the *Yangian*. It suddenly became clear that one should try to reformulate the theory in a way which would keep all these powerful symmetries manifest.

However, any formulation of quantum field theory based on Feynman diagrams derived from a Lagrangian—a manifestly *local* function on spacetime—must choose a particular spacetime in which to make locality manifest, scattering amplitudes computed with Feynman diagrams are inherently biased toward one particular set of superconformal symmetries at the cost of obfuscating the others. Manifest locality, and by extension unitarity—traditionally the salient *features* of the Feynman expansion—seem directly opposed to the underlying simplicity of scattering amplitudes in $\mathcal{N} = 4$.

This strongly suggested that an entirely new formulation of quantum field theory should exist—especially for the case of $\mathcal{N} = 4$, but also for quantum field theory more generally. Such a dual theory was proposed two years ago by Arkani-Hamed *et al.* [10], and this formulation has already led to several major breakthroughs in our understanding of scattering amplitudes and—arguably—in our understanding of quantum field theory more generally. In this new framework, amplitudes are calculated as contour integrals in an auxiliary space, the space of k -dimensional planes in n -dimensions, a space known to mathematicians as the Grassmannian, $G(k, n)$. Shortly after the appearance of [10], it was shown that Grassmannian contour integrals generate all Yangian invariants [11].

Since the Grassmannian proposal was made, it has led to a near-continuous succession of major breakthroughs. For example, together with Arkani-Hamed, Cachazo, and Trnka,

Chapter 1, it was found that formulae derived for scattering amplitudes using the BCFW recursion relations can be smoothly deformed into the forms computed by either the Risager or the CSW expansions. Shortly thereafter, we demonstrated how yet another smooth deformation of the contours for scattering amplitudes connect these forms to those obtained in Witten’s twistor string theory [12], described in Chapters 2 and 3. And in Chapter 6, the connection between the Grassmannian integral and all of the known dual-formulations of quantum field theory will be completed by illustrating how also the local Berends-Giele recursion relations can be realized in the Grassmannian, [13].

Giving this framework a foundation independent of traditional quantum field theory, we will show in Chapter 2 how the particular integrals in the Grassmannian which compute scattering amplitudes arise in a precise way by merely endowing the Grassmannian with a ‘particle interpretation’: every n -point scattering amplitude can be obtained by simply ‘adding a particle’ to the contour defining the $(n - 1)$ -point amplitude—in an essentially unique way, [12]. And so it became possible to imagine ‘boot-strapping’ all tree-amplitudes in $\mathcal{N} = 4$ from only the most elementary by successively adding particles one at a time. This vision will be fully-realized in Chapter 3 in which we describe work done together with Trnka, Volovich, and Wen, deriving a new closed-formula for all tree-amplitudes in $\mathcal{N} = 4$, [14].

But during the past two years, it has become increasingly clear that there is much, much more to learn from this story than what had been seen at tree-level. For one thing, it turns out that the contours defining tree-amplitudes can in fact be extended to all orders of perturbation theory by systematically integrating-out particles from lower-order amplitudes, [15]—giving both a compelling new picture for the origin of quantum mechanics, and supplying an incredibly powerful new tool with which to compute scattering amplitudes to high order. This is described in Chapter 4. It is worth emphasizing this second—essentially technological—implication of having such a recursive definition of the S-Matrix: from the moment we understood how to obtain loop-amplitudes from trees, it required less than twenty-four hours for us to compute amplitudes *well*-beyond what was then deemed essentially intractable by experts. Indeed, endowed by this powerful set of new tools, we were able to present in [15] the ‘two-loop’ (or, next-to-next-to-leading-order) generalization of equation (0.1)—collapsing the then known result which spanned ten pages [16]—to essentially a single term—a simplification not unlike that captured in

equation (0.1) itself.

Indeed, in the time since [15] was published, many new and exciting forms of multi-loop amplitudes have been found, including a one-line formula for the ‘next-to-next-to-next-to-leading-order’ (3-loop) corrections to (0.1), and a similarly-compact formula for all 2-loop ‘NMHV’ amplitudes (a class of amplitudes which—before the advent of the tools described in Chapter 4—were so challenging that no examples were known in the literature). These expressions are particularly remarkable because they are free of any unphysical propagators, and are therefore called ‘local.’ This will be discussed in Chapter 5. In some cases, the remarkable simplicity enjoyed by these *local* forms of loop amplitudes have been found to be closely connected with an extremely elegant geometric interpretation for what they are computing: the volumes of simplices. This is described in Chapter 6, also reported in [13]. It is not yet known to what extent this geometric picture extends beyond some simple examples, but Chapter 6 provides a striking example of very different organizing principle behind computations in quantum field theory.

The situation today is not unlike the situation in string theory a little over a decade ago, when many disparate theoretical frameworks were suddenly seen to be different aspects of a single underlying theory, named M-theory. This unification gave rise to many important, previously unanticipated breakthroughs. And so it seems to be with the Grassmannian. Within a relatively short period of time, it may be possible to understand $\mathcal{N} = 4$ *completely*. Indeed, it does not seem unreasonable to expect this research to give rise to important new insights in several branches of pure mathematics, to generate powerful new tools for practical computations relevant to collider physics, and to continue to deepen our understanding of quantum field theory in general.

Chapter 1

Contour Deformation and CSW Recursion

1.1 $\mathcal{N} = 4$ SYM and the Grassmannian

A dual formulation for the S-Matrix of $\mathcal{N} = 4$ SYM was recently been proposed in [10], where the leading singularities of the n -particle N^{k-2} MHV amplitudes—to all orders in perturbation theory—are associated with a remarkably simple integral over the Grassmannian $G(k, n)$:

$$\mathcal{L}_{n,k}(\mathcal{W}) = \frac{1}{\text{vol}(GL_k)} \int \frac{d^{k \times n} C_{\alpha a}}{(12 \cdots k)(23 \cdots k+1) \cdots (n1 \cdots k-1)} \prod_{\alpha=1}^k \delta^{4|4}(C_{\alpha a} \mathcal{W}_a). \quad (1.1.1)$$

Let us quickly review the notation appearing in (1.1.1). First, the Grassmannian $G(k, n)$ is the space of k -planes in n dimensions, an element of which can be represented by a collection of k n -vectors in the n -dimensional space whose span specifies the plane. These vectors can be put together into the $k \times n$ matrix $C_{\alpha a}$, where $\alpha = 1, \dots, k$ and $a = 1, \dots, n$. With this, we write

$$(m_1 m_2 \cdots m_k) = \epsilon^{\alpha_1 \cdots \alpha_k} C_{\alpha_1 m_1} \cdots C_{\alpha_k m_k} \quad (1.1.2)$$

for the minor of the $k \times n$ matrix $C_{\alpha a}$ made from the columns (m_1, \dots, m_k) . Since any $k \times k$ linear transformation on these k vectors leaves the k -plane invariant, there is a GL_k “gauge symmetry” $C_{\alpha a} \mapsto L_{\alpha}^{\beta} C_{\beta a}$; our integral is “gauge-fixed” by dividing by the volume of GL_k . The amplitude is given in dual twistor space, $\mathcal{W}_a = (\tilde{\mu}_a, \tilde{\lambda}_a | \tilde{\eta}_a)$, where $\tilde{\mu}_a$ is the (half-Fourier transform) conjugate of $\tilde{\lambda}_a$, and $\tilde{\eta}_a$ is a SUSY Grassmann parameter.

This expression can be trivially transformed back to momentum space—the only dependence is in the $\delta^{4|4}(C_{\alpha a} \mathcal{W}_a)$ factor, which transforms into

$$\delta^{4|4}(C_{\alpha a} \mathcal{W}_a) \rightarrow \int d^{2 \times k} \rho^{\alpha} \prod_{a=1}^n \delta^2(\rho^{\alpha} C_{\alpha a} - \lambda_a) \times \prod_{\alpha=1}^k \delta^2(C_{\alpha a} \tilde{\lambda}_a) \times \delta^4(C_{\alpha a} \tilde{\eta}_a). \quad (1.1.3)$$

In words, this equation embodies a simple new way of thinking about momentum conservation. The kinematical data is given by specifying n individual λ_a 's and $\tilde{\lambda}_a$'s, each of

which has two Lorentz indices. We can think of each (Lorentz) component as specifying some n -vector in the n -dimensional space of particle labels. Actually, given that the Lorentz group is $SL_2 \times SL_2$, the Lorentz-invariant statement is that there is a two-plane λ and another two-plane $\tilde{\lambda}$; momentum conservation $\sum \lambda_a \tilde{\lambda}_a = 0$ is the statement that the two-planes λ and $\tilde{\lambda}$ are orthogonal. Equation (1.1.3) interprets this in a different way, by introducing an auxiliary object—the k -plane C —and forcing C to contain the λ -plane (the first factor) and be orthogonal to the $\tilde{\lambda}$ -plane (the second factor).

The final, Grassmann δ -function in equation (1.1.3) ensures that the object is invariant under all of GL_k (and not just SL_k). In fact, we could have motivated the entire construction leading to equation (1.1.1) from this picture of momentum conservation: the measure in the integral over the Grassmannian is simply the nicest GL_k -invariant one with manifest cyclic symmetry. Note also that while (1.1.1) makes superconformal invariance manifest, the momentum-space form involving (1.1.3) makes parity manifest: the action of parity is just the obvious map between $G(k, n)$ and $G(n-k, n)$. This can be seen explicitly by choosing a natural gauge-fixing of GL_k , where k of the columns of C are set to an orthonormal basis, corresponding to the “link-representation” [10, 17].

The geometric picture of momentum conservation motivates yet another representation of $\mathcal{L}_{n,k}$, which makes *dual* superconformal invariance manifest [18, 19]. Since momentum conservation requires that the C -plane contains the λ two-plane, it is possible to re-write the integral as one over only the space of $(k-2)$ -planes, D , which are complementary to λ in C . This can be done using a gauge-fixing of GL_k which forces the first two rows of the C -matrix to coincide with the λ -plane—thereby manifestly encoding the fact that the Grassmannian includes the λ -plane. A further linear transformation maps

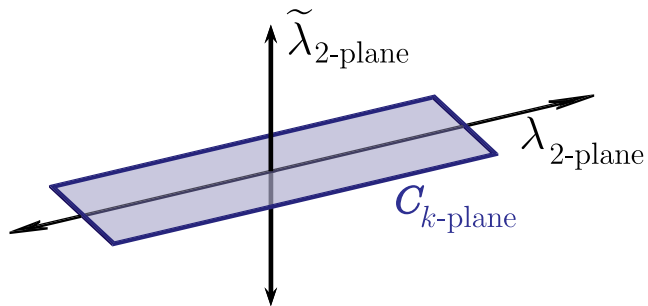
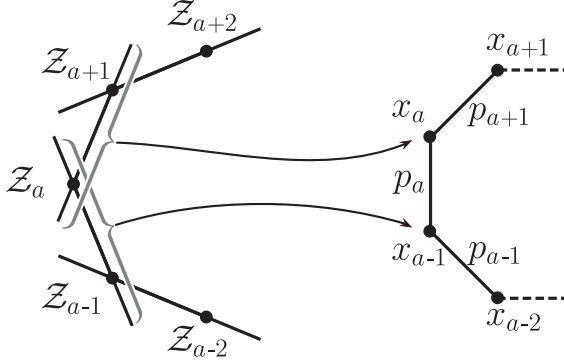


Figure 1.1: The geometric realization of momentum conservation.

Figure 1.2: The relationship between momentum-twistors and dual-spacetime points.



$k \times k$ minors to $(k-2) \times (k-2)$ minors, and we find that we can write

$$\mathcal{L}_{n,k}(\lambda, \tilde{\lambda}, \tilde{\eta}) = \frac{\delta^4(\sum_a \lambda_a \tilde{\lambda}_a) \delta^8(\sum_a \lambda_a \tilde{\eta}_a)}{\langle 12 \rangle \langle 23 \rangle \cdots \langle n1 \rangle} \times \mathcal{R}_{n,k}, \quad (1.1.4)$$

where

$$\mathcal{R}_{n,k}(\mathcal{Z}) = \frac{1}{\text{vol}(GL_{k-2})} \int \frac{d^{(k-2) \times n} D_{\hat{\alpha}a} \prod_{\hat{\alpha}=1}^{k-2} \delta^{4|4}(D_{\hat{\alpha}a} \mathcal{Z}_a)}{(12 \cdots k-2)(23 \cdots k-1) \cdots (n1 \cdots k-3)}. \quad (1.1.5)$$

Here, the \mathcal{Z}_a are the “momentum-twistor” variables introduced by Hodges [20], which are the most natural variables with which to discuss *dual* superconformal invariance. External particles are associated with points x_a in the dual space, with $p_a = x_{a+1} - x_a$. The point x_a is associated with a line in *its* associated momentum-“twistor space”; and since $x_a - x_{a+1}$ is null, the line in momentum-twistor space associated with x_a intersects the line associated with x_{a+1} . Therefore, we can associate x_a with a canonical pair of momentum-twistors $(\mathcal{Z}_a, \mathcal{Z}_{a-1})$ defined by the intersection of lines. This is illustrated in the figure below. The momentum twistor \mathcal{Z}_a is composed of $\mathcal{Z}_a = (\mu_a, \lambda_a | \eta_a)$, where the variables $\tilde{\lambda}_a, \tilde{\eta}_a$ are determined by μ_a, η_a . Explicitly, they are given by

$$\begin{aligned} \tilde{\lambda}_a &= \frac{\langle a-1 \ a \rangle \mu_{a+1} + \langle a \ a+1 \rangle \mu_{a-1} + \langle a+1 \ a-1 \rangle \mu_a}{\langle a-1 \ a \rangle \langle a \ a+1 \rangle} \\ \tilde{\eta}_a &= \frac{\langle a-1 \ a \rangle \eta_{a+1} + \langle a \ a+1 \rangle \eta_{a-1} + \langle a+1 \ a-1 \rangle \eta_a}{\langle a-1 \ a \rangle \langle a \ a+1 \rangle}. \end{aligned} \quad (1.1.6)$$

Dual superconformal transformations [8, 19–21] are just linear transformations of the \mathcal{Z}_a , which is a manifest symmetry of equation (1.1.5), just as ordinary superconformal transformations are linear transformations on \mathcal{W}_a making them a manifest symmetry of equation (1.1.1). Thus, equation (1.1.1) makes *all* the important symmetries of $\mathcal{N} = 4$ SYM amplitudes manifest.

The momentum-space formula for $\mathcal{L}_{n,k}$ is to be interpreted as a contour integral in $(k-2) \times (n-k-2)$ variables, which can be thought of as specifying the unfixed degrees of freedom of a $(k-2)$ -plane orthogonal to both the $\tilde{\lambda}$ - and λ -planes. In [10], evidence was given that the residues of the integrand are associated with leading singularities up to 2 loops, motivating the conjecture that *all* leading singularities are contained as residues. This conjecture carries even more weight given the realization that all the residues are both superconformal *and* dual superconformal invariant, which further means they are invariant under the full Yangian symmetry [8]. Leading singularities are data associated with scattering amplitudes that are free of IR-divergences—at loop level, they can be thought of as being associated with loop integrals over compact contours—and should therefore reflect all the symmetries of the theory. In fact, the residues of our object can be thought of as generating (likely all) Yangian invariants that are algebraic functions of the external spinor-helicity variables. Furthermore, as emphasized in [10], higher-dimensional residue theorems encode highly non-trivial relations between these invariants, many of which have striking physical interpretations such as loop-level infrared equations.

It is clear that there is an enormous amount of fascinating structure to be uncovered in the properties of the individual residues of $\mathcal{L}_{n,k}$, since they are invariants of the most remarkable integrable structure we have ever seen in physics! Recent work [22, 23] as well as work to appear [24] gives strong evidence that infinite classes of all-loop leading singularities are indeed contained amongst the residues of $\mathcal{L}_{n,k}$.

There is however something even more remarkable than the properties of residues taken individually: they can be combined in such a way as to produce amplitudes with a local space-time interpretation. Consider for instance NMHV tree amplitudes ($k=3$). A given residue is associated with putting $(k-2)(n-k-2) = (n-5)$ minors to zero, which can be labeled as $(m_1) \cdots (m_{n-5})$, where (m) denotes that the minor $(m \ m+1 \ m+2)$ has been set to zero. In [10], it was shown that a natural BCFW expansion for the NMHV amplitudes is given by a sum of residues

$$M_{n,\text{NMHV}}^{\text{BCFW}} = \sum \underbrace{(o_1)(e_2)(o_3) \cdots}_{n-5 \text{ terms}} \quad (1.1.7)$$

where the sum is over all strictly-increasing series of $(n-5)$ alternating odd (o) and even

(e) integers; to be explicit the 6-,7- and 8-particle amplitudes are given by

$$\begin{aligned}
M_{6,\text{NMHV}}^{\text{BCFW}} &= (1) + (3) + (5); \\
M_{7,\text{NMHV}}^{\text{BCFW}} &= (1)(2) + (1)(4) + (1)(6) + (3)(4) + (3)(6) + (5)(6); \\
M_{8,\text{NMHV}}^{\text{BCFW}} &= (1)(2)(3) + (1)(2)(5) + (1)(2)(7) + (1)(4)(5) + (1)(4)(7) \\
&\quad + (1)(6)(7) + (3)(4)(5) + (3)(4)(7) + (3)(6)(7) + (5)(6)(7).
\end{aligned}
\tag{1.1.8}$$

We remind the reader of a fact that will be important repeatedly: residues are naturally alternating in the arguments, so that e.g. $(i_1)(i_2) = -(i_2)(i_1)$. The P(BCFW) form of the amplitudes has exactly the same form as BCFW, but switching the role of even and odd integers:

$$M_{n,\text{NMHV}}^{\text{P(BCFW)}} = (-1)^{n-5} \underbrace{\sum (e_1)(o_2)(e_3) \cdots}_{n-5 \text{ terms}}.
\tag{1.1.9}$$

As shown in [10], the equality $M^{\text{BCFW}} = M^{\text{P(BCFW)}}$ is a (quite non-trivial) consequence of global residue theorems, which further guarantees the cyclic invariance of the amplitude.

This presentation of the NMHV amplitudes makes all of its symmetries manifest, and is strikingly “combinatorial” in nature. One thing that is seemingly *not* manifest, however, is that this object has anything whatsoever to do with a local space-time Lagrangian! Each term individually has “non-local” poles, which magically cancel in the odd/even/odd combination defining the amplitude. The cancelation of these non-local poles can be understood indirectly by the equality $M^{\text{BCFW}} = M^{\text{P(BCFW)}}$, since the non-local poles appearing in the two forms turn out to be different. However, this is very far from establishing that this object comes from a local Lagrangian, and one would certainly like to see the emergence of space-time in a much more direct and explicit way.

In this chapter, we will argue that the local space-time description of tree scattering amplitudes is actually hiding in plain sight in the BCFW sum over residues in the Grassmannian. We will show that a very natural and canonical contour deformation converts the BCFW form of tree scattering amplitudes to the CSW/Risager expansion, which is a direct reflection of the space-time Lagrangian in light-cone gauge!

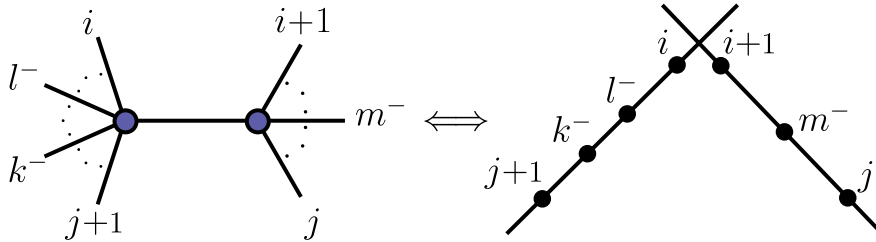
1.2 Brief Review of CSW and Risager

To set the stage, let us quickly review the story of the CSW recursion relations [5, 25, 26] and the very closely-related Risager recursion relations [6, 27]. The CSW rules are simply Feynman rules [28], except that the vertices are off-shell continuations of MHV amplitudes, where the λ 's for internal lines with momentum P are defined by

$$\lambda_P = P|\zeta], \quad (1.2.10)$$

where ζ is an auxiliary spinor. Note that we use a different notation for this auxiliary spinor than the usual one in the literature, $\tilde{\eta}$, in order to not confuse this object with the SUSY Grassmann parameters. The similarity with usual Feynman rules and the hidden Lorentz invariance of this expansion is not a coincidence: the CSW rules can be derived from the Yang-Mills Lagrangian by going to a more sophisticated version of light-cone gauge [28, 29]; the auxiliary spinor ζ is associated with the light-like direction defining the light-cone gauge. As usual in light-cone gauge, we have only physical degrees of freedom, the two polarizations \pm of the gluons. There are cubic interactions $(++-)$, $(--+)$ and the quartic interaction $(++--)$. From this, it is possible to make a field redefinition to remove the anti-MHV $(++-)$ interaction; this forces the introduction of an infinite number of new MHV vertices, which must—on-shell—reproduce the MHV amplitudes. The resulting Lagrangian is precisely the one that gives the CSW rules. The equivalence between the MHV rules in a light-cone gauge and usual Lorentz-invariant formulation of the (super) Yang-Mills Lagrangian $\mathcal{L} = -\frac{1}{4}\text{tr}F_{\mu\nu}^2 + \dots$ was nicely established in a different way in [30]. Beginning with a twistor space action with a large amount of gauge symmetry, one gauge-fixing leads to the usual manifestly Lorentz-invariant Yang-Mills action, while a different gauge-fixing yields the MHV Lagrangian in light-cone gauge. Thus, the CSW rules should be thought of as directly reflecting the Yang-Mills Lagrangian in light-cone gauge, encoding local space-time physics in the most succinct possible way.

For future reference, we remind the reader that the terms in the CSW expansion of the N^{k-2} MHV amplitude are localized on $(k-1)$ intersecting lines in the \mathcal{Z} -twistor space: the MHV vertices in the CSW diagrams are associated with lines in twistor space, while the internal lines are associated with points where these lines intersect. Thus, a general term in the CSW expansion of NMHV amplitudes with particles m, k , and l of negative helicity is localized in twistor space as shown below.



The Risager deformation is closely related, providing an alternate derivation of the CSW rules that closely parallels the logic leading the BCFW recursion relations [7,31–33]. As with BCFW, it involves a deformation of the spinor helicity variables; specifically, it begins by canonically deforming the $\tilde{\lambda}_i$'s for all the negative helicity particles:

$$\tilde{\lambda}_i \rightarrow \tilde{\lambda}_i + \alpha_i z \zeta. \quad (1.2.11)$$

In order to conserve overall momentum, the α_i must satisfy the constraint

$$\sum_i \alpha_i \lambda_i = 0. \quad (1.2.12)$$

Thus, for k negative helicity gluons, the most general Risager deformation is labeled by $(k - 2)$ parameters. It is possible to show that under this deformation the amplitude vanishes as $z \rightarrow \infty$, so that the familiar BCFW logic leads to recursion relations (see, e.g. [32,34]). Remarkably, Risager showed that repeated recursive use of this deformation leads to the CSW rules [6].

Below we will study the Risager expansion for $\overline{\text{MHV}}$ amplitudes in the split-helicity configuration. In this case, the Risager diagrams consist only of ones with a three-point vertex and the lower-point $\overline{\text{MHV}}$ amplitude connected by a propagator. We will find it useful to look at Risager deformations in momentum-twistor variables μ_a , for which the general $N^{k-2}\text{MHV}$ split helicity amplitude $A(1^-, 2^-, \dots, (k-1)^-, k^+, \dots, (n-1)^+, n^-)$ takes the remarkably simple form:

$$\hat{\mu}_a = \begin{cases} \mu_a + z\beta_a\zeta & \text{for } a = 1, \dots, k-2 \quad (\beta_a \text{ arbitrary}) \\ \mu_a & \text{for } a = k-1, \dots, n \end{cases}. \quad (1.2.13)$$

Note that this deforms $(k - 2)$ terms, which is exactly the number of independent α 's in (1.2.11). There are no constraints on the β_a since—by construction—any choice of μ_a is guaranteed to produce $\tilde{\lambda}_a$'s that satisfy momentum conservation. This choice of β_a

determines the deformation of the negative helicity particles α_i as

$$\alpha_i = \frac{\langle i \ i-1 \rangle \beta_{i+1} + \langle i+1 \ i \rangle \beta_{i-1} + \langle i-1 \ i+1 \rangle \beta_i}{\langle i+1 \ i \rangle \langle i \ i-1 \rangle}. \quad (1.2.14)$$

1.3 Relaxing δ -Functions

We now describe the contour deformation that will lead us from the BCFW contour in the Grassmannian to the space-time Lagrangian in light-cone gauge, passing through the CSW and Risager expansions of tree amplitudes. We begin with the form of $\mathcal{L}_{n,k}$ in momentum space. It is most convenient to use the momentum-twistor form, since this explicitly exhibits the (super) momentum-conserving δ -functions in the pre-factor, and we can study instead the object $\mathcal{R}_{n,k}$.

There is something seemingly unnatural in the expression for $\mathcal{R}_{n,k}$: it is a nice, holomorphic contour integral, but it has explicit δ -function factors! This is not unnatural at all, since these are in fact to be thought of “holomorphic” δ -functions, which are properly interpreted as poles. In other words, we may interpret $\delta^2(\mu)$ as being really

$$\delta^2(\mu) = \frac{1}{\mu_1} \times \frac{1}{\mu_2}; \quad (1.3.15)$$

or more generally, introducing a pair of auxiliary spinors χ, ζ , we write

$$\delta^2(\mu) = \frac{[\chi \zeta]}{[\chi \mu][\zeta \mu]} \quad (1.3.16)$$

where we also demand that the contour of integration enforce the poles where $[\chi \mu] = [\zeta \mu] = 0$. Note that the expression in equation (1.3.16) is not manifestly Lorentz invariant—but of course the residue obtained on the pole of both factors *is* Lorentz invariant. The reason for using the notation “ $\delta^2(\mu)$ ” is to emphasize the Lorentz invariance of the final object. Thus, when we say that the expression for $\mathcal{R}_{n,k}$ is a contour integral in $(k-2)(n-k-2)$ variables, we really mean that we started with a larger $(k-2)(n-k+2)$ -dimensional integral and have already fixed part of the contour by specifying that it enforces $4(k-2)$ poles associated with the Bosonic parts of the $\delta^4(D_{\hat{a}a} \mathcal{Z}_a)$ -factors. Similarly, what we have been referring to as “the” residues of $\mathcal{R}_{n,k}$ are really particular residues in this higher-dimensional integral, evaluated on $4(k-2)$ extra poles, with an extra $(k-2)(n-k-2)$ conditions involving the minors needed to fully-specify the residue.

This way of thinking about the δ -functions explicitly as poles naturally suggests something very remarkable. We can “relax” any one of the δ -functions, using a residue theorem to move the contour off one of its associated poles, and thereby express a manifestly Lorentz-invariant residue as a sum over non-Lorentz invariant terms which involve putting an extra minor to zero. Inspired by this, we will take one of the δ^2 -factors and replace it by

$$\delta^2(\mu) = \delta([\zeta \mu]) \times \frac{[\chi \zeta]}{[\chi \mu]}, \quad (1.3.17)$$

where we mean that the pole at $[\zeta \mu] = 0$ is still being enforced while we allow ourselves the freedom to deform the contour off the pole at $[\chi \mu] = 0$. Note that while this expression is not Lorentz-invariant away from both poles, it *is* independent of the choice of χ . The reason is that on the zero of $[\zeta \mu] = 0$, μ is proportional to ζ and we may write $\mu = d \times \zeta$, and so $[\chi \zeta]/[\chi \mu] = 1/d$ is χ -independent. Thus, relaxing the δ -function in this way expresses a Lorentz-invariant residue as a sum over non-Lorentz invariant terms which are a function of only a single auxiliary spinor ζ . Concretely, we can do this for one of the $\delta^2(D_{\hat{\alpha}a}\mu_a)$ factors—e.g. that of $\hat{\alpha} = 1$ —by making the replacement

$$\delta^2(D_{1a}\mu_a) \rightarrow \delta(D_{1a}[\zeta \mu_a]) \times \frac{[\chi \zeta]}{D_{1a}[\chi \mu_a]} \quad (1.3.18)$$

and deforming the contour off the $D_{1a}[\chi \mu_a]$ pole.

Clearly, this operation can be extended to relax even more δ -functions; but we will see that relaxing just one δ -function “blows up” Lorentz-invariant residues into a sum of non-Lorentz invariant terms with a beautiful physical interpretation. For the NMHV case, we will see that some of the terms in the sum are *precisely* the ones that appear in the CSW expansion of NMHV amplitudes. This is strongly suggested—even without a direct computation—by the localization properties of these terms both in the Grassmannian and twistor space, and the precise equality can be easily verified. Other terms in the sum do not have the appropriate localization properties and are not associated with CSW terms. The CSW terms have a local space-time interpretation and are therefore free of non-local poles, while the others do contain non-local poles. In a sense our δ -relaxing contour deformation has performed a particularly powerful partial fraction expansion of the residue into a sum over local and non-local pieces. Remarkably, in the sum over residues with the alternating odd/even structure of equation (1.1.9), all the non-CSW

terms appear precisely twice with opposite signs and cancel in pairs, while the remaining terms are exactly the terms of the CSW expansion of the amplitude!

For $k > 3$, it is easy to see that relaxing a single δ -function can not directly produce CSW terms. Nonetheless, such a canonical operation must have a physical meaning, and the only natural candidate for a non-manifestly Lorentz invariant form of amplitudes depending on a single auxiliary spinor is the Risager expansion. This raises a puzzle, however, since the Risager expansion is not unique, but is labeled by $(k - 2)$ degrees of freedom. We establish the precise equivalence and understand the origin of these degrees of freedom for the case of split-helicity $\overline{\text{MHV}}$ amplitudes, where the $(k - 2)$ free parameters of the Risager deformation are seen to be quite non-trivially determined by the degrees of freedom associated with the GL_{k-2} “gauge symmetry” of the momentum-twistor formula.

As was shown by Risager [6], a recursive application of the Risager recursion eventually yields the CSW expansion for general amplitudes. Although we won’t pursue this direction further in this chapter, this strongly suggests that the CSW expansion for general amplitudes can be directly obtained by recursively relaxing many δ -function factors.

1.4 NMHV and CSW from δ -Relaxation

I. Preliminaries

Let us work in the momentum-twistor picture, where

$$\mathcal{L}_{n,3} = M_{MHV} \times \int \frac{d^{n-5} D_{1a}}{(1)(2) \cdots (n)} \delta^{4|4}(D_{1a} \mathcal{Z}_a). \quad (1.4.19)$$

Here the 1×1 minors (j) are of course just single variables D_{1j} ; we remind the reader that the linear transformation from the $G(k, n)$ to the $G(k-2, n)$ picture makes the $(k - 2) \times (k - 2)$ minor $(23 \cdots k-1)_D$ proportional to the $k \times k$ minor $(12 \cdots k)_C$, so that e.g. the minor (2) in the momentum-twistor picture is proportional to the minor (123) in the $G(3, n)$ picture. For convenience we will denote the elements of the $1 \times n$ matrix $D_{\hat{a}a}$ as

$$(D_1, D_2, \dots, D_n). \quad (1.4.20)$$

In other words, we remove the index \hat{a} when $k = 3$ since it takes a single value.

A given residue is associated with setting $(n - 5)$ of the minors to zero as is obvious: after gauge-fixing any one of the D_a , setting $(n - 5)$ of the D_a ’s to zero allows us to use

the Bosonic δ -function to solve for the remaining four D 's. We denote this residue as $\overline{(a_1)(a_2)(a_3)(a_4)(a_5)}$, which instructs us to write all minors in cyclic order starting from (1), with $(a_1), \dots, (a_5)$ left off. As an example with $n = 8$, $\overline{(2)(3)(4)(6)(7)}$ denotes the residue (1)(5)(8) where the minors (1), (5), (8) are set to zero. We remind the reader once again that residues of functions in several complex variables are antisymmetric objects, so that the order in which the minors are presented matters, and e.g., (1)(5)(8) = $-(5)(1)(8)$.

We will be looking at explicit gluon amplitudes in what follows, so we need to integrate over the SUSY Grassmann parameters to extract these. This is a completely straightforward exercise. We set the gluons with $a \in I$ to have negative helicity, strip-off the ordinary momentum-conserving δ -function, and we write $\mathcal{L}_{n,k} \equiv \delta^4(\sum_a \lambda_a \tilde{\lambda}_a) L_{n,k}$ with

$$L_{n,k} = \frac{1}{\text{vol}(GL_{k-2})} \int \frac{d^{(k-2) \times n} D_{\hat{\alpha}a} (\det \tilde{D})^4 \times \delta^4(D_{\hat{\alpha}a} \mathcal{Z}_a)}{(1\ 2 \ \dots \ k-2)(2\ 3 \ \dots \ k-1) \dots (n\ 1 \ \dots \ k-3)} \quad (1.4.21)$$

where \tilde{D} is a $k \times k$ matrix

$$\tilde{D}_{\alpha I} = \begin{pmatrix} \lambda_{\alpha I} \\ \hat{D}_{\alpha I} \end{pmatrix} \text{ with } \hat{D}_{\alpha I} = \Theta(I-1) \sum_{a=I+1}^n D_{\alpha a} \langle I\ a \rangle; \quad (1.4.22)$$

here, $\Theta(x)$ is 1 for $x > 0$ and 0 otherwise.

Note that while in this expression particle “1” appears to play a special role, it could be replaced by any other starting point, with all the expressions for $L_{n,k}$ agreeing on the support of the δ -functions.

Returning to the $k = 3$ case, a general residue is explicitly given by

$$\overline{(a_1)(a_2)(a_3)(a_4)(a_5)} = \int \frac{dD_{a_1} \dots dD_{a_5}}{D_{a_1} \dots D_{a_5}} (\det \tilde{D})^4 \delta^4(D_{a_1} \mathcal{Z}_{a_1} + \dots + D_{a_5} \mathcal{Z}_{a_5}); \quad (1.4.23)$$

we can relax the δ -function for the μ -term by making the replacement

$$\delta^2(D_a \mu_a) \rightarrow \delta(D_a [\mu_a \zeta]) \times \frac{[\chi \zeta]}{(D_a [\mu_a \chi])} \equiv \frac{1}{d} \delta(D_a [\mu_a \zeta]). \quad (1.4.24)$$

Then, we can use a residue theorem to deform the contour off $D_a [\chi \mu_a] = 0$, or equivalently off $d = 0$, and write

$$\overline{(a_1)(a_2)(a_3)(a_4)(a_5)} = \sum_{\sigma \in \mathbb{Z}_5} \left[\overline{(a_{\sigma(1)})(a_{\sigma(2)})(a_{\sigma(3)})(a_{\sigma(4)} d (a_{\sigma(5)})} \right], \quad (1.4.25)$$

where the sum is over cyclic permutations of $\{1, 2, 3, 4, 5\}$. For example,

$$\left[\overline{(a_1)(a_2)(a_3)(a_4)d(a_5)} \right]$$

is given by

$$\int_{D_{a_5}=0} \frac{dD_{a_1} \cdots dD_{a_5}}{D_{a_1} \cdots D_{a_5}} (\det \tilde{D})^4 \frac{1}{d} \delta^2(D_{a_1} \lambda_{a_1} + \cdots + D_{a_5} \lambda_{a_5}) \delta(D_{a_1} [\zeta \mu_{a_1}] + \cdots + D_{a_5} [\zeta \mu_{a_5}]). \quad (1.4.26)$$

II. Localization Properties of the Grassmannian

Before we demonstrate the complete equivalence of the CSW expansion and the terms generated by “blowing-up” each residue of the NMHV contour, it is worthwhile to give an intuitive understanding of why this should work.

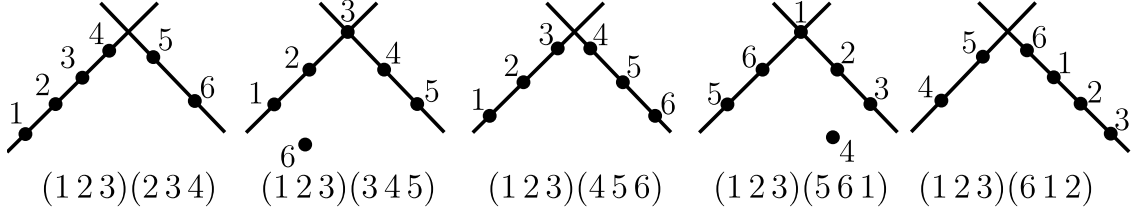
One of the strongest hints that there should be a direct connection between the CSW expansion and $\mathcal{L}_{n,k}$ is how the localization *in twistor-space* implied by CSW is mirrored by a *localization within the Grassmannian itself*. We can see this directly by Fourier-transforming the kinematical δ -function $\delta^{4|4}(C_{\alpha a} \mathcal{W}_a)$ from the \mathcal{W} -twistor variables to their (ordinary) dual twistor-space variables \mathcal{Z} :

$$\prod_{\alpha=1}^k \delta^{4|4}(C_{\alpha a} \mathcal{W}_a) \rightarrow \int d^{4|4} z^\alpha \prod_{\alpha=1}^k \delta^{4|4}(\mathcal{Z}_a - C_{\alpha a} z^\alpha). \quad (1.4.27)$$

(These twistors \mathcal{Z}_a are ordinary twistors, which are the duals of \mathcal{W}_a , and should not be confused with momentum-twistors.)

If we think of each column of $G(k, n)$ as projectively defining a point in \mathbb{CP}^{k-1} , then the vanishing of a minor of $G(k, n)$ —consecutive or otherwise—is equivalent to some localization condition among these points in \mathbb{CP}^{k-1} . The first nontrivial example of this can be easily seen for $G(3, n)$, where a minor $(i \ j \ k) = 0$ if and only if the corresponding points i, j , and k are collinear in \mathbb{CP}^2 . It is not hard to see that the twistor-space “collinearity operator” $\epsilon_{IJKL} Z_i^I Z_j^J Z_k^K$, which vanishes whenever the (Bosonic parts of the) twistors Z_i, Z_j , and Z_k are collinear [4], manifestly annihilates any residue of the Grassmannian supported where the minor $(i \ j \ k)$ vanishes. Similarly, for $k = 4$, the “coplanarity operator” $\epsilon_{IJKL} Z_i^I Z_j^J Z_k^K Z_l^L$ which test whether Z_i, \dots, Z_l are coplanar, will annihilate any residue for which the minor $(i \ j \ k \ l) = 0$. (Although beyond the scope

momentum-twistor picture. Let us look at the 5 terms in the blow-up of the residue (1 2 3); these terms have the the following localizations structure in twistor space:



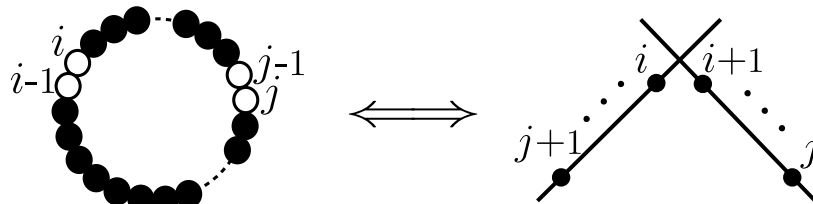
Note that while the terms $[(1)(2)]$, $[(1)(4)]$, $[(1)(6)]$ *do* have CSW localization properties, the terms $[(1)(3)]$ and $[(1)(5)]$ *do not*. Similarly, the terms $[(3)(1)]$ and $[(3)(5)]$ in the blow-up of (3), and the terms $[(5)(1)]$, $[(5)(3)]$ in the blow-up of (5) do not have CSW localization. However, and quite remarkably, these 6 non-local terms cancel each other in pairs due to the antisymmetric property of the residues, as e.g. $[(1)(3)] + [(3)(1)] = 0$. The 9 remaining terms all have CSW localization and are indeed in perfect correspondence with the 9 CSW diagrams for this amplitude!

This pattern holds for all NMHV amplitudes. It is easiest to see this pictorially: let the sum over residues giving the BCFW form of the amplitude be represented as follows,

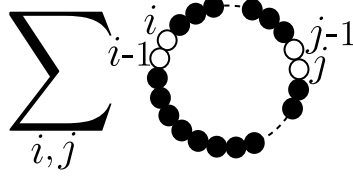
$$\sum_{1 < i < j < n} \text{Diagram}$$

where each term represents $\overline{(i-1)(i)(j-1)(j)(n)}$, i.e., the open circles correspond to the minors that are not being set to zero.

Now, when we blow up each residue with our contour deformation, we have a sum over terms setting an extra minor tacked-on at the end of the chain to zero, which can be represented in the picture by summing over terms “coloring-in” one of the white dots, leaving us with 4 minors that are not set to zero. Each of these has some localization properties, but it is easy to see that the only ones that have CSW localization are the ones of the form:



over all CSW terms



III. Establishing the CSW Equivalence

We finally prove that each of the remaining residues in the sum above precisely corresponds to the corresponding term in the CSW expansion of the NMHV amplitude. To begin with, it is convenient to introduce the following notation

$$\{a b c\} = \mu_a \langle b c \rangle + \mu_b \langle c a \rangle + \mu_c \langle a b \rangle \quad (1.4.30)$$

so that, e.g.,

$$\tilde{\lambda}_i = \frac{\{i+1 i i-1\}}{\langle i+1 i \rangle \langle i i-1 \rangle}. \quad (1.4.31)$$

Let us compute each of the residues $\overline{(i)(i+1)(j)(j+1)d}$, corresponding to the vanishing of all D 's except $D_i, D_{i+1}, D_j, D_{j+1}$ and d .

Recall that we have three δ -functions to impose:

$$\begin{aligned} & \delta^2(D_i \lambda_i + D_{i+1} \lambda_{i+1} + D_j \lambda_j + D_{j+1} \lambda_{j+1}) \\ & \times \delta(D_i [\mu_i \zeta] + D_{i+1} [\mu_{i+1} \zeta] + D_j [\mu_j \zeta] + D_{j+1} [\mu_{j+1} \zeta]). \end{aligned} \quad (1.4.32)$$

Using GL_1 to fix $D_i = 1$, it is easy to solve explicitly for the rest of the D 's

$$\begin{aligned} D_{i+1} &= \frac{[\{i j j+1\} \zeta]}{[\{i+1 j j+1\} \zeta]}, \\ D_j &= \frac{[\{i i+1 j+1\} \zeta]}{[\{i+1 j j+1\} \zeta]}, \quad D_{j+1} = \frac{[\{i i+1 j\} \zeta]}{[\{i+1 j j+1\} \zeta]}. \end{aligned} \quad (1.4.33)$$

Here $[\{abc\} \zeta]$ means the Lorentz invariant contraction of spinors.

The three δ -functions in (1.4.32) yield a Jacobian

$$J = \frac{1}{[\{i+1 j j+1\} \zeta]} \quad (1.4.34)$$

while the product of D 's in the denominator of the residue becomes

$$\frac{1}{D_i D_{i+1} D_j D_{j+1}} = \frac{[\{i+1 j j+1\} \zeta]^3}{[\{i+1 i j+1\} \zeta][\{i+1 i j\} \zeta][\{i j j+1\} \zeta]}. \quad (1.4.35)$$

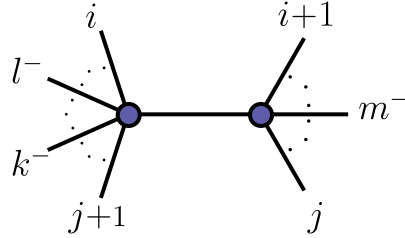
Finally,

$$d = \langle Z_i Z_{i+1} Z_j Z_{j+1} \rangle \quad (1.4.36)$$

where $\langle Z_i Z_{i+1} Z_j Z_{j+1} \rangle = \epsilon^{IJKL} Z_{i,I} Z_{i+1,J} Z_{j,K} Z_{j+1,L}$ is the *dual* conformal invariant inner product of four momentum-twistors. In fact, this particular combination has a special meaning,

$$\frac{\langle Z_j Z_{j-1} Z_i Z_{i-1} \rangle}{\langle j \ j-1 \rangle \langle i \ i-1 \rangle} = (x_j - x_i)^2 = (p_i + p_{i+1} + \cdots + p_{j-1})^2 \quad (1.4.37)$$

which is nothing but the propagator in the corresponding CSW diagram!



In this computation we are taking as the minus-helicity particles gluons k, l and m . Therefore, the helicity-factor $(\det \tilde{D})$ has the form

$$(\det \tilde{D}) = \begin{vmatrix} \lambda_m & \lambda_k & \lambda_l \\ \hat{D}_m & \hat{D}_k & \hat{D}_l \end{vmatrix}. \quad (1.4.38)$$

In the case where particle m is on the right-side and k, l on the left-side as in the figure above, referring to equation (1.4.22), we can write

$$\hat{D}_m = D_j \langle m \ j \rangle + D_{j+1} \langle m \ j+1 \rangle = \frac{[\{j+1 \ i \ i-1\} \zeta] \langle m \ j \rangle - [\{j+1 \ i \ i-1\} \zeta] \langle m \ j \rangle}{[\{i+1 \ j \ j+1\} \zeta]} \quad (1.4.39)$$

while $\hat{D}_k = \hat{D}_l = 0$. Then $(\det \tilde{D}) = \langle k l \rangle \hat{D}_m$.

The residue $\overline{(i)(i+1)(j)(j+1)d}$, which equals $J(\det \tilde{D})^4 / (d D_i D_{i+1} D_j D_{j+1})$, becomes

$$\frac{([\{j+1 \ i+1 \ i\} \zeta] \langle m \ j \rangle - [\{j \ i+1 \ i\} \zeta] \langle m \ j+1 \rangle)^4 \langle k l \rangle^4}{\langle Z_{j+1} Z_j Z_{i+1} Z_i \rangle [\{j+1 \ i+1 \ i\} \zeta] [\{j+1 \ j \ i+1\} \zeta] [\{i \ j+1 \ j\} \zeta] [\{j \ i+1 \ i\} \zeta]}. \quad (1.4.40)$$

A simple computation using, e.g.,

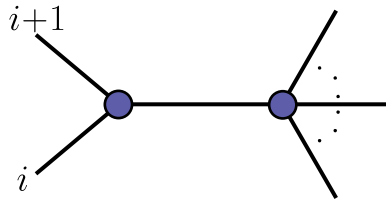
$$\begin{aligned} (p_j + \cdots + p_{i+1}) |i\rangle &= \frac{\{j+1 \ j \ i\}}{\langle j+1 \ j \rangle}, \\ \langle j+1 | (p_j + \cdots + p_i) &= \frac{\{j+1 \ i \ i-1\}}{\langle i \ i-1 \rangle}, \end{aligned} \quad (1.4.41)$$

reveals that equation (1.4.40) precisely reproduces the CSW contribution associated to the corresponding diagram.

1.5 Risager from δ -Relaxation

For $k > 3$, it is easy to see that relaxing a single δ -function does not directly lead to the CSW expansion. This is obvious since localization in the Grassmannian associated with putting $k \times k$ minors to zero for $k > 3$ is not directly associated with localization on lines in twistor space. The only natural interpretation of our deformation is as the Risager expansion. An immediate question with this interpretation is precisely how the $(k - 2)$ degrees of freedom of the Risager deformation are reflected in the Grassmannian picture—exactly which Risager expansion are we landing on? In this section we establish the correspondence with Risager, and also understand the origin of the Risager degrees of freedom, by examining $\overline{\text{MHV}}$ amplitudes. This will determine precisely which Risager expansion must be associated with our contour deformation for general (n, k) .

The only Risager diagrams that contribute involve the points $i, i + 1$ and the internal line P on one side, connected with a propagator to the lower-point $\overline{\text{MHV}}$ amplitude on the other side



which can be nicely simplified to the form

$$A_i^{\text{Risager}} = \frac{[kl]^4}{[\widehat{1\ 2}] \dots [\widehat{i-1\ i}][i\ i+1][\widehat{i+1\ i+2}] \dots [\widehat{n\ 1}]} \quad (1.5.42)$$

Here, the deformation parameter z is evaluated where $P^2(z^*) = 0$. We will now see that this expansion is reproduced for the first non-trivial case of the split-helicity 6-particle $\overline{\text{MHV}}$ amplitude $A(1^-, 2^-, 3^-, 4^+, 5^+, 6^-)$. The D -matrix in the momentum twistor form of the Grassmannian is

$$D = \begin{pmatrix} D_{11} & D_{12} & D_{13} & D_{14} & D_{15} & D_{16} \\ D_{21} & D_{22} & D_{23} & D_{24} & D_{25} & D_{26} \end{pmatrix}. \quad (1.5.43)$$

As before, we will be relaxing one of the $\delta(D_{1a}\mu_a)$ -factors. Our strategy is to use four δ -function constraints for the second row, and to solve for D_{23}, \dots, D_{26} in terms of D_{21}

and D_{22} , and to use the remaining three δ -functions to solve for D_{14}, \dots, D_{16} in terms of D_{11}, D_{12} , and D_{13} . Now, in deforming the contour, we will get a sum over terms where a given minor (j) is set to zero. Here, we use the notation (j) to refer to the minor ($j \ j + 1 \ \dots \ j + k - 3$). We can use the condition of the vanishing of this minor to solve for D_{13} and plug it back into our equations for D_{14}, \dots, D_{16} . Notice that we can gauge-fix the GL_2 so that e.g. $D_{11}, D_{12}, D_{21}, D_{22}$ are anything we like, but we will leave them arbitrary for now. The reason is that while the sum over all the terms will be GL_2 -invariant, each individual term will not, and as we will see the dependence on gauge degrees of freedom will precisely mirror the freedom in the Risager deformations.

A somewhat lengthy computation yields a lovely result for the term where the minor (j) is set to zero; we find that it precisely corresponds to a term in the Risager expansion

$$[(j)] = A_{j+3}^{\text{Risager}} \quad (1.5.44)$$

where the Risager deformation is particularly simple and is given in terms of the following deformation on momentum twistor variables $\hat{\mu}_i = \mu_i + \beta_i z \zeta$ with

$$\beta_1 = D_{22}, \quad \text{and} \quad \beta_2 = D_{21}. \quad (1.5.45)$$

That is, as advertised, the degrees of the freedom in the Risager expansion are contained in the GL_2 -freedom of the momentum-twistor Grassmannian formula!

Moving on to the 7-point amplitude $A(1^-, 2^-, 3^-, 4^-, 5^+, 6^+, 7^-)$ we find exactly the same pattern: we find that the sum over terms setting a minor to zero precisely matches the Risager expansion of the amplitude, with the β -deformations now with

$$\beta_1 = M_{23}, \quad \beta_2 = M_{13}, \quad \text{and} \quad \beta_3 = M_{12}, \quad (1.5.46)$$

where the M_{ij} are determined by the GL_3 gauge degrees of freedom as

$$M_{i,j} = \begin{vmatrix} D_{2i} & D_{2j} \\ D_{3i} & D_{3j} \end{vmatrix}. \quad (1.5.47)$$

The case for general split-helicity amplitudes follows the same pattern. We use the D_{ij} , $i, j = 1, \dots, n - 4$, as free gauge-fixing parameters. We solve for D_{ij} , $i = 2, \dots, n - 4$, $j = n - 3, \dots, n$ in terms of gauge-fixed parameters D_{ij} , $j = 1, \dots, n - 4$, and then solve for the D_{1j} , $j = n - 2, n - 1, n$ in terms of gauge fixing parameters D_{ij} , $j = 1, \dots, n - 4$,

and D_{1n-3} . Then, for each individual residue characterized by some vanishing minor (j), we determine D_{1n-3} , and substitute it back into other D_{1j} . We can then calculate all minors and Jacobian factors, and compare with the Risager expansion. Remarkably the two expressions agree using a Risager shift most nicely given in terms of a deformations of μ 's:

$$\beta_j = \begin{vmatrix} D_{2,1} & \dots & D_{2,j-1} & D_{2,j+1} & \dots & D_{2,n-4} \\ \vdots & \vdots & \vdots & \vdots & \vdots & \vdots \\ D_{n-4,1} & \dots & D_{n-4,j-1} & D_{n-4,j+1} & \dots & D_{n-4,n-4} \end{vmatrix}. \quad (1.5.48)$$

Again, the general pattern is that the deformations are constructed just from gauge-fixing parameters. This just demonstrates the fact that the freedom in choosing Risager deformations β_j is included in the GL_{k-2} redundancy in the Grassmannian.

1.6 Concluding Remarks

We have argued that a simple and canonical “ δ -relaxing” contour deformation takes us from the Grassmannian formulation of BCFW tree amplitudes—which has a remarkably “combinatorial” form making all symmetries manifest—to the CSW expansion, which manifests the local space-time Lagrangian in light-cone gauge. Relaxing a single δ -function already yields the full CSW expansion for NMHV amplitudes, and must lead to the Risager expansion for general k as we established for the $\overline{\text{MHV}}$ case. It would be interesting to see this more explicitly, and also to understand whether the recursive application of the Risager expansion leading to the CSW expansion has a natural interpretation in terms of relaxing multiple δ -functions.

The operation we have found gives a natural way of “blowing up” residues into components, separating pieces with a local space-time interpretation from the non-local ones. This allows us to give the sum over Grassmannian residues corresponding to the tree contour a “particle interpretation” in space-time. As we will see in [35], there is a second natural operation on the sum over residues—rather than blowing each residue up into many pieces, we can instead unify them together as the zero set of a single map. This manifests an even more surprising feature than a particle interpretation in space-time—the integral localizes on configurations with a “particle interpretation” *in the Grassmannian*, allowing us to construct higher-point tree amplitudes by “adding one particle at a time”

to lower-point ones. Furthermore, a natural deformation not simply of the contour but of the integrand itself directly connects our Grassmannian picture with the connected prescription [36] of Witten’s twistor string theory [4, 37–39].

We find it remarkable that almost all the concepts surrounding perturbative scattering amplitudes in this decade—the twistor string theory, CSW, BCFW and Risager recursion relations, infrared equations, leading singularities and dual superconformal invariance—are unified in the Grassmannian integral we have been exploring. The only important object that has yet to make a direct appearance in this story is the light-like Wilson loop (see e.g. [40–46])—making this connection will surely tell us how to extract loop-level information beyond the all-loop leading singularities that are already clearly present in the Grassmannian.

Chapter 2 *The Unification of Residues and Grassmannian Dualities*

2.1 Scattering Amplitudes and the Grassmannian

A new duality was conjectured in [10] between leading singularities of color-stripped n -particle N^{k-2} MHV amplitudes in $\mathcal{N} = 4$ SYM and a simple contour integral of the form

$$\mathcal{L}_{n,k}(\mathcal{W}_a) = \frac{1}{\text{vol}(GL_k)} \int \frac{d^{k \times n} C_{\alpha a} \prod_{\alpha=1}^k \delta^{4|\sum_{a=1}^n C_{\alpha a} \mathcal{W}_a|}}{(1\,2 \cdots k)(2\,3 \cdots k+1) \cdots (n\,1 \cdots k-1)}, \quad (2.1.1)$$

where the \mathcal{W}_a in the (ordinary) dual twistor space and carry all the information about the external particles. The integral is over $k \times n$ matrices $C_{\alpha a}$ modulo a GL_k -action on the right. This space is also known as the Grassmannian $G(k, n)$ —the space of configurations of k -planes in \mathbb{C}^n . The rows in the matrix $C_{\alpha a}$ define k n -vectors which together span a k -plane that contains the origin. Since GL_k -transformations simply reflect a change of basis for the k -plane, the action of GL_k must be modded-out. The formulation in (2.1.1) makes manifest that any object computed from $\mathcal{L}_{n,k}$ is superconformal invariant.

Fourier-transforming from dual twistors to ordinary momentum-space, one finds that

$$\begin{aligned} \mathcal{L}_{n,k} = \frac{1}{\text{vol}(GL_k)} \int \frac{d^{k \times n} C}{(1\,2 \cdots k)(2\,3 \cdots k+1) \cdots (n\,1 \cdots k-1)} \\ \times \prod_{\alpha=1}^k \delta^4(C_{\alpha a} \tilde{\eta}_a) \delta^2(C_{\alpha a} \tilde{\lambda}_a) \int d^2 \rho_\alpha \delta^2(\rho_\beta C_{\beta a} - \lambda_a). \end{aligned} \quad (2.1.2)$$

Gauge-fixing the GL_k -redundancy in such a way that k columns of the matrix $C_{\alpha a}$ make up the unit $k \times k$ matrix takes (2.1.2) into the link representation of [17]. This gauge-fixing makes parity manifest by making it equivalent to the obvious geometric statement that $G(k, n)$ is isomorphic to $G(n - k, n)$. The δ -functions in (2.1.2) restrict the integration to k -planes that contain the λ -plane and are orthogonal to the $\tilde{\lambda}$ -plane. Using a different gauge-fixing, one can make the first two rows of the C -matrix be identical to the two

n -vectors defining the λ -plane. A simple linear algebra argument together with a further gauge fixing that leaves a GL_{k-2} subgroup of GL_k unfixed reduces the integral to one over $(k-2)$ -planes in \mathbb{C}^n , i.e. , over $G(k-2, n)$ [18]. The resulting form, in terms of a $(k-2) \times n$ matrix D is given by [18, 19],

$$\mathcal{L}_{n,k} = \mathcal{A}_{\text{MHV}} \frac{1}{\text{vol}(GL_{k-2})} \int \frac{d^{(k-2) \times n} D \prod_{\hat{\alpha}=1}^{k-2} \delta^{4|4}(D_{\hat{\alpha}a} \mathcal{Z}_a)}{(1\ 2 \cdots k-2)(2\ 3 \cdots k-1) \cdots (n\ 1 \cdots k-3)}, \quad (2.1.3)$$

where \mathcal{A}_{MHV} is the tree-level MHV superamplitude which contains the momentum-conserving δ -function and its superpartner. The remaining integral is now defined in terms of what are called momentum-supertwistors \mathcal{Z}_a . These are the objects introduced by Hodges [20] in order to make *dual*-superconformal invariance [21, 40, 47, 48] manifest.

After all δ -functions in (2.1.2) are used, $\mathcal{L}_{n,k}$ becomes a contour integral in $(k-2)(n-k-2)$ variables. As usual with contour integrals, there is really no integral at all and we are interested in the residues. Each of these residues is simultaneously superconformal and dual-superconformal invariant, and is thus invariant under the full Yangian symmetry of the theory [8, 49]. Higher-dimensional analogues of Cauchy’s residue theorem encode highly non-trivial relations between these invariants. The residues give a basis for the leading singularities of all loop amplitudes. Evidence for this fact for up to two-loops was given in [10], and evidence to all orders has been recently given by [22, 23]. Tree-level amplitudes are known to be expressible as sums over one-loop leading singularities—via the BCFW recursion relations [7, 31] (see also, e.g., [50])—and therefore they become sums of residues of $\mathcal{L}_{n,k}$. This can be expressed by providing a contour of integration for $\mathcal{L}_{n,k}$ which we denote $\Gamma_{n,k}^{\mathcal{L}}$. Note that this contour is not uniquely defined, since residue theorems can be used to express the same sum in many different forms. We will nonetheless loosely refer to this equivalence class of contours as “the” contour.

The contour $\Gamma_{n,k}^{\mathcal{L}}$ must have a remarkable property. While the residues are all Yangian invariant, they do not individually have a local space-time interpretation; for instance, they are riddled with non-local poles. The non-local poles magically cancel in the sum over residues of $\Gamma_{n,k}$. In the previous Chapter 1, we showed that a natural contour deformation “blows up residues” into a sum over local and non-local terms, making the local spacetime description as manifest as possible by connecting to the light-cone gauge Lagrangian via the CSW/Risager [5, 6, 25–27] rules. In this chapter we discuss a natural

counterpart to this operation: instead of “blowing up” residues, we will see that there is a natural way of *unifying* them into a single algebraic variety. This will expose something perhaps even more surprising than the emergence of local space-time physics: we will see that the contour $\Gamma_{n,k}^{\mathcal{L}}$ can be thought of as localizing the integral over $G(k, n)$ to a sub-manifold with a “particle interpretation” *in the Grassmannian*. This allows us to construct higher-point tree amplitudes by simply “adding one particle at a time” to lower-point ones, with soft limits manifest. Furthermore, this unified form of the amplitude is intimately connected to CSW localization in twistor space, and—as we will see for N^2 MHV—is generally distinct from any contour derived using BCFW.

Having discovered the possibility of a particle interpretation in the Grassmannian, it is natural to ask whether there is a formulation that makes such an interpretation manifest while also keeping manifest cyclic invariance (which would not ordinarily be completely explicit in a picture which “adds one particle at a time”). This motivates us to start anew, keeping only the Grassmannian kinematics encoded in the δ -function factor $\delta^{4|4}(C_{\alpha a} \mathcal{W}_a)$. A simple counting argument leads us to an extremely natural way of implementing the Grassmannian particle interpretation: by integrating over a sub-manifold in the Grassmannian associated with the “Veronese map” from $G(2, n) \rightarrow G(k, n)$. The resulting object can be easily recognized as the connected prescription [52] for Witten’s twistor string theory [4] (see also [37–39, 53–63]; for a review, see [64]); indeed this discussion can be thought of as a physical motivation for and derivation of this theory from the Grassmannian viewpoint.

Cast as integrals over the Grassmannian, the integrand corresponding to our first discovery of the particle interpretation—motivated by realizing the contour $\Gamma_{n,k}^{\mathcal{L}}$ as a single algebraic variety—will not be the same as the second form, leading to the connected prescription for twistor string theory. In the simplest examples, one can use the global residue theorem (see e.g. [65]) to show that while the integrands are different, the contour integrals agree (see e.g. [66]). However, this way of establishing the equality requires some gymnastics; a significant insight into why this miracle can happen is obtained by noticing that the two integrands can be *smoothly deformed into each other* by introducing a deformation parameter t ; we demonstrate t -independence explicitly for both NMHV and N^2 MHV amplitudes. The equality between the objects must then be a consequence of a more general statement about amplitudes, which should follow from a simple residue

theorem. We identify this simple residue theorem for all NMHV amplitudes—it is the same as the “ δ -relaxing” deformation used in Chapter 1 to expose the CSW recursion relations.

The outline for this chapter is as follows. In the next two sections we give a general introduction to our two main themes. In section 2.4 we discuss the relationship between the two different kinds of Grassmannian particle interpretations we encounter. In section 2.5 we discuss NMHV tree amplitudes. In section 2.6 we move on to the N^2 MHV amplitudes, and in particular, give a detailed discussion of the 8-particle N^2 MHV amplitude. We end with brief concluding remarks in section 2.7.

2.2 Unification of Residues

We begin by returning to the momentum space formula for $\mathcal{L}_{n,k}$ given in equation (2.1.2). Gauge-fixing the GL_k -invariance, leaves $kn - k^2 = k(n - k)$ integration variables, and after imposing all $2n$ of the δ -functions, we end up with an overall momentum-conserving δ -function and an integral over $k(n - k) - (2n - 4) = (k - 2)(n - k - 2)$ variables. For brevity, we will denote this total number of integration variables by M ,

$$M \equiv (k - 2)(n - k - 2), \tag{2.2.1}$$

and denote the free variables by τ_1, \dots, τ_M . In the following, we strip-off all overall factors and concentrate on

$$\int d^M \tau \frac{1}{(1\ 2 \cdots k)(2\ 3 \cdots k+1) \cdots (n\ 1 \cdots k-1)(\tau)}. \tag{2.2.2}$$

This is a holomorphic integral—i.e. , it is over τ and not $\bar{\tau}$; therefore, it must be interpreted as a contour integral in M complex variables.

I. Local Residues

There is a very natural way of defining “local residues” for functions of M complex variables $\tau = (\tau_1, \dots, \tau_M)$. Consider a rational function of the form

$$f = \frac{g(\tau)}{p_1(\tau)p_2(\tau) \cdots p_N(\tau)} \tag{2.2.3}$$

where $N \geq M$. A residue is naturally associated with locations τ_* in τ space where M of the polynomial factors $p_{i_1}(\tau_*), \dots, p_{i_M}(\tau_*) = 0$. It is natural to re-write

$$f = \frac{h_{i_1, \dots, i_M}(\tau)}{p_{i_1}(\tau) \cdots p_{i_M}(\tau)} \quad \text{with} \quad h_{i_1, \dots, i_M}(\tau) = \frac{g(\tau_*)}{\prod_{j \neq i_1, \dots, i_M} p_j(\tau_*)}. \quad (2.2.4)$$

In the neighborhood of such a point we can change variables from $(p_{i_1}, \dots, p_{i_M}) \rightarrow (u_1, \dots, u_M)$, and up to a Jacobian, the integral becomes $\int du_1/u_1 \cdots du_M/u_M$, which is naturally defined to have residue 1. We denote the residue as $(p_{i_1})(p_{i_2}) \cdots (p_{i_M})$, given by

$$(p_{i_1})(p_{i_2}) \cdots (p_{i_M})|_{\tau_*} = \frac{h_{i_1, \dots, i_M}(\tau_*)}{\det \left(\frac{\partial(p_{i_1}, \dots, p_{i_M})}{\partial(\tau_1, \dots, \tau_M)} \right) (\tau_*)}. \quad (2.2.5)$$

Note that this definition of the residue depends on the order in which the polynomials enter in the Jacobian and is naturally antisymmetric in the labels: different orders can give answers which differ by a sign. This is a reflection of the fact that we were supposed to choose an orientation for the contour. The contour is in fact topologically a collection of circles $T^m = \{\tau : |p_i(\tau)| = \epsilon_i\}$ and the orientation that produces (2.2.5) is given by $d(\arg(p_{i_1})) \wedge \cdots \wedge d(\arg(p_{i_M}))$.

The NMHV tree amplitudes are given as a sum over these simple local residues. Consider the $n = 7$ NMHV amplitude. In [10], the BCFW-contour for the amplitude was found to be given as

$$\Gamma_{7,3}^{\mathcal{L}} = (2) [(3) + (5) + (7)] + (4) [(5) + (7)] + (6)(7). \quad (2.2.6)$$

Each term is of the form $(i)(j)$ with (i) representing the minor $(i \ i+1 \ i+2)$. The BCFW-contour for general NMHV amplitudes is of the form

$$\Gamma_{n,3}^{\mathcal{L}} = \sum \underbrace{(e_1)(o_2)(e_3) \cdots}_{n-5 \text{ terms}}, \quad (2.2.7)$$

where the sum is over all strictly-increasing series of $(n-5)$ alternating even (e) and odd (o) integers. Again, this form is not unique: as shown in [10]: using residue theorems one can exchange the role of even and odd integers in this sum in many ways—and this fact was important to the proof given in [10] of the cyclic-invariance of the entire contour.

For $k > 3$, it is clear that for large-enough n , the simplistic definition of a local residue described above is inadequate to localize the integrand: we have n minors, but

$(k - 2)(n - k - 2)$ variables, which exceeds n for any $k > 3$ for some sufficiently-large n . However, as explained in more detail in [10], our object allows for a more refined notion of “composite residue” which is applicable when there are fewer polynomial factors than there are variables. This allows residues to be defined for any n and k . A simple illustration of a composite residue is given by the function of three variables x, y, z ,

$$\frac{1}{x(x + yz)}. \tag{2.2.8}$$

Note that there are only two polynomial factors in the denominator, and so it is not possible to define a local residue in the standard way. Nonetheless, on the locus where the first polynomial factor vanishes, $x = 0$, the second polynomial factorizes as $y \cdot z$, and one should reasonably define this to have residue 1. Note that such a “composite” residue is only possible for very special functions: had we replaced the second polynomial factor with $(x + yz + a)$ for $a \neq 0$, no such identification would be possible. Geometrically, for $a = 0$, the set of points where both the polynomials vanish splits into two infinite families $(x = 0, y = 0, z)$ and $(x = 0, y, z = 0)$, and the point where the residue is defined is the intersection of these infinite families. As discussed in [10], exactly the same phenomenon happens with the minors of the $\mathcal{L}_{n,k}$: on the zeros of some of the minors, other minors factor into pieces, each of which can be individually set to zero to define composite residues. Already for the 8-point N²MHV-amplitude, some of the objects appearing the BFCW form of the tree amplitude are composite residues. Below, we will find a very natural way of thinking about composites that is a natural consequence of our new picture for unifying residues into a single variety: composite residues can be thought of as *ordinary* residues, but associated with putting minors made of *non-consecutive* columns to zero.

II. Tree-Amplitude Contours as Algebraic Varieties

The NMHV tree contour defined by $\Gamma_{n,3}^{\mathcal{L}}$ in (2.2.7) is perfectly clear as given. However, there is something somewhat unnatural about it: it is not precisely a “contour” in the sense used by mathematicians. The reason is that we haven’t presented the set of residues we are summing-over as a subset of the zeros of a *single* mapping from $\mathbb{C}^M \rightarrow \mathbb{C}^M$; in other words, we haven’t identified a fixed set of M polynomials (f_1, \dots, f_M) , such that the tree contour is contained in a subset of the solutions to $f_i = 0$. In fact for NMHV

amplitudes it is possible to do this for $n = 6, 7$, taking the f 's to be made of products of the consecutive minors appearing in the denominator of $\mathcal{L}_{n,k}$. However, already for $n = 8$, we'll see that it is impossible to do this using only *consecutive* minors. Thus, we seem to reach an impasse: from a mathematical point of view, it would clearly be natural to “glue” all the residues together as zeros of a single map—to think of the contour as a single algebraic variety. But the physical contour for tree amplitudes does not seem to admit such an interpretation.

However, we will see that it *is* possible to naturally unify the residues into a single variety—the apparent obstruction to doing so was merely a consequence of the myopia of only considering minors composed of consecutive columns of $C_{\alpha a}$.

By iteratively adding one particle at a time, we will soon see that the tree-level amplitude *can* be given in the form

$$\int_{\mathbf{f}=0} d^M \tau \frac{h(\tau)}{f_1(\tau) \cdots f_M(\tau)}, \quad (2.2.9)$$

where we sum over all the zeros of $\mathbf{f} \equiv (f_1, \dots, f_M) = 0$. Note that $h(\tau)$ is not just a polynomial, but a ratio of polynomials—otherwise this sum would vanish by the global residue theorem! The remarkable fact is that, as rational functions,

$$\frac{h}{f_1 \cdots f_m} = \frac{1}{(1\ 2 \cdots k)(2\ 3 \cdots k+1) \cdots (n\ 1 \cdots k-1)}, \quad (2.2.10)$$

but the numerator of h and f_1, \dots, f_M are polynomials *in the minors* of $C_{\alpha a}$ of degree larger than n , and all the non-consecutive minors appearing in the f_i 's are cancelled by those in the numerator of h . This is how they manage to encode the information about the contour.

For instance, we will show that *all* NMHV amplitudes can be written in the form

$$A_n^{(3)} = \int_{\mathbf{f}_n=0} \frac{\prod_{j=6}^{n-1} [(1\ 2\ j)(2\ 3\ j-1)]}{(n-1)(1)(3) f_6 \cdot f_7 \cdots f_n}, \quad (2.2.11)$$

where $\mathbf{f}_n = (f_6, \dots, f_n)$ and each $f_k : \mathbb{C} \rightarrow \mathbb{C}$ is given by the product of minors,

$$f_k = (k-2\ k-1\ k)(k\ 1\ 2)(2\ 3\ k-2). \quad (2.2.12)$$

Similarly, each N²MHV amplitude can be written as

$$A_n^{(4)} = \int_{\mathbf{f}_n=0} \frac{\prod_{j=7}^{n-1} [(1\ 2\ 3\ j)(2\ 3\ j-2\ j-1)(1\ j-2\ j-1\ j)] \prod_{j=4}^{n-3} [(1\ 3\ j\ j+1)(1\ 2\ j\ j+3)]}{(n-1)(1)(3) \mathcal{F}_7 \cdot \mathcal{F}_8 \cdots \mathcal{F}_n}, \quad (2.2.13)$$

where $\mathbf{f}_n \equiv (f_{7_a}, f_{7_b}, f_{8_a}, f_{8_b}, \dots, f_{n_a}, f_{n_b})$ with

$$\begin{aligned} f_{\ell_a} &\equiv (\ell-3 \ell-2 \ell-1 \ell)(\ell-3 \ell 1 2)(\ell-3 2 3 \ell-2); \\ \text{and } f_{\ell_b} &\equiv (1 \ell-2 \ell-1 \ell)(1 \ell 2 3)(1 3 \ell-3 \ell-2); \end{aligned} \tag{2.2.14}$$

and for which $\mathcal{F}_\ell \equiv f_{\ell_a} \cdot f_{\ell_b}$.

Note that as stated the definitions of h and f include minors built out of *non-consecutive* columns. We will see that their presence is crucial for allowing us to unify all the residues into a single algebraic-variety. As a by-product, they will also teach us how to think about “ordinary” and “composite” residues of $\mathcal{L}_{n,k}$ in a more uniform way, as “composite” residues can be understood as ordinary residues involving non-consecutive minors.

III. Manifest Soft-Limits and the Particle Interpretation

We motivated the gluing-together of tree-amplitude residues into a single variety from a mathematical point of view. There is also a physical reason to be dissatisfied with the usual way of presenting tree-amplitudes as a sum over disparate local residues: soft-limits of the amplitude would then not then manifest themselves as an obvious feature of the contour. Suppose we take the holomorphic soft-limit of particle n , where $\lambda_n \rightarrow 0$ while keeping $\tilde{\lambda}_n$ fixed. In this limit, the most singular part of the amplitude connects directly to the lower point amplitude with the usual multiplicative soft factor

$$A_n \rightarrow \frac{\langle n-1 \ 1 \rangle}{\langle n-1 \ n \rangle \langle n \ 1 \rangle} A_{n-1}. \tag{2.2.15}$$

This means that there must be a connection between $\Gamma_{n,k}^{\mathcal{L}}$ and $\Gamma_{n-1,k}^{\mathcal{L}}$; but this is not at all manifest for the NMHV tree contour given by equation (2.2.7). It is important to mention that from the mathematical point of view, the *inverse* operation is in fact more natural. In other words, it is more natural to think about the inclusion of $G(k, n-1)$ into $G(k, n)$ than to think about the projection of some contour in $G(k, n)$ down to $G(k, n-1)$. Indeed, in [24], we will show that there is a natural notion of an “inverse-soft” operation on individual residues, that maps a residue of $\mathcal{L}_{n,k-1}$ to a residue of $\mathcal{L}_{n,k}$. However what we are after here is a remarkable feature not of individual residues but of the way they are combined into $\Gamma_{n,k}^{\mathcal{L}}$.

Quite beautifully, the unification of residues in equation (2.2.10) allows us to think of the n -particle amplitude by “adding a particle” to the $(n - 1)$ -particle amplitude in a way that makes the soft-limits manifest. In fact, we can write

$$\frac{h_n}{f_1 \cdots f_{M_n}} = \frac{h_{n-1}}{f_1 \cdots f_{M_{n-1}}} \times \mathcal{S}_{(n-1) \rightarrow n} \quad (2.2.16)$$

and recursively build the contour for higher point amplitudes in this way. Furthermore, in the soft limit, $\lambda_n \rightarrow 0$, we find that (after an application of the global residue theorem) the τ integral localizes so that

$$\mathcal{S}_{(n-1) \rightarrow n} \rightarrow \frac{\langle n-1 \ 1 \rangle}{\langle n-1 \ n \rangle \langle n \ 1 \rangle}, \quad (2.2.17)$$

which precisely reproduces the needed soft factor!

IV. Connection to CSW Localization

The attentive reader may have noticed that the forms of f_i presented above for the NMHV and N²MHV amplitudes contain the product of three minors; moreover the denominator of h_n is the product of the three consecutive minors $(n-1)$, (1) and (3) . This is not an accident: these forms are intimately connected to localization of amplitudes on CSW configurations in twistor space! In order to understand why, let us begin by noting that it is natural to think of the matrix $C_{\alpha a}$ as a collection of n k -vectors, or n points in \mathbb{C}^k . In fact, due to the little group symmetry which rescales each column of $C_{\alpha a}$ independently, we can think of these points projectively as n points in \mathbb{CP}^{k-1} . Since the contour of integration is the variety where $\mathbf{f} = 0$, it is natural to ask whether there is anything special about the points in \mathbb{CP}^{k-1} for which \mathbf{f} vanishes? In fact, there is an even more interesting question, which we can best discuss with some new notation. Let us define the “expectation value” of some “operator” built out of minors of $C_{\alpha a}$, by

$$\langle \mathcal{O} \rangle = \int_{\mathbf{f}=0} \frac{h}{f_1 \cdots f_M} \mathcal{O}. \quad (2.2.18)$$

Note that with this definition, the amplitude itself is $\langle 1 \rangle$, and trivially $\langle f_i \rangle = 0$. However there are also other operators with vanishing expectation values. For instance, taking the operator to be the denominator of h_n , we find that $\langle (n-1)(1)(3) \rangle = 0$ as a consequence of the global residue theorem. One might ask whether there exists a different way of

writing the integral where all these vanishing expectation values are understood on the same footing trivially, as part of the definition of the contour of integration. In this case the answer is “yes”: the “ δ -relaxing” contour-deformation used in Chapter 1 does this. We see that this form of the amplitude makes a certain localization property of the amplitude manifest—associated with the vanishing “expectation value” of objects built out of the product of three minors. If we further use the (independently proven) information that the amplitude is cyclically invariant, we get a very large number of constraints, which we can loosely think of as localizing the integral in the Grassmannian.

Now, for $k \leq 4$, there is a very close connection between *localization in the Grassmannian* and *localization in (Z) twistor space*. In order to see this, it suffices to Fourier-transform the bosonic parts of the kinematical δ -functions $\delta^{4|4}(C_{\alpha a} \mathcal{W}_a)$ into the Z twistor space:

$$\prod_{\alpha} \delta^4(C_{\alpha a} \mathcal{W}_a) \rightarrow \int d^4 z^{\alpha} \prod_a \delta^4(Z_a - C_{\alpha a} z^{\alpha}). \quad (2.2.19)$$

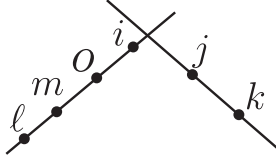
Note that for $k = 3$, the twistor space “collinearity operator” $\epsilon_{IJKL} Z_i^I Z_j^J Z_k^K$ acts on the amplitude as

$$(Z_i Z_j Z_k)^I A_n = \int d^4 z (z z z)^I \langle (i j k) \rangle. \quad (2.2.20)$$

We can think of the “localization in the Grassmannian” implied by $\langle (i j k) \rangle = 0$ as telling us that the points $\{i, j, k\}$ in the \mathbb{CP}^2 associated with the columns of $G(3, n)$ are (projectively) collinear. By virtue of equation (2.2.20) this tells us that this sense of localization in the Grassmannian is sharply reflected as localization in twistor space.

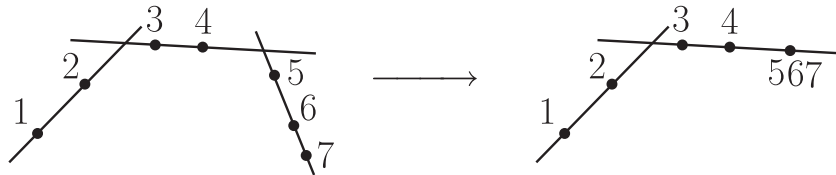
All of this is interesting because the set of twistor space collinearity operators that test for CSW localization precisely involve products of *three* of them—which translate to the vanishing expectation value for the product of three minors in the Grassmannian. It is very easy to see that for any configuration of n cyclically ordered points localized on two lines in \mathbb{CP}^2 , the product of three minors $(i x j)(k y l)(m z o)$ vanishes, where $i < x < j \leq k < y < l \leq m < z < o$. To prove it, let’s assume that the first two factors are not equal to zero, which means that $(i x j), (k y l)$ can not be collinear. This forces the points to be distributed on the two lines as in:

But then m, z, o are forced to be on the same line, and so the last factor $(m z o) = 0$. This shows why two minors are insufficient but three suffice. Furthermore, having sufficiently



many of the operators of this form vanish is enough to *guarantee* CSW-localization. Something similar is true for $k = 4$. Here the coplanarity operator $(Z_i Z_j Z_k Z_l)$ in twistor space maps to the 4×4 minor $(i j k l)$ in the Grassmannian. Perhaps a little surprisingly, collections of coplanarity operators suffice to ensure CSW-localization on lines. This can happen if the coplanarity conditions involve non-consecutive points.

For $k > 4$, it is in general difficult to find a set operators testing localization for CSW configurations of $(k - 1)$ intersecting lines in the \mathbb{CP}^3 of twistor space; the reason is that the \mathbb{CP}^3 is too “small”. It is however much easier to talk about localization to CSW-like configurations of $(k - 1)$ lines in \mathbb{CP}^{k-1} , and this is precisely the natural question associated with vanishing operator expectation values from the Grassmannian point of view! It is amusing to ask what “Grassmannian CSW” operators test for this Grassmannian notion of localization. It is easy to exhibit two large classes of such operators, always made from the products of three minors for any k . One class is similar to set we described for $k = 3$: the product of three $(k \times k)$ minors $(i \cdots j)(k \cdots l)(m \cdots n)$ vanishes for CSW-like configurations in \mathbb{CP}^{k-1} . Another class of operators can be easily constructed recursively. Given any configuration localized on lines in \mathbb{CP}^{k-1} , we can project down along one of the lines to get a another set of points (with some co-incident) localized on $(k - 2)$ lines in \mathbb{CP}^{k-2} , as shown below in an example with $k = 4$:



Since any particle I belongs to a unique line, by considering $(k \times k)$ minors that all include I , we are projecting-down along the line containing I to the problem in \mathbb{CP}^{k-2} . Thus the set of operators obtained by attaching column I to the ones just discussed—of the form $(I i \cdots j)(I k \cdots l)(I m \cdots o)$ —will also vanish on these configurations. Given that localization to “Grassmannian” CSW configurations implies localization on CSW configurations in twistor space, this strongly suggests that this “three-minor” form of the maps obtained in unifying tree amplitudes should persist for all k .

A very non-trivial check on this picture can be made by examining the simplest

amplitude with $k = 5$ —the split helicity 10-particle amplitude. There are 20 different BCFW terms in the amplitude, which can all be easily identified as residues of $\mathcal{L}_{10,5}$. We can test for localization in the Grassmannian by computing $\langle \mathcal{O}_{\text{CSW}} \rangle$ for the class of Grassmannian CSW operators we have just defined. Since we know the form of the C -matrix explicitly for each residue, this simply amounts to taking each BCFW term and multiplying it by the relevant product of three minors of its associated C -matrix. We have checked that the correct linear combination of twenty BCFW terms weighted with \mathcal{O}_{CSW} in this way indeed vanishes. Something even stronger is true: we checked that if we leave the coefficients of all 20 BCFW terms arbitrary, demanding that all the “localization on intersecting lines in \mathbb{CP}^4 ” operators annihilate the amplitude completely fixes the 20 terms up to a single overall scale. We will return to further investigate these fascinating issues at greater length in a future work.

2.3 Veronese Particle Interpretation

In the previous section, we discovered the particle interpretation and CSW localization of the tree amplitudes as a happy consequence of gluing together the residues of $\mathcal{L}_{n,k}$ contributing to the tree amplitude into a single variety. But the particle interpretation was not manifest from the outset—nor was the cyclic-invariance of the amplitude.

This motivates us to start anew, and construct a Grassmannian theory which makes the particle interpretation and cyclic-symmetry as manifest as possible. We will find that this straightforward exercise leads us essentially uniquely to the connected prescription [52] of Witten’s twistor string theory [4]. As an additional bonus, in addition to cyclic symmetry, this formulation will make the famous U_1 -decoupling identity manifest, which is a remarkable property of amplitudes that is only “obvious” from the Lagrangian point of view.

Going back to the beginning, the central object encoding “Grassmannian kinematics” are the twistor-space δ -functions which contain the only dependence on space-time variables $\prod_{\alpha} \delta^{4|4}(C_{\alpha a} \mathcal{W}_a)$. As seen recently in [22, 23], this factor alone goes a long way in explaining how the (non-trivial) kinematics of leading singularities can be encoded in $\mathcal{L}_{n,k}$, even without using any specific properties of the measure made from consecutive minors, so clearly we should stick with this structure. Transforming back to momentum

space it becomes

$$\prod_{\alpha} \delta^2(C_{\alpha a} \tilde{\lambda}_a) \delta^4(C_{\alpha a} \tilde{\eta}_a) \int d^{2 \times k} \rho^{\alpha} \prod_a \delta^2(\rho^{\alpha} C_{\alpha a} - \lambda_a). \quad (2.3.1)$$

The bosonic δ -functions impose $(2n - 4)$ constraints on $C_{\alpha a}$, enforcing the geometric constraint that the k -plane $C_{\alpha a}$ be orthogonal to the 2-plane $\tilde{\lambda}$ and contains the 2-plane λ . Now, in equation (2.1.2), in interpreting the integral over $G(k, n)$ as a contour integral, we place a further $(k - 2) \times (n - k - 2)$ constraints on $C_{\alpha a}$, which is equivalent to declaring that we are performing the integral over a $k \times (n - k) - (k - 2) \times (n - k - 2) = (2n - 4)$ -dimensional sub-manifold in $G(k, n)$. We can generalize this idea to define a whole class of “Grassmannian theories”, which enforce the “kinematic” constraints on the space-time variables associated with $\delta^{4|4}(C_{\alpha a} \mathcal{W}_a)$. We simply choose some $(2n - 4)$ dimensional subspace Σ of the Grassmannian, a general point of which we represent as $C_{\alpha a}^*(\zeta_I)$ for $I = 1, \dots, (2n - 4)$. Then we consider the object

$$\int_{\Sigma} d^{2n-4} \zeta \mu(\zeta) \prod_{\alpha} \delta^{4|4}(C_{\alpha a}^*(\zeta_I) \mathcal{W}_a), \quad (2.3.2)$$

where $\mu(\zeta)$ is a measure factor.

Now, of all such Grassmannian theories, there is a special class that we can motivate physically as having a “particle interpretation”. Ordinarily, the configuration space for n -particles is thought of as n copies of a given space on which each of the particles “live”. In order for a Grassmannian theory to have such a “particle interpretation”, then, we would like to loosely think of $\Sigma = (\Sigma_{\text{base}})^n$. Now, $\dim(\Sigma) = (2n - 4)$ (let us leave the -4 offset for a moment, and) note that at large n , the only way we can make such an identification is if $\dim(\Sigma_{\text{base}}) = 2$; and so the most natural choice is $\Sigma_{\text{base}} = \mathbb{C}^2$. The “ -4 ” can arise from a GL_2 -redundancy acting on \mathbb{C}^2 . We can therefore conclude that we are looking for a $(2n - 4)$ sub-manifold of the Grassmannian, that can be thought of as a mapping of $(\mathbb{C}^2)^n / GL_2$ into $G(k, n)$. It only remains to discuss how to determine this mapping from $(\mathbb{C}^2)^n / GL_2 \rightarrow G(k, n)$ explicitly.

Let us denote a general point in \mathbb{C}^2 by $\sigma = (A, B)$. It is natural to look for a mapping into a point we will denote by $\sigma^V(\sigma)$ in \mathbb{C}^k , such that the GL_2 -action on σ turns into some GL_k -action on σ^V . There is a canonical map from $\mathbb{C}^2 \rightarrow \mathbb{C}^k$, familiar from elementary

algebraic geometry which does this precisely and is known as the Veronese map:

$$\sigma : \begin{pmatrix} A \\ B \end{pmatrix} \rightarrow \begin{pmatrix} A^{k-1} \\ A^{k-2}B \\ \vdots \\ B^{k-1} \end{pmatrix} \equiv \sigma^V(\sigma). \quad (2.3.3)$$

We can assemble the n k -dimensional vectors σ_a^V , for $a = 1, \dots, n$, into the $k \times n$ dimensional matrix $C_{\alpha\alpha}^V[\sigma]$ which denotes the Veronese map from $(\mathbb{C}^2)^n/GL_2 \rightarrow G(k, n)$

$$C^V[\sigma] = \begin{pmatrix} \vdots & \vdots & \cdots & \vdots \\ \sigma^V[\sigma_1] & \sigma^V[\sigma_2] & \cdots & \sigma^V[\sigma_n] \\ \vdots & \vdots & \cdots & \vdots \end{pmatrix}; \quad (2.3.4)$$

or written more succinctly

$$C_{\alpha\alpha}^V[\sigma] = A_a^{k-\alpha} B_a^{\alpha-1}. \quad (2.3.5)$$

We group all the σ_a together into $2 \times n$ matrix which, given the GL_2 -action, we can think of as an element of $G(2, n)$. Thus we can also think of C^V as giving the Veronese map from $G(2, n) \rightarrow G(k, n)$.

I. Twistor String Theory

In order to complete our story and fully define a Grassmannian theory, we need to integrate over the two-dimensional vectors σ_a with a natural GL_2 -invariant measure. By analogy with the simple choice for the GL_k -invariant measure chosen in equation (2.1.2), the simplest possibility is to soak-up the GL_2 weights with a product of consecutive 2×2 minors and define

$$\mathcal{T}_{n,k}(\mathcal{W}) = \frac{1}{\text{vol}(GL_2)} \int \frac{d^2\sigma_1 \cdots d^2\sigma_n}{(\sigma_1\sigma_2)(\sigma_2\sigma_3) \cdots (\sigma_n\sigma_1)} \prod_{\alpha} \delta^{4|4}(C_{\alpha\alpha}^V[\sigma]\mathcal{W}_\alpha). \quad (2.3.6)$$

In the case of equation (2.1.2) for $\mathcal{L}_{n,k}$, the choice of measure with consecutive minors had much more than aesthetic benefits: only with this choice was it possible to prove the equivalence with equation (2.1.3) and establish dual superconformal invariance. Similarly, in the present case, the choice of measure with the product of the $(\sigma_i\sigma_{i+1})$ in the denominator makes a remarkable feature of scattering amplitudes manifest which

is normally only obvious from the spacetime Lagrangian. This property is the famous “ U_1 -decoupling identity”. While we normally talk about color-stripped amplitudes, in reality the full amplitude is given by a sum over permutations

$$\mathcal{A}_n = \sum_{P \in S_n / \mathbb{Z}_n} \text{Tr}(T^{a_{P(1)}} T^{a_{P(2)}} \dots T^{a_{P(n)}}) A(P(1), \dots, P(n)). \quad (2.3.7)$$

When the gauge group is taken to be any product of $SU(N_i)$ factors (including U_1 's), the Lagrangian description makes it obvious that the amplitude for producing particles in the adjoint of $SU(N_i)$ from $SU(N_j)$ -particles must vanish. This implies many relations among the partial amplitudes $A(P(1), \dots, P(n))$ with different orderings. The simplest of these relations is called the U_1 -decoupling identity, which is obtained when the gauge group is taken to be $U_n = U_1 \times SU_n$. Now, the dependence on the external spacetime variables in $\delta^{4|4}(C_{\alpha a}^V[\sigma] \mathcal{W}_a)$ is fully permutation-invariant; the only factor that breaks the permutation invariance down to cyclic invariance is the factor $(\sigma_1 \sigma_2)(\sigma_2 \sigma_3) \dots (\sigma_n \sigma_1)$, and it is trivial to see that this satisfies the identity necessary for $\mathcal{T}_{n,k}(\mathcal{W}_a)$ to satisfy the U_1 -decoupling identity.

We have motivated equation (2.3.6) as a beautiful way of writing a theory enforcing a Grassmannian “particle interpretation”. It is also nothing other than the connected prescription [52] for Witten’s twistor string theory [4] (see also [33] where the Grassmannian form of the twistor string theory is presented). To see this, we Fourier-transform from the \mathcal{W}_a to the \mathcal{Z}_a variables in order to return to Witten’s original setting:

$$\prod_{\alpha} \delta^{4|4}(C^V[\sigma]_{\alpha a} \mathcal{W}_a) \rightarrow \int d^{4|4} z^{(\alpha)} \prod_a \delta^{4|4}(\mathcal{Z}_a - C^V[\sigma]_{\alpha a} z^{(\alpha)}). \quad (2.3.8)$$

If we further write $\sigma_a = (A_a B_a) = \xi_a(1 \rho_a)$, the GL_2 -action has a GL_1 -rescaling the ξ and an SL_2 -symmetry acting on ρ , with (1ρ) being thought of as inhomogeneous co-ordinates on \mathbb{CP}^1 . Then, $(\sigma_i \sigma_{i+1}) = (\xi_i \xi_{i+1})(\rho_i - \rho_{i+1})$, and we have

$$\mathcal{T}_{n,k}(\mathcal{Z}_a) = \frac{1}{\text{vol}(GL_2)} \int \frac{d\rho_1 \dots d\rho_n}{(\rho_1 - \rho_2)(\rho_2 - \rho_3) \dots (\rho_n - \rho_1)} \prod_a \delta^{3|4}(\mathcal{Z}_a - \sum_{\alpha=0}^{k-1} z^{(\alpha)} \rho_a^{\alpha}), \quad (2.3.9)$$

where $\delta^{3|4}(\mathcal{Z} - \mathcal{Z}')$ is a projective δ -function in $\mathbb{CP}^{3|4}$:

$$\delta^{3|4}(\mathcal{Z} - \mathcal{Z}') = \int \frac{d\xi}{\xi} \delta^{4|4}(\mathcal{Z} - \xi \mathcal{Z}'). \quad (2.3.10)$$

Equation (2.3.9) is exactly the connected prescription for computing tree amplitudes from twistor string theory, integrating over the moduli space (parametrized by the $z^{(\alpha)}$)

of degree- $(k - 1)$ curves in $\mathbb{CP}^{3|4}$. However, notice that from the point of view of the Grassmannian, there is a more fundamental notion of localization: under the action of the little group, $\mathcal{W}_a \rightarrow t_a \mathcal{W}_a$, we have $C_{\alpha a} \rightarrow t_a^{-1} C_{\alpha a}$, and therefore we can think of each column of $C_{\alpha a}$ projectively as giving a point in \mathbb{CP}^{k-1} . The Veronese condition of equation (2.3.4) is then nothing but the statement that all these points in \mathbb{CP}^{k-1} lie on a degree- $(k - 1)$ mapping of $\mathbb{CP}^1 \rightarrow \mathbb{CP}^{k-1}$. This localization to degree- $(k - 1)$ curves in \mathbb{CP}^{k-1} associated with the Grassmannian implies, via equation (2.3.9), localization on degree- $(k - 1)$ curves in twistor space.

We can cast the expression for $\mathcal{T}_{n,k}$ in a form that will most directly facilitate a comparison with $\mathcal{L}_{n,k}$, by writing $\mathcal{T}_{n,k}$ as an integral over the full Grassmannian $G(k, n)$, with $(k - 2) \times (n - k - 2)$ δ -functions imposing the constraint that the k -planes have the Veronese form of equation (2.3.4) with a ‘‘particle interpretation’’. We do this by formally introducing ‘‘1’’ in the form

$$1 = \frac{1}{\text{vol}(GL_k)} \int d^{k \times n} C_{\alpha a} d^{k \times k} L_{\alpha}^{\beta} (\det L)^n \prod_{\alpha, a} \delta(C_{\alpha a} - L_{\alpha}^{\beta} C_{\beta a}^V[\sigma]); \quad (2.3.11)$$

here the integral over L_{α}^{β} is just one over all $k \times k$ linear transformations, and by gauge-fixing to $L_{\alpha}^{\beta} = \delta_{\alpha}^{\beta}$, we get ‘‘1’’ trivially.

We can then integrate over the σ_a , and we are left with

$$\mathcal{T}_{n,k}(\mathcal{W}_a) = \frac{1}{\text{vol}(GL_k)} \int d^{k \times n} C_{\alpha a} F(C) \delta^{4|4}(C_{\alpha a} \mathcal{W}_a), \quad (2.3.12)$$

where

$$F(C) = \frac{1}{\text{vol}(GL_2)} \int \frac{d^2 \sigma_1 \cdots d^2 \sigma_n}{(\sigma_1 \sigma_2)(\sigma_2 \sigma_3) \cdots (\sigma_n \sigma_1)} d^{k \times k} L_{\alpha}^{\beta} \prod_{\alpha, a} \delta(C_{\alpha a} - L_{\alpha}^{\beta} C_{\beta a}^V[\sigma]). \quad (2.3.13)$$

Clearly, by construction $F(C)$ will contain $(k - 2) \times (n - k - 2)$ δ -function factors localizing the integral over the C 's to have the Veronese form. Really these δ -functions are to be thought of holomorphically, in other words, we think of ‘‘ $\delta(x) \rightarrow 1/x$ ’’, where the contour of integration is forced to enclose $x = 0$ (see [51]). Therefore, $\mathcal{T}_{n,k}$ will have the form

$$\mathcal{T}_{n,k} = \frac{1}{\text{vol}(GL_k)} \int_{S_1 = \cdots = S_M = 0} d^{k \times n} C_{\alpha a} \frac{H(C)}{S_1(C) \cdots S_M(C)}. \quad (2.3.14)$$

We will call the $S(C)$'s ‘‘Veronese operators’’, whose vanishing is necessary for the matrix $C_{\alpha a}$ to be put into the Veronese form by some GL_k -transformation.

The first non-trivial example to study is the six-particle NMHV amplitude $n = 6, k = 3$; the computation was first presented in [37, 39], having gauge-fixed the GL_k -symmetry on the C 's in the “link representation” where k of the columns of $C_{\alpha a}$ are set to an orthonormal basis; it is very easy to translate these results in a general GL_k -invariant form, as has also been recently done in [66]. The result for $H(C)$ is

$$H(C) = \frac{(1\ 3\ 5)}{(1\ 2\ 3)(3\ 4\ 5)(5\ 6\ 1)} \quad (2.3.15)$$

while there is a single $S(C)$ given by

$$S(C) \equiv S_{123456}(C) = (1\ 2\ 3)(3\ 4\ 5)(5\ 6\ 1)(2\ 4\ 6) - (2\ 3\ 4)(4\ 5\ 6)(6\ 1\ 2)(3\ 5\ 1). \quad (2.3.16)$$

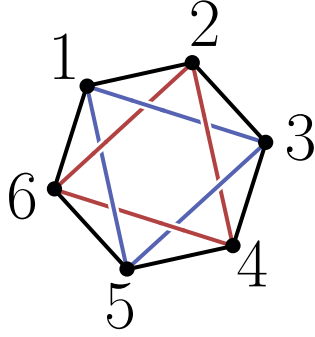
II. Veronese Operators for Conics

The object $S_{123456}(C)$ will play a fundamental role in the story of the connected prescription, so we pause to discuss its salient properties. For $n = 6, k = 3$, the Veronese condition is simply that 6 points on \mathbb{CP}^2 lie on a conic. Now, any 5 generic points determine a conic, and there is clearly a single constraint for a 6th additional point to lie on the conic determined by the first 5; this is what $S_{123456} = 0$ imposes. We can see that this is the constraint by looking at the form of the C^V matrix

$$C^V = \begin{pmatrix} 1 & \cdots & 1 \\ \rho_1 & \cdots & \rho_6 \\ \rho_1^2 & \cdots & \rho_6^2 \end{pmatrix}, \quad (2.3.17)$$

where we have used the little group freedom to rescale the elements of the first row to all be 1. Clearly, the Veronese condition should be GL_k -invariant, and hence we are looking for a relationship between the minors of $C_{\alpha a}$ that is a consequence of this special form. Note any 3×3 matrix made from columns of $C_{\alpha a}$ has the Vandermonde form and so the minors $(i\ j\ k)$ are very simple: $(i\ j\ k) = (\rho_i - \rho_j)(\rho_j - \rho_k)(\rho_k - \rho_i)$. In order to discover the relationship between minors implied by the Veronese condition in this case, examine the “star of David” figure below:

Each link in the figure connecting $(i\ j)$ represents a factor of $(\rho_i - \rho_j)$ (in cyclic order). We can interpret the product of the links $(1\ 2)(2\ 3)(1\ 3)$ in the figure as the minor $-(1\ 2\ 3)$, the product $(3\ 4)(4\ 5)(3\ 5)$ as $-(3\ 4\ 5)$, the product $(5\ 6)(6\ 1)(5\ 1)$ as $-(5\ 6\ 1)$, and the remaining links $(2\ 4)(4\ 6)(2\ 6) = -(2\ 4\ 6)$. Thus the product of all the links in the figure



is $(1\ 2\ 3)(3\ 4\ 5)(5\ 6\ 1)(2\ 4\ 6)$. However the picture is clearly cyclically invariant, so the product is also $(2\ 3\ 4)(4\ 5\ 6)(6\ 1\ 2)(1\ 3\ 5)$, and thus we have found the single relation we are looking for

$$S_{123456} = (1\ 2\ 3)(3\ 4\ 5)(5\ 6\ 1)(2\ 4\ 6) - (2\ 3\ 4)(4\ 5\ 6)(6\ 1\ 2)(3\ 5\ 1) = 0. \quad (2.3.18)$$

Clearly the condition that 6 points lie on a conic is invariant under the permutation of the points, so that if $S_{123456} = 0$, then $S_{P(1)P(2)\dots P(6)} = 0$ as well. In fact something even stronger is true. Even though it is not manifest, the object S_{123456} is permutation invariant in its labels (up to the sign of the order of the permutation); in other words,

$$S_{P(1)P(2)\dots P(6)} = (-1)^P S_{12\dots 6}. \quad (2.3.19)$$

It is trivial to see that S picks up a minus sign under a cyclic shift of the labels $i \rightarrow i + 1$, and it can be further checked that $S_{123456} = -S_{213456}$ as a simple consequence of the Schouten identity.

Let us move on to examine the 7-particle NMHV amplitude [37, 39, 66] where the integrand for \mathcal{T} is of the form

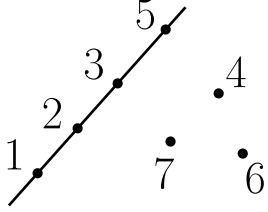
$$\frac{H(C)}{S_{123456} S_{123567}} \quad (2.3.20)$$

with

$$H(C) = \frac{(1\ 3\ 5)(6\ 1\ 2)(1\ 3\ 6)(2\ 3\ 5)}{(6\ 7\ 1)(1\ 2\ 3)(3\ 4\ 5)}. \quad (2.3.21)$$

Here the role of the two S 's in the denominator is clear. The 5 points $\{1, 2, 3, 5, 6\}$ determine a conic; $S_{123456} = 0$ enforces that the point 4 lies on this conic, while $S_{123567} = 0$ enforces that 7 lies on this conic; together they impose that all 7 points lie on the same conic. Actually there is a loophole in this argument, which nicely explains the role of the many factors in the numerator of $H(C)$. If the points $\{1, 2, 3, 5, 6\}$ lie on a *degenerate*

conic, it is possible for both S 's to vanish without having all 7 points on conic. For instance, suppose that any four of the points $\{1, 2, 3, 5, 6\}$ are collinear; this would make each S vanish trivially, even if the other three points are in general positions, for instance,



The numerator factors in $H(C)$ vanish on these “spurious” configurations and ensure that they don’t contribute to the integrand; in this example, this configuration is killed by the (235) factor in the numerator of H . It is easy to check that *all* spurious solutions are dispatched by factors in the numerator in this way.

For general NMHV amplitudes, we will have $(n-5)$ S 's. We stress that there are many equivalent ways of writing equation (2.3.14), using different collections of $(n-5)$ Veronese operators in the denominator to enforce that the n points lie on a conic. For instance, one canonical choice involves using a fixed set of 5 points $\{1, 2, 3, 4, 5\}$ to determine the conic, and then simply choosing the $(n-5)$ S 's to be S_{12345j} for $j = 6, \dots, n$. However, this is not the only possibility; all that is needed is for the labels of the S 's to overlap sufficiently to guarantee all n points to lie on the same conic; but we will find other choices to be more natural for our purposes.

III. General Veronese Operators

Moving beyond NMHV amplitudes, we must encounter Veronese operators that enforce n points to live on a degree- $(k-1)$ curve in $\mathbb{C}\mathbb{P}^{k-1}$. The conditions must again be GL_k -invariant and must therefore be written in terms of $k \times k$ minors. Fortunately, it is very easy to see that the conditions are always a collection of constraints of exactly the same form as $S_{123456} = 0$, involving the difference of the product of 4 minors. Physically this is because we can use parity to relate the Veronese conditions for (n, k) to those for $(n, n-k)$. It is illuminating to see this explicitly, since it also allows us to make contact with the work of [37]. Parity is manifest in the link representation, so let us study what the Veronese C^V matrices look like in this representation. Suppose we gauge-fix the

first k columns to the $k \times k$ identity matrix, and denote the remaining entries as c_{iI} for $i = 1, \dots, k$ and $I = k + 1, \dots, n$. Instead of finding the explicit GL_k transformation that takes the C^V matrix to this form, we can note that the c_{iI} can be written in a GL_k -invariant way as the ratio of two minors:

$$c_{iI} = \frac{(12 \cdots \widehat{i} \cdots kI)}{(12 \cdots k)}, \quad (2.3.22)$$

where in the numerator \widehat{i} denotes that the column i is not included. Since this ratio is GL_k -invariant, we can compute it directly for the form C^V , easily finding

$$c_{iI} = \frac{\kappa_I}{\kappa_i} \frac{1}{\rho_I - \rho_i} \quad (2.3.23)$$

where

$$\kappa_I = \prod_{j=1}^k (\rho_I - \rho_j), \quad \kappa_i = \prod_{j \neq i=1}^k (\rho_i - \rho_j). \quad (2.3.24)$$

So the Veronese operators must check whether the $k \times (n - k)$ variables c_{iI} can be expressed in the form of equation (2.3.22) [37, 39]. As discussed in [37], equation (2.3.22) is equivalent to demanding that the $k \times (n - k)$ matrix with entries c_{iI}^{-1} has rank two, which is equivalent to demanding that all 3×3 sub-determinants of this matrix vanish, giving rise to conditions on the c_{iI} which are sextic polynomials in the variables. However even without examining these conditions in detail, it is clear the conditions are the same swapping the matrix c_{iI} with its transpose, which is the statement of $G(k, n) = G(n - k, n)$ (i.e. parity). Now, under parity, a given $k \times k$ minor $(m_1 m_2 \cdots m_k)$ of $G(k, n)$ is mapped to its complement $\overline{(m_1 \cdots m_k)}$ in $G(n - k, n)$, where the $\overline{(\quad)}$ denotes that the $(n - k)$ columns that are *not* m_1, \dots, m_k are used. Explicitly,

$$\overline{(m_1 \cdots m_k)} = \epsilon_{m_1 \cdots m_k l_1 \cdots l_{n-k}} (l_1 \cdots l_{n-k}). \quad (2.3.25)$$

Thus, we see that written in a GL_k -invariant way, the $(k - 2) \times (n - k - 2)$ Veronese conditions for some (n, k) are equivalent to the same number of conditions for $(n, n - k)$ replacing the $k \times k$ minors with their complements. For instance, consider the case $k = 4$, where the Veronese operators check whether points lie on the degree-3 curve known as the twisted cubic. (This has been known for a long time—see, e.g. [67]). Any 6 generic points define a twisted cubic. For 7 points, the case with $k = 4$ is the same as

$k = 3$ that we have already studied: the condition for 7 points to be on a conic can be written as, e.g., $S_{123456} = 0, S_{123567} = 0$; so to get the condition for 7 points to lie on a twisted cubic we may just take the parity conjugate—i.e. replace the factor (123) with $\overline{(123)} = (4567)$ and so on. This gives us the pair of conditions for 7 points to lie on the twisted cubic determined by the first 6. But then we can use this pair of conditions to test that any number of further points lie on the twisted cubic. In general, for any k , any $k + 2$ points like on the degree- k curve, and we can determine the conditions for $(k + 3)$ points to lie on that curve by looking at the parity conjugate case where $(k + 3)$ points must lie on a conic. These are $(k + 3 - 5) = (k - 2)$ conditions of the form $S_{i_1 \dots i_6} = 0$, which we can translate to the original value of k by replacing 3×3 minor with its $[(k + 3) - 3] \times [(k + 3) - 3] = k \times k$ complement. Having determined these $(k - 2)$ conditions for $(k + 3)$ particles to lie on the degree- k curve, we get a total of $(n - (k + 3) + 1) \times (k - 2) = (k - 2) \times (n - k - 2)$ conditions for checking that all n points lie on the curve.

From this discussion, we may conclude that a manifestly GL_k -invariant Grassmannian formulation of the connected prescription for twistor string theory will necessarily involve a denominator with $(k - 2) \times (n - k - 2)$ S 's, each of which is given as the difference of a product of four minors.

2.4 Deformation and Duality

We have now seen two apparently quite different formulations of Grassmannian theories with a particle interpretation. The first was motivated by unifying the residues of $\mathcal{L}_{n,k}$ contributing to the tree amplitude into a single algebraic variety, which allowed us to think about adding particles one at a time to construct higher-point amplitudes while keeping the Yangian symmetry manifest. The cyclic invariance of this object is not completely manifest, although at least for NMHV amplitude, the cyclic invariance of the amplitude obtained from $\Gamma^{\mathcal{L}}$ follows straightforwardly from residue theorems. Finally, the U_1 -decoupling identity is not manifest at all.

One might like to see the cyclic symmetry and U_1 -decoupling identities in a much more manifest way. This is what the connected prescription for twistor string theory accomplishes beautifully, by showing that the amplitude is *almost* permutation invariant,

only breaking down to cyclic invariance because of the “MHV” factor on the worldsheet $\frac{1}{(\sigma_1\sigma_2)\cdots(\sigma_n\sigma_1)}$. The price is that dual superconformal invariance is not manifest.

Despite appearances, the remarkable statement is that the amplitudes computed in these two apparently very different ways should agree:

$$\mathcal{T}_{n,k} = \mathcal{L}_{n,k}^{\Gamma\mathcal{C}}. \quad (2.4.1)$$

We would like to understand why this miracle can happen, beginning with the NMHV amplitudes. It is a good start that both forms are written as integrals over a single variety—but to go further in making the comparison, we need to deal with the problem that the maps f_k involve the product of *three* minors while the Veronese operators involve the product of *four* minors. Clearly we need to find a modified form of the f_k , which involves a fourth minor. We can also motivate the need for finding a modified form of the f_k 's with a fourth minor in another way. Since we will soon be interested in deforming the f_k , in order to have a consistent behavior under the scaling of each column vector of the matrix $C_{\alpha a}$ —i.e. under little group rescalings—we have to deform each component of the map $f_k = (k-2 \ k-1 \ k)(k \ 1 \ 2)(2 \ 3 \ k-2)$ by something that preserves the original scaling. Note that it is impossible to *add* a polynomial in the minors to f_k to achieve this. However, we can modify each f_k as follows

$$f_k^{\text{modif}} = (k-2 \ k-1 \ k)(k \ 1 \ 2)(2 \ 3 \ k-2)(1 \ 3 \ k-1). \quad (2.4.2)$$

By doing this we can deform it while keeping the map holomorphic. The reader might worry about the fact that the new factor $(1 \ 3 \ k-1)$ has introduced new poles. It is not hard to show that if h_n is modified as

$$h_n^{\text{modif}} = \frac{\prod_{j=6}^{n-1} [(1 \ 2 \ j)(2 \ 3 \ j-1)] \prod_{\ell=5}^{n-1} (1 \ 3 \ \ell)}{(n-1)(1)(3)}, \quad (2.4.3)$$

then the proof presented in section III. is not affected.

Even more surprising is the fact that in the new form, f_k^{modif} admits *a continuous family of deformations* in such a way that the amplitude is independent of the deformation parameter! Let us denote the deformed f_k^{modif} by $S_k(t_k)$ in anticipation to the connection with the twistor string. More precisely, the deformation we would like to perform is the following

$$\begin{aligned} S_k(t_k) = & \quad (k-2 \ k-1 \ k)(k \ 1 \ 2)(2 \ 3 \ k-2)(k-1 \ 1 \ 3) \\ & - t_k(k-1 \ k \ 1)(1 \ 2 \ 3)(3 \ k-2 \ k-1)(k \ 2 \ k-2), \end{aligned} \quad (2.4.4)$$

where t_k is a real parameter (the restriction of reality is to ensure that for generic λ 's and $\tilde{\lambda}$'s, no pole of the form $1/(i \ i+1 \ i+2)$ will be hit by any of the $S_k(t_k)$). (The minus sign in (2.4.4) is introduced for later convenience.)

Let us denote the family of maps $\mathbf{S}_t \equiv (S_6(t_6), \dots, S_n(t_n))$. In a moment, we will show that the contour integral

$$\int_{\mathbf{S}_t} d^{n-5} \tau \frac{H_n}{S_6(t_6) S_7(t_7) \cdots S_n(t_n)} \quad (2.4.5)$$

is t -independent using a contour deformation and global residue theorems. Here, $H_n = h_n^{\text{modif}}$. When $t_k = 1$, $S_k(1)$ becomes the Veronese operator checking the localization of the six points $\{k-2, k-1, k, 1, 2, 3\}$ on a conic in \mathbb{CP}^2 , but lacks any convenient geometric interpretation for $t \neq 0$.

We have checked by explicitly computing the factor $F(C)$ from equation (2.3.13), along the lines of the computations in [37, 39], that choosing these Veronese operators to appear in the holomorphic δ -functions, the numerator factor $H(C)$ precisely coincides with $h(C)$. Thus, t -independence proves the equality of $\mathcal{T}_{n,3}$ and $\mathcal{L}_{n,3}$ equipped with contour $\Gamma_{n,3}^{\mathcal{L}}$. As we already remarked, this establishes that the amplitude satisfies the remarkable U_1 -decoupling identity.

It only remains to prove the t -independence of the amplitude, which follows from a straightforward argument using the observations of Chapter 1. Using the notation of Chapter 1, we think of one of the δ -function factors as a pole $\frac{1}{d}$, and we use the global residue theorem grouping with the $(n-5)+1$ polynomial factors being the $(n-5)$ f_i 's, together with the remaining three minors in the denominator and d , $(n-1)(1)(3)d$, for the last polynomial. Now, as in Chapter 1, we deform the pole away from $d = 0$, getting a sum over terms setting $(1) = 0$, $(3) = 0$ and $(n-1) = 0$. Now, in all of our deformations, the coefficient of t contains a factor $(1 \ 2 \ 3)$, so the term with $(1) = 0$ kills the t -dependence of all these terms and is trivially t -independent. The terms with $(n-1) = 0$ and $(3) = 0$ make t -independent the first and the last of the f 's respectively, and are seen to be t -independent by induction, down to the $n = 6$ case which is trivially seen to be t -independent. Note that this argument can also be thought of as a direct contour-deformation argument relating the connected prescription of the twistor string theory to the disconnected prescription given by the CSW rules!

Note that even without this explicit argument, the form of the connected prescription

given by equation (2.4.5) (at $t_k = 1$) betrays its connection to CSW. The reason is the presence of the product of three minors $(n-1)(1)(3)$ in the denominator of H_n : the global residue theorem tells us that $\langle (n-1)(1)(3) \rangle = 0$, where the “expectation value” is here defined with the integrand of the connected prescription. But this is a CSW operator! Furthermore, since the twistor string starting point is manifestly cyclically invariant, we must have have that $\langle (i-2)(i)(i+2) \rangle = 0$ for all i . This is a much stronger constraint than the vanishing of the Veronese operators, and is the way the connected prescription alerts us to CSW localization.

For general k , we expect a similar analysis to hold. Each of the f_i can be modified to be written as a product of 4 minors in the form

$$f_i^{\text{modif}} = M_1^i M_2^i M_3^i M_4^i . \quad (2.4.6)$$

We can now consider deformation by a parameter t_i of the form

$$f_i(t) = M_1^i M_2^i M_3^i M_4^i - t_i M_1^{i'} M_2^{i'} M_3^{i'} M_4^{i'} \quad (2.4.7)$$

and at $t_i = 1$, this deformed f_i coincides precisely with Veronese operators S_i

$$S_i = M_1^i M_2^i M_3^i M_4^i - M_1^{i'} M_2^{i'} M_3^{i'} M_4^{i'} . \quad (2.4.8)$$

Furthermore, for this choice of Veronese operators, the numerator factors in the two forms should become identical

$$h(C) = H(C). \quad (2.4.9)$$

In our discussion of N^2 MHV amplitudes, we will present very strong evidence supporting this claim with direct verification through the 10-point amplitude. Given this remarkable fact, it is very natural to look for a generalization of the very simple contour deformation argument we gave for NMHV amplitudes to establish the t -independence of the amplitude.

Assuming that the argument holds for all n and k , we find not only a duality between $\mathcal{T}_{n,k}$ and $\mathcal{L}_{n,k}$ equipped with $\Gamma_{n,k}^{\mathcal{L}}$, but equality for an infinite class of theories labeled by the continuous parameter t . In a whimsical sense, we might think of t as representing an “RG” flow. In this analogy the $\mathcal{L}_{n,k}$ description at $t = 0$ is the “ultraviolet” theory, with the individual residues being the “gluons”, with all symmetries manifest, while the $\mathcal{T}_{n,k}$

description is the “infrared” picture with the unified residues combined into “hadrons”, where the “macroscopic” properties of the collection of residues—the cyclic symmetries and U_1 -decoupling identities—are manifest.

2.5 NMHV Amplitudes

Having described the central ideas of this chapter in general terms, we turn to examining them in detail for the simplest non-trivial case of NMHV amplitudes. We will begin by showing the sum over residues with the even/odd/even structure of given by $\Gamma^{\mathcal{L}}$ in equation (2.2.7) can be unified into a single variety in a natural way. We will then show that this ansatz can be t -deformed to the amplitude computed from the connected prescription for twistor string theory. We end the section by comparing these two ways of unifying the residues into a single variety.

Let’s start by explicitly constructing a holomorphic map $\mathbf{f}_n : \mathbb{C}^{n-5} \rightarrow \mathbb{C}^{n-5}$ defined in terms of $n - 5$ polynomials $\mathbf{f} \equiv (f_6, \dots, f_n)$ and a function h_n , such the tree level amplitude is given as

$$A_n^{(3)} = \int_{\mathbf{f}_n=0} d^{n-5}\tau \frac{h_n}{f_6 \cdot f_7 \cdots f_n}. \quad (2.5.1)$$

The reason for the offset in the labeling of the polynomials f_i will become clear below. The construction is such that taken as rational functions one has,

$$\frac{h_n}{f_6 \cdot f_7 \cdots f_n} = \frac{1}{(1\ 2\ 3)(2\ 3\ 4) \cdots (n\ 1\ 2)}. \quad (2.5.2)$$

It is natural to try to construct the map f from consecutive minors as those are the ones that enter in (2.5.2). However, it is easy to see that for $n \geq 8$ it is impossible to construct a holomorphic map from consecutive minors such that the contour given in [10] is contained in the set of zeros of the map. It is instructive to see the obstruction already for $n = 8$. The contour $\Gamma_{8,3}^{\mathcal{L}}$ is given by

$$\begin{aligned} \Gamma_{8,3}^{\mathcal{L}} = & (1)(2) [(3) + (5) + (7)] + (3)(4) [(5) + (7)] + (5)(6)(7) \\ & + (1)(4) [(5) + (7)] \quad + (3)(6)(7) \\ & + (1)(6)(7). \end{aligned} \quad (2.5.3)$$

Let's try to construct a mapping $\mathbf{f}_8 : \mathbb{C}^3 \rightarrow \mathbb{C}^3$, with f_i polynomials in the minors (k). Consider the terms (1)(2)(3), (1)(4)(5) and (3)(4)(5). From the first term we learn that (1) and (3) must belong to different f_i 's, while combining the information from the second and third we learn that (1) and (3) must be on the same f_i , which is a contradiction.

Having seen the need for a different way to construct \mathbf{f}_n we now show that the construction is very natural and recursive. The reason it is recursive has a beautiful physical interpretation: it is equivalent to the operation of adding one particle at a time!

In order to motivate the construction, consider first the six-particle amplitude. (In this section, k is always 3 and will therefore be frequently suppressed). The contour given in [10] is $\Gamma_{6,3}^{\mathcal{L}} = (234) + (456) + (612)$. By this we mean three terms, the first of which is

$$\int_{(234)=0} d\tau \frac{1}{(123)(234)(345)(456)(561)(612)}. \quad (2.5.4)$$

Clearly, if we define the map $f_6 : \mathbb{C} \rightarrow \mathbb{C}$ as $f_6 = (234)(456)(612)$, then

$$A_6^{(3)} = \int_{f_6=0} d\tau \frac{h_6(\tau)}{f_6(\tau)} \quad (2.5.5)$$

with $h_6 = 1/(123)(345)(561)$.

In order to find a recursive way of constructing the map for all n , let us consider the five particle integrand,

$$\frac{1}{(123)(234)(345)(451)(512)}, \quad (2.5.6)$$

and ask what factor would convert this into the six-particle integrand. Clearly,

$$\mathcal{S}_{5 \rightarrow 6}^{k=3} = \frac{1}{(561)} \times \frac{(451)(512)(234)}{f_6}, \quad (2.5.7)$$

where $f_6 = (456)(612)(234)$, does what is needed. It might be puzzling at first why we introduced (234) both in the numerator and in the denominator. The reason for this is clear from the previous discussion. Recall that we have to define h_6 and f_6 independently. Multiplying (2.5.6) by $\mathcal{S}_{5 \rightarrow 6}$ we immediately find h_6 .

We interpret the operation of multiplying by $\mathcal{S}_{5 \rightarrow 6}$ as that of adding particle six to the five-particle amplitude. We will see that this interpretation is justified when we show that in general this corresponds to building an object with the right holomorphic soft-limit.

I. Recursive Construction

From the six-particle example, we are motivated to construct the n -particle amplitude recursively as follows. Let $\mathbf{f}_{(n-1)} : \mathbb{C}^{n-6} \rightarrow \mathbb{C}^{n-6}$ be the holomorphic map and h_{n-1} the meromorphic function such that

$$A_n^{(3)} = \int_{\mathbf{f}_{(n-1)}=0} d^{n-6}\tau \frac{h_{n-6}}{f_6 f_7 \cdots f_{n-1}}. \quad (2.5.8)$$

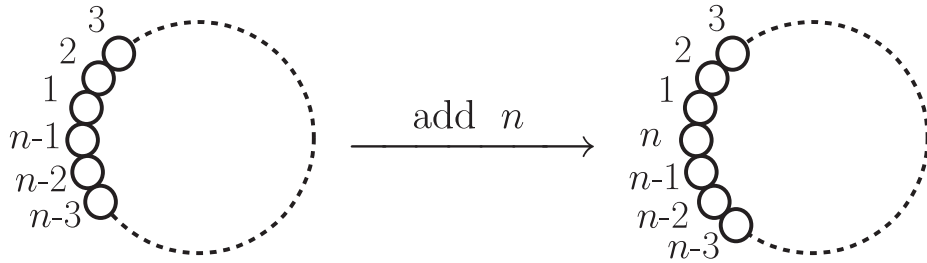
Then the n -particle amplitude is obtained by “multiplying” the integrand by

$$\mathcal{S}_{(n-1) \rightarrow n} = \frac{1}{(n-1 \ n \ 1)} \times \frac{(n-2 \ n-1 \ 1)(n-1 \ 1 \ 2)(2 \ 3 \ n-2)}{f_n} \quad (2.5.9)$$

with $f_n = (n-2 \ n-1 \ n)(n \ 1 \ 2)(2 \ 3 \ n-2)$. By “multiplying” we mean extending the map $(f_6, f_7, \dots, f_{n-1})$ to a map $\mathbf{f}_n : \mathbb{C}^{n-5} \rightarrow \mathbb{C}^{n-5}$ by adding f_n as the last component—i.e., forming $\mathbf{f}_n = (f_6, f_7, \dots, f_{n-1}, f_n)$. Likewise, we have a new h_n given by

$$h_n = h_{n-1} \frac{(n-2 \ n-1 \ 1)(n-1 \ 1 \ 2)(2 \ 3 \ n-2)}{(n-1 \ n \ 1)}. \quad (2.5.10)$$

Note that what we are doing can be interpreted as adding the particle n between $(n-1)$ and 1:



Given that we are dealing with 3×3 minors for NMHV amplitudes, it is reasonable that the “add particle n ” operation could involve particles $(n-3)$ up to 3. There are a number of choices we could make for how to do this, but the one we have presented accomplishes the task of unifying the residues in the nicest way that also manifests a number of important properties that we will discuss at greater length at the end of this section.

II. The $n = 7, 8$ Amplitudes

For now, let us show how this construction works explicitly for $n = 7$ and $n = 8$. The seven particle NMHV contour is given by

$$\Gamma_{7,3}^{\mathcal{L}} = (2) [(3) + (5) + (7)] + (4) [(5) + (7)] + (6)(7). \quad (2.5.11)$$

Using the recursive construction, we multiply the six-particle h_6/f_6 by

$$\mathcal{S}_{6 \rightarrow 7} = \frac{1}{(671)} \times \frac{(561)(612)(235)}{f_7} \quad (2.5.12)$$

with $f_7 = (567)(712)(235)$.

Putting everything together we find the seven-particle amplitude to be

$$A_7^{(3)} = \int_{\mathbf{f}_7=0} d^2\tau \frac{h_7(\tau)}{f_6(\tau)f_7(\tau)} \quad \text{with} \quad h_7(\tau) = \frac{(612)(235)}{(671)(123)(345)}, \quad (2.5.13)$$

while the map $\mathbf{f}_7 = (f_6, f_7)$ where,

$$f_6(\tau) = (234)(456)(612) \quad \text{and} \quad f_7(\tau) = (567)(712)(235). \quad (2.5.14)$$

The claim is that the tree-level contour is nothing but the sum over the residues of all the 9 zeros of \mathbf{f}_7 . At first sight this might seem surprising because by naïvely simplifying $h_7/(f_6 f_7)$ one would find the original object

$$\frac{1}{(123)(234)(345)(456)(567)(671)(712)}, \quad (2.5.15)$$

integrated over $[(2) + (4)][(5) + (7)]$. This only gives four terms of the six terms in (2.5.11) and therefore it cannot be the correct amplitude. The resolution to this naïve puzzle is that we should not cancel terms and forget about them! Recall that the map \mathbf{f}_7 is independent of the function h and we are supposed to carefully study all 9 residues. It turns out that only six are nonzero, and these add up to the amplitude. Among the six, four of them are the ones we got from the naïve analysis. Let us present the other two.

The first term missed in the naïve cancelation is the residue at the point located where $(234) = 0$ and $(235) = 0$. Note that (235) is also a factor in the numerator, and this is why naïvely may not be expected to contribute. The reason it does contribute is that when we impose the condition that the points 2, 3, 5 be (projectively) collinear and points 2, 3, 4 be collinear, it follows that 3, 4, 5 must also be collinear, and hence

$(345) = 0$. But (345) is a factor in the denominator of h_7 and therefore is a pole with non-vanishing residue. In order to compute the residue in these cases we will use the following simple result: given linear polynomials, A, B and C in two variables, such that $C = 0$ when $A = B = 0$ one has the identity

$$\int_{|A|=\epsilon_1, |B|=\epsilon_2} d^2\tau \frac{A}{ABC} = \int_{|B|=\epsilon_1, |C|=\epsilon_2} d^2\tau \frac{A}{ABC} = \int_{|B|=\epsilon_1, |C|=\epsilon_2} d^2\tau \frac{1}{BC}, \quad (2.5.16)$$

for any ϵ_1 and ϵ_2 arbitrarily small. This means that what we called the residue at $A = B = 0$ is the same as the residue at $B = C = 0$.

Using the identity we find that the pole at $(234) = (235) = 0$ can also be thought of as a pole at $(234) = (345) = 0$. Canceling (235) in the numerator and the denominator we find that it is what we call residue $(2)(3)$.

The second term is at $(612) = (712) = 0$. At this point we also have $(671) = 0$ which is a pole of h_7 . Using the same identity one finds the residue $(6)(7)$.

All other remaining 3 out of the original 9 residues vanish due to the factors in the numerator as they do not set any other factors in the poles h_7 to zero.

Putting together the first four terms we found in the naïve analysis plus the two new terms we find (2.5.11),

$$(2) [(3) + (5) + (7)] + (4) [(5) + (7)] + (6)(7). \quad (2.5.17)$$

Aside: A Subtlety in the Use of the Global Residue Theorem

Before continuing on to the eight particle example, it is important to discuss a subtlety which appears in the application of the global residue theorem (GRT) to residue integrals of the sort we are dealing with. In fact, as we will illustrate for the seven particle example, a naïve application of the global residue theorem leads to a contradiction. Let us recall that the global residue theorem asserts that given a holomorphic map $f : \mathbb{C}^m \rightarrow \mathbb{C}^n$ with $m \leq n$ and a holomorphic function s in \mathbb{C}^m , then for any way of constructing a map $g : \mathbb{C}^m \rightarrow \mathbb{C}^m$ by combining several f_i 's into single g_i 's such that g only has isolated zeros then

$$\sum_{p \in g^{-1}(0)} \int_{T_p^m} d^m\tau \frac{s(\tau)}{f_1(\tau) \cdots f_m(\tau) f_{m+1}(\tau) \cdots f_n(\tau)} = 0 \quad (2.5.18)$$

where the sum is over all zeros of g and the contour T_p^m is defined by translating $p \in \mathbb{C}^m$ to the origin and having $|g_i| = \epsilon_i$ with ϵ_i a sufficiently small positive real number. The theorem holds provided there is no contribution at infinity, which is true when $\deg s \leq \sum_{i=1}^m \deg g_i - (m+1)$. Suppose that the i^{th} component of g is given by $g_i = f_k f_l$ for some k and l . Using (2.5.18) one could conclude that

$$\sum_{p \in \Gamma_k} \int_{T_p^m} d^m \tau \frac{s(\tau)}{f_1(\tau) \cdots f_n(\tau)} = - \sum_{p \in \Gamma_l} \int_{T_p^m} d^m \tau \frac{s(\tau)}{f_1(\tau) \cdots f_n(\tau)}, \quad (2.5.19)$$

where Γ_k (or by Γ_l) are the zeros of the map g where g_i is replaced by f_k (or by f_l). In one complex dimension this is the usual way Cauchy's theorem is applied. Consider now the 7-particle amplitude. We can set $m = 2$, $s(\tau) = (6\ 1\ 2)(2\ 3\ 5)$, and introduce $f_5 = (6\ 7\ 1)(1\ 2\ 3)(3\ 4\ 5)$ in addition to f_6 and f_7 . This gives a map $f^{\text{new}} : \mathbb{C}^2 \rightarrow \mathbb{C}^3$. According to the theorem we have to construct a map $g : \mathbb{C}^2 \rightarrow \mathbb{C}^2$ out of the three components of f^{new} . One possible choice is $g_1 = f_6$ and $g_2 = f_5 f_7 = (6\ 7\ 1)(1\ 2\ 3)(3\ 4\ 5) f_7$, with f_6 and f_7 given in (2.5.14). Recalling that each minor is linear in τ 's we find that the degree condition for the application of the GRT is satisfied. Using (2.5.19) one finds

$$\int_{\{f_6, f_7\}} d^2 \tau \frac{(6\ 1\ 2)(2\ 3\ 5)}{(6\ 7\ 1)(1\ 2\ 3)(3\ 4\ 5) f_6 f_7} = - \int_{\{f_5, f_6\}} d^2 \tau \frac{(6\ 1\ 2)}{(5\ 6\ 7)(7\ 1\ 2) f_5 f_6}. \quad (2.5.20)$$

The LHS has been shown to give $A_7^{(3)}$ in the first part of this section. Let us now compute the RHS where the contour is a sum over the zeros of $\{(6\ 7\ 1)(1\ 2\ 3)(3\ 4\ 5), f_6\}$. A straightforward computation reveals that this is the sum over the usual residues of $\mathcal{L}_{n,k}$ given by

$$- (6)[(4) + (2) + (7)] - (1)[(4) + (2)] - (3)[(4) + (2)]. \quad (2.5.21)$$

We can use a GRT as was done in [10] to bring this into a more recognizable form. We will use that $(6)[(1) + (2) + (3) + (4) + (5) + (7)] = 0$ in (2.5.21) and a rearrangement of terms (recalling that $(i)(j) = -(j)(i)$) to get

$$- (1)[(2) + (4) + (6)] - (3)[(4) + (6)] - (5)(6) + (2)(3). \quad (2.5.22)$$

The first six terms give rise to the parity-conjugate version of the BCFW-contour as explained in [10] and therefore equal $A_7^{(3)}$. This means that (2.5.22) equals

$$A_7^{(3)} + (2)(3), \quad (2.5.23)$$

which is a contradiction, as advertised. As mentioned at the beginning of the discussion, there is an implicit assumption in using the GRT (2.5.18) to derive (2.5.19). The implicit assumption is that Γ_k and Γ_l as sets of points in \mathbb{C}^m are disjoint. This is exactly what fails in our seven particle example. Indeed, note that the point $(2) = (3) = 0$ appears in both contours! In order to see this, note that the map defined by $g_1 = f_6$ and $g_2 = (6\ 7\ 1)(1\ 2\ 3)(3\ 4\ 5) f_7$, with $f_7 = (5\ 6\ 7)(7\ 1\ 2)(2\ 3\ 5)$, has a double zero at $(2\ 3\ 4) = (3\ 4\ 5) = 0$ since $(2\ 3\ 5)$ also vanishes there. This means that while the GRT is valid as given in (2.5.18), the splitting into two parts must be defined independently in this situation. In other words, one has to decide where to keep $(2)(3)$. In our construction we have defined the amplitude in such a way that $(2)(3)$ is kept where the contour is defined by $\{f_6, f_7\}$ and therefore should be subtracted from the second form, i.e. ,

$$A_7^{(3)} = - \int_{\{f_5, f_6\}} d^2\tau \frac{(6\ 1\ 2)}{(5\ 6\ 7)(7\ 1\ 2) f_5 f_6} - (2)(3) . \quad (2.5.24)$$

This is very reminiscent of what happened in [37], where some forms for the connected prescription gave rise to the amplitude only after subtracting “spurious” configurations. Note that the same exercise can be repeated but using $g_1 = f_5 f_6$ and $g_2 = f_7$. We leave it to the reader to show that the same phenomena happens when this time the shared point is given by $(6) = (7) = 0$. Recall that $(2)(3)$ and $(6)(7)$ were precisely the special points in the previous discussion of the seven particle amplitude.

Eight-Particle Example

The eight particle amplitude can be analyzed in a similar manner to the seven particle example. Following the same steps as before we find

$$\int_{\mathbf{f}_8=0} d^3\tau \frac{h_8(\tau)}{f_6 f_7 f_8} \quad \text{with} \quad h_8(\tau) = \frac{(6\ 1\ 2)(2\ 3\ 5)(7\ 1\ 2)(2\ 3\ 6)}{(7\ 8\ 1)(1\ 2\ 3)(3\ 4\ 5)} \quad (2.5.25)$$

while the map $\mathbf{f}_8 \equiv (f_6, f_7, f_8)$ and for which the f_i are given by

$$f_6 = (2\ 3\ 4)(4\ 5\ 6)(6\ 1\ 2), \quad f_7 = (5\ 6\ 7)(7\ 1\ 2)(2\ 3\ 5), \quad f_8 = (6\ 7\ 8)(8\ 1\ 2)(2\ 3\ 6). \quad (2.5.26)$$

Once again, the naïve cancelation of terms when $h_8/(f_6 f_7 f_8)$ is thought of as a rational function leads the contour $[(2) + (4)](5)[(6) + (8)]$ which is clearly wrong as it misses 6 terms!

Four of the missing terms are of the same origin as the two missing terms in the seven particle amplitude. We simply list the map and leave the geometric proofs an elementary exercises for the reader:

$$\begin{aligned}
\{(234), (235), (678)\} &\longrightarrow \{(234), (345), (678)\} = (2)(3)(6); \\
\{(234), (235), (812)\} &\longrightarrow \{(234), (345), (812)\} = (2)(3)(8); \\
\{(234), (712), (812)\} &\longrightarrow \{(234), (781), (812)\} = (2)(7)(8); \\
\{(456), (712), (812)\} &\longrightarrow \{(456), (781), (812)\} = (4)(7)(8).
\end{aligned} \tag{2.5.27}$$

The final two missing terms are more interesting. One of the missing terms from the $\mathcal{L}_{n,k}$ -contour is $(2)(3)(4) = \{(234), (345), (567)\}$. Note that this singularity has the geometric interpretation of imposing that points 2, 3, 4, 5, 6 and 7 be collinear in the \mathbb{CP}^2 -sense.

Let us now look at the map \mathbf{f}_8 at the point $(234) = (235) = (236) = 0$. Note that this imposes exactly the same geometric constraint and it is therefore the same point in (τ_1, τ_2, τ_3) space. Since by construction we have zeros in h_8 where $(235) = 0$ and $(236) = 0$ we need two poles in the denominator to vanish. These are (456) in f_6 and (345) in h_8 . Recalling that the residue is computed using a T^3 -contour $|(234)| = \epsilon_1$, $|(235)| = \epsilon_2$ and $|(236)| = \epsilon_3$ one can show that the answer is the same as if we used the contour $|(234)| = \epsilon_1$, $|(345)| = \epsilon_2$ and $|(456)| = \epsilon_3$ and therefore the residue is identical to what we call $(2)(4)(5)$.

Moreover, this also shows that the same point in \mathbb{C}^3 is determine by $(456) = (235) = (236) = 0$. This means that this is not a distinct zero of \mathbf{f}_8 and therefore does not give rise to a new residue.

Exactly the same happens to the second missing term but this time we have to start with $\{(612), (712), (812)\}$ and realize that (678) in f_8 and (781) in h_8 vanish. Summarizing the new kind of terms

$$\begin{aligned}
\{(234), (235), (236)\} &= \{(456), (235), (236)\} \longrightarrow \{(234), (345), (456)\} = (2)(3)(4); \\
\{(612), (712), (812)\} &= \{(612), (712), (678)\} \longrightarrow \{(678), (781), (812)\} = (6)(7)(8);
\end{aligned}$$

and collecting all these results we find 10 residues which agree with $\Gamma_{8,3}^{\mathcal{L}}$ given in (2.5.3).

III. General Proof For All n

Let us now prove that

$$A_n^{(3)} = \int_{\mathbf{f}_n} \frac{h_n}{f_6 f_7 \cdots f_n}, \quad (2.5.28)$$

reproduces the correct tree-level amplitude as defined by $\Gamma_{n,3}^{\mathcal{L}}$ for all NMHV amplitudes in full generality. The proof proceeds by induction. In fact, it is a simple generalization of the computation we have already seen for eight particles—which is the simplest case where all the general ingredients appear.

Let us state more precisely what we want to prove. Consider the n -particle amplitude. Given that as rational functions

$$\frac{1}{(1)(2) \cdots (n-2)(n-1)(n)} = \frac{h_n}{f_6 \cdot f_7 \cdots f_{n-1} \cdot f_n}, \quad (2.5.29)$$

all we need to show is that the points in \mathbb{C}^{n-5} determined by

$$\underbrace{\mathcal{E}_n \star \mathcal{O}_n \star \mathcal{E}_n \star \cdots}_{(n-5) \text{ factors}} \quad (2.5.30)$$

are zeros of \mathbf{f}_n . These zeros are guaranteed to give the right residues while all other zeros of \mathbf{f}_n have zero residue by virtue of (2.5.29)! Recall from [10] that the \star -product is such that $(i) \star (j) = 0$ if $i > j$, and

$$\mathcal{E}_n = (2) + (4) + \cdots + (2[n/2]) \quad \text{and} \quad \mathcal{O}_n = (1) + (3) + \cdots + (2[n/2] + 1). \quad (2.5.31)$$

A note on notation: in this discussion we use (i) for a consecutive minor of the n -particle amplitude. Any other minor will be written explicitly as $(i \ j \ k)$.

Induction Argument

Start by assuming that the statement is true for $(n-1)$ -particles. In other words, we can freely start with

$$\frac{1}{(1)(2)(3) \cdots (n-3)(n-2 \ n-1 \ 1)(n-1 \ 1 \ 2)} \quad (2.5.32)$$

and consider only the zeros of $f_{(n-1)}$ corresponding to

$$\underbrace{\mathcal{E}_{n-1} \star \mathcal{O}_{n-1} \star \mathcal{E}_{n-1} \star \cdots}_{(n-6) \text{ factors}} \quad (2.5.33)$$

where the subscript is there to indicate that the minors in (2.5.32) are being used.

Recall that in order to get the n -particle formula all we have to do is to multiply by $h_{n-1}/f_6 \cdots f_{n-1}$ by

$$\mathcal{S}_{(n-1) \rightarrow n}^{(3)} = \frac{(n-2 \ n-1 \ 1)(n-1 \ 1 \ 2)(n-2 \ 2 \ 3)}{(n-1 \ n \ 1) f_n} \quad (2.5.34)$$

with $f_n = (n-2)(n)(n-2 \ 2 \ 3)$. For the purpose of the proof, all we need to show is that all the points in \mathbb{C}^{n-5} given by (2.5.30) are also points in

$$[\mathcal{E}_{n-1} \star \mathcal{O}_{n-1} \star \mathcal{E}_{n-1} \star \cdots] \times [(n-2) + (n) + (n-2 \ 2 \ 3)]. \quad (2.5.35)$$

The multiplication sign ‘ \times ’ is there to stress that every single term on the left must be multiplied by every term on the right (unlike the symbol \star).

The first two terms in the last factor of (2.5.35), i.e. , $[(n-2)]$ and $[(n)]$, directly give terms in (2.5.30) except when they hit terms of the form $[\dots \star (n-1 \ 1 \ 2)]$ or $[\dots \star (n-2 \ n-1 \ 1) \star (n-1 \ 1 \ 2)]$. The reason for splitting these two cases will become clear in a moment.

Terms of the form $[\dots \star (n-1 \ 1 \ 2)] \times (n-2)$ vanish because no other consecutive minor is set to zero, while terms of the form $[\dots \star (n-1 \ 1 \ 2)] \times (n)$ make $(n-1 \ n \ 1) = 0$ and give rise to $[\dots \star (n-1)](n) = [\dots] \star (n-1) \star (n)$. The situation is different and much more interesting for the second class. Note that $[\dots] \star (n-2 \ n-1 \ 1) \star (n-1 \ 1 \ 2) \times (n-2)$ and $[\dots] \star (n-2 \ n-1 \ 1) \star (n-1 \ 1 \ 2) \times (n)$ define the same point in \mathbb{C}^{n-5} ! This particular point is precisely the one where minors $(n-2) = (n-1) = (n) = 0$. This means that they give rise to the terms in (2.5.30) of the form $[\dots] \star (n-2) \star (n-1) \star (n)$.

This shows that as sets of points in \mathbb{C}^{n-5}

$$[\mathcal{E}_{n-1} \star \mathcal{O}_{n-1} \star \mathcal{E}_{n-1} \star \cdots] \star [(n-2) + (n)] = [\mathcal{E}_n \star \mathcal{O}_n \star \mathcal{E}_n \star \cdots] \star [(n-2) + (n)]. \quad (2.5.36)$$

The only difference between this formula and what we want is a $(n-4)$ term in the final factor. The reason is that with $(n-5)$ total factors, the \star -product forces any factor of the form $(n-k)$ with $k \geq 2$ in the last factor to vanish in (2.5.30). Moreover, it

is clear that only one term in (2.5.30) has $(n-4)$ as the final factor. This is the term $(2) \star (3) \star (4) \star \dots \star (n-5) \star (n-4)$. In order to generate this term, note that $(n-2 \ 2 \ 3) = 0$ in (2.5.35) together with $(2) = (3) = \dots = (n-1) = 0$ implies that $(n-4)$, which explicitly is given by $(n-4 \ n-3 \ n-2)$, vanishes which is what we wanted to show.

As an aside, note that this proof motivates us to write the $\mathcal{L}_{n,k}$ -contour as \star -multiplication of the $(n-1)$ -particle contour by $[(n) + (n-2) + (n-4)]$, in other words, it shows that it is given as

$$[(6) + (4) + (2)] \star [(7) + (5) + (3)] \star [(8) + (6) + (4)] \star \dots \star [(n) + (n-2) + (n-4)]. \quad (2.5.37)$$

Note that we have unified the residues of this contour into a single variety; both the contour itself as well as the unification are not manifestly cyclically invariant. The cyclic invariance of $\Gamma_{n,3}^{\mathcal{L}}$ was shown to follow simply from the global residue theorem in [10], and hence the unified form we have given it also gives rise to a cyclically invariant amplitude.

IV. “Inverse-Soft” Interpretation

It remains to show that the “add one particle at a time” construction we have given has an interpretation more specifically as an “inverse-soft” operation, by showing that the multiplicative factor $\mathcal{S}_{(n-1) \rightarrow n}^{(3)}$ turns into the soft factor for particle n in the limit $\lambda_n \rightarrow 0$. Recall that

$$\mathcal{S}_{(n-1) \rightarrow n}^{(3)} = \frac{(n-2 \ n-1 \ 1)(n-1 \ 1 \ 2)(n-2 \ 2 \ 3)}{(n-1 \ n \ 1) f_n} \quad (2.5.38)$$

with

$$f_n = (n-2)(n)(n-2 \ 2 \ 3). \quad (2.5.39)$$

Now, in order to exhibit the soft limit, we will use the global residue theorem, choosing $(n-6)$ of the polynomials to be the f ’s for the $(n-1)$ -particle amplitude, and the remaining polynomial to be f_n times the remaining denominator factors, which among others include the minor $(n-1 \ n \ 1)$. The residue theorem gives us a sum over terms putting the remaining denominator factors to zero. It is easy to show in general (as will be discussed in detail in [24]), that none of these contributions can be singular in the soft limit, except the one where the minor $(n-1 \ n \ 1)$ is set to zero. Focusing only on this contribution, it will also be shown that *every* residue of $\mathcal{L}_{n,3}$ setting $(n-1 \ n \ 1)$ and any

other collection of minors to zero maps, in the soft limit $\lambda_n \rightarrow 0$, to the usual soft factor multiplied by the corresponding residue of $G(3, n - 1)$ determined by the vanishing of these other minors. This guarantees that the soft limits are manifest as claimed.

V. Connection to the Twistor String

As already mentioned in section 2.4, there is a continuous deformation of the map $f_{(n)}$ which does not affect the sum over residues and which gives rise to an integral over the Grassmannian which can be shown to come from the twistor string formulation of the amplitude and which wonderfully manifests the cyclic-symmetry and U_1 -decoupling identities of the amplitude.

It is instructive to note that both the cyclic invariance and U_1 -decoupling identities can be established without performing the explicit calculation relating our form of the object to the connected prescription. By construction, the Veronese operators localize the integral over the $C_{\alpha a}$'s to be over matrices with the Veronese form; computing the residue tells us to look at what is happening to first order in a Laurent expansion in $(n - 5)$ variables in the vicinity of the Veronese form. Let us consider such a first-order perturbation away from the Veronese form given by the following parametrization of the $C_{\alpha a}$ matrix,

$$C = \begin{pmatrix} \xi_1 + \sum_{j=1}^{n-5} \epsilon_j \rho_1^j & \xi_2 + \sum_{j=1}^{n-5} \epsilon_j \rho_2^j & \cdots & \xi_n + \sum_{j=1}^{n-5} \epsilon_j \rho_n^j \\ \xi_1 \rho_1 & \xi_2 \rho_2 & \cdots & \xi_n \rho_n \\ \xi_1 \rho_1^2 & \xi_2 \rho_2^2 & \cdots & \xi_n \rho_n^2 \end{pmatrix}, \quad (2.5.40)$$

one finds that the leading order in ϵ of the Veronese polynomials is linear in ϵ and can be denoted by $S_k^{\text{leading}}(1)$. This means that the following change of variables $u_k = S_k^{\text{leading}}(1)$ from $(\epsilon_1, \dots, \epsilon_{n-5})$ to u_k is linear and the contour integral around the point $S_k^{\text{leading}} = 0$ can be written as follows

$$G(\xi_i, \rho_i) = \int d^{n-5} u \frac{1}{u_6 u_7 \cdots u_n}, \quad (2.5.41)$$

where the contour computes the residue at $u_k = 0$ which gives one. Of course, to get the final result for the tree amplitude one would still have to integrate over the ρ 's, but this form already allows us to see both the cyclic-symmetries and U_1 -decoupling identity. This is because straightforward computation of the function $G(\xi_i, \rho_i)$ reveals a very beautiful

property: it is almost permutation invariant. In fact, it is given by

$$G(\xi_i, \rho_i) = \frac{1}{(\rho_1 - \rho_2)(\rho_2 - \rho_3) \cdots (\rho_n - \rho_1)} \times \tilde{G}(\xi_i, \rho_i) \quad (2.5.42)$$

where $\tilde{G}(\xi_i, \rho_i)$ is fully permutation invariant! Despite the non-manifest cyclic invariance of this integrand, this residue *is* cyclically invariant, and this conclusion is not changed in performing the integral over ρ 's giving the tree amplitude. Similarly, since the only breaking of permutation invariance is in the pre-factor, which is just the same twistor-string measure guaranteeing the U_1 -decoupling identity.

2.6 Generalization to N^2 MHV

Returning to the Grassmannian, it is not difficult to extend our results for general NMHV amplitudes to higher- k by first using parity-conjugation to obtain the contour for $\overline{\text{NMHV}}$, and then view this as the result of having added a particle to an $\overline{\text{MHV}}$ amplitude. It will be instructive to work this out in detail for N^2 MHV, because there are several new structures that emerge first for $k = 4$ that will be important for all higher- k ; these new structures will be discussed in section I. After deriving a general formula (2.6.10) for the N^2 MHV amplitude computed in the Grassmannian, we will check it in detail for the 8-particle amplitude in section II. This will allow us to discuss many of the new structures that emerge beyond NMHV, and which are prerequisite to understanding higher- k .

The method by which we will obtain the contour for N^2 MHV is roughly as follows. We will first write the contour for the 7-particle N^2 MHV(= $\overline{\text{NMHV}}$) amplitude by parity-conjugating the result for $k = 3$. We will see that this can be viewed as having been obtained from the 6-particle N^2 MHV(= $\overline{\text{MHV}}$) amplitude by acting with an operator which adds a particle while preserving k , similar to the operator discussed above to derive the NMHV contour. This operator naturally generalizes to higher- n , and through its repeated application to the 6-particle amplitude, we obtain a closed-form result for all n .

As discussed in section 2.3, parity acts in the Grassmannian by exchanging C with its dual \tilde{C} , and trading all minors for their complements (see near (2.3.25)). For example, in going from $G(3, 7) \rightarrow G(4, 7)$, the minor $(1\ 2\ 3) \mapsto \overline{(1\ 2\ 3)} = (4\ 5\ 6\ 7)$. Knowing this, we can immediately write down the 7-point N^2 MHV amplitude from the NMHV amplitude

given above. It is,

$$A_7^{(4)} = \int_{\tilde{f}_7=0} \frac{(3\ 4\ 5\ 7)(4\ 6\ 7\ 1)}{(2)(4)(6) \left\{ \underbrace{[(7)(3\ 4\ 5\ 7)(5)]}_{\tilde{f}_6} \underbrace{[(1)(3)(4\ 6\ 7\ 1)]}_{\tilde{f}_7} \right\}}, \quad (2.6.1)$$

where we have used \tilde{f}_j to denote the parity-conjugates of ‘ f_j ’, and we have used a single label in parentheses to denote any *consecutive* minors of $G(4, n)$ —e.g., $(2) \equiv (2\ 3\ 4\ 5)$. Although equation (2.6.1) is correct as written, we will find it useful to exploit the cyclic-symmetry of the Grassmannian to bring (2.6.1) into a form more reminiscent of our result for NMHV. Specifically, by rotating all particle labels in (2.6.1) by $j \mapsto j - 3$, we obtain an expression remarkably similar to our form of the NMHV amplitude:

$$A_7^{(4)} = \int_{\mathbf{f}_7^{(4)}=0} \frac{(4\ 7\ 1\ 2)(1\ 3\ 4\ 5)}{(6)(1)(3)} \frac{1}{\mathcal{F}_{4567\ 123}}, \quad (2.6.2)$$

where we have grouped the (cyclically-rotated) parity-conjugates of f_6 and f_7 into the object

$$\mathbf{f}_7^{(4)} \equiv \left\{ f_{7_a}^{(4)}, f_{7_b}^{(4)} \right\} \equiv \left\{ (4)(4\ 7\ 1\ 2)(2), (5)(7)(1\ 3\ 4\ 5) \right\}, \quad (2.6.3)$$

and where $\mathcal{F}_{4567\ 123} \equiv f_{7_a}^{(4)} \cdot f_{7_b}^{(4)}$. To motivate this notation, observe that adding a particle to an n -point amplitude while preserving k necessarily introduces $(k - 2)$ new integration variables that must be fixed by the contour, and each $f_n^{(4)}$ accounts for one of these new variables. For $k = 4$, therefore, it is the *pair* of maps $\left\{ f_{7_a}^{(4)}, f_{7_b}^{(4)} \right\} \equiv \mathbf{f}_7^{(4)}$ —taken together—which fixes the contour, and $\mathcal{F}_{4567\ 123} = f_{7_a}^{(4)} \cdot f_{7_b}^{(4)}$ which appears in the integrand. (The indices ‘4567 123’ below \mathcal{F} are meant to make explicit the fact that \mathcal{F} involves the *seven* particles numbering 4567 123—presented in this order. This notation will be useful below, when we consider adding particles to a general n -point amplitude.)

Let us now re-write the 7-particle amplitude in such a way that makes manifest that it could have been obtained by acting on the 6-particle N²MHV amplitude with an ‘inverse-soft’ operator similar to that discussed above for NMHV. Knowing $A_7^{(4)}$ from above, this is very easy to do:

$$A_7^{(4)} = \int A_6^{(4)} \times_{6 \rightarrow 7} \mathcal{S}^{(4)} = \int_{\mathbf{f}_7^{(4)}=0} \frac{1}{(1)(2)(3)(4\ 5\ 6\ 1)(5\ 6\ 1\ 2)(6\ 1\ 2\ 3)} \mathcal{S}_{6 \rightarrow 7}^{(4)}, \quad (2.6.4)$$

where

$$\mathcal{S}_{6 \rightarrow 7}^{(k=4)} = \frac{(4561)(5612)(6123)(4712)(4235)(1345)}{(6712)} \frac{1}{\mathcal{F}_{4567123}}. \quad (2.6.5)$$

Two important aspects of $\mathcal{S}_{6 \rightarrow 7}^{(4)}$ will allow it to be generalized to higher n in a way which does not alter its form. First, it correctly maps the measure of $\mathcal{L}_{6,4}$ to that of $\mathcal{L}_{7,4}$: by ‘removing’ the three minors of $G(4,6)$ which are not consecutive in $G(4,7)$ —namely, (4561) , (5612) , and (6123) —by including them in the numerator of $\mathcal{S}^{(4)}$; also, by adding to the measure each of the four consecutive minors of $G(4,7)$ which were not present in $\mathcal{L}_{6,4}$. One of these minors— (6712) —is manifest in (2.6.5), while the other three minors involving particle 7 are part of \mathcal{F} . Notice that *all* the non-consecutive minors appearing in \mathcal{F} are manifestly part of the numerator of (2.6.5). The second important aspect of \mathcal{S} is that, by including \mathcal{F} in its definition, it describes the contour of integration for the new integration variables added when going from $\mathcal{L}_{6,4}$ to $\mathcal{L}_{7,4}$ (of course, there were no integration variables for the 6-point $N^2\text{MHV}(=\overline{\text{MHV}})$ amplitude).

Let us now see how we can generalize $\mathcal{S}_{6 \rightarrow 7}^{(4)}$ to one which adds particle 8 to the 7-particle amplitude. It turns out there is a very natural way of doing this. Notice that for $k = 4$, the four consecutive minors of $G(4,n)$ involving n —which were not present in $G(4,n-1)$ and—which must be added to the measure by \mathcal{S} involves exactly seven columns: $n-3, \dots, n, 1, 2, 3$. And because $\mathcal{S}_{6 \rightarrow 7}^{(4)}$ and $\mathcal{F}_{4567123}$ both involve only seven fixed columns of the Grassmannian, there is a *canonical* way to generalize these to higher n . Concretely, in going from the $(n-1)$ -point amplitude to the n -point amplitude, the inverse-soft operator must involve the minors

$$(n-3 \ n-2 \ n-1 \ n), \quad (n-2 \ n-1 \ n \ 1), \quad (n-1 \ n \ 1 \ 2), \quad \text{and} \quad (n \ 1 \ 2 \ 3) \quad (2.6.6)$$

in the denominator. It is easy to see how these can be kept manifest in \mathcal{F} through its natural generalization to \mathcal{F}_n by

$$\mathcal{F}_n \equiv \frac{\mathcal{F}}{(n-3)(n-2)(n-1)n \ 123} \equiv f_{n_a}^{(4)} \cdot f_{n_b}^{(4)} \quad (2.6.7)$$

where

$$\begin{aligned} f_{n_a}^{(4)} &\equiv (n-3 \ n-2 \ n-1 \ n)(n-3 \ n \ 1 \ 2)(n-3 \ 2 \ 3 \ n-2); \\ \text{and} \quad f_{n_b}^{(4)} &\equiv (1 \ n-2 \ n-1 \ n)(1 \ n \ 2 \ 3)(1 \ 3 \ n-3 \ n-2). \end{aligned} \quad (2.6.8)$$

Notice that (2.6.7) is simply the same as (2.6.3) with the substitution $\{4, 5, 6, 7\} \mapsto \{n-3, n-2, n-1, n\}$ while keeping $\{1, 2, 3\}$ fixed.

In a similar manner, we can generalize the inverse-soft operator to

$$\mathcal{S}_{(n-1) \rightarrow n}^{(4)} = \frac{(n-3 \ n-2 \ n-1 \ 1)(n-2 \ n-1 \ 1 \ 2)(n-1 \ 1 \ 2 \ 3)(n-3 \ n \ 1 \ 2)(n-3 \ 2 \ 3 \ n-2)(1 \ 3 \ n-3 \ n-2)}{(n-1 \ n \ 1 \ 2) \cdot \mathcal{F}_n} \quad (2.6.9)$$

By repeatedly applying this inverse-soft operator to the 6-particle N^2 MHV amplitude, we can obtain any higher-point amplitude we like. Indeed, it is not difficult to obtain the general result for any number of particles. Doing this explicitly, we find that the n -particle N^2 MHV amplitude is given by

$$A_n^{(4)} = \int_{\mathcal{J}_n^{(4)}=0} \frac{\prod_{j=7}^{n-1} [(1 \ 2 \ 3 \ j) (2 \ 3 \ j-2 \ j-1) (1 \ j-2 \ j-1 \ j)] \prod_{j=4}^{n-3} [(1 \ 3 \ j \ j+1) (1 \ 2 \ j \ j+3)]}{(n-1)(1)(3) \ \mathcal{F}_7 \cdot \mathcal{F}_8 \cdots \mathcal{F}_n}. \quad (2.6.10)$$

As we will see below, this ansatz correctly gives the 8-particle N^2 MHV amplitude, and it does so in a remarkably-novel way—involving only four one-loop leading singularities together with sixteen two-loop (all the residues of $G(4, 8)$ are at most two-loop leading singularities, [24]).

I. The Geometry of Residues in the Grassmannian

The 8-particle N^2 MHV amplitude not only offers us an extremely good test of the ansatz (2.6.10), but it also allows us the opportunity to discuss some of the more general structures involved in amplitudes (and their contours) for $k > 3$. Most of these arise as a simple consequence of the fact that for $k > 3$, minors of the Grassmannian are typically irreducible polynomials of degree greater than one and therefore vanish along cycles in $G(k, n)$ which multiply intersect each other (and themselves). This is true of the cycles defined by the vanishing of the (mostly non-consecutive) minors which define the tree contour in (2.6.10), and it is true for the purely consecutive minors which are relevant to $\mathcal{L}_{n,k}$.

One obvious consequence of the fact that any given set of cycles can multiply-intersect is that more data is necessary to identify any particular residue than just which minors vanish on its support. And it is not true in general that distinct residues supported along the vanishing of the same set of minors are at all related. This fact becomes increasingly apparent as n grows large, but is already striking for $n = 9$: for example, while two of

the five residues supported along by the vanishing of the minors “(1)(2)(3)(4)(6)(8)” are the leading singularities of four-mass boxes, the other three residues associated with the vanishing of these minors are simply rational functions.

As discussed in [10], the number of isolated solutions to setting a given set of minors to zero is described by Littlewood-Richardson formula. For $k = 4$ these are simply the Catalan numbers: there are generally 2 solutions to setting 4 minors to zero in $G(4, 8)$; 5 solutions to setting 6 minors to zero in $G(4, 9)$; 14 solutions for $G(4, 10)$; 42 for $G(4, 11)$; 132 for $G(4, 12)$; and simple residues cease to exist for $n > 12$. While we may be able to get away with labeling the 2 solutions for each set of four minors of $G(4, 8)$ by simply ‘1’ and ‘2,’ it is clear that something more is needed in general.

As we will see below, one very powerful way to identify *all* the distinct residues in $G(k, n)$ is simply through the projective geometry of the Grassmannian viewed in the particle interpretation. And, perhaps even more importantly, this geometric data is closely-related to physically-important information, such as soft-limits (see [24]). Of course, when each column of the $C_{\alpha a}$ -matrix is viewed as a point in \mathbb{CP}^{k-1} , *every* minor represents *some* geometric test. Consider the following concrete example, which arises frequently in $G(4, n)$. It is easy to show that

$$(2345) = (3456) = 0 \implies \begin{cases} \mathbf{A} & \text{all the points } \{2, 3, 4, 5, 6\} \text{ are coplanar;} \\ \mathbf{B} & \text{the points } \{3, 4, 5\} \text{ are collinear.} \end{cases} \quad (2.6.11)$$

In case **A**, we know as a consequence that $(2346) = 0$, for example (similarly for any other choice of 4 from among $\{2, 3, 4, 5, 6\}$); and in the case of **B**, we know as a consequence that $(3458) = 0$ (or, more generally, $(345m) = 0$ for any m). Notice that the natural way to test either case would be through the vanishing of a *non-consecutive* minor. Indeed, one way to uniquely identify every residue of the Grassmannian is to give an exhaustive list of all the minors—both consecutive and non-consecutive—which vanish on its support. (This is actually quite obvious: any point in the Grassmannian can be identified by its Plücker coordinates, which in turn can be written as a sequence of (typically non-consecutive) minors.)

One of the most remarkable features of the form of the tree-contour derived in (2.6.10) is that the non-consecutive minors used to define the contour appear to *automatically* collapse any possible ambiguity about which particular residues are included in the con-

tour. This turns out to be possible because for $n > 7$, at least one factor among the \mathcal{F}_n 's given in (2.6.7) is always composed entirely of non-consecutive minors!

Another remarkable feature of the contour given in (2.6.10) is that it is given *entirely* in terms of ‘simple’ residues—that is, simple residues involving both consecutive and non-consecutive minors. As we will see, the 8-point contour fixed by the contour in (2.6.10) turns out to contain 9 residues which are ‘composite’ in terms of consecutive minors—and yet all of them arise as the *simple* residues of the contour. Moreover, for higher n , there are always $\dim(\tau)$ maps among the \mathcal{F} 's which define the contour, and so: *all residues—composites and non-composites alike—are generated as simple residues involving both consecutive and non-consecutive minors!*

On the Naming of Residues

Before we calculate the actual residues of $G(4, 8)$ which contribute to the contour given above, it is necessary for us to develop some notation to describe the residues concretely. From our discussion above, it is clear that any residue can be uniquely identified by giving a sufficiently-exhaustive list of the minors which vanish at its support. Naturally, we would like to represent this data as concisely as possible. While we will not prove it here, (see [24]), it turns out that there is a natural, physically-motivated, concise way to represent all the necessary information: *any* residue of $G(4, n)$ can be uniquely identified by the following:¹

1. a list of the consecutive minors which vanish on its support, which we write in the form, e.g., “(2)(4)(6)(8)” (where the order of these labels determines the sign of the residue);
2. all triples of consecutive, collinear points, which we indicate by a blue subscript labeling the middle of the consecutive triple; so, e.g., by “(2)(3)(7)(8)₁₄” we mean the particular solution to (2)(3)(7)(8) for which the triples (812) and (345) are collinear;

¹This is only strictly true if we consider each conjugate-pair of residues associated with the leading singularities of a four-mass box as equivalent.

and, although not strictly necessary to identify each residue, we find it useful² to further indicate

3. all triples of consecutive points *whose parity conjugates* are coplanar, indicated with a red superscript labeling the middle of triple of points; so, e.g., by “(2)(3)(7)(8)⁵⁸” we mean the particular solution to (2)(3)(7)(8) for which all the particles *in the complements of (456) and (781)* are coplanar—i.e., for which (78123) and (23456) are coplanar.

With this notation, our example (2.6.11) can be rewritten:

$$(2)(3) \implies \begin{cases} (2)(3)^8 \\ (2)(3)_4 \end{cases}. \quad (2.6.12)$$

As a statement about functions, (2.6.12) reads $(3) = (3)'(2) + (3)^8 \cdot (3)_4$, which is to say, the minor (3) factorizes on the support of (2) (and vice versa).

It is worth keeping in mind that the collinearity and coplanarity operators are actually *stronger* constraints than minors alone. Specifically,

- each $(\dots)_m$ implies that $(m-1 \ m \ m+1 \ p) = 0$ for *any* p ; and in particular, it implies that the minors $(m-1) = (m-2) = 0$;
- each $(\dots)^q$ implies that any minor forming a subset of $\overline{(q-1 \ q \ q+1)}$ vanishes; in particular, it implies that $(q+2) = \dots = (q+n-5) = 0$.

Notice that it is possible for a residue to be supported where *both* factors of a given minor vanish simultaneously. For example, if $(2) = 0$ and both $(3)^8 = (3)_4 = 0$, then a total of *three* constraints would be imposed by these two minors. Because of the symmetry between (3) factorizing on (2) and (2) factorizing on (3), we choose to indicate this extra constraint by writing $[(2)(3)]_4^8$. Notice that either of the labels $()^8$ and $()_4$ imply that minors (2) *and* (3) vanish. An example of this type of composite for $n = 8$ is the residue $[(2)(3)](8)_4^8$ —which will in fact contribute to the tree contour as we will see below. Similarly, if we were to know that all of the points 3, 4, 5, and 6 were collinear, then we would have a residue adorned by both $()_4$ and $()_5$; but $()_5$ implies that $(3) = (4) = 0$,

²This is particularly relevant for $n = 8$, as it is the ‘parity-conjugate of three points being collinear’; for higher n , this geometric constraint becomes increasingly constraining.

while $()_4$ implies $(2) = (3) = 0$, and so minor (3) is doubly-constrained. In this case, we would name the residue $(2)(3)^2(4)_{45}^{81}$ (here, the coplanarity labels are a consequence of the collinearity).

Although we will not have room to discuss this here (see [24]), in addition to fully-specifying each distinct residue the Grassmannian, these labels also have an important, physically-motivated interpretation. They indicate how each particular residue—when viewed as a function of the kinematical variables—can be constructed out of an analogous lower-point residue in a canonical way through the action of an ‘inverse-soft operator’ analogous to the one discussed above, but applicable to each individual residue alone and without reference to the entire amplitude. Specifically, whenever a residue involves three points being collinear in $G(k, n)$, it is canonically-related to a residue in $G(k, n - 1)$ where the middle particle has been removed. Similarly, because the coplanarity of $(n - 3)$ points is the parity-conjugate of three points being collinear, a coplanarity label indicates that a residue is canonically-related to a residue of $G(k - 1, n - 1)$ in which the labelled particle has been removed.

II. The 8-Particle N^2 MHV Amplitude

We now are fully prepared to write down and compute the 8-point N^2 MHV amplitude as given by the general formula (2.6.10). Explicitly, we have

$$A_8^{(4)} = \int_{f_8^{(4)}=0} \frac{(5671)(7123)(2356)(1247)(1345)(1258)(1356)}{(7)(1)(3) \mathcal{F}_7 \cdot \mathcal{F}_8}, \quad (2.6.13)$$

where, from (2.6.7),

$$\begin{aligned} \mathcal{F}_7 &= \left[(4)(4712)(2) \right] \times \left[(1237)(3451)(5671) \right], \\ \text{and } \mathcal{F}_8 &= \left[(5)(5812)(5236) \right] \times \left[(6)(8)(1356) \right]. \end{aligned} \quad (2.6.14)$$

This multidimensional contour integral involves a few subtleties beyond those already encountered for NMHV contours. As discussed at length above, the principle new subtlety encountered for $k = 4$ is that the minors which define the contour are generically quadratic polynomials, whose cycles of zeros typically intersect each other (and themselves) multiply. Another novelty first encountered for $k = 4$ is that it is possible for some of the minors within the f_i 's to factorize on a solution of the others, leading to

multiple branches which can sometimes can have very different structures. These potential subtleties are best understood through example. Therefore, in the next subsection, we will work through a number of the contributions (and potential contributions) to the tree amplitude coming from the contour above, trying to sample all of the possible types of contributions.

Before we begin our series of examples, it is useful to lay-out the form we expect the answer to take, and the type of calculation that will be involved in the evaluating (2.6.13). Because setting any 4 minors of $G(4, 8)$ to zero will typically have 2 isolated solutions, we may first expect that by pairing any of the three minor-factors of the f_i 's together, we would find $\lesssim 3^4 * 2 = 162$ isolated poles in the Grassmannian 'encompassed' by the contour. Of course, the numerator of (2.6.13) ensures that any pole generated by the f_i 's which is not a pole of *consecutive minors* will have a vanishing residue. Therefore, we expect that the vast-majority of isolated solutions to $f_i = 0$, for $i = 1, \dots, 4$ will not contribute anything to the amplitude. Indeed, it turns out that among all the 3^4 choices of factors from among the f_i 's (and all of their multiple solutions), only 20 poles will contribute a non-vanishing residue to the contour—and these terms have been checked to add-up to precisely the 8-particle amplitude, matching right-down to the sign of every term.

Example Contributions from the Contour

In order to gain some understanding of how each of the 20 non-vanishing residues are generated by the contour, it is worthwhile to analyze a few examples in detail. Let us start by rewriting the maps f_i which define the contour in a slightly more transparent way:

$$\begin{aligned} f_1 &= [(2345)(4567)(7124)], & f_3 &= [(5678)(2356)(8125)], \\ f_2 &= [(1237)(3451)(5671)], & f_4 &= [(6781)(8123)(3561)]. \end{aligned} \tag{2.6.15}$$

Notice that the contour is naturally composed of some 3^4 parts coming from the simultaneous vanishing of any choice of factors from among the f_i 's. However, because f_2 is entirely composed of non-consecutive minors, most poles of the contour will have vanishing residue and contribute nothing to the tree amplitude. The exceptional cases are those for which the solution to $f_1 = \dots = f_4 = 0$ is also a pole in $\mathcal{L}_{8,4}$. The complete

list of such contributions is given in Table 2.1 at the end of this section. Each of these contributions is quite easy to understand geometrically, and considering a few exercises in particular will illustrate the role of projective geometry in the general contour.

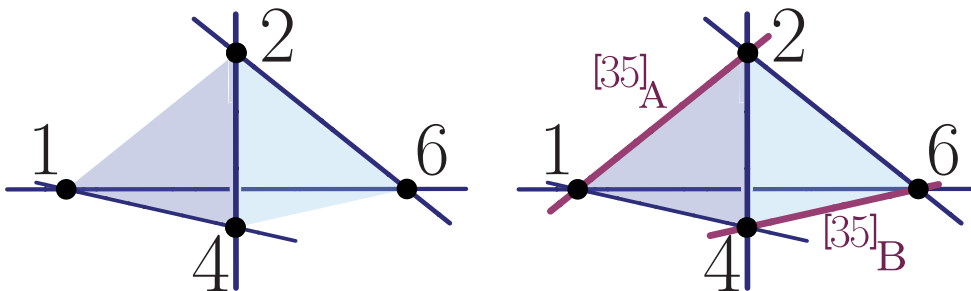
- $(2345)(3451)(2356)(1356) \implies (2)(3)^2(4)_{45}^{81}$

Notice that this choice of minors from the f_i 's includes only one consecutive minor, (2345) , together with the three non-consecutive minors (1345) , (2356) , and (1356) . The important thing to notice about these four minors is that they all involve points 3 and 5. This means that the geometry problem at hand is merely the classic problem of Schubert calculus of finding the set of lines—in this case the lines $[35]$ —which intersect four given lines in \mathbb{P}^3 .

Here, the four lines which $[35]$ must intersect are $[14]$, $[42]$, $[26]$, $[61]$. Notice that these four lines mutually intersect at points 4, 2, 6, and 1, forming a closed loop. This is illustrated on the left-hand side of the figure below. It is not hard to see that the only two solutions are those shown on the right-hand side of the same figure, $[35]_A$ and $[35]_B$.

The solution $[35]_A$ involves all four points $\{1, 2, 3, 5\}$ being collinear. While this configuration implies that minors (8) and (1) vanish, it does not provide a fourth constraint coming from a consecutive minor, and therefore the residue associated with this pole will vanish in the contour.

The solution $[35]_B$, on the other hand, involves all the points $\{3, 4, 5, 6\}$ being collinear. Recall that when 3, 4, 5 are collinear, minors (2) and (3) vanish, and when 4, 5, 6 are collinear, minors (3) and (4) vanish. Thus, the minor (3) is doubly-constrained, and we find that this geometric configuration contributes the residue $(2)(3)^2(4)_{45}^{81}$ to the amplitude.



- $(2345)(3451)(2356)(8123) \implies [(2)(3)](8)_4^8$

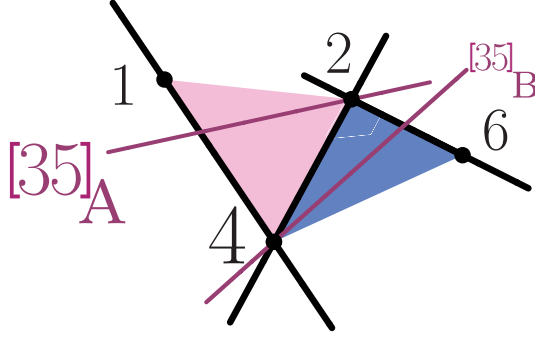


Figure 2.1: The two classes of solutions to setting minors (2345) , (1345) , and (2356) , to zero. In solution **A**, line $[35]$ lies on the plane $[124]$ and passes through the point 2; for **B**, the line $[35]$ lies on the plane $[624]$ and passes through the point 4.

The first three minors of this problem are the same as in the last problem. Let us start by considering these minors by themselves. As before, because all three minors involve the particles 3 and 5, we are looking for the configurations of lines $[35]$ which intersect the three given lines $[14]$, $[42]$, and $[26]$. There are two families of such solutions which are illustrated in Figure 2.1. Specifically, these two solutions are:

- A** the line $[35]$ passes through the point 2 and lies on the plane $[142]$, or
- B** the line $[35]$ passes through the point 4 and lies on the plane $[642]$.

Now let us consider imposing the additional constraint $(8123) = 0$ to each of the two cases. In case **A**, $(8123) = 0$ implies that the line $[81]$ intersect $[23] = [25] = [35]$. The only configuration then, is where the line $[35]$ lies along $[12]$, which was the same case we encountered in the previous geometry problem—and one that does not involve enough consecutive minors to contribute to the amplitude.

For case **B**, the line $[81]$ will intersect the plane $[246]$ at some point through which $[35]$ must pass; this will fix the angular freedom of $[35]$ on the plane $[246]$. Therefore, we have that 3, 4, and 5 are collinear, *and* the points 2, 3, 4, 5, 6 are coplanar. Both of these conditions set the minors (2) and (3) to zero, and so the two minors $[(2)(3)]_4^8$ contribute a total of three constraints. When combined with minor (8), we obtain the composite residue $[(2)(3)](8)_4^8$.

- $(2345)(5671)(5678)(8123) \implies (2)(4)(5)(8)_6$ and $(2)(6)(5)(8)_3$

Recall how consecutive minors factorized in the example (2.6.12). Just as in that case, because minors (5 6 7 8) and (5 6 7 1) overlap on three columns, we may conclude that, on the support of (5), $(5\ 6\ 7\ 1) \rightarrow (6)^3 \cdot (4)_6$. What this means for this case is that the two solutions to $(5\ 6\ 7\ 1) = (5\ 6\ 7\ 8) = 0$ are $(4)(5)_6$ and $(5)(6)^3$. Combining these two constraints with the minors (2) and (8) from f_1 and f_4 , respectively, we find that the two solutions are: $(2) \left[(4)_6 + (6)^3 \right] (5)(8) = (2)(4)(5)(8)_6 + (2)(6)(5)(8)^3$.

Before we move on to the next example, it is worth emphasizing that the *ordering* of minors appearing in the residue “ $(2)(6)(5)(8)^3$ ” was fixed by the ordering of the f_i ’s: minor (5 6 7 1) appearing in f_2 contributed the ‘(6),’ while f_3 contributed minor (5). This completely fixes the signs of the tree-contour.

- $(4\ 5\ 6\ 7)(5\ 6\ 7\ 1)(5\ 6\ 7\ 8)(6\ 7\ 8\ 1) \implies (4)(5)^2(6)^{2\ 3}_{6\ 7}$

Let us start this problem by first considering the three minors (4 5 6 7), (5 6 7 8) and (6 7 8 1). Here, we have that the line [6 7] must intersect the three lines [4 5], [5 8], and [8 1]. This case should be familiar from before, and is illustrated in Figure 2.2. There are two infinite families of solutions:

- A.** the line [6 7] passes through the point 5 and lies on the plane [1 5 8], or
- B.** the line [6 7] passes through the point 8 and lies on the plane [4 5 8].

Let us first consider case **A**. Here, we see that there is an apparent problem: when the points $\{5, 6, 7, 8, 1\}$ are coplanar, we *automatically* have that minor (5 6 7 1) = 0, and so f_2 vanishes everywhere over this entire infinite ‘sheet’ which solves the first three constraints! Clearly, when $f_2 = 0$ everywhere over a surface, it does not generate a

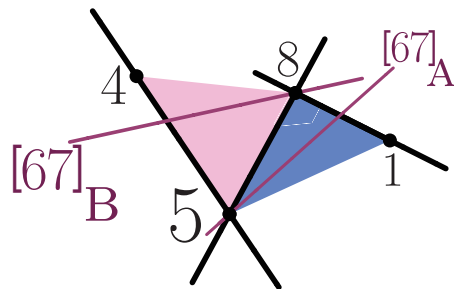


Figure 2.2: The two classes of solutions to setting minors $(4\ 5\ 6\ 7) = (5\ 6\ 7\ 8) = (6\ 7\ 8\ 1) = 0$, where the possible configurations for the line [6 7] are indicated.

transversally-supported pole. Said another way, f_2 vanishes *trivially* for this class of solutions, and only because the non-consecutive minor (5 6 7 1) vanishes. But this also vanishes everywhere in the numerator and so it effectively imposes no constraint at all.

In case **B**, however, (5 6 7 1) is *not* manifestly zero. Here, in fact, the vanishing of (5 6 7 1) imposes the non-trivial constraint that [6 7] intersects the point 5. Notice that this is actually where *both* of the factors of minor (5 6 7 1) = 0—one factor which tests the coplanarity of the points {5, 6, 7, 1} and the other which tests the collinearity of the points {5, 6, 7}. For this solution, the line [6 7] must lie along the line [5 8], and hence the points {5, 6, 7, 8} are all collinear! Similar to our first example above, the collinearity of {5, 6, 7} implies that minors (4) and (5) vanish, while the collinearity of {6, 7, 8} implies that the minors (5) and (6) vanish. This leads to the composite residue (4)(5)²(6)₆₇²³.

Residue	Geometry Problem:				Residue	Geometry Problem:			
	f_1	f_2	f_3	f_4		f_1	f_2	f_3	f_4
(2)(3) ² (4) ₄₅ ⁸¹	(2345)	(3451)	(2356)	(1356)	(2)(3)(5)(6) ₄₇	(2345)	(3451)	(5678)	(6781)
[(2)(3)](6) ₄ ⁸	(2345)	(3451)	(2356)	(6781)	(2)(5)(3)(6) ³⁸	(2345)	(5671)	(2356)	(6781)
[(2)(3)](8) ₄ ⁸	(2345)	(3451)	(2356)	(8123)	(2)(3)(5)(8) ₄	(2345)	(3451)	(5678)	(8123)
(2)[(5)(6)] ₇ ³	(2345)	(5671)	(5678)	(6781)	(2)(3)(7)(8) ₁₄	(2345)	(3451)	(8125)	(8123)
(2)[(7)(8)] ₁ ⁵	(2345)	(1237)	(8125)	(8123)	(2)(7)(3)(8) ⁵⁸	(2345)	(1237)	(2356)	(8123)
(4)(5) ² (6) ₆₇ ²³	(4567)	(5671)	(5678)	(6781)	(2)(4)(5)(8) ₆	(2345)	(5671)	(5678)	(8123)
[(4)(5)](8) ₆ ²	(4567)	(5671)	(5678)	(8123)	(2)(6)(5)(8) ³	(2345)	(5671)	(5678)	(8123)
(4)[(7)(8)] ₁ ⁵	(4567)	(1237)	(8125)	(8123)	(2)(7)(5)(8) ⁵	(2345)	(1237)	(5678)	(8123)
(6)(7) ² (8) ₈₁ ⁴⁵	(7124)	(7123)	(8125)	(8124)	(4)(5)(7)(8) ₁₆	(4567)	(5671)	(8125)	(8123)
(2)(1)(5)(8) ₂ ⁷	(2345)	(7123)	(5678)	(8123)	(4)(7)(5)(8) ²⁵	(4567)	(1237)	(5678)	(8123)

Table 2.1: All of the non-vanishing residues contributing to the 8-point N²MHV amplitude as given in (2.6.13), and the corresponding ‘geometry problem’ that gives rise to each.

Summary of 8-Point N²MHV Results

Continuing to solve the various geometry-problems in this manner, we would eventually find that the complete contour given in (2.6.13) contributes only 20 non-vanishing residues

to the tree-amplitude. These 20 terms are as follows:

$$\begin{aligned}
A_8^{(4)} = & (2)(3)^2(4)_{45}^{81} + [(2)(3)](6)_4^8 + [(2)(3)](8)_4^8 + (6)(7)^2(8)_{81}^{45} + (2)[(7)(8)]_1^5 \\
& + (4)[(7)(8)]_1^5 + (2)[(5)(6)]_7^3 + (4)(5)^2(6)_{76}^{32} + [(4)(5)](8)_6^2 + (2)(1)(5)(8)_2^7 \\
& + (2)(3)(5)(6)_{47} + (2)(5)(3)(6)^{38} + (2)(3)(5)(8)_4 + (2)(3)(7)(8)_{14} + (2)(7)(3)(8)^{58} \\
& + (2)(4)(5)(8)_6 + (2)(6)(5)(8)^3 + (2)(7)(5)(8)^5 + (4)(5)(7)(8)_{16} + (4)(7)(5)(8)^{25}
\end{aligned} \tag{2.6.16}$$

We have checked that this correctly matches the result calculated in field theory. The geometric origin of each of these terms is summarized in Table 2.1.

One of the remarkable features of (2.6.16) is that among all the residues of the contour, only 4 are primitive one-loop leading singularities—namely, $(2)(3)^2(4)_{45}^{81}$, $(4)(5)^2(6)_{67}^{23}$, $(6)(7)^2(8)_{81}^{45}$, and $(2)(1)(5)(8)_2^7$, of which the first three are cyclic-variants of the function ‘ X ’ of [31], while the last is cyclically-related to ‘ V ’ (see also [10]). All the other residues appearing in (2.6.16) are two-loop leading singularities; these and similar facts were discussed at length in a paper specifically focused on residues in $G(k, n)$ for $k \geq 4$, [24].

One may naturally wonder if there is any similarity between the structure of the tree-contour in (2.6.16) and the even/odd structure of the NMHV contour. In some sense there is: knowing how each of the factors of each f_i contributes to the non-vanishing terms in (2.6.16), we find that the tree-contour can be re-written (somewhat schematically) as,

$$A_8^{(4)} = \left[(2)+(4)+(6)_{81} \right] \left[(5)^3+(7)^5+(1)_2^7+(3)_4+(5)_6 \right] \left[(3)_5+(7)_1+(5)+(7)^4+(3)^8 \right] \left[(4)^{81}+(6)+(8) \right].$$

By expanding this formula and keeping only the terms that are consistent with the constraints implied by the collinearity/coplanarity operators, precisely the 20 terms of the tree-contour given in (2.6.16) are found.

III. Connection to the Twistor String

We can now take our proposal for all N^2 MHV amplitudes and deform it along the lines explained in section 5 in order to get an integral over the Grassmannian localized on C -matrices of the Veronese form. In other words we take

$$A_n^{(4)} = \int_{\mathcal{S}_n^{(4)}=0} \frac{\mathcal{H}_n^{(4)}}{\mathcal{S}_7^{(4)} \cdot \mathcal{S}_8^{(4)} \cdots \mathcal{S}_n^{(4)}}, \tag{2.6.17}$$

where

$$\mathcal{H}_n^{(4)} = \frac{\prod_{j=7}^{n-1} [(1\ 2\ 3\ j)(2\ 3\ j-2\ j-1)(1\ j-2\ j-1\ j)] \prod_{j=4}^{n-3} [(1\ 3\ j\ j+1)(1\ 2\ j\ j+3)(1\ 3\ j\ j+2)(1\ 2\ j\ j+2)]}{(n-1)(1)(3)}, \quad (2.6.18)$$

and $\mathbf{S}_n^{(4)} \equiv \{S_{7_a}^{(4)}, S_{7_b}^{(4)}, \dots, S_{n_a}^{(4)}, S_{n_b}^{(4)}\}$ with

$$\begin{aligned} S_{k_a}^{(4)} \equiv & (k-3\ k-2\ k-1\ k)(k-3\ k\ 1\ 2)(k-3\ 2\ 3\ k-2)(k-3\ k-1\ 1\ 3) \\ & - (k-3\ k-1\ k\ 1)(k-3\ 1\ 2\ 3)(k-3\ 3\ k-2\ k-1)(k-3\ k\ 2\ k-2); \end{aligned} \quad (2.6.19)$$

$$\begin{aligned} \text{and } S_{k_b}^{(4)} \equiv & (1\ k-2\ k-1\ k)(1\ k\ 2\ 3)(1\ 3\ k-3\ k-2)(1\ k-1\ 2\ k-3) \\ & - (1\ k-1\ k\ 2)(1\ 2\ 3\ k-3)(1\ k-3\ k-2\ k-1)(1\ k\ 3\ k-2); \end{aligned}$$

and each $\mathcal{S}_k^{(4)}$ represents the product the two Veronese operators $S_{k_a}^{(4)} \cdot S_{k_b}^{(4)}$.

The natural question at this point is whether this form agrees with the twistor string formula. In order to check this we take the twistor string formula equation (2.3.13) and gauge fix GL_2 using ξ_1, ρ_1, ρ_2 and ρ_3 and gauge fix GL_4 to some link representation. Therefore we get an integral of the form [39]

$$J_{GL_2} \int \frac{d\rho_4 d\rho_5 \cdots d\rho_n}{(\rho_1 - \rho_2)(\rho_2 - \rho_3) \cdots (\rho_n - \rho_1)} \int \prod_{i=2}^n \frac{d\xi_i}{\xi_i} \prod_{i,J} \delta \left(c_{iJ} - \frac{\xi_i \xi_J}{\rho_i - \rho_J} \right) \quad (2.6.20)$$

where $J_{GL_2} = \xi_1(\rho_1 - \rho_2)(\rho_2 - \rho_3)(\rho_3 - \rho_1)$. Here, i runs over four indices (the ones chosen for the link representation), while J runs over the remainder $n - 4$. And we can now expand around any fixed configuration $\widehat{c}_{iJ} = \widehat{\xi}_i \widehat{\xi}_J / (\widehat{\rho}_i - \widehat{\rho}_J)$. In other words, we may take $c_{iJ} = \widehat{c}_{iJ} + h_{iJ}^a \epsilon_a$ where h_{iJ}^a are some generic functions of $\widehat{\rho}$'s and $\widehat{\xi}$'s, where $a = 1, \dots, 2(n-6)$. Now we take the system of $4(n-4)$ equations given by the δ -functions as a system that 'locks' all $2(n-6)$ ϵ 's to zero and all $n-3$ ρ 's and all $n-1$ ξ 's to their hatted values. This means that (2.6.20) becomes

$$\mathcal{I}_{\text{Twistor-String}} \equiv \frac{\widehat{\xi}_1(\widehat{\rho}_1 - \widehat{\rho}_2)(\widehat{\rho}_2 - \widehat{\rho}_3)(\widehat{\rho}_3 - \widehat{\rho}_1)}{(\widehat{\rho}_1 - \widehat{\rho}_2)(\widehat{\rho}_2 - \widehat{\rho}_3) \cdots (\widehat{\rho}_n - \widehat{\rho}_1)} \times J_{4(n-4)}(\widehat{\rho}, \widehat{\xi}, 0), \quad (2.6.21)$$

where $J_{4(n-4)}(\widehat{\rho}, \widehat{\xi})$ is the Jacobian of the $4(n-4)$ equations $E_{iJ} = \widehat{\xi}_i \widehat{\xi}_J / (\widehat{\rho}_i - \widehat{\rho}_J) + h_{iJ}^a \epsilon_a - \frac{\xi_i \xi_J}{\rho_i - \rho_J}$ evaluated on the hatted values and $\epsilon = 0$ —i.e. ,

$$J_{4(n-4)} = \frac{\partial(E_{iJ})}{\partial(\epsilon's, \xi's, \rho's)}. \quad (2.6.22)$$

On the Grassmannian side, we gauge-fix GL_4 in the same way and expand $c_{iJ} = \widehat{c}_{iJ} + h_{iJ}^a \epsilon_a$. Using this expansion, each of the $2(n-6)$ Veronese operators becomes linear in ϵ 's to leading order. Therefore we can evaluate the integral (2.6.17) and obtain

$$\mathcal{I}_G \equiv \mathcal{H}_n^{(4)} \Big|_{c_{iJ}=\widehat{c}_{iJ}} \times J_{2(n-6)}, \quad (2.6.23)$$

where the Jacobian $J_{2(n-6)}$ is given by

$$\frac{\partial(S_{7a}^{(4)}, \dots, S_{n_b}^{(4)})}{\partial(\epsilon_1, \dots, \epsilon_{2(n-6)})} \Big|_{\epsilon=0}. \quad (2.6.24)$$

We have checked that $\mathcal{I}_{\text{Twistor-String}} = \mathcal{I}_G$ for $n = 7, 8, 9$ and 10 . It would be interesting to find a general proof for all n .

2.7 Discussion

The expression for $\mathcal{L}_{n,k}$ as a contour integral over the Grassmannian $G(k, n)$ makes the Yangian symmetry [49] of $\mathcal{N} = 4$ SYM manifest. Since conformal and dual superconformal symmetries act on mutually non-local spaces, it is not surprising that each individual residue of $\mathcal{L}_{n,k}$ does not have a good local space-time interpretation; rather, there is by now a great deal of evidence for the conjecture of [10], that the residues compute leading singularities of scattering amplitudes at all loop orders. Even at tree-level, however, a central issue is to understand how local space-time physics emerges. As we saw in Chapter 1, for the special contours associated with the tree amplitude, a canonical contour deformation can expose the spacetime Lagrangian in light-cone gauge via the CSW/Risager rules. But the more fundamental question remains: what is invariantly special about this contour? Is there a question intrinsic to the Grassmannian that singles it out? In this chapter we have clearly seen the outlines of the answer to this question. Demanding that our integral over $G(k, n)$ has a “particle interpretation” *in the Grassmannian* picks out a contour that gives us the tree amplitudes with a good space-time interpretation. The notion of a particle interpretation in the Grassmannian seems more primitive and fundamental than locality in space-time, since it is formulated in a setting that exhibits all the symmetries of the theory. Unifying the residues of $\Gamma_{n,k}^{\mathcal{L}}$ into a single variety leads to an “add one at a time” particle interpretation which makes the Yangian symmetry manifest. The Veronese particle interpretation is equivalent to the connected prescription

for twistor string theory. Quite beautifully, these apparently different sorts of Grassmannian theories are simply related by a deformation parameter t . The theory at $t = 0$ corresponds directly to the unified form of $\mathcal{L}_{n,k}$ with contour $\Gamma_{n,k}^{\mathcal{L}}$, while the connected prescription amplitude $\mathcal{T}_{n,k}$ corresponds to $t = 1$. Thinking of t as analogous to RG time, $\mathcal{L}_{n,k}$ is like the “ultraviolet” theory, where the full Yangian symmetry is manifest, while $\mathcal{T}_{n,k}$ is akin to the confined description in the infrared, where the “macroscopic” properties of the collection of residues—especially the cyclic symmetries and U_1 -decoupling identities—are manifest. For NMHV amplitudes a simple residue theorem demonstrates t -independence, and we expect a generalization of this argument should be possible for all k . Indeed, while we have restricted our discussion in this chapter to NMHV and N^2 MHV amplitudes, we fully expect the basic physical picture for tree amplitudes we have presented in this chapter to generalize for arbitrary k . A number of new issues arise for $k > 4$ —in particular the distinction between the more natural localization in \mathbb{CP}^{k-1} versus localization in the \mathbb{CP}^3 of twistor space first becomes apparent for $k = 5$ —and we will return to examine these issues in future work.

We have focused exclusively on tree amplitudes in this chapter, yet clearly the most exciting feature of $\mathcal{L}_{n,k}$ is that it contains all-loop information. Can the “particle interpretation” picture in the Grassmannian be generalized to include full loop-level amplitudes, not just leading singularities?

Chapter 3

The Grassmannian and the Twistor String: Unifying all Tree Amplitudes in $\mathcal{N} = 4$

3.1 Introduction

There is now a vast and growing body of evidence to support the duality conjectured by Arkani-Hamed, Cachazo, Cheung and Kaplan [10] between the leading singularities¹ of planar $N^{(k-2)}$ MHV scattering amplitudes in $\mathcal{N} = 4$ super Yang-Mills and certain contour integrals denoted $\mathcal{L}_{n,k}$ over the Grassmannian manifold $G(k, n)$ of k -planes in n -dimensions [10–12, 18, 19, 22–24, 39, 51, 63, 66, 68–71]. Parameterizing $G(k, n)$ in terms of a $k \times n$ matrix $C_{\alpha a}$ —composed of k representative vectors in \mathbb{C}^n which span a given plane— $\mathcal{L}_{n,k}$ is given by

$$\mathcal{L}_{n,k} = \frac{1}{\text{vol}(GL_k)} \oint_{\Gamma_{n,k}} \frac{d^{k \times n} C_{\alpha a}}{(1)(2)(3) \cdots (n-1)(n)} \prod_{\alpha=1}^k \delta^{4|4}(C_{\alpha a} \mathcal{W}_a), \quad (3.1.1)$$

where $a = 1, \dots, n$ labels each particle, each $\mathcal{W}_a \equiv (\tilde{\mu}, \tilde{\lambda} | \tilde{\eta})_a$ denotes a supertwistor which encodes the external momenta and helicities, and ‘ (j) ’ represents the j^{th} $k \times k$ -minor of $C_{\alpha a}$ built out of *consecutive* columns of the matrix $C_{\alpha a}$,²

$$(j) \equiv (j \ j+1 \ \cdots \ j+k-1) \equiv \epsilon^{\alpha_1 \alpha_2 \cdots \alpha_k} C_{\alpha_1 j} C_{\alpha_2 j+1} \cdots C_{\alpha_k j+k-1}. \quad (3.1.2)$$

Of course, as a contour integral, equation (3.1.1) is nothing but the sum of the residues of the poles ‘encompassed’ by the contour of integration $\Gamma_{n,k}$. The combinations of residues which compute tree amplitudes can be obtained by a variety of field-theoretic

¹Leading singularities are L -loop integrals in field-theory evaluated along T^{4L} -contours which put $4L$ internal propagators on-shell.

²We will often use a single label—e.g. ‘(1)’—to denote a *consecutive* minor beginning with the indicated column. More generally, a $k \times k$ minor constructed out of columns $[\ell_1, \dots, \ell_k]$ $C_{\alpha a}$ will be denoted $(\ell_1 \dots \ell_k)$.

techniques, including the BCFW recursion relations [7,31] (which can be efficiently translated in terms of the residues of $\mathcal{L}_{n,k}$, [22–24], including the form derived from BCFW in [50]). It was not until recently, however, that the contours $\Gamma_{n,k}$ which compute tree amplitudes in $\mathcal{L}_{n,k}$ were understood in a way purely intrinsic to the Grassmannian. This understanding made manifest a deep connection between the Grassmannian integral $\mathcal{L}_{n,k}$ and Witten’s twistor string theory. Because this connection is crucial to our main result, we briefly review it here before presenting our proposal for the contours which give all tree amplitudes in $\mathcal{N} = 4$ super Yang-Mills.

Amplitudes in Witten’s twistor string theory [4] can be computed via the ‘connected prescription’ written down by Roiban, Spradlin and one of the authors in [52, 53, 53] as integrals of an open string correlator over the moduli space of curves in a supertwistor space. Although geometrically very beautiful, these integrals turned out to be technically very difficult to evaluate because of the presence of highly non-linear equations. Using the link variables described in [39, 63], Dolan and Goddard [63] wrote contour integrals which compute all tree amplitudes as rational functions, and checked explicitly that these lead to the correct formulae for many particular amplitudes (see also [39]), and for all split-helicity amplitudes in [70]. The key insight of Dolan and Goddard was to use a sequence of global residue theorems³ which connect the connected prescription contours to $\mathcal{L}_{n,k}$. Significantly, the twistor string construction—especially when expressed in the framework of the connected prescription—carries with it the knowledge of a natural, preferred choice of integration contour which computes each tree amplitude. But only by combining the connected prescription with the particle interpretation described in Chapter 2 does this preferred contour become computationally tractable.

The equivalence between the connected prescription for the twistor string and $\mathcal{L}_{n,k}$ was recently proven for all NMHV amplitudes in [12, 66]. These proofs rely on repeated use of the global residue theorem, and show that the combination of residues contributing to any NMHV amplitude computed via the twistor string can be re-expressed as a direct sum of residues of $\mathcal{L}_{n,k}$. Moreover, an amazing and much stronger property was observed: the two integrands were in fact related by a *smooth deformation* which interpolates between the connected prescription of twistor string theory and the Grassmannian integrand of $\mathcal{L}_{n,k}$.

³The global residue theorem is the multi-dimensional generalization of Cauchy’s theorem for ordinary contour integrals in one complex dimension (see, e.g. [65]).

The deformation connecting the two descriptions moves the locations of each pole, and changes the value of each residue; but the sum of residues which define the tree amplitude is itself found to be invariant. Taking together the results of [12, 66], that the twistor string connected prescription provides a preferred choice of integration contour and that its integrand may be smoothly deformed to the integrand $\mathcal{L}_{n,k}$, we conclude therefore that the twistor string may be used to generally answer the important open question of determining the appropriate contours in the Grassmannian for computing general tree-amplitudes in $\mathcal{N} = 4$ super Yang-Mills. For this to be the case, it is necessary that the contour given for the connected prescription continue to make manifest the connection between the twistor string and the Grassmannian through a contour deformation similar to that described in [12, 66] for NMHV amplitudes.

In this chapter, we propose a new, explicit formula for all $N^{(k-2)}$ MHV tree amplitudes in $\mathcal{N} = 4$, generalizing the NMHV results of [12, 66]. In section 2 we will present our main formula, equation (3.2.3), and discuss its smooth deformation to a contour in $\mathcal{L}_{n,k}$. In section 3 we will describe how this formula can be obtained by iteratively ‘adding particles’ in a natural way to the first non-trivial tree amplitude, the 6-point NMHV amplitude, while making sure that soft limits and parity are manifest at every stage. In section 4 we will make a series of transformations to map our formula to that of [63], thereby deriving it from twistor string connected prescription.

3.2 All Tree Amplitudes in $\mathcal{N} = 4$ superYang-Mills

We propose that the general, tree-level, planar, color-stripped, n -point $N^{(k-2)}$ MHV amplitude is given by

$$\mathcal{A}_n^{(k)} = \frac{1}{\text{vol}(GL_k)} \oint_{\mathcal{F}_n^{(k)} = \vec{0}} \frac{dC_{\alpha a} \mathcal{H}_n^{(k)}}{(n-1)(1)(3) \mathcal{F}_n^{(k)}} \prod_{\alpha=1}^k \delta^{4|4}(C_{\alpha a} \mathcal{W}_a), \quad (3.2.3)$$

where the contour $\mathcal{F}_n^{(k)} = \vec{0}$ is the zero-locus of $\mathcal{F}_n^{(k)} : \mathbb{C}^{(n-k-2)(k-2)} \rightarrow \mathbb{C}^{(n-k-2)(k-2)}$, defined in terms of the $(n-k-2)(k-2)$ Veronese maps F_ℓ^j ,

$$\mathcal{F}_n^{(k)} \equiv \prod_{\ell=k+3}^n \left(\prod_{j=1}^{k-2} F_\ell^j \right), \quad (3.2.4)$$

where each F_ℓ^j can be written in terms of the minors of $C_{\alpha a}$ according to

$$\begin{aligned} F_\ell^j \equiv & (\sigma_\ell^j \ell-2 \ell-1 \ell) (\sigma_\ell^j \ell j j+1) (\sigma_\ell^j j+1 j+2 \ell-2) (\sigma_\ell^j \ell-1 j j+2) \\ & - (\sigma_\ell^j j j+1 j+2) (\sigma_\ell^j j+2 \ell-2 \ell-1) (\sigma_\ell^j \ell-1 \ell j) (\sigma_\ell^j j+1 \ell-2 \ell), \end{aligned} \quad (3.2.5)$$

with σ_ℓ^j representing collectively the columns $[1, \dots, j-1] \cup [j+\ell-k, \dots, \ell-3]$ of $C_{\alpha a}$, and where $\mathcal{H}_n^{(k)}$ is the product of all the *non-consecutive* minors in the *first line* of equation (3.2.5); explicitly,

$$\begin{aligned} \mathcal{H}_n^{(k)} = & \mathcal{H}_{n-1}^{(k)} \times (\sigma_{n-1}^{k-2} n-1 k-2 k-1) \\ & \times \prod_{j=1}^{k-3} [(\sigma_n^j n j j+1)(\sigma_{n-1}^{j+1} n-3 n-2 n-1)] \prod_{j=1}^{k-2} [(\sigma_n^j n-1 j j+2)(\sigma_n^j j+1 j+2 n-2)]. \end{aligned}$$

Noticing that all the minors appearing in a given map F_ℓ^j involve the same set of columns σ_ℓ^j , and that the rest are organized according to a ‘ 3×3 ’ Veronese operator, we may encode the structure of equation (3.2.5) by writing⁴

$$\begin{aligned} F_\ell^j \equiv & \sigma_\ell^j \bowtie S_{\ell-2 \ell-1 \ell j j+1 j+2}, \\ & \equiv \left([1, \dots, j-1] \cup [j+\ell-k, \dots, \ell-3] \right) \bowtie S_{\ell-2 \ell-1 \ell j j+1 j+2}, \end{aligned} \quad (3.2.6)$$

where S_{abcdef} represents the primitive Veronese operator which, when acting on \mathbb{P}^2 , tests if the six points a, \dots, e lie on a conic,

$$S_{abcdef} \equiv (abc)(cde)(efa)(bdf) - (bcd)(def)(fab)(cea). \quad (3.2.7)$$

⁴This simplified notation can be justified by observing that only 6 of the $k+3$ columns which are relevant to a given Veronese operator F_ℓ^j change from one term to another.

As will be described below, the structure of the numerators $\mathcal{H}_n^{(k)}$ is dictated entirely by the proposed duality between equation (3.2.3) and a related expression in $\mathcal{L}_{n,k}$. Following the theme of [12, 66], let us introduce a deformation parameter t_ℓ^j for each map F_ℓ^j ,

$$F_\ell^j(t_\ell^j) \equiv \begin{aligned} & (\sigma_\ell^j \ell-2 \ell-1 \ell) (\sigma_\ell^j \ell j j+1) (\sigma_\ell^j j+1 j+2 \ell-2) (\sigma_\ell^j \ell-1 j j+2) \\ & - t_\ell^j (\sigma_\ell^j j j+1 j+2) (\sigma_\ell^j j+2 \ell-2 \ell-1) (\sigma_\ell^j \ell-1 \ell j) (\sigma_\ell^j j+1 \ell-2 \ell). \end{aligned} \quad (3.2.8)$$

Then the integral $\mathcal{A}_n^{(k)}(t_\ell^j)$, with all F_ℓ^j in (3.2.3) replaced by $F_\ell^j(t_\ell^j)$, will map precisely to the one appearing for $\mathcal{L}_{n,k}$ in limit of $t_\ell^j \rightarrow 0$ for all ℓ, j . This is because, together with the three minors manifest in equation (3.2.3) (namely, $(n-1)$, (1) , and (3)) the factors which constitute $\mathcal{F}_n^{(k)}(t_\ell^j)$ when $t_\ell^j \rightarrow 0$ will contribute exactly one copy of each of the consecutive minors present in the measure of the integral $\mathcal{L}_{n,k}$:

$$\mathcal{F}_n^{(k)} = \underbrace{\left(F_{k+3}^1 \cdots F_{k+3}^{k-2} \right)}_{(2),(4)} \underbrace{\left(F_{k+4}^1 \cdots F_{k+4}^{k-2} \right)}_{(5)} \underbrace{\left(F_{k+5}^1 \cdots F_{k+5}^{k-2} \right)}_{(6)} \cdots \underbrace{\left(F_{n-1}^1 \cdots F_{n-1}^{k-2} \right)}_{(n-k)} \underbrace{\left(F_n^1 \cdots F_n^{k-2} \right)}_{(n-k+1), \dots, (n-2), (n)}.$$

And since $\mathcal{H}_n^{(k)}$ is composed of all the *non-consecutive* minors present in the *first* factors of each F_ℓ^j , we have that

$$\lim_{t_\ell^j \rightarrow 0} \left(\frac{\mathcal{H}_n^{(k)}}{(n-1)(1)(3) \mathcal{F}_n^{(k)}} \right) = \frac{1}{(n-1)(1)(3)} \frac{1}{(2)(4)(5) \cdots (n-3)(n-2)(n)}, \quad (3.2.9)$$

making the connection between the twistor string and $\mathcal{L}_{n,k}$ manifest.

We strongly suspect that formula (3.2.3) is unchanged by any of the deformations introduced by the parameters t_ℓ^j in (3.2.8). For NMHV amplitudes, t_ℓ^j -independence has been rigorously proven by a direct application of the global residue theorem, [12, 66], and we suspect that similar arguments can be used to prove t_ℓ^j -independence more generally. We have checked this numerically for several nontrivial N²MHV amplitudes, including the alternating-helicity amplitude for eight gluons, but we leave the question of proving complete t_ℓ^j -independence to future researches.

Let us end this section by presenting explicitly the $t_\ell^j \rightarrow 0$ limit of the deformed twistor-string contour (3.2.3), illustrating some of the key differences between the two formulations. When $t_\ell^j \rightarrow 0$, each Veronese operator factorizes into the product of the four minors listed in the first line of (3.2.8). In general, all but $n-3$ of these factors will be non-consecutive, and therefore are included among the factors of the numerator $\mathcal{H}_n^{(k)}$.

Although it is generally ill-advised to ‘cancel terms’ between the contour-defining maps defining $\mathcal{F}_n^{(k)}$ and the numerator, there is a good physical reason for suspecting that the ‘fourth’ minors of each of the $F_\ell^j(t_\ell^j \rightarrow 0)$ —which are never consecutive—contribute no non-vanishing residues to the contour.⁵ As described in [12, 51], CSW operators, when translated into the Grassmannian, are constructed from products of three minors. Although beyond the scope of the present discussion, ensuring that each pole of the integrand is composed of three-minor operators helps one to connect the CSW, or ‘disconnected’, support of tree amplitudes to the ‘connected’ support of the twistor string through a series of global residue theorems. At any rate, there is now enough direct evidence that general tree-contours are entirely supported on the vanishing first three factors of each F_ℓ^j when $t_\ell^j \rightarrow 0$ to justify the simplification to a ‘3-minor’ form of each map in the contour.

Taking each $t_\ell^j \rightarrow 0$, the twistor-string contour $\mathcal{A}_n^{(k)}(t_\ell^j)$ becomes,

$$\mathcal{A}_n^{(k)}(t_\ell^j) \xrightarrow[t_\ell^j \rightarrow 0]{} \mathcal{A}_n^{(k)} = \frac{1}{\text{vol}(GL_k)} \oint_{\mathcal{F}_n^{(k)} = \vec{0}} \frac{dC_{\alpha a} \mathcal{H}_n^{(k)}}{(n-1)(1)(3) \mathcal{F}_n^{(k)}} \prod_{\alpha=1}^k \delta^{4|4}(C_{\alpha a} \mathcal{W}_a), \quad (3.2.10)$$

where

$$\mathcal{F}_n^{(k)} \equiv \prod_{\ell=k+3}^n \left(\prod_{j=1}^{k-2} f_\ell^j \right) \quad \text{with} \quad f_\ell^j \equiv \sigma_\ell^j \bowtie (\ell-2 \ \ell-1 \ \ell) (\ell \ j \ j+1) (j+1 \ j+2 \ \ell-2), \quad (3.2.11)$$

with σ_ℓ^j as before, and where

$$\mathcal{H}_n^{(k)} = \frac{\mathcal{H}_n^{(k)}}{\prod_{\ell=k+3}^n \prod_{j=1}^{k-2} (\sigma_\ell^j \ \ell-1 \ j \ j+2)}, \quad (3.2.12)$$

which, as before, represents the product of all non-consecutive minors among the maps f_ℓ^j .

Alternatively, we could have started with formula (3.2.10) for $\mathcal{A}_n^{(k)}$ and obtained formula (3.2.3) for $\mathcal{A}_n^{(k)}$ by ‘adding a missing minor’ to each map of f according to

$$\begin{aligned} f &= \sigma \bowtie (abc)(cde)(efa) \\ \Rightarrow F &= \sigma \bowtie [(abc)(cde)(efa)(bdf) - (bcd)(def)(fab)(cea)], \end{aligned} \quad (3.2.13)$$

⁵The reason why naïve cancellation of factors between $\mathcal{H}_n^{(k)}$ and those in $\mathcal{F}_n^{(k)}(t_\ell^j \rightarrow 0)$ can be misleading is described with several examples in Chapter 2; for example, even the poles supported by purely non-consecutive minors of the F_ℓ^j ’s can have the interpretation of being supported by consecutive minors, and thereby contributing a residue to the contour.

in order to supply a simple geometric meaning to the contour—the maps F 's having the natural interpretation of testing the localization of points in $\mathbb{P}^{(k-1)}$.

Both formulae give all tree-level amplitudes in $\mathcal{N} = 4$ super Yang-Mills in terms of a specific contour integral. The first one, equation (3.2.3), naturally arises from twistor string theory, and its contour $\mathcal{F}_n^{(k)} = \vec{0}$ has a nice geometric meaning: it is the constraint for n points to lie on a degree- $(k-1)$ curve in twistor space. On the other hand, the formula (3.2.10) provides the integration contour for Grassmannian $\mathcal{L}_{n,k}$, and thereby ensures that each contribution is itself manifestly Yangian invariant.

3.3 Building the Contour one Particle at a Time

In this section we describe how the general contour for any tree amplitude (3.2.3) can be obtained by sequentially extending the contour of the first non-trivial amplitude, the 6-point NMHV amplitude, by adding one particle at a time. Before doing so, however, it will be useful to briefly discuss some of the generally-desirable features that any such contour-prescription should have.

Let us consider what would be necessary to extend a formula valid for $\mathcal{L}_{n-1,k}$ to one valid for $\mathcal{L}_{n,k}$ while keeping k fixed. Recall that the integral $\mathcal{L}_{n,k}$'s measure is given by the product of the n consecutive $k \times k$ minors of $C_{\alpha a}$. The n^{th} particle, being represented by the n^{th} column of $C_{\alpha a}$ participates in k of these consecutive minors; and these k minors, taken together, span a range of $\min(n, 2k-1)$ columns of $C_{\alpha a}$. This suggests that, fixing k , only for $n \geq 2k-1$ will a tree contour be sufficiently general to have a natural extension to all n . Conveniently however, the $n = (2k-1)$ -point N^{k-2} MHV amplitude, $\mathcal{A}_{n=2k-1}^{(k)}$, is nothing but the parity-conjugate of the n -point N^{k-3} MHV amplitude, $\mathcal{A}_{n=2k-1}^{(k-1)}$, allowing it to be uniquely related to a contour with strictly lower- k . And so we should not be too surprised that it is possible to ‘bootstrap’ a formula valid for any fixed k to one valid for all k , using parity when $n = 2k-1$ as the bridge which connects each k to $k+1$.

Just as there are several equally-valid formulae for the general NMHV tree contour (see, e.g. [12, 39, 63, 66]), there are several ways of writing the general $N^{(k-2)}$ MHV tree contour. The one that we derive here is obtained by starting with the particular NMHV tree contour given in Chapter 2 and extending it in such a way that the general contour prescription is invariant under parity for all n, k . As we will see, these criteria lead

uniquely to the contour given here which defines our general result given in equation (3.2.3).⁶

I. NMHV amplitudes

Let us begin with the simplest amplitude which requires a non-trivial contour to be specified. The 6-point NMHV amplitude's contour is essentially unique up to a global residue theorem, and can be written [10, 12, 39, 63, 66],

$$\mathcal{A}_6^{(3)} = \frac{1}{\text{vol}(GL_3)} \oint_{\mathcal{F}_6^{(3)}=\vec{0}} dC_{\alpha a} \frac{\mathcal{H}_6^{(3)}}{(5)(1)(3) \mathcal{F}_6^{(3)}} \prod_{\alpha=1}^3 \delta^{4|4}(C_{\alpha a} \mathcal{W}_a), \quad (3.3.14)$$

where

$$\mathcal{F}_6^{(3)} = \left[(4)(6)(2)(135) - (561)(123)(345)(624) \right] = S_{456123} \quad (3.3.15)$$

$$\text{and } \mathcal{H}_6^{(3)} = (135).$$

(Here, we have chosen to de-emphasize the minors which do not appear in the analogous expressions for $\mathcal{L}_{n,k}$ by colouring them grey, and we have chosen to highlight each of the *consecutive* minors which participate in the contour by colouring them red. This highlighting will be useful when we consider amplitudes involving more particles and with $k > 3$.)

As demonstrated in Chapter 2, this contour can be extended to all NMHV amplitudes in the following way,

$$\mathcal{A}_n^{(3)} = \frac{1}{\text{vol}(GL_3)} \oint_{\mathcal{F}_n^{(3)}=\vec{0}} dC_{\alpha a} \frac{\prod_{\ell=6}^{n-1} [(12\ell)(23\ell-1)] \prod_{\ell=6}^n [(13\ell-1)]}{(n-1)(1)(3) \mathcal{F}_n^{(3)}} \prod_{\alpha=1}^3 \delta^{4|4}(C_{\alpha a} \mathcal{W}_a), \quad (3.3.16)$$

where

$$\begin{aligned} \mathcal{F}_n^{(3)} &= \prod_{\ell=6}^n \left[(\ell-2 \ell-1 \ell)(\ell 1 2)(2 3 \ell-2)(\ell-1 1 3) - (\ell-1 \ell 1)(1 2 3)(3 \ell-2 \ell-1)(\ell 2 \ell-1) \right] \\ &= \prod_{\ell=6}^n S_{\ell-2 \ell-1 \ell 1 2 3}. \end{aligned}$$

⁶We have also found other parity-symmetric contour prescriptions by starting from each of the different forms of the NMHV tree amplitude. We have checked that each of these extensions to all n, k is unique and that each leads to correct formulae for general tree amplitudes. In addition, there are further possibilities if one foregoes the connection between $\mathcal{L}_{n,k}$ and the twistor string, but these will not be considered here.

Notice that the only operator that involves particle n is the last, $F_{\ell=n}^{j=1}$, and this operator includes in general all but one of the consecutive minors which involve column n —namely, all but minor $(n-1)$. Indeed, each F_ℓ^1 can be seen as an operator which adds particle ℓ to the $(\ell-1)$ -point contour.

Consider for example the contour for $n=7$,

$$\mathcal{F}_7^{(3)} = \left\{ \begin{array}{l} F_6^1 = (4) \quad (612) \quad (2) \quad (513) - (561)(123)(345)(624) = S_{456123} \\ F_7^1 = (5) \quad (7) \quad (235)(613) - (671)(123)(356)(725) = S_{567123} \end{array} \right\}. \quad (3.3.17)$$

By recognizing that $\mathcal{A}_7^{(3)}$ is nothing but the parity-conjugate of $\mathcal{A}_7^{(4)}$, we may use this contour to directly obtain the contour of the first non-trivial N²MHV tree-amplitude.

II. N²MHV Amplitudes

As mentioned above, because the parity-conjugate⁷ of the 7-point NMHV amplitude is the 7-point N²MHV amplitude, we may use the general NMHV contour to obtain our first non-trivial contour for $k=4$,

$$\mathcal{F}_7^{(4)} = \widetilde{\mathcal{F}_7^{(3)}} = \left\{ \begin{array}{l} F_7^1 = (4) \quad (4712) \quad (2) \quad (4613) - (4123)(4356)(4671)(4268) = [4] \bowtie S_{567123} \\ F_7^2 = (5) \quad (7) \quad (1345)(1624) - (1234)(1456)(1672)(1357) = [1] \bowtie S_{567234} \end{array} \right\}.$$

From here, there are several ways in which the above contour can be extended to one for all n . For example, one could make the identification made in Chapter 2, that

$$F_7^{1,2} = \left\{ \begin{array}{l} [4] \bowtie S_{567123} \\ [1] \bowtie S_{567234} \end{array} \right\} \implies F_\ell^{1,2} \Leftrightarrow \left\{ \begin{array}{l} [\ell-3] \bowtie S_{\ell-2 \ell-1 \ell 1 2 3} \\ [1] \bowtie S_{\ell-2 \ell-1 \ell 2 3 \ell-3} \end{array} \right\}. \quad (3.3.18)$$

However, this extension of the 7-point N²MHV amplitude leads to a form of the 8-point N²MHV contour which is not manifestly self-conjugate under parity, and which therefore unnecessarily obfuscates the extension to all N^(k-2)MHV amplitudes.⁸ We suggest that the following extension is more natural,

$$F_7^{1,2} = \left\{ \begin{array}{l} [4] \bowtie S_{567123} \\ [1] \bowtie S_{567234} \end{array} \right\} \implies F_\ell^{1,2} \Leftrightarrow \left\{ \begin{array}{l} [\ell-3] \bowtie S_{\ell-2 \ell-1 \ell 1 2 3} \\ [1] \bowtie S_{\ell-2 \ell-1 \ell 2 3 4} \end{array} \right\}. \quad (3.3.19)$$

⁷Here, we should point out that we are using a definition of ‘parity’ that both exchanges the column-labels of each minor with their complements, and maps each column $j \mapsto (n+1) - j$. This appears to be the most natural definition of parity in the Grassmannian.

⁸That being said, we have every reason to suspect the formula given in Chapter 2 is in fact just as correct as the one we present here.

Notice that the only difference between the contour prescriptions in (3.3.18) and (3.3.19) is that the former associates S_{567234} with $S_{\ell-2\ell-1\ell23\ell-3}$ while the latter associates S_{567234} with $S_{\ell-2\ell-1\ell234}$.

Using this prescription, we find that the 8-point N²MHV may be written,

$$\mathcal{A}_8^{(4)} = \frac{1}{\text{vol}(GL_4)} \oint_{\mathcal{F}_8^{(4)}=\vec{0}} \frac{dC_{\alpha a} \mathcal{H}_8^{(4)}}{(7)(1)(3) \mathcal{F}_8^{(4)}} \prod_{\alpha=1}^4 \delta^{4|4}(C_{\alpha a} \mathcal{W}_a), \quad (3.3.20)$$

where $\mathcal{F}_8^{(4)} = F_7^1 F_7^2 \cdot F_8^1 F_8^2$ with the F_ℓ^j given explicitly by⁹

$$\mathcal{F}_8^{(4)} = \left\{ \begin{array}{l} F_7^1 = (4) \quad (4712) \quad (2) \quad (4613) - (4123)(4356)(4671)(4268) = [4] \bowtie S_{567123} \\ F_7^2 = (1567)(1237)(1345)(1624) - (1234)(1456)(1672)(1357) = [1] \bowtie S_{567234} \\ F_8^1 = (5) \quad (5812)(5623)(5713) - (5123)(5367)(5781)(5268) = [5] \bowtie S_{678123} \\ F_8^2 = (6) \quad (8) \quad (1346)(1724) - (1234)(1467)(1782)(1368) = [1] \bowtie S_{678234} \end{array} \right\} \quad (3.3.21)$$

and $\mathcal{H}_8^{(4)}$ is the product of all *non-consecutive* minors of the first factors of the F_ℓ^j 's,

$$\begin{aligned} \mathcal{H}_8^{(4)} = & (4712)(1567)(1237)(1345)(5812)(5623)(1346) \\ & \times (4613)(1624)(5713)(1724). \end{aligned} \quad (3.3.22)$$

It is not hard to see that this contour is manifestly parity self-conjugate. (We should point out that this contour differs from the one given in Chapter 2 by only single minor appearing in F_8^2 ; however, this minor difference turns out to leave essentially all the geometry problems described in Chapter 2 unchanged, and so the contour (3.3.21) leads to precisely the same sum of twenty residues described in Chapter 2, and therefore reproduces the correct 8-point N²MHV tree amplitude for all helicity configurations.)

As a further test of the validity of our contour prescription, let us briefly mention the tree-amplitude obtained for the 9-point N²MHV amplitude. As above, we may write,

$$\mathcal{A}_9^{(4)} = \frac{1}{\text{vol}(GL_4)} \oint_{\mathcal{F}_9^{(4)}=\vec{0}} \frac{dC_{\alpha a} \mathcal{H}_9^{(4)}}{(8)(1)(3) \mathcal{F}_9^{(4)}} \prod_{\alpha=1}^4 \delta^{4|4}(C_{\alpha a} \mathcal{W}_a), \quad (3.3.23)$$

⁹Here, we have highlighted each of the primary ‘consecutive subparts’ of each of the minors in the contour by colouring them blue. These tend to be the most important minors when computing a tree amplitude as a series of ‘geometry problems’ as described in Chapter 2.

where $\mathcal{F}_9^{(4)} = F_7^1 F_7^2 \cdot F_8^1 F_8^2 \cdot F_9^1 F_9^2$ with each F_ℓ^j given explicitly by,

$$\mathcal{F}_9^{(4)} = \left\{ \begin{array}{l} F_7^1 = (4) \quad (4712) \quad (2) \quad (4613) - (4671)(4123)(4356)(4725) = [4] \rtimes S_{567123} \\ F_7^2 = (1567)(1237)(1345)(1246) - (1672)(1234)(1456)(1735) = [1] \rtimes S_{567234} \\ F_8^1 = (5) \quad (5812)(5623)(5713) - (5781)(5123)(5367)(5826) = [5] \rtimes S_{678123} \\ F_8^2 = (1678)(1238)(1346)(1247) - (1782)(1234)(1467)(1836) = [1] \rtimes S_{678234} \\ F_9^1 = (6) \quad (6912)(6723)(6813) - (6891)(6123)(6378)(6927) = [6] \rtimes S_{789123} \\ F_9^2 = (7) \quad (9) \quad (1347)(1824) - (1892)(1234)(1478)(1937) = [1] \rtimes S_{789234} \end{array} \right. , \quad (3.3.24)$$

Deforming this contour from the twistor string to $\mathcal{L}_{9,4}$ by sending each $t_\ell^j \rightarrow 0$ —removing all the contributions shown in coloured grey in (3.3.24)—the problem of computing the tree-amplitude reduces to a series of ‘geometry problems’—finding the localization in the Grassmannian induced by requiring that each of the six maps f_ℓ^j vanish, and determining which of these configurations are supported entirely by the vanishing of consecutive minors.¹⁰ The six maps f_ℓ^j are given explicitly by,

$$\mathcal{F}_9^{(4)} = \left\{ \begin{array}{l} f_7^1 = (4) \quad (4712) \quad (2) \\ f_7^2 = (1567)(1237)(1345) \end{array} \right\} \cup \left\{ \begin{array}{l} f_8^1 = (5) \quad (5812)(5623) \\ f_8^2 = (1678)(1238)(1346) \end{array} \right\} \cup \left\{ \begin{array}{l} f_9^1 = (6)(6912)(6723) \\ f_9^2 = (7) \quad (9) \quad (1347) \end{array} \right\}. \quad (3.3.25)$$

We have found that there are precisely 50 non-vanishing, consecutively-supported residues along the contour (3.3.24) and that these residues perfectly reproduce the fully-supersymmetric 9-point N²MHV tree amplitude.

These 50 residues, together with the ‘geometry problems’ giving rise to each, are collected in appendix B, where we have followed the conventions of Chapter 2 for the naming of each residue according to its localization in $C_{\alpha a}$.

III. N³MHV Amplitudes and Beyond

As was the case for the 7-point amplitude, the parity conjugate of the 9-point N²NHV amplitude represents the first sufficiently-general N³MHV amplitude from which we may ‘bootstrap’ the general N³MHV result. We will see that by requiring the 9-point N³MHV amplitude to be iteratively-related to the 8-point N³MHV amplitude—itsself obtained as

¹⁰Any configuration along the contour not entirely supported by consecutive minors will have vanishing residue because of the non-consecutive minors which constitute $\mathcal{H}_9^{(4)}$.

the parity-conjugate of the 8-point NMHV amplitude—will uniquely fix the structure of the ansatz for all further amplitudes in $\mathcal{N} = 4$ super Yang-Mills.

Taking the parity-conjugate of the 9-point $k = 4$ contour (3.3.24), we find,

$$\mathcal{F}_9^{(5)} = \widetilde{\mathcal{F}_9^{(4)}} = \left\{ \begin{array}{l} F_8^1 = [45] \bowtie S_{678123} \\ F_8^2 = [15] \bowtie S_{678234} \\ F_8^3 = [12] \bowtie S_{678345} \end{array} \right\} \cup \left\{ \begin{array}{l} F_9^1 = [56] \bowtie S_{789123} \\ F_9^2 = [16] \bowtie S_{789234} \\ F_9^3 = [12] \bowtie S_{789345} \end{array} \right\}. \quad (3.3.26)$$

Notice that only the last three F_ℓ^j 's—those of the second set above—involve column 9. Moreover, all of the F_ℓ^j 's for $\ell = 8$ involve column 8. Therefore, the requirement that the 9-point N³MHV contour is the extension of the 8-point N³MHV contour, uniquely fixes the ℓ -dependence of the maps F_ℓ^j . With this, it is not hard to see that the general solution for all N³MHV amplitudes must be given by

$$\mathcal{F}_n^{(5)} = \prod_{\ell=8}^n (F_\ell^1 \cdot F_\ell^2 \cdot F_\ell^3), \quad \text{with} \quad \left\{ \begin{array}{l} F_\ell^1 = [\ell-4 \ell-3] \bowtie S_{\ell-2 \ell-1 \ell 1 2 3} \\ F_\ell^2 = [1 \ell-3] \bowtie S_{\ell-2 \ell-1 \ell 2 3 4} \\ F_\ell^3 = [1 2] \bowtie S_{\ell-2 \ell-1 \ell 3 4 5} \end{array} \right\}. \quad (3.3.27)$$

As one further, concrete illustration of this prescription for the tree-amplitude contour, let us briefly consider the 10-point N³MHV amplitude,

$$\mathcal{A}_{10}^{(5)} = \frac{1}{\text{vol}(GL_5)} \oint_{\mathcal{F}_{10}^{(5)} = \vec{0}} \frac{dC_{\alpha a} \mathcal{H}_{10}^{(5)}}{(9)(1)(3) \mathcal{F}_{10}^{(5)}} \prod_{\alpha=1}^5 \delta^{4|4} (C_{\alpha a} \mathcal{W}_a), \quad (3.3.28)$$

where $\mathcal{F}_{10}^{(5)} = F_8^1 F_8^2 F_8^3 \cdot F_9^1 F_9^2 F_9^3 \cdot F_{10}^1 F_{10}^2 F_{10}^3$, and with each F_ℓ^j given by

$$\mathcal{F}_{10}^{(5)} = \left\{ \begin{array}{l} F_8^1 = (4) \quad (45812) \quad (2) \quad (45713) - (45123)(45367)(45781)(45268) = [45] \bowtie S_{678123} \\ F_8^2 = (15678)(12358)(13456)(15724) - (15234)(15467)(15782)(15368) = [15] \bowtie S_{678234} \\ F_8^3 = (12678)(12348)(12456)(12735) - (12345)(12567)(12783)(12468) = [12] \bowtie S_{678345} \\ F_9^1 = (5) \quad (56912)(23567)(56813) - (56123)(56378)(56891)(56279) = [56] \bowtie S_{789123} \\ F_9^2 = (16789)(12369)(13467)(16824) - (16234)(16478)(16892)(16379) = [16] \bowtie S_{789234} \\ F_9^3 = (12789)(12349)(12457)(12835) - (12345)(12578)(12893)(12479) = [12] \bowtie S_{789345} \\ F_{10}^1 = (6) \quad (671012)(23678)(67913) - (67123)(67389)(679101)(672810) = [67] \bowtie S_{8910123} \\ F_{10}^2 = (7) \quad (710123)(13478)(17924) - (17234)(17489)(179102)(173810) = [17] \bowtie S_{8910234} \\ F_{10}^3 = (8) \quad (10) \quad (12458)(12935) - (12345)(12589)(129103)(124810) = [12] \bowtie S_{8910345} \end{array} \right.$$

where again $\mathcal{H}_{10}^{(5)}$ can be simply read-off from F_ℓ^j 's:

$$\begin{aligned} \mathcal{H}_{10}^{(5)} = & (45812)(15678)(15823)(15346)(12678)(12834)(12456) \\ & \times (56912)(56237)(16789)(16923)(16347)(12789)(12934) \\ & \times (12457)(671012)(67238)(171023)(17348)(12458) \\ & \times (45713)(15724)(12735)(56813)(16824)(12835)(67913)(17924)(12935). \end{aligned}$$

Although it would require more space than warranted by an appendix, we have explicitly verified that the contour above includes 175 non-vanishing residues which precisely matches the general, 10-point N^3 MHV amplitude.

Continuing in this manner, we arrive at the general formula (3.2.3),

$$\mathcal{A}_n^{(k)} = \frac{1}{\text{vol}(GL_k)} \oint_{\mathcal{F}_n^{(k)} = \bar{0}} \frac{dC_{\alpha a} \mathcal{H}_n^{(k)}}{(n-1)(1)(3) \mathcal{F}_n^{(k)}} \prod_{\alpha=1}^k \delta^{4|4} (C_{\alpha a} \mathcal{W}_a),$$

where $\mathcal{F}_n^{(k)} = (F_{k+3}^1 \cdots F_{k+3}^{k-2}) \cdot (F_{k+4}^1 \cdots F_{k+4}^{k-2}) \cdots (F_n^1 \cdots F_n^{k-2})$ with each F_ℓ^j given by

$$F_\ell^j \equiv \sigma_\ell^j \bowtie S_{\ell-2 \ell-1 \ell j j+1 j+2}. \quad (3.3.29)$$

IV. General Properties of the Result

Parity

One of the important features of the general contour obtained in the previous subsections is that it is manifestly parity-symmetric. By this, we mean that the parity-conjugate of a given amplitude's contour is the contour for the parity-conjugate amplitude. For example, for all $n = 2k$, the contour given by $\mathcal{F}_{n=2k}^{(k)}$ is manifestly parity self-conjugate.

To see how this works more generally, consider the role played by each of the n columns of the Grassmannian $C_{\alpha a}$ in the definition of the Veronese map $F_\ell^j \equiv \sigma_\ell^j \bowtie S_{\ell-2 \ell-1 \ell j j+1 j+2}$. In general, the n columns break into six contiguous groups,

$$\underbrace{[1 \ 2 \ \cdots \ j-1]}_{\in \sigma_\ell^j} \underbrace{[j \ j+1 \ j+2]}_{\in S} [j+3 \ \cdots \ j+(k-\ell)-1] \underbrace{[j+(k-\ell) \ \cdots \ \ell-3]}_{\in \sigma_\ell^j} \underbrace{[\ell-2 \ \ell-1 \ \ell]}_{\in S} [\ell+1 \ \cdots \ n],$$

where the columns of $C_{\alpha a}$ which do not participate at all in F_ℓ^j have been coloured grey to emphasize the 'gaps' in the roles played by various columns. Importantly, parity does

not change the ‘contiguousness’ of these six groups, or the roles they played by the six columns of the primitive Veronese map $S_{\ell-2\ell-1\ell j j+1 j+2}$ (coloured red above); parity merely changes the labels we assign each column, and exchanges the $k-6$ columns involved in *all* the minors of F_ℓ^j —those of σ_ℓ^j , coloured blue above—with the $n-k-6$ columns involved in *none* of the minors of F_ℓ^j —those coloured grey above. That is,

$$\left\{ \begin{array}{l} [1 \cdots j-1] \\ [j \ j+1 \ j+2] \\ [j+3 \cdots j+(k-\ell)-1] \\ [j+(k-\ell) \cdots \ell-3] \\ [\ell-2 \ \ell-1 \ \ell] \\ [\ell+1 \cdots n] \end{array} \right\} \xrightarrow[\substack{k \mapsto (n-k) \\ i \mapsto (n+1)-i}]{\text{parity}} \left\{ \begin{array}{l} [n-j+2 \cdots n] \\ [n-j-1 \ n-j \ n-j+1] \\ [n+\ell-j-k \cdots n-j-2] \\ [n-\ell+4 \cdots n+\ell-j-k-1] \\ [n-\ell+1 \ n-\ell+2 \ n-\ell+3] \\ [1 \cdots n-\ell] \end{array} \right\}. \quad (3.3.30)$$

This shows that,

$$F_\ell^j \xrightarrow[\substack{k \mapsto (n-k) \\ i \mapsto (n+1)-i}]{\text{parity}} \widetilde{F}_\ell^j = F_{(n-j+1)}^{(n-\ell+1)} \equiv F_{\ell'}^{j'}, \quad (3.3.31)$$

so that

$$\mathcal{F}_n^{(k)} = \prod_{\ell=k+3}^n \left(\prod_{j=1}^{k-2} F_\ell^j \right) \xrightarrow[\substack{k \mapsto (n-k) \\ i \mapsto (n+1)-i}]{\text{parity}} \mathcal{F}_n^{(n-k)} = \prod_{\ell=k+3}^n \left(\prod_{j=1}^{k-2} \widetilde{F}_\ell^j \right) = \prod_{j'=1}^{k'-2} \left(\prod_{\ell'=k'+3}^n F_{\ell'}^{j'} \right) = \prod_{\ell'=k'+3}^n \left(\prod_{j'=1}^{k'-2} F_{\ell'}^{j'} \right), \quad (3.3.32)$$

where $k' \equiv (n-k)$, which is that which it was required to demonstrate.

Manifest Soft-Limits and the Particle Interpretation

As we have seen, the contour integral giving the $n-1$ -particle $N^{(k-2)}$ MHV scattering amplitude, is related to that giving the n -particle $N^{(k-2)}$ MHV scattering amplitude by a single overall factor which relates $\mathcal{H}_n^{(k)}$ to $\mathcal{H}_{n-1}^{(k)}$, together with a partial contour specification,

$$\begin{aligned} \mathcal{A}_n^{(k)} &= \frac{1}{\text{vol}(GL_k)} \oint_{\mathcal{F}_n^{(k)}=\vec{0}} dC_{\alpha a} \frac{\mathcal{H}_n^{(k)}}{(n-1)(1)(3) \mathcal{F}_n^{(k)}} \\ &= \frac{1}{\text{vol}(GL_k)} \oint_{\mathcal{F}_{n-1}^{(k)}=\vec{0}} dC_{\alpha \hat{a}} \frac{\mathcal{H}_{n-1}^{(k)}}{(1)(3) \mathcal{F}_{n-1}^{(k)}} \times \oint_{\substack{F_n^1=0 \\ \vdots \\ F_n^{k-2}=0}} dC_{\alpha n} \frac{\mathcal{H}_n^{(k)} / \mathcal{H}_{n-1}^{(k)}}{(n-1) F_n^1 \cdot F_n^2 \cdots F_n^{k-2}}, \end{aligned} \quad (3.3.33)$$

where $\hat{a} = 1, \dots, n-1$ and the ratio $\mathcal{H}_n^{(k)}/\mathcal{H}_{n-1}^{(k)}$ was given explicitly after equation (3.2.5) in section 2. This separation of the integral is warranted because only the maps F_n^1, \dots, F_n^{k-2} involve the variables of the n^{th} column of $C_{\alpha a}$. We can anticipate which contour should be specified for these $k-2$ variables to extract the soft-limit by considering the duality between the geometry of the columns of $C_{\alpha a}$, viewed as points in \mathbb{P}^{k-1} , and \mathcal{Z} -twistor-space geometry [12]. In twistor space, the soft-limit is achieved when the three twistors $\mathcal{Z}_{n-1}, \mathcal{Z}_n$, and \mathcal{Z}_1 become (projectively) collinear, and so we can extract the soft limit from $\mathcal{A}_n^{(k)}$ by choosing a contour for which the column-vectors $C_{\alpha n-1}, C_{\alpha n}$, and $C_{\alpha 1}$ become linearly-dependent. This fixes exactly $(k-2)$ variables of integration, and so should completely specify the integral factor in (3.3.33) relating $\mathcal{A}_n^{(k)}$ to $\mathcal{A}_{n-1}^{(k)}$.

Recalling the definition of the maps $F_n^1, F_n^2, \dots, F_n^{k-1}$, it is easy to see that when the columns $n-1, n, 1$ become linearly-dependent, F_n^2, \dots, F_n^{k-2} all vanish, while F_n^1 factorizes into simply the product of four minors. Importantly, notice that $\mathcal{H}_n^{(k)}, \mathcal{H}_{n-1}^{(k)}$, and all the factors of $\mathcal{F}_{n-1}^{(k)}$ are regular in this limit. Because of this, we can apply the global residue theorem in (3.3.33) to trade F_n^1 for the minor $(n-1)$ —which does vanish in this limit.

This allows us to view the contour integral for the twistor string entirely in $\mathcal{L}_{n,k}$, and refer to some well-known facts [12,24] relating residues in $\mathcal{L}_{n,k}$ to those of $\mathcal{L}_{n-1,k}$ to see how the soft-factor arises. It turns out that the contour which sets three consecutive columns of the Grassmannian to be linearly dependent is particularly nice, and is nothing but a holomorphic inverse soft-factor times the ratio of the k consecutive minors containing n to the $k-1$ minors which were consecutive only prior to ‘adding particle n ’ to $G(k, n-1)$. Recall that this ratio of minors is explicitly built-into the definition of $\mathcal{H}_n^{(k)}$

3.4 Transformation to the Twistor String

In this section we demonstrate the equivalence of the twistor string amplitude [36, 53] (when expressed in link variables as in [39, 63]) to our main formula (3.2.3) above. This is accomplished via repeated application of the identity transformation

$$\delta(S_{ijklrst})\delta(S_{ijkrsu}) \sim \frac{(jkt)(irt)}{(jks)(irs)}\delta(S_{ijklrst})\delta(S_{ijkrtu}); \quad (3.4.34)$$

here, \sim is used to indicate that the replacement may be made at the level of the integrand only strictly for *physical configurations* along the contour of integration. This transformation has played an important role in the analysis of [66], [70]. Note that this relation

indicates a specific change in the contour prescription: the $\delta(S_{ijkrsu})$ on the left-hand side may localize the integral on fewer (or more) poles than the $\delta(S_{ijkrtu})$ on the right, in which case the extra (or missing) poles on the right-hand side are provided by zeros of the minors in the denominator (or cancelled by zeros of the minors in the numerator).

In the next two subsections we first focus on following the transformation of the $\delta(F_\ell^i)$'s from equation (3.2.3) to the formula (4.12) in [63]. We then collect all the pre-factors which pile-up along the way and demonstrate precise agreement with [63]. It is very easy to check the agreement between our formula and that of [63] for NMHV using [66]. We may proceed by induction at step n , beginning with the assumption that equation (3.2.3) agrees with [63] for the $(n-1)$ -point amplitudes.

I. Transforming the $\delta(F_\ell^j)$'s

Let us first transform the $\delta(F_\ell^j)$'s from equation (3.2.3) to the corresponding ones in [63]. Because we will use induction, we only need to consider F_n^j and for the simplicity we will denote it as F_j . In order to compare with the formula in [63] we must first change the common piece in F_j , namely $\sigma_n^j = [1, \dots, j-1] \cup [j+n-k, \dots, n-3]$ in (3.2.6), into a subset of the columns $[1, 2, \dots, k]$.¹¹ In this sense F_1 is the ‘worst’ of the F 's and F_{k-2} is the ‘best’, so the strategy will be to first make all transformations on F_1 , then to make all transformations on F_2 , and continue in the same way (as far as possible) until F_{k-3} . In this way we gradually transform all of the original $\delta(F_j)$'s into ‘real sextics’ (objects which are indeed sextics in a certain gauge). In the following we show a first few steps and then move on to the final conclusion.

- Let us first show how to transform F_1 to F_1'' ,

$$\begin{aligned} F_1 &= [n-k+1 \cdots n-3] \bowtie S_{1 \ 2 \ 3 \ n-2 \ n-1 \ n} \\ \rightarrow F_1'' &= [n-k+2 \cdots n-3 \ 2] \bowtie S_{1 \ 3 \ 4 \ n-2 \ n-1 \ n}. \end{aligned} \tag{3.4.35}$$

Step one is to use the identity

$$\delta(F_1)\delta(F_2') \sim J_1^{(1)}\delta(F_1')\delta(F_2'), \tag{3.4.36}$$

¹¹The meaning of this will become clear by looking at the final result, equation (3.4.44).

where the sextics and the Jacobian are

$$\begin{aligned}
F'_2 &= [n - k + 2 \cdots n - 3 \ 1] \bowtie S_{2 \ 3 \ n-k+1 \ n-2 \ n-1 \ n} \\
F'_1 &= [n - k + 2 \cdots n - 3 \ 2] \bowtie S_{1 \ 3 \ n-k+1 \ n-2 \ n-1 \ n} \\
J_1^{(1)} &= [n - k + 2 \cdots n - 3] \bowtie \frac{(n \ 1 \ 2 \ 3)(n - 2 \ n - 1 \ 1 \ 2)}{(n \ 1 \ 3 \ n - k + 1)(n - 2 \ n - 1 \ 1 \ n - k + 1)}.
\end{aligned} \tag{3.4.37}$$

This identity follows from (3.4.34) by setting a particular gauge, namely to use GL_k -symmetry to set k columns $[1, 2, 3, n - k + 1, \dots, n - 3]$ of $k \times n$ matrix $(C_{\alpha a})$ to be an identity square matrix, and we will denote the gauge as $\{1, 2, 3, n - k + 1, \dots, n - 3\}$. Note that we also transformed F_2 into F'_2 which generated a Jacobian J which will end up canceling, so we will not write it explicitly.

Next we further transform F'_1 by using

$$\delta(F'_1)\delta(F_1^{(n-1)}) \sim J_1^{(2)}\delta(F''_1)\delta(F_1^{(n-1)}), \tag{3.4.38}$$

where

$$\begin{aligned}
F_1^{(n-1)} &= [n - k + 2 \cdots n - 3 \ 2] \bowtie S_{1 \ 3 \ n-k+1 \ n-2 \ n-1 \ 4}, \\
F''_1 &= [n - k + 2 \cdots n - 3 \ 2] \bowtie S_{1 \ 3 \ 4 \ n-2 \ n-1 \ n}, \\
J_{1_j}^{(2)} &= [n - k + 2 \cdots n - 3 \ \bar{j}] \bowtie \frac{(n - 1 \ 4 \ j)(3 \ n - 2 \ 4)}{(n - 1 \ n - k + 1 \ j)(3 \ n - 2 \ n - k + 1)},
\end{aligned} \tag{3.4.39}$$

with $j = 1$ and $\bar{j} = 2$. Note that in carrying out this transformation we have made use of the constrain $\delta(F_1^{(n-1)})$ which can be obtained by transforming F_{n-1}^j of the $(n - 1)$ -point amplitudes.

The third step is to transform F'_2 back to F_2 , which generates a Jacobian J^{-1} .

To summarize the construction so far, we have shown how to transform the original F_1 into a “better” quantity F''_1 at the cost of inserting the Jacobian factor $J_1^{(1)}J_{1_1}^{(2)}$ into the integrand.

• Next we would like to similarly process F_2 with F''_1 . By applying (3.4.34) for the new F''_1 and the old F_2

$$\begin{aligned}
F''_1 &= [n - k + 2 \cdots n - 3 \ 2] \bowtie S_{1 \ 3 \ 4 \ n-2 \ n-1 \ n}, \\
F_2 &= [n - k + 2 \cdots n - 3 \ 1] \bowtie S_{2 \ 3 \ 4 \ n-2 \ n-1 \ n},
\end{aligned} \tag{3.4.40}$$

we get the new quantities

$$\begin{aligned}
F'''_1 &= [n - k + 3 \cdots n - 3 \ 2 \ 3] \bowtie S_{1 \ 4 \ 5 \ n-2 \ n-1 \ n}, \\
F'''_2 &= [n - k + 3 \cdots n - 3 \ 1 \ 3] \bowtie S_{2 \ 4 \ 5 \ n-2 \ n-1 \ n}.
\end{aligned} \tag{3.4.41}$$

The Jacobians generated from this step are

$$J_2^{(1)} J_{2_1}^{(2)} J_2^{(1)} J_{2_2}^{(2)}, \quad (3.4.42)$$

where

$$\begin{aligned} J_2^{(1)} &= [n-k+3 \cdots n-3] \bowtie \frac{(n \ 1 \ 2 \ 3 \ 4)(n-2 \ n-1 \ 1 \ 2 \ 3)}{(n \ 1 \ 2 \ 4 \ n-k+2)(n-2 \ n-1 \ 1 \ 2 \ n-k+2)}, \\ J_{2_j}^{(2)} &= [n-k+3 \cdots n-3 \ \bar{j}] \bowtie \frac{(n-1 \ 5 \ j)(4 \ n-2 \ 5)}{(n-1 \ n-k+2 \ j)(4 \ n-2 \ n-k+2)}, \end{aligned} \quad (3.4.43)$$

with $j = 1, 2$ and $\bar{1} \equiv (2, 3)$, $\bar{2} \equiv (1, 3)$.

• We proceed by transforming the original F_3 together with the new F_1''', F_2''' into three new quantities $F_1''''', F_2''''', F_3'''''$. We continue in this manner until we reach F_{k-3}''''' . In each step we will always make two-type transformations like the ones described above. At the end of the day, we have new quantities

$$F_j = [1, 2, \dots, \not{j}, \dots, k-2] \bowtie S_j \ k-1 \ k \ n-2 \ n-1 \ n, \quad (3.4.44)$$

where $1 \leq j \leq k-2$. The Jacobians generated during the whole process are products of

$$\begin{aligned} J_l^{(1)} &= [n-k+l+1 \cdots n-3] \bowtie \frac{(n \ 1 \ 2 \ \cdots \ l+2)(n-2 \ n-1 \ 1 \ \cdots \ l+1)}{(n \ 1 \ \cdots \ l \ l+2 \ n-k+l)(n-2 \ n-1 \ 1 \ \cdots \ l \ n-k+l)}, \\ J_{\bar{l}_j}^{(2)} &= [n-k+l+1 \cdots n-3 \ \bar{j}] \bowtie \frac{(n-1 \ l+3 \ j)(l+2 \ n-2 \ l+3)}{(n-1 \ n-k+l \ j)(l+2 \ n-2 \ n-k+l)}, \end{aligned} \quad (3.4.45)$$

where $\bar{j} \equiv (1, 2, \dots, \not{j}, \dots, l+1)$, $1 \leq l \leq k-3$ and $1 \leq j \leq l$.

Finally let us choose a gauge $\{1, 2, 3, \dots, k\}$, in which case $F_j = S_j \ k-1 \ k \ n-2 \ n-1 \ n$ may be found in (3.4.44). Thus we have mapped our F_n^j 's to the sextics in [63], and all we are left to compare is the corresponding prefactor.

II. Collecting Prefactors

Let us now verify that performing the above procedure on our formula (3.2.3) leads to precisely the same prefactor inside the integral as in [63]. We only need to compare the ratio between n -point amplitude and $(n-1)$ -point amplitude which for our formula

(3.2.3) reads

$$\begin{aligned}
A_n = \frac{\mathcal{H}_n^{(k)}}{\mathcal{H}_{n-1}^{(k)}} &= \frac{1}{(n-1 \ n \ 1 \ \dots \ k-2)} \left[\prod_{j=1}^{k-1} (n-k+j \ \dots \ n-1 \ 1 \ \dots \ j) \right. \\
&\quad \times (n-k+j \ \dots \ n-3 \ n \ 1 \ \dots \ j+1)(n-k+j \ \dots \ n-2 \ 1 \ \dots \ j-1 \ j+1 \ j+2) \\
&\quad \left. \times (n-k+i \ \dots \ n-3 \ n-1 \ 1 \ \dots \ j \ j+2) \right].
\end{aligned} \tag{3.4.46}$$

The corresponding ratio in twistor string is given by the formula (4.12) of [63]. Taking into account the Jacobian from the transformations described in the previous subsection, we find the ratio of our formula (3.2.3) to that in [63] is precisely equal to one. This completes the proof.

Chapter 4

The All-Loop Extension of the BCFW Recursion Relations

4.1 The Loop *Integrand* for $\mathcal{N} = 4$ SYM Amplitudes

Scattering amplitudes in gauge theories have extraordinary properties that are completely invisible in the textbook formulation of local quantum field theory. The earliest hint of this hidden structure was the remarkable simplicity of the Parke-Taylor formula for tree-level MHV amplitudes [2, 3]. Witten’s 2003 proposal of twistor string theory [4] gave a strong impetus to rapid developments in the field, inspiring the development of powerful new tools for computing tree amplitudes, including CSW diagrams [5] and BCFW recursion relations [7, 21, 31, 72]. At one-loop, very efficient on-shell methods now exist [73, 74] and at higher-loop level generalizations of the unitarity-based method [75–78] have made a five-loop computation possible [79], which should soon determine the five-loop cusp anomalous dimension [80].

The BCFW recursion relations in particular presented extremely compact expressions for tree amplitudes using building blocks with both local and non-local poles. In a parallel development, an amazing hidden symmetry of planar $\mathcal{N} = 4$ SYM—dual conformal invariance—was noticed first in multi-loop perturbative calculations [47] and then at strong coupling [40], leading to a remarkable connection between null-polygonal Wilson loops and scattering amplitudes [8, 40, 42, 43, 45, 46, 81–84]. It was quickly realized that the BCFW form of the tree amplitudes manifested both full superconformal and *dual* superconformal invariance, which together close into an infinite-dimensional Yangian symmetry algebra [49]. Understanding the role of this remarkable integrable structure in the full quantum theory, however, was clouded by the IR-divergences that appear to almost completely destroy the symmetry at loop-level, leaving only the anomalous action of the (Bosonic) dual conformal invariance [44, 48, 85, 86].

I. Grassmannian Duality for Leading Singularities

In [10], a strategy for making progress on these questions was suggested. The idea was to find objects closely associated with scattering amplitudes which are completely free of IR-divergences; the action of the symmetries would be expected to be manifest on such objects, and they would provide “data” that might be the output of a putative dual theory of the S-Matrix.

The leading singularities of scattering amplitudes are precisely objects of this sort. Thinking of loop amplitudes as multi-dimensional complex integrals, leading singularities arise from performing the integration not on the usual non-compact ‘contours’ over all real loop-momenta, but on compact contours ‘encircling’ isolated (and generally complex) poles in momentum space. As such, they are free of IR-divergences and well-defined at any loop order, yielding algebraic functions of the external momenta. Leading singularities were known to have strange inter-relationships and satisfy mysterious identities not evident in their field-theoretic definition. Morally they are also expected to be Yangian-invariant, although even this is not completely manifest¹. Thus leading singularities seem to be prime candidates for objects to be understood and computed by a dual theory.

Such a duality was proposed in [10], connecting leading singularities of color-stripped, n -particle N^k MHV scattering amplitudes in $\mathcal{N} = 4$ SYM to a simple contour integral over the Grassmannian $G(k, n)$:

$$\mathcal{Y}_{n,k}(\mathcal{Z}) = \frac{1}{\text{vol}(GL_k)} \int \frac{d^{k \times n} C_{\alpha a}}{(1 \cdots k)(2 \cdots k+1) \cdots (n \cdots k-1)} \prod_{\alpha=1}^k \delta^{4|4}(C_{\alpha a} \mathcal{Z}_a). \quad (4.1.1)$$

Here $a = 1, \dots, n$ labels the external particles, and \mathcal{Z}_a are variables in $\mathbb{CP}^{3|4}$. The original formulation of this object worked with twistor variables $\mathcal{W}_a = (W_a | \tilde{\eta}_a)$, and was given as $\mathcal{L}_{n,k+2}(\mathcal{W}) = \mathcal{Y}_{n,k+2}(\mathcal{W})$. This was quickly realized [18] to be completely equivalent to a second form in *momentum* twistor space [19], with $\mathcal{L}_{n,k+2}(\lambda, \tilde{\lambda}, \tilde{\eta}) = M_{\text{MHV}}^{\text{tree}} \times \mathcal{Y}_{n,k}(\mathcal{Z})$. Here the variables $\mathcal{Z}_a = (Z_a | \eta_a)$ are the “momentum-twistors” introduced by Hodges [20], which are the most natural variables with which to discuss *dual* superconformal invariance. Furthermore, these momentum twistors are simple algebraic functions of the external momenta, upon which scattering amplitudes conventionally depend².

¹Indeed we will give a proof of this basic fact in the next section; a different argument for the same result is given in [87].

² To quickly establish notation and conventions, the momentum of particle a is given by $p_a^\mu =$

Since the Grassmannian integral is invariant under both ordinary and dual superconformal transformations, it enjoys the full Yangian symmetry of the theory, as has been proven more directly in [68]. In fact, it has been argued that these contour integrals in $G(k, n)$ generates *all* Yangian invariants.³ [11, 69].

Leading singularities are associated with residues of the Grassmannian integral. Residue theorems [65] imply many non-trivial and otherwise mysterious linear relations between leading singularities. These relations are associated with important physical properties such as locality and unitarity [10].

Further investigations [12] identified a new principle, the Grassmannian “particle interpretation”, which determines the correct contour of integration yielding the BCFW form of tree amplitudes [50]. Quite remarkably, a deformation of the integrand connects this formulation to twistor string theory [12, 14, 66]. Furthermore, another contour deformation produces the CSW expansion of tree amplitudes [51], making the emergence of local space-time a derived consequence from the more primitive Grassmannian starting point.

The Grassmannian integral and Yangian-invariance go hand-in-hand and are essentially synonymous; indeed, the Grassmannian integral is the most concrete way of thinking about Yangian invariants, since not only the symmetries but also the non-trivial relationship between different invariants are made manifest; even connections to non-manifestly Yangian-invariant but important physical objects (such as CSW terms) are made transparent.

Given these developments, we are encouraged to ask again: is there an analogous structure underlying not just the leading singularities but the full loop amplitudes? Does Yangian-invariance play a role? And if so, how can we see this through the thicket of IR-divergences that appear to remove almost all traces of these remarkable symmetries

$x_{a+1}^\mu - x_a^\mu$, and the point x_a^μ in the dual co-ordinate space is associated with the line $(Z_{a-1} Z_a)$ in the corresponding momentum-twistor space. This designation ensures that the lines $(Z_{a-1} Z_a)$ and $(Z_a Z_{a+1})$ intersect, so that correspondingly, $x_{a+1}^\mu - x_a^\mu = p_a$ is null. (Bosonic) dual-conformal invariants are made with 4-brackets $\langle a b c d \rangle = \epsilon_{IJKL} Z_a^I Z_b^J Z_c^K Z_d^L$. An important special case is $\langle i-1 i j-1 j \rangle = \langle i-1 i \rangle \langle j-1 j \rangle (x_j - x_i)^2$; 2-brackets $\langle ij \rangle$ are computed using the upper-two components of Z_i, Z_j and cancel out in dual-conformal expressions. For more detail see [18–20].

³The residues of $G(k, n)$ are Yangian-invariant for generic momenta away from collinear limits. See [88, 89] for important discussions of the fate of Yangian invariance in the presence of collinear singularities.

in the final amplitudes?

II. The Planar Integrand

Clearly, we need to focus again on finding well-defined objects associated with loop amplitudes. Fortunately, in *planar* theories, there is an extremely natural candidate: the loop *integrand* itself!

Now, in a general theory, the loop integrand is not obviously a well-defined object. Consider the case of 1-loop diagrams. Most trivially, in summing over Feynman diagrams, there is no canonical way of combining different 1-loop diagrams under the same integral sign, since there is no natural origin for the loop-momentum space. The situation is different in planar theories, however, and this ambiguity is absent. This is easy to see in the dual x -space co-ordinates [47]. The ambiguity in shifting the origin of loop momenta is nothing other than translations in x -space; but fixing the x_1, \dots, x_n of the external particles allows us to canonically combine all the diagrams. Alternatively, in a planar theory it is possible to unambiguously define the loop momentum common to all diagrams to be the one which flows from particle “1” to particle “2”.

At two-loops and above, we have a number of loop integration variables in the dual space x, y, \dots, z , and the well-defined loop integrand is completely symmetrized in these variables.

So the loop integrand is well-defined in the planar limit, and any dual theory should be able to compute it. All the symmetries of the theory should be manifest at the level of the integrand, only broken by IR-divergences in actually carrying out the integration—the symmetries of the theory are broken only by the choice of integration contour.

III. Recursion Relations for All Loop Amplitudes

Given that the integrand is a well-defined, rational function of the loop variables and the external momenta, we should be able to determine it using BCFW recursion relations in the familiar way⁴. At loop-level the poles have residues with different physical meaning. The first kind is the analog of tree-level poles and correspond to factorization channels.

⁴We note that [90] have conjectured that the loop amplitudes can be determined by CSW rules, manifesting the superconformal invariance of the theory.

The second kind has no tree-level analog; these are single cuts whose residues are forward limits of lower-loop amplitudes. Forward limits are naïvely ill-defined operations but quite nicely they exist in any supersymmetric gauge theory, as was shown to one-loop level in [91]. There it was also argued that forward limits are well-defined to higher orders in perturbation theory in $\mathcal{N} = 4$ SYM. In principle, this is all we need for computing the loop integrand in $\mathcal{N} = 4$ SYM to all orders in perturbation theory. However, our goal requires more than that. We would like to show that the integrand of the theory can be written in a form which makes all symmetries—the full Yangian—manifest. The Yangian-invariance of BCFW terms at tree-level becomes obvious once they are identified with residues of the Grassmannian integral, we would like to achieve the same at loop-level.

This is exactly what we will do in this chapter. We will give an explicit recursive construction of the all-loop integrand, in exact analogy to the BCFW recursion relations for tree amplitudes, making the full Yangian symmetry of the theory manifest.

The formulation also provides a new physical understanding of the meaning of loops, associated with simple operations for “removing” particles in a Yangian-invariant way. Loop amplitudes are associated with removing pairs of particles in an “entangled” way. We describe all these operations in momentum-twistor space, since this directly corresponds to familiar momentum-space loop integrals; presumably an ordinary twistor space description should also be possible.

As is familiar from the BCFW recursion relations at tree-level, the integrand is expressed as a sum over non-local terms, in a form very different than the familiar “rational function \times scalar integral” presentation that is common in the literature. Nonetheless, the Yangian-invariance guarantees that every term in the loop amplitude has Grassmannian residues as its leading singularities.

The integrands can of course be expressed in a manifestly-local form if desired, and are most naturally written in momentum-twistor space [92, 93]. As we will see, the most natural basis of local integrands in which to express the answer is not composed of the familiar scalar loop-integrals, but is instead made up of chiral tensor integrals with unit leading-singularities, which makes the physics and underlying structure much more transparent.

Of course the integrand is a well-defined rational function which is computed in four-dimensions without any regulators. The regularization needed to carry out the integra-

tions is a very physical one, given by moving out on the Coulomb branch [94] of the theory. This can be beautifully implemented, both conceptually and in practice, with the momentum-twistor space representation of the integrand [92, 93].

Quite apart from the conceptual advantages of this way of thinking about loops, our new formulation is also completely systematic and practical, taking the “art” out of the computation of multi-loop amplitudes in $\mathcal{N} = 4$ SYM. As simple applications of the general recursive formula, we present a number of new multi-loop results, including the two-loop NMHV 6- and 7-particle integrands. We also include very concise, local expressions for all 2-loop MHV integrands and for the 5-particle MHV integrand at 3-loops. All multiplicity results for the so-called “parity even” part of two-loop amplitudes in the MHV sector were obtained by Vergu in [16], extending previous work done for 5-particles [79] and 6-particles [83, 95] in dimensional regularization. The “parity even” part of the 6-particle amplitude in dimensional regularization has been computed in work in progress by Kosower, Roiban, and Vergu [96]. Complete integrands have been computed at two-loop order for 5-particles in [79] using D -dimensional unitarity and for 5- and 6-particles in [95, 97] using the leading singularity technique developed in [97, 98]. Also using the leading singularity technique, the 5-point 3-loop integrand was presented in [99]. Combining D -dimensional unitarity with a generalization of quadruple cuts to higher loop order [98], a method called maximal cuts was introduced in [79] and used for the computation of the 4-point 5-loop integrand. The 4-point amplitude integrand at $l = 2, 3, 4$ loop-level were computed in [100], [101], and [102], respectively. The method to be used in this chapter is, however, very different both in philosophy and in practice from the leading singularity or generalized unitarity approaches.

In this chapter, we give a brief and quite telegraphic outline of our arguments and results; we will present a much more detailed account of our methods and further elaborate on many of the themes presented here in upcoming work [35]. In section 4.2, we describe a number of canonical operations on Yangian invariants—adding and removing particles, fusing invariants—that generate a variety of important physical objects in our story. In section 4.3 we describe the origin of Yangian-invariant loop integrals as arising from the “hidden entanglement” of pairs of removed particles. In section 4.4 we describe the main result of this Chapter: a generalization of the BCFW recursion relation to all loop amplitudes in the theory, and discuss some of its salient features through simple

1-loop examples. In section 4.5 we set the stage for presenting loop amplitudes in a manifestly local form by describing the most natural way of doing this in momentum-twistor space. In section 4.6 we present a number of new multi-loop integrands computed using the recursion relation and translated into local form for the convenience of comparing with known results where they are available. We conclude in section 4.7 with a discussion of a number of directions for future work. We discuss indications that not only the integrands but also the loop integrals should be “simple”. The idea of determining the loop integrand for planar amplitudes is a general one that can generalize well beyond maximally supersymmetric theories with Yangian symmetry, and we also very briefly discuss these prospects.

4.2 Canonical Operations on Yangian Invariants

As a first step towards the construction of the all-loop integrand for $\mathcal{N} = 4$ SYM in manifestly Yangian form, we study simple operations that can map Yangian invariants $Y_{n,k}(\mathcal{Z}_1, \dots, \mathcal{Z}_n)$ to other Yangian invariants. In this discussion it will not matter whether the \mathcal{Z} ’s represent variables in twistor-space or momentum-twistor space; we will simply be describing mathematical operations that mapping between invariants. Combining these operations in various ways yields many objects of physical significance [35]. The same physical object will arise from different combinations of these operations in twistor-space vs. momentum-twistor space; we will content ourselves here by presenting mostly the momentum-twistor space representations.

As mentioned in the introduction, understanding these operations is not strictly necessary if we simply aim to find *a* formula for the integrand. The reason is that the BCFW recursion relations we introduce in section 4.4 can be developed independently for theories with less supersymmetry, which do not enjoy a Yangian symmetry. Our insistence in keeping the Yangian manifest however will pay off in two ways. The first is conceptual: the Yangian-invariant formulation will introduce a new physical picture for meaning of loops. The second is computational: the Yangian-invariant formulation gives a powerful way to compute the novel “forward-limit” terms in the BCFW recursions in momentum-twistor space, using the Grassmannian language.

We will begin by discussing how to add and remove particles in a Yangian-invariant

way. One motivation is an unusual feature of the Grassmannian integral—the space of integration depends on the number n of particles. It is natural to try and connect different n 's by choosing a contour of integration that allows a “particle interpretation”, by which we mean simply that the variety defining the contour for the scattering amplitudes of $(n+1)$ particles differs from the one for n particles only by specifying the extra constraints associated with the new particle [12]. Following this “add one particle at a time”-guideline completely specifies the contour for all tree amplitudes [12, 14], along the way exposing a remarkable connection with twistor string theory [4, 39, 52, 63, 66]. As we will see in this chapter, loops are associated with interesting “entangled” ways of *removing* particles from higher-point amplitudes. We will then move on to discuss how to “fuse” two invariants together. Using these operations we demonstrate the Yangian invariance of all leading singularities, and discuss the important special case of the “BCFW bridge” in some detail.

I. Adding Particles

Let us start with a general Yangian-invariant object

$$Y_{n,k}(\mathcal{Z}_1, \dots, \mathcal{Z}_n). \quad (4.2.2)$$

We will first describe operations that will add a particle to lower-point invariants to get higher-point invariants known as applying “inverse soft factors” [24], which are so named because taking the usual soft limit of the resulting object returns the original object. This can be done preserving k or increasing $k \mapsto k + 1$. We can discuss these in both twistor- and momentum-twistor space; for the purposes of this chapter we will describe these inverse-soft factor operations in momentum-twistor space.

The idea is that there are residues in $G(k, n)$ which are trivially related to residues in $G(k, n - 1)$ or $G(k - 1, n - 1)$. The k -preserving operation $Y_{n-1,k} \mapsto Y_{n,k}$ is particularly simple, being simply the identification

$$Y'_{n,k}(\mathcal{Z}_1, \dots, \mathcal{Z}_{n-1}, \mathcal{Z}_n) = Y_{n-1,k}(\mathcal{Z}_1, \dots, \mathcal{Z}_{n-1}); \quad (4.2.3)$$

that is, where we have simply added particle n as a label (but have not altered the functional form of Y in any way); thanks to the momentum-twistor variables, momentum

conservation is automatically preserved. The k -increasing inverse soft factor is slightly more interesting. There is always a residue of $G(k, n)$ which has a C -matrix of the form

$$\begin{pmatrix} * & * & 0 & \cdots & 0 & * & * & 1 \\ * & \cdots & \cdots & \cdots & \cdots & \cdots & * & 0 \\ \vdots & \ddots & \ddots & \ddots & \ddots & \ddots & * & \vdots \end{pmatrix}. \quad (4.2.4)$$

Here, the non-zero elements in the top row, $* * * * 1$ correspond to particles $1, 2, (n-2), (n-1), n$, and we have generic non-zero entries in the lower $(k-1) \times (n-1)$ matrix. The corresponding residue is easily seen to be associated with

$$Y'_{n,k}(\dots, \mathcal{Z}_{n-1}, \mathcal{Z}_n, \mathcal{Z}_1, \dots) = [n-2 \ n-1 \ n \ 1 \ 2] \times Y_{n-1,k-1}(\dots, \widehat{\mathcal{Z}}_{n-1}, \widehat{\mathcal{Z}}_1, \dots) \quad (4.2.5)$$

where

$$[a \ b \ c \ d \ e] = \frac{\delta^{0|4}(\eta_a \langle b \ c \ d \ e \rangle + \eta_b \langle c \ d \ e \ a \rangle + \eta_c \langle d \ e \ a \ b \rangle + \eta_d \langle e \ a \ b \ c \rangle + \eta_e \langle a \ b \ c \ d \rangle)}{\langle a \ b \ c \ d \rangle \langle b \ c \ d \ e \rangle \langle c \ d \ e \ a \rangle \langle d \ e \ a \ b \rangle \langle e \ a \ b \ c \rangle} \quad (4.2.6)$$

is the basic ‘NMHV’-like R -invariant⁵ and the $\widehat{\mathcal{Z}}_{n-1,1}$ are deformed momentum twistor variables. The Bosonic components of the deformed twistors have a very nice interpretation: $\widehat{\mathcal{Z}}_1$ is simply the intersection of the line $(1 \ 2)$ with the plane $(n-2 \ n-1 \ n)$, which we indicate by writing $\widehat{\mathcal{Z}}_1 \equiv (n-2 \ n-1 \ n) \cap (1 \ 2)$; and $\widehat{\mathcal{Z}}_{n-1}$ is the intersection of the line $(n-2 \ n-1)$ with the plane $(1 \ 2 \ n)$, written $\widehat{\mathcal{Z}}_{n-1} \equiv (n-2 \ n-1) \cap (1 \ 2 \ n)$. Fully supersymmetrically, we have

$$\begin{aligned} \widehat{\mathcal{Z}}_1 &\equiv (n-2 \ n-1 \ n) \cap (1 \ 2) = \mathcal{Z}_1 \langle 2 \ n-2 \ n-1 \ n \rangle + \mathcal{Z}_2 \langle n-2 \ n-1 \ n \ 1 \rangle; \\ \widehat{\mathcal{Z}}_{n-1} &\equiv (n-2 \ n-1) \cap (n \ 1 \ 2) = \mathcal{Z}_{n-2} \langle n-1 \ n \ 1 \ 2 \rangle + \mathcal{Z}_{n-1} \langle n \ 1 \ 2 \ n-2 \rangle. \end{aligned} \quad (4.2.7)$$

II. Removing Particles

We can also remove particles to get lower-point Yangian invariants from higher-point ones. This turns out to be more interesting than the inverse-soft factor operation, though physically one might think it is even more straightforward. After all, we can remove a particle simply by taking its soft limit. However, while this is a well-defined operation on *e.g.* the full tree amplitude, it is *not* a well-defined operation on the individual residues

⁵When two sets of the twistors are consecutive, these “ R -invariants” are sometimes written $R_{r;s,t} \equiv [r \ s-1 \ s \ t-1 \ t]$. These invariants were first introduced in [8] in dual super-coordinate space.

(BCFW terms) in the tree amplitude. The reason is the presence of spurious poles: each term does not individually have the correct behavior in the soft limit.

Nonetheless, there *are* completely canonical and simple operations for removing particles in a Yangian-invariant way. One reduces $k \mapsto k - 1$, the other preserves k . The k -reducing operation removes particle n by integrating over its twistor co-ordinate

$$Y'_{n-1,k-1}(\mathcal{Z}_1, \dots, \mathcal{Z}_{n-1}) = \int d^{3|4} \mathcal{Z}_n Y_{n,k}(\mathcal{Z}_1, \dots, \mathcal{Z}_{n-1}, \mathcal{Z}_n). \quad (4.2.8)$$

This gives a Yangian-invariant for any closed contour of integration—meaning that under the Yangian generators for particles $1, \dots, n - 1$, this object transforms into a total derivative with respect to \mathcal{Z}_n . This statement can be trivially verified by directly examining the action of the level-zero and level-one Yangian generators on the integral. It is also very easy to verify directly from the Grassmannian integral. Note that depending on the contour that is chosen, a given higher-point invariant can in general map to several lower-point invariants.

The k -preserving operation “merges” particle n with one of its neighbors, $n - 1$ or 1 . For example,

$$Y'_{n-1,k}(\mathcal{Z}_1, \dots, \mathcal{Z}_{n-1}) = Y_{n,k}(\mathcal{Z}_1, \dots, \mathcal{Z}_{n-1}, \mathcal{Z}_n \mapsto \mathcal{Z}_{n-1}). \quad (4.2.9)$$

The Yangian-invariance of this operation is slightly less obvious to see by simply manipulating Yangian generators, but it can be verified easily from the Grassmannian formula.

We stress again that these operations are perfectly well-defined on *any* Yangian-invariant object, regardless of whether the standard soft-limits are well defined. Of course, they coincide with the soft limit when acting on *e.g.* the tree amplitude.

III. Fusing Invariants

Finally, we mention a completely trivial way of combining two Yangian invariants to produce a new invariant. Start with two invariants which are functions of a disjoint set of particles, which we can label $Y_1(\mathcal{Z}_1, \dots, \mathcal{Z}_m)$ and $Y_2(\mathcal{Z}_{m+1}, \dots, \mathcal{Z}_n)$. Then, it is easy to see that the simple product

$$Y'(\mathcal{Z}_1, \dots, \mathcal{Z}_n) = Y_1(\mathcal{Z}_1, \dots, \mathcal{Z}_m) \times Y_2(\mathcal{Z}_{m+1}, \dots, \mathcal{Z}_n) \quad (4.2.10)$$

is also Yangian-invariant. Only the vanishing under the level-one generators requires a small comment. Note that the cross terms vanish because the corresponding level-zero

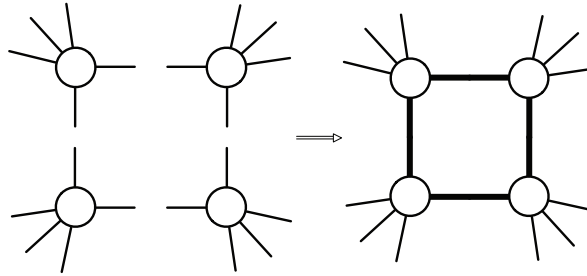
generators commute and therefore the level-one generators cleanly splits into the smaller level-one generators.

IV. Leading Singularities are Yangian Invariant

Combining these operations builds new Yangian invariants from old ones; all of which have nice physical interpretations. An immediate consequence is a simple proof that all leading singularities are Yangian invariant. For this subsection only, we work in ordinary twistor space. Then we take any four Yangian invariants for disjoint sets of particles and we make a new invariant by taking the product of all of them,

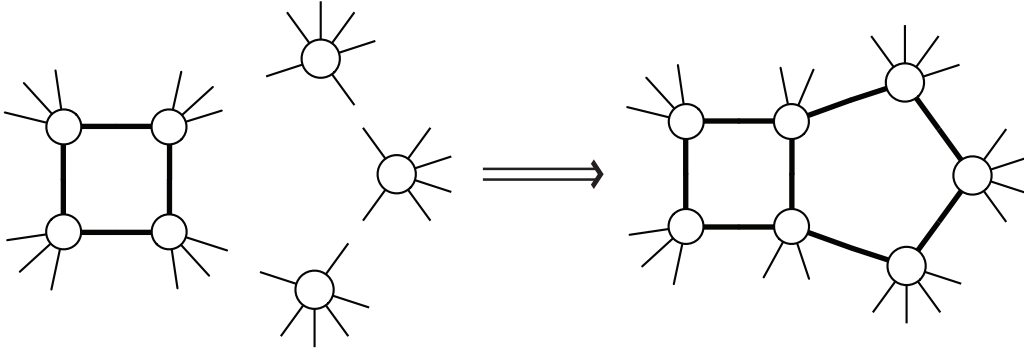
$$Y_1(\mathcal{W}_1, \dots, \mathcal{W}_m) Y_2(\mathcal{W}_{m+1}, \dots, \mathcal{W}_l) Y_3(\mathcal{W}_{l+1}, \dots, \mathcal{W}_p) Y_4(\mathcal{W}_{p+1}, \dots, \mathcal{W}_q).$$

We then “merge” m and $m + 1$, l and $l + 1$, p and $p + 1$, and q with 1. We then integrate over m, l, p, q . This precisely yields the twistor-space expression for a “1-loop” leading singularity topology [22, 23].



In the figure, a thick black line denotes the merging of the two particles at the ends of the line, and integrating over the remaining variable. The generalization to all leading singularities is obvious; for instance, starting with the “1-loop” leading singularity we have already built, we can use the same merge and integrate operations to build “2-loop”

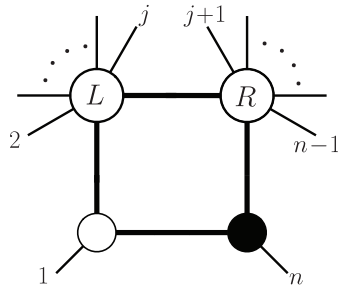
leading singularity topologies such as that shown below.



We conclude that all leading singularities are Yangian invariant. Given that all Yangian invariants are Grassmannian residues, this proves (in passing) the original conjecture in [10] that all leading singularities can be identified as residues of the Grassmannian integral.

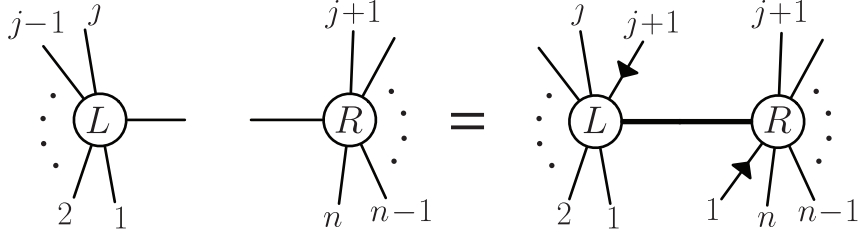
V. The BCFW Bridge

A particularly important way of putting together two Yangian invariants to make a third is the “BCFW bridge” [17, 21, 34], associated with the familiar “two-mass hard” leading singularities drawn below in twistor space [17, 33, 34, 103]:



Here, the open and dark circles respectively denote MHV and $\overline{\text{MHV}}$ three-particle amplitudes, respectively. We remark in passing that the inverse-soft factor operations mentioned above are special cases of the BCFW bridge where a given Yangian invariant is bridged with an $\overline{\text{MHV}}$ three-point vertex (for the k -preserving case) or an MHV three-point vertex (for the k -increasing case).

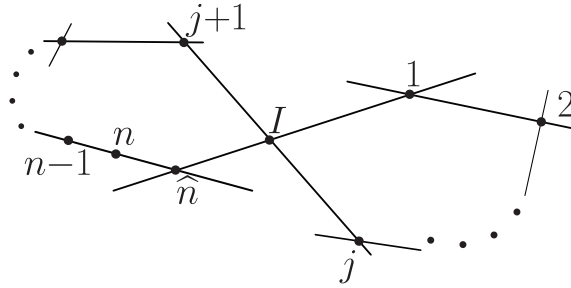
We will find it useful to also see the bridge expressed as a composition of our basic operations in momentum-twistor space, as



This is a pretty object since it uses all of our basic operations in an interesting way. In the figure, the solid arrows pointing inward indicate that particle-“1” is added as a k -increasing inverse soft factor on Y_L , and $j+1$ is added as a k -increasing inverse soft factor on Y_R . We are also using the merge operation to identify the repeated “1” and “ $j+1$ ” labels across the bridge. The internal line, which we label as \mathcal{Z}_I , is integrated over. The contour of integration is chosen to encircle the $\langle n-1 \ n \ 1 \ I \rangle$ -pole from the $[n-1 \ n \ 1 \ I \ j+1]$ -piece of the inverse-soft factor on Y_L , and the $\langle 1 \ I \ j+1 \ j \rangle$ - and $\langle I \ j+1 \ j \ j-1 \rangle$ -poles from the $[1 \ I \ j+1 \ j \ j-1]$ -piece of the inverse soft factor on Y_R . The deformation on \mathcal{Z}_n induced by the inverse-soft factor adding particle-1 on Y_L is of the form

$$\mathcal{Z}_n \mapsto \widehat{\mathcal{Z}}_n = \mathcal{Z}_n + z\mathcal{Z}_{n-1}, \quad \text{where} \quad \langle \widehat{\mathcal{Z}}_n Z_1 Z_j Z_{j+1} \rangle = 0. \quad (4.2.11)$$

This is the momentum-twistor space version of the BCFW deformation, which corresponds to deforming $\lambda_n, \widetilde{\lambda}_1$ in momentum-space. We remind ourselves of this deformation by placing the little arrow pointing from $n \mapsto n-1$ in the figure for the bridge. The momentum-twistor space geometry associated with this object is



which precisely corresponds to the expected BCFW deformation and the corresponding factorization channel.

We leave a detailed derivation of this picture to [35], but in fact the momentum-twistor structure of the BCFW bridge can be easily understood. Note that Y_L, Y_R have

k -charge k_L, k_R , while $Y_L \otimes Y_R$ has k -charge $k_L + k_R + 1$; given that the \mathcal{Z}_I decreases the k -charge by 1, we must start with Y_L and Y_R and get objects with k -charge $(k_L + 1)$ and $(k_R + 1)$ on the left and right. This can be canonically done by acting with k -increasing inverse soft factors; the added particle on Y_L must be adjacent to n in order to affect a deformation on \mathcal{Z}_n . Finally, the data associated with the “extra” particles introduced by the inverse soft factor must be removed in the only way possible, by using the merge operation. Explicitly, the final result for $Y_L \otimes_{\text{BCFW}} Y_R$ is

$$\left(Y_L \otimes_{\text{BCFW}} Y_R\right)(1, \dots, n) = [n-1 \ n \ 1 \ j \ j+1] \times Y_R(1, \dots, j, I) \times Y_L(I, j+1, \dots, n-1, \widehat{n}) \quad (4.2.12)$$

with

$$\widehat{n} = (n-1 \ n) \cap (j \ j+1 \ 1), \quad \text{and} \quad I = (j \ j+1) \cap (n-1 \ n \ 1). \quad (4.2.13)$$

Starting with the tree amplitude $M_{n,k,\text{tree}}$ ⁶, the BCFW deformation $\mathcal{Z}_n \mapsto \mathcal{Z}_n + z\mathcal{Z}_{n-1}$ can be used to recursively construct tree amplitudes in the familiar way: by writing,

$$M_{n,k,\text{tree}} = \oint \frac{dz}{z} \widehat{M}_{n,k,\text{tree}}(z), \quad (4.2.14)$$

it is clear that the desired amplitude $\widehat{M}_{n,k,\text{tree}}(z)$ is obtained by summing-over all the residues of the RHS *except* the pole at origin $z = 0$. Notice that there is a non-zero pole at infinity in this deformation: as $z \rightarrow \infty$, $\mathcal{Z}_n \rightarrow \mathcal{Z}_{n-1}$ projectively, and so the tree amplitude gets a contribution from $M_n(\mathcal{Z}_1, \dots, \mathcal{Z}_{n-1}, \mathcal{Z}_n) \rightarrow M_{n-1}(\mathcal{Z}_1, \dots, \mathcal{Z}_{n-1})$ ⁷. The pole at $z \rightarrow \infty$ corresponds to the term in the usual momentum-space BCFW formula using an $\overline{\text{MHV}}$ three-point vertex bridged with M_{n-1} , which simply acts as a k -preserving inverse-soft factor. The remaining physical poles are of the form $\langle i \ i+1 \ j \ j+1 \rangle$. Under $\mathcal{Z}_n \mapsto \mathcal{Z}_n + z\mathcal{Z}_{n-1}$, we only access the poles where $\langle Z_n(z) Z_1 Z_j Z_{j+1} \rangle \rightarrow 0$, and the corresponding residues are computed by the BCFW bridge indicated above, with Y_L, Y_R being the lower-point tree amplitudes.

⁶We remind the reader that we are working in momentum-twistor space, so that what we are calling M_{tree} here is obtained after stripping off the MHV tree-amplitude factor from the full amplitude in momentum space.

⁷Note that $z \rightarrow \infty$ here does *not* correspond to going to infinity in the familiar momentum-space version of BCFW. The pole at infinity in ordinary momentum space here corresponds to a pole involving the infinity twistor $\langle Z_n(z) I Z_1 \rangle = 0$. Of course we do not expect such a pole to arise in a dual-conformal invariant theory, not only at tree-level, but at all-loop order, as will be relevant to our subsequent discussion. A direct proof of this fact, not assuming dual conformal invariance, should follow from the “enhanced spin-lorentz symmetry” arguments of [34].

4.3 Loops From Hidden Entanglement

Let's imagine starting with some scattering amplitude or Grassmannian residue, and begin removing particles. The operation that decreases k in particular demands a choice for the contour of integration. If we remove particle Z_A by integrating over it as $\int d^{3|4} Z_A$, it is natural to choose a T^3 -contour of integration for the Bosonic $d^3 Z_A$ integral and compute a simple residue⁸.

We can then proceed to remove a subsequent particle either by merging, or performing further integrals $\int d^{3|4} Z_B$ and so on. In this way we will simply proceed from higher-point Grassmannian residues to lower-point ones. In particular, if these operations are performed on a higher-point tree amplitude, we arrive at lower-point tree amplitudes, and don't encounter any new objects.

But we can imagine a more interesting way of removing not just one but a pair of particles. Consider removing particle A and subsequently removing the adjacent particle B . Instead of first integrating-out A and then B on separate T^3 's, let's consider an "entangled" contour of integration, which we will discover to yield, instead of lower-point Grassmannian residue, a loop integral.

Consider as a simple example removing two particles from the 6-particle $N^2\text{MHV} = \overline{\text{MHV}}$ tree amplitude, $M_{6,4,\ell=0}(1234AB)$. Performing the $d^{0|4}\eta_A, d^{0|4}\eta_B$ integrals is trivial, and this gives

$$\int d^3 z_A d^3 z_B \frac{\langle 1234 \rangle^3}{\langle 234z_A \rangle \langle 34z_A z_B \rangle \langle 4z_A z_B 1 \rangle \langle z_A z_B 12 \rangle \langle z_B 123 \rangle} \quad (4.3.15)$$

where we have chosen to label the Bosonic momentum twistors with lower-case z 's for later convenience. As we have claimed, on any closed contour, these integrals should give a Yangian-invariant answer. Indeed, computing the z_B integral by residue on any contour leaves us with

$$\int d^3 z_A \frac{\langle 1234 \rangle^3}{\langle z_A 123 \rangle \langle z_A 234 \rangle \langle z_A 341 \rangle \langle z_A 412 \rangle} \quad (4.3.16)$$

⁸Residues of rational functions in m complex variables are computed by choosing m polynomial factors f_i 's from the denominator and integrating along a particular T^m -contour, *i.e.* the product of m circles given as the solutions of $|f_i| = \epsilon$ with $\epsilon \ll 1$ and near a common zero of the f_i 's. See [65] for more details.

and computing any of the simple residues of this remaining z_A integral gives 1, which is of course the only Yangian invariant for MHV amplitudes.

We will now see that starting with exactly the same integrand but choosing a different contour of integration yields, instead of “1”, the 4-particle 1-loop amplitude. Geometrically, the points z_A, z_B determine a line in momentum-twistor space, which is interpreted as a point in the dual x -space, or equivalently, a loop-integral’s four-momentum. We will first integrate over the positions of z_A, z_B on the line (AB) , and then integrate over all lines (AB) .

This contour can be described explicitly by parametrizing $z_{A,B}$ as

$$z_A = \begin{pmatrix} \lambda_A \\ x\lambda_A \end{pmatrix}, \quad z_B = \begin{pmatrix} \lambda_B \\ x\lambda_B \end{pmatrix} \quad (4.3.17)$$

where x will be the loop momentum. The measure is

$$d^3z_A d^3z_B = \langle \lambda_A d\lambda_A \rangle \langle \lambda_B d\lambda_B \rangle \langle \lambda_A \lambda_B \rangle^2 d^4x. \quad (4.3.18)$$

The λ_A, λ_B integrals will be treated as contour integrals on $\mathbb{CP}^1 \times \mathbb{CP}^1$, while the x -integral will be over real points in the (dual) Minkowski space.

Using that $\langle z_A z_B j-1 j \rangle = \langle \lambda_A \lambda_B \rangle \langle j-1 j \rangle (x-x_j)^2$ our integral becomes

$$\int d^4x \frac{x_{13}^2 x_{24}^2}{(x-x_1)^2 (x-x_2)^2 (x-x_4)^2} \int \frac{\langle 1234 \rangle \langle 23 \rangle \langle \lambda_A d\lambda_A \rangle \langle \lambda_B d\lambda_B \rangle}{\langle z_A 123 \rangle \langle 234 z_B \rangle \langle \lambda_A \lambda_B \rangle}. \quad (4.3.19)$$

The factor $\langle z_A 234 \rangle$ is linear in the projective variable λ_A while the factor $\langle 123 z_B \rangle$ is linear in λ_B . This implies that there is a unique way to perform the λ_A and λ_B integrals by contour integration, which gives us

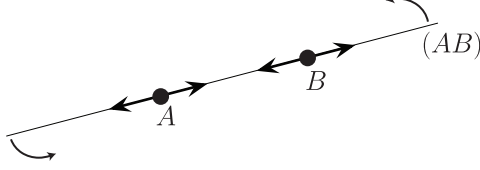
$$\int d^4x \frac{x_{13}^2 x_{24}^2}{(x-x_1)^2 (x-x_2)^2 (x-x_3)^2 (x-x_4)^2}. \quad (4.3.20)$$

This is precisely the 1-loop MHV amplitude!

We have thus seen that, removing a pair of particles with this “entangled” contour of integration, where we first integrate over the position of two points along the line joining them and then integrate over all lines, naturally produces objects that look like loop integrals.

There is a nicer way of characterizing this “entangled” contour that is also more convenient for doing calculations, let us describe it in detail. Given z_A, z_B , a general

GL_2 -transformation on the 2-vector (z_A, z_B) moves A, B along the line (AB) . Thus, in integrating over $d^3 z_A d^3 z_B$, we'd like to “do the GL_2 -part of the integral first” to leave us with an integral that only depends on the line (AB) :



We can do this explicitly by writing

$$\begin{pmatrix} z_A \\ z_B \end{pmatrix} = \begin{pmatrix} c_A^{(A)} & c_A^{(B)} \\ c_B^{(A)} & c_B^{(B)} \end{pmatrix} \begin{pmatrix} Z_A \\ Z_B \end{pmatrix}; \quad (4.3.21)$$

then

$$d^3 z_A d^3 z_B = \langle c_A d c_A \rangle \langle c_B d c_B \rangle \langle c_A c_B \rangle^2 \left[\frac{d^4 Z_A d^4 Z_B}{\text{vol}(GL_2)} \right], \quad (4.3.22)$$

and our integral becomes—this time writing it out fully:

$$\int \left[\frac{d^4 Z_A d^4 Z_B}{\text{vol}(GL_2)} \right] \frac{\langle 1234 \rangle^3}{\langle AB 12 \rangle \langle AB 34 \rangle \langle AB 41 \rangle} \int \frac{\langle c_A d c_A \rangle \langle c_B d c_B \rangle}{\langle c_A c_B \rangle \langle c_A \psi_A \rangle \langle c_B \psi_B \rangle}, \quad (4.3.23)$$

where

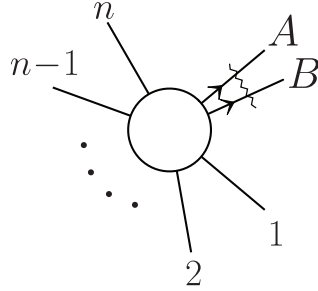
$$\psi_A = \begin{pmatrix} \langle A234 \rangle \\ \langle B234 \rangle \end{pmatrix}, \quad \psi_B = \begin{pmatrix} \langle A123 \rangle \\ \langle B123 \rangle \end{pmatrix}. \quad (4.3.24)$$

The c_A, c_B integral is naturally performed on a contour ‘encircling’ $c_A = \psi_A, c_B = \psi_B$, yielding $\frac{1}{\langle \psi_A \psi_B \rangle} = \frac{1}{\langle AB 23 \rangle \langle 1234 \rangle}$. More generally, if “234” and “123” in the definitions of ψ_A, ψ_B were to be replaced by arbitrary “ abc ” and “ xyz ”, $\langle \psi_A \psi_B \rangle = \langle Axyz \rangle \langle Babc \rangle - \langle Aabc \rangle \langle Bxyz \rangle \equiv \langle AB (abc) \cap (xyz) \rangle$ where $(abc) \cap (xyz)$ is the line corresponding to the intersection of the planes (abc) and (xyz) . We are then left with

$$\int \left[\frac{d^4 Z_A d^4 Z_B}{\text{vol}(GL_2)} \right] \frac{\langle 1234 \rangle^2}{\langle AB 12 \rangle \langle AB 23 \rangle \langle AB 34 \rangle \langle AB 41 \rangle}, \quad (4.3.25)$$

where the integration region is such that the line (AB) corresponds to a real point in the (dual) Minkowski space-time. We recognize this object as the 1-loop MHV amplitude, exactly as above.

We can clearly perform this operation starting with any Yangian invariant object $Y[\mathcal{Z}_A, \mathcal{Z}_B, \mathcal{Z}_1, \dots]$, which we will graphically denote as:



and write as

$$\int_{GL_2} Y[\dots, \mathcal{Z}_n, \mathcal{Z}_A, \mathcal{Z}_B, \mathcal{Z}_1, \dots] \quad (4.3.26)$$

This object is formally Yangian-invariant, in the precise sense that the integrand will transform into a total derivative under the action of the Yangian generators for the external particles. Of course, such integrals may have IR-divergences along some contours of integration, which is how Yangian-invariance is broken in practice.

The usual way of writing the loop amplitudes as “leading singularity \times scalar integral” ensures that the leading singularities of the individual terms are Yangian-invariant, but the factorized form seems very un-natural, and there is no obvious action of the symmetry generators on the integrand. By contrast, the loop integrals we have defined, as we will see, will not take the artificial “residue \times integral” form, but of course their leading singularities are automatically Grassmannian residues. The reason is that a leading singularity of the (AB) -integral can be computed as a simple residue of the underlying $d^{3|4}z_A d^{3|4}z_B$ integral, which is free of IR-divergences and guaranteed to be Yangian-invariant.

4.4 Recursion Relations For All Loop Amplitudes

Having familiarized ourselves with the basic operations on Yangian invariants, we are ready to discuss the recursion relations for loops in the most transparent way. The loop integrand is a rational function of both the loop integration variables and the external kinematical variables. Just as the BCFW recursion relations allow us to compute a rational function from its poles under a simple deformation, the loop integrand can be determined in the same way. Consider the l -loop integrand $M_{n,k,\ell}$, and consider again

the (supersymmetric) momentum-twistor deformation

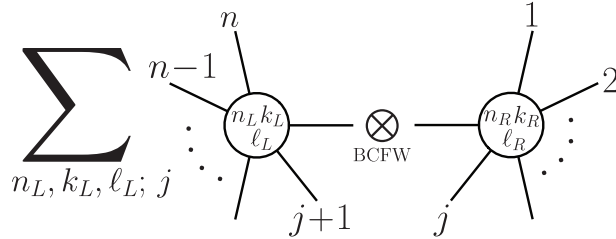
$$\mathcal{Z}_n \mapsto \mathcal{Z}_n + z\mathcal{Z}_{n-1}. \quad (4.4.27)$$

Then

$$M_{n,k,\ell} = \oint \frac{dz}{z} \widehat{M}_{n,k,\ell}(z) \quad (4.4.28)$$

and we sum over all the residues of the RHS away from the origin, all of which can be determined from lower-point/lower-loop amplitudes. This recursion relation can be derived in a large class of theories and is not directly tied to $\mathcal{N} = 4$ SYM or Yangian-invariance. However our experience with building Yangian-invariant objects will help us to understand (and compute) the terms in the recursion relations in a transparent way, and also easily recognize them as manifestly Yangian-invariant objects.

As in our discussion of the BCFW bridge at tree-level, the pole at infinity is simply the lower-point integrand with particle n removed. All the rest of the poles in z also have a simple interpretation: in general, all the poles arise either from $\langle Z_n(z) Z_1 Z_j Z_{j+1} \rangle \rightarrow 0$ or $\langle (AB)_q Z_n(z) Z_1 \rangle \rightarrow 0$, where $(AB)_q$ denotes the line in momentum twistor space associated with the q^{th} loop-variable. The first type of pole simply corresponds to factorization channels, and the corresponding residue is computed by the BCFW bridges between lower-loop/lower-point amplitudes:

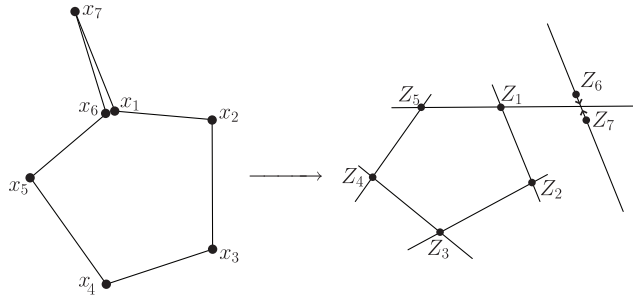


where $n_L + n_R = n + 2$, $k_L + k_R = k - 1$, $\ell_L + \ell_R = \ell$. Note that we treat all the poles (including the pole at infinity) on an equal footing by declaring the term with $j = 2$ to be given by the k -preserving inverse soft-factor acting on lower-point amplitude.

This is the most obvious generalization of the BCFW recursion relation from trees to loops, but it clearly can't be the whole story, since it would allow us to recursively reduce loop amplitudes to the 3-particle loop amplitude, which vanishes! Obviously, at loop-level, a “source” term is needed for the recursive formula.

I. Single-Cuts and the Forward-Limit

This source term is clearly provided by the second set of poles, arising from $\langle (AB)_q Z_n(z) Z_1 \rangle \rightarrow 0$. For simplicity of discussion let's first consider the 1-loop amplitude. This pole corresponds to cutting the loop momentum running between n and 1, and is therefore given by a tree-amplitude with two additional particles sandwiched between $n, 1$, with momenta $q, -q$, summing-over the multiplet of states running around the loop. These single-cuts associated with “forward-limits” of lower-loop integrands are precisely the objects that make an appearance in the context of the Feynman tree theorem [91]. The geometry of the forward limit is shown below for both in the dual x -space and momentum-twistor space:

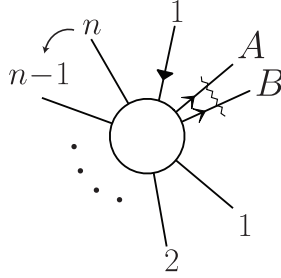


Here, between particles 5 and 1, we have particles 6,7 with momenta $q^\mu, -q^\mu$, where $q^\mu = x_1^\mu - x_7^\mu$ is a null vector. In momentum-twistor space, the null condition means that the line (76) intersects (15), while in the forward limit both Z_6 and Z_7 approach the intersection point $(76) \cap (15)$.

In a generic gauge theory, the forward limits of tree amplitudes suffer from collinear divergences and are not obviously well-defined. However remarkably, as pointed out in [91], in supersymmetric theories the sum over the full multiplet makes these objects completely well-defined and equal to single-cuts!

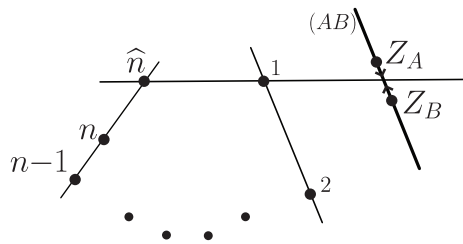
Indeed, we can go further and express this single-cut “forward limit” term in a manifestly Yangian-invariant way. It turns out to to be a beautiful object, combining the

entangled removal of two particles with the “merge” operation:



Here a particle $(n + 1)$ is added adjacent to A, B as a k -increasing inverse soft factor, then A, B are removed by entangled integration. The GL_2 -contour is chosen to encircle points where both points A, B on the line (AB) are located at the intersection of the line (AB) with the plane $(n-1 \ n \ 1)$. Note that there is no actual integral to be done here; the GL_2 -integral is done on residues and is computed purely algebraically. Finally, the added particle $(n + 1)$ is merged with 1.

As in our discussion of the BCFW bridge, this form can be easily understood by looking at the deformations induced by the “1” inverse soft factors; the associated momentum-twistor geometry turns out to be

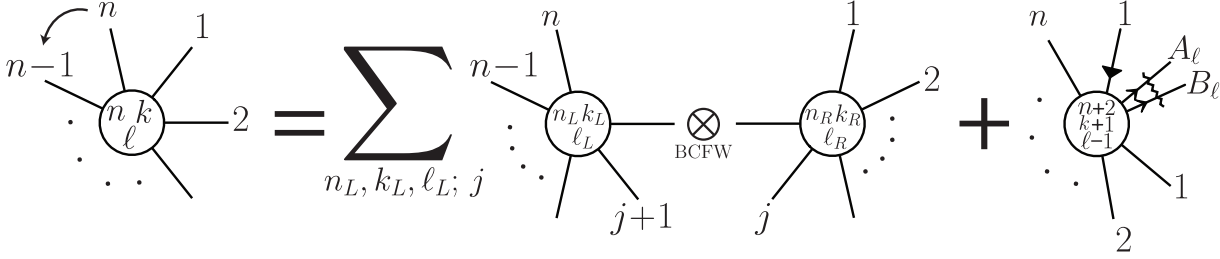


exactly as needed. The picture is the same for taking the single cut of any Yangian-invariant object.

Note that we were able to identify the BCFW terms in a straightforward way since the residues of the poles of the integrand have obvious “factorization” and “cut” interpretations. This is another significant advantage of working with the integrand, since as is well known, the full loop amplitudes (after integration) have more complicated factorization properties [104]. This is due to the IR-divergences which occur when the loop momenta becomes collinear to external particles, when the integration is performed.

II. BCFW For All Loop Amplitudes

Putting the pieces together, we can give the recursive definition for all loop integrands in planar $\mathcal{N} = 4$ SYM as



To be fully explicit, the recursion relation is

$$\begin{aligned}
 M_{n,k,\ell}(1, \dots, n) &= M_{n-1,k,\ell}(1, \dots, n-1) \\
 &+ \sum_{n_L, k_L, \ell_L; j} [j \ j+1 \ n-1 \ n \ 1] M_{n_R, k_R, \ell_R}^R(1, \dots, j, I_j) M_{n_L, k_L, \ell_L}^L(I_j, j+1, \dots, \widehat{n}_j) \\
 &+ \int_{GL_2} [AB \ n-1 \ n \ 1] \times M_{n+2, k+1, \ell-1}(1, \dots, \widehat{n}_{(AB)}, \widehat{A}, B).
 \end{aligned} \tag{4.4.29}$$

where $n_L + n_R = n + 2$, $k_L + k_R = k - 1$, $\ell_L + \ell_R = \ell$ and the shifted momentum (super-)twistors that enter are

$$\begin{aligned}
 \widehat{n}_j &= (n-1 \ n) \cap (j \ j+1 \ 1), & I_j &= (j \ j+1) \cap (n-1 \ n \ 1); \\
 \widehat{n}_{(AB)} &= (n-1 \ n) \cap (AB \ 1), & \widehat{A} &= (AB) \cap (n-1 \ n \ 1).
 \end{aligned} \tag{4.4.30}$$

Beyond 1-loop, it is understood that this expression is to be fully-symmetrized with equal weight in all the loop-integration variables $(AB)_\ell$; it is easy to see that this correctly captures the recursive combinatorics. Recall again that GL_2 -integral is done on simple residues and is thus computed purely algebraically; the contour is chosen so that the points A, B are sent to $(AB) \cap (n-1 \ n \ 1)$. As we will show in [35], recursively using the BCFW form for the lower-loop amplitudes appearing in the forward limit allows us to carry out the GL_2 -integral completely explicitly, but the form we have given here will suffice for this chapter.

III. Simple Examples

In [35], we will describe the loop-level BCFW computations in detail; here we will just highlight some of the results for some simple cases, to illustrate some of the important

properties of the recursion and the amplitudes that result. We start by giving the BCFW formula for all one-loop MHV amplitudes.

In this case the second line in the above formula vanishes, and the recursion relation trivially reduces to a single sum. To compute the NMHV tree amplitudes which enters through the third line, it is convenient to use the tree BCFW deformation $\tilde{\mathcal{Z}}_B = \mathcal{Z}_B + z\hat{\mathcal{Z}}_A$ which leads to

$$M_{\text{MHV}}^{1\text{-loop}} = \int_{(AB)} \int_{GL_2} \sum_j [AB j j+1 1] \times \left(\sum_{i < j} [\hat{A}B 1 i i+1] + \dots \right), \quad (4.4.31)$$

where we have defined

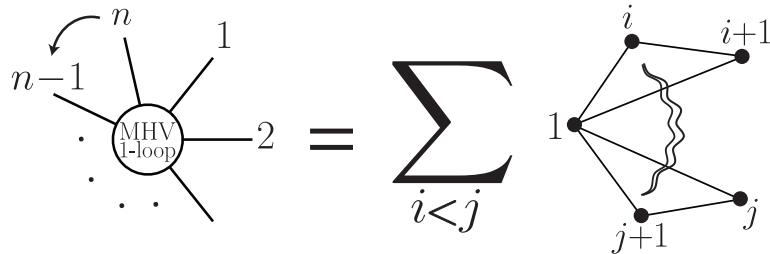
$$\int_{(AB)} \equiv \int \left[\frac{d^{4|4} \mathcal{Z}_A d^{4|4} \mathcal{Z}_B}{\text{vol}(GL_2)} \right], \quad (4.4.32)$$

and where the omitted terms are independent of \mathcal{Z}_B and vanish upon Fermionic-integration. The GL_2 - and Fermion-integrals are readily evaluated, as explained above, reducing this to

$$M_{\text{MHV}}^{1\text{-loop}} = \int_{(AB)} \sum_{i < j} \frac{\langle AB(1 i i+1) \cap (1 j j+1) \rangle^2}{\langle AB 1 i \rangle \langle AB i i+1 \rangle \langle AB i+1 1 \rangle \langle AB 1 j \rangle \langle AB j j+1 \rangle \langle AB j+1 1 \rangle}. \quad (4.4.33)$$

This is the full one-loop integrand for MHV amplitudes.

As expected on general grounds from Yangian-invariance, and also as familiar from BCFW recursion at tree-level, the individual terms in this formula contain both local and non-local poles. We will graphically denote a factor $\langle AB xy \rangle$ in the denominator by drawing a line (xy) ; the numerators of tensor integrals (required by dual conformal invariance) will be denoted by wavy- and dashed-lines—the precise meaning of which will be explained shortly. In this notation, this result is



Notice that all the terms have 6 factors in the denominator, and hence by dual conformal invariance we must have two factors containing (AB) in the numerators. These are denoted by the wavy lines: the numerator is $\langle AB(1 i i+1) \cap (1 j j+1) \rangle^2 \equiv (\langle A 1 i i+1 \rangle \langle B 1 j j+1 \rangle) -$

$\langle B 1 i i+1 \rangle \langle A 1 j j+1 \rangle^2$, where the power of 2 has been indicated by the line's multiplicity.

Notice that when $i + 1 = j$, the numerator cancels the two factors $\langle AB 1 j \rangle^2$ in the denominator: by a simple use of the Schouten identity it is easy to see that

$$[\langle A 1 j-1 j \rangle \langle B 1 j j+1 \rangle - \langle A 1 j j+1 \rangle \langle B 1 j-1 j \rangle]^2 = [\langle AB 1 j \rangle \langle 1 j-1 j j+1 \rangle]^2. \quad (4.4.34)$$

In general, all of these terms contain both physical as well as spurious poles. Physical poles are denominator factors of the form $\langle AB i i+1 \rangle$ and $\langle i i+1 j j+1 \rangle$ while spurious poles are all other denominator factors. We often refer to physical poles as local poles and to spurious poles as non-local. A small explanation for the “non-local” terminology is in order. Consider the 5-particle amplitude as an example, where there are three terms in the integrand. These three terms are

$$\frac{\langle 1234 \rangle^2}{\langle AB 12 \rangle \langle AB 23 \rangle \langle AB 34 \rangle \langle AB 14 \rangle} + \frac{\langle AB (123) \cap (145) \rangle^2}{\langle AB 12 \rangle \langle AB 23 \rangle \langle AB 31 \rangle \langle AB 14 \rangle \langle AB 45 \rangle \langle AB 51 \rangle} \\ \frac{\langle 3451 \rangle^2}{\langle AB 34 \rangle \langle AB 45 \rangle \langle AB 51 \rangle \langle AB 31 \rangle}. \quad (4.4.35)$$

The spurious poles are $\langle AB 14 \rangle$ and $\langle AB 13 \rangle$. The line defined by Z_1 and Z_3 corresponds to a complex point, but what makes $\langle AB 13 \rangle$ non-local? The reason is that in field theory $1/\langle AB 13 \rangle$ could only come from a loop integration, *e.g.* it is generated by a local one-loop integral of the form

$$\int \left[\frac{d^4 Z_C d^4 Z_D}{\text{vol}(GL_2)} \right] \frac{\langle CD (512) \cap (234) \rangle}{\langle CD AB \rangle \langle CD 51 \rangle \langle CD 12 \rangle \langle CD 23 \rangle \langle CD 34 \rangle}. \quad (4.4.36)$$

(This is also the secret origin of the non-local poles in BCFW at tree-level.)

Back to the 5-particle example, $\langle AB 14 \rangle$ and $\langle AB 31 \rangle$ occur each in two of the three terms and they cancel in pairs. Indeed upon collecting denominators we find, after repeated uses of the Schouten identity, the result for the sum

$$\frac{\langle AB 12 \rangle \langle 2345 \rangle \langle 1345 \rangle + \langle AB 23 \rangle \langle 1345 \rangle \langle 1245 \rangle + \langle AB 13 \rangle \langle 1245 \rangle \langle 3245 \rangle + \langle AB 45 \rangle \langle 1234 \rangle \langle 1235 \rangle}{\langle AB 12 \rangle \langle AB 23 \rangle \langle AB 34 \rangle \langle AB 45 \rangle \langle AB 51 \rangle}. \quad (4.4.37)$$

This is furthermore cyclically-invariant, albeit in a nontrivial way involving Schouten identities.

Let us also briefly discuss the 6-particle NMHV amplitude at 1-loop. The full integrand has 16 terms which differs even more sharply from familiar local forms of writing

the amplitude. As we will review in the next section, the usual box decomposition of 1-loop amplitudes does not match the full integrand (only the “parity-even” part of the integrand); even so, there is a natural generalization of the basis of integrals that can be used to match the full integrand in a manifestly dual conformal invariant form. Any such representation, however, will have the familiar form “leading singularity/Grassmannian residue \times loop integral”. However, this is *not* the form we encounter with loop-level BCFW. Instead, the supersymmetric η -variables are entangled with the loop integration variables in an interesting way. For instance, one of the terms from the forward limit contribution to the 6-particle NMHV amplitude integrand is the following,

$$\frac{\delta^{0|4} \left(\begin{array}{l} \eta_1 \langle AB 1(23) \cap (456) \rangle + \eta_2 \langle 4561 \rangle \langle AB 31 \rangle + \eta_3 \langle 4561 \rangle \langle AB 12 \rangle \\ + \eta_4 \langle AB (123) \cap (561) \rangle + \eta_5 \langle AB 1(46) \cap (123) \rangle + \eta_6 \langle AB 1(123) \cap (45) \rangle \end{array} \right)}{\langle 4561 \rangle \langle AB 45 \rangle \langle AB 61 \rangle \langle AB 12 \rangle \langle AB 23 \rangle \langle AB 13 \rangle \langle AB 41 \rangle \langle AB (123) \cap (456) \rangle \langle AB (123) \cap (561) \rangle}$$

The full expression is given in appendix C. Note the presence of the explicit (AB) -dependence in the argument of the Fermionic δ -function. Seemingly miraculously, when the residues of this integral are computed on its leading singularities, the η -dependence precisely reproduces the standard NMHV R -invariants. Of course this miracle is guaranteed by our general arguments about the Yangian-invariance of these objects.

IV. Unitarity as a Residue Theorem

The BCFW construction of tree-level amplitudes make Yangian-invariance manifest, but are not manifestly cyclic-invariant. The statement of cyclic-invariance is then a remarkable identity between rational functions. Of course one could say that the field theory derivation of the recursion relation gives a proof of these identities, but this is quite a circuitous argument. One of the initial striking features of the Grassmannian picture for tree amplitudes was that these identities were instead a direct consequence of the global residue theorem applied to the Grassmannian integral. This observation ultimately led to the “particle interpretation” picture for the tree contour, giving a completely autonomous and deeper understanding of tree amplitudes, removed from the crutch of their field theory origin.

In complete analogy with BCFW at tree-level, the BCFW construction of the loop integrand is not manifestly cyclically-invariant. Again cyclic-invariance is a remarkable

identity between rational functions, and again this identity can be thought of as a consequence of the field theory derivation of the recursion relation. But of course we strongly suspect that there is an extension of the “particle interpretation” picture that gives a completely autonomous and deeper understanding of loop amplitudes, independent of any field theoretic derivation.

Just as at tree-level, a first step in this direction is to find a new understanding of the cyclic-invariance identities. To wit, we have understood how the cyclic-identity for the 1-loop MHV amplitude can be understood as a residue theorem; we very briefly outline the argument here, deferring a detailed explanation to [35]. The idea is to identify the terms appearing in the MHV 1-loop formulas as the residues of a new Grassmannian integral. All the terms in the MHV 1-loop formula can actually be thought of as arising from $\int d^{3|4} \mathcal{Z}_A d^{3|4} \mathcal{Z}_B Y_{n+2, k=2}(\mathcal{Z}_A, \mathcal{Z}_B, \dots)$, where $Y_{n+2, k=2}$ is computed from the $G(2, n+2)$ Grassmannian integral. Note that $\mathcal{Z}_A, \mathcal{Z}_B$ appear in the δ -functions of the integral in the combination $C_{\beta A} \mathcal{Z}_A + C_{\beta B} \mathcal{Z}_B$, so the GL_2 -action on $(\mathcal{Z}_A, \mathcal{Z}_B)$ also acts on $(C_{\beta A}, C_{\beta B})$. Performing the $\eta_{A,B}$ and GL_2 -integrals leaves us with a new Grassmannian integral:

$$\int d^{2 \times (n+2)} C_{\beta a} \frac{\delta^4(C_{\beta i} Z_i + C_{\beta A} Z_A + C_{\beta B} Z_B)(AB)^2}{(12)(23) \cdots (n1)}. \quad (4.4.38)$$

By construction, this integral has a GL_2 -invariance acting on columns (A, B) and (Z_A, Z_B) , and hence all of its residues are only a function of the line $(Z_A Z_B)$. In particular all terms appearing in the MHV 1-loop formula, after GL_2 integration, are particular residues of this Grassmannian integral.

As we will discuss at greater length in [35], the equality of cyclically-related BCFW expressions of the 1-loop amplitude follows from a residue theorem applied to this integral. In fact, it can be shown that the *only* combination of these residues that is free of spurious poles is the physical 1-loop amplitude.

At tree level, the cyclic-identity applied to *e.g.* NMHV amplitudes ensures the absence of spurious poles. The same is true at 1-loop level. Since the BCFW formula manifestly guarantees that one of the single cuts is correctly reproduced, cyclicity guarantees that *all* the single cuts are correct. Having all correct single cuts, automatically ensures that all higher cuts—and in particular unitarity cuts—are correctly reproduced. Unitarity then finds a deeper origin in this residue theorem.

4.5 The Loop Integrand in Local Form

We have seen that the loop integrand produced by BCFW consists of a sum over non-local terms. In order to present the results in a more familiar form, and also as a powerful check on the formalism, it is interesting to instead re-write the integrand in a manifestly local way (which will of course spoil the Yangian-invariance of each term). We will do this for a number of multi-loop examples in the next section, but first we must describe a new basis of local loop integrals which differs in significant ways from the standard scalar integrals, but which will greatly simplify the results and make the physics much more transparent.

Loop amplitudes are normally written as scalar integrals⁹ with rational coefficients. Obviously this form can not match the full loop integrand, since scalar integrals are even under parity but the amplitude is chiral. Let's consider one-loop integrals to begin the discussion. In the usual way of discussing the integral reduction procedure, manipulations at the level of the integrand reduces integrals down to pentagons [105]. The final reduction to the familiar boxes uses the fact that the parity-odd parts of the integrand integrate to zero.

We are instead interested in the full integrand, however, and since the amplitudes aren't parity symmetric, there is no natural division between "parity-odd" and "parity-even". In fact, for the purpose of writing recursion relations, it is crucial to know both. Furthermore, the BCFW recursion relation guarantees that the loop integrand is dual conformally invariant and thus most usefully discussed in momentum-twistor space. We are then led to construct a novel basis of naturally chiral integrals written directly in momentum-twistor space, as we now briefly describe. These issues will be discussed at much greater length in [35].

Let's look at a few quick examples of local integrals written in momentum-twistor space. We have encountered the simplest example already; the zero mass integral at 1-loop

$$\int \left[\frac{d^4 Z_A d^4 Z_B}{\text{vol}(GL_2)} \right] \frac{\langle 1234 \rangle^2}{\langle AB 12 \rangle \langle AB 23 \rangle \langle AB 34 \rangle \langle AB 41 \rangle}. \quad (4.5.39)$$

⁹Here we abuse terminology and use the term "scalar", which is appropriate at one-loop, to refer to possibly tensor integrals at higher-loop order where the tensor structure is the product of "local" factors, *i.e.*, of the form $\langle (AB)_\ell i i+1 \rangle$ and $\langle (AB)_\ell (AB)_k \rangle$.

Henceforth, we will drop the integration measure and only write the integrand. The most general 1-loop integrand is of the form

$$\frac{\langle AB Y_1 \rangle \dots \langle AB Y_{n-4} \rangle}{\langle AB 12 \rangle \langle AB 23 \rangle \dots \langle AB n1 \rangle}, \quad (4.5.40)$$

where $Y_1^{IJ}, \dots, Y_{n-4}^{IJ}$ are general 4×4 antisymmetric matrices or ‘bitwistors’; with 6 independent components. Momentum-twistors make integral reduction trivial. Suppose there are 6 or more local propagator factors including $\langle AB j_1 j_1+1 \rangle \dots \langle AB j_6 j_6+1 \rangle$ in the denominator. We can always expand all the Y^{IJ} ’s in a basis of the 6 bitwistors $Z_{j_1}^{[I} Z_{j_1+1}^{J]}, \dots, Z_{j_6}^{[I} Z_{j_6+1}^{J]}$. Inserting this expansion into the integrand, each term knocks-out a propagator from the denominator. Thus we can reduce any integral down to pentagons.

These will contain 5 “(AB)” factors in the denominator and a single “(AB)” factor in the numerator. In the literature, x -space loop integrals are written with numerator factors like $(x - x_j)^2$, which in momentum-twistor space correspond to $\langle AB j j+1 \rangle$. However, we will find more general numerators to be more natural. For instance, a typical pentagon integrand we consider takes the form

$$\frac{\langle AB 14 \rangle \langle 5123 \rangle \langle 2345 \rangle}{\langle AB 12 \rangle \langle AB 23 \rangle \langle AB 34 \rangle \langle AB 45 \rangle \langle AB 51 \rangle}. \quad (4.5.41)$$

We can trivially translate this integral into x -space; the numerator is proportional to $(x - x_{14})^2$, where x_{14} is a complex point associated with the line (14) in momentum-twistor space; specifically, the pentagon-integral (4.5.41) is given by

$$\frac{\langle 14 \rangle \langle 23 \rangle}{\langle 12 \rangle \langle 34 \rangle} \int d^4 x \frac{(x - x_{14})^2 x_{13}^2 x_{35}^2}{(x - x_1)^2 (x - x_2)^2 (x - x_3)^2 (x - x_4)^2 (x - x_5)^2}, \quad (4.5.42)$$

with

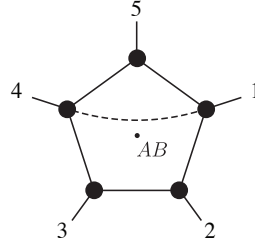
$$x_{14} \equiv \frac{|1\rangle x_4 |4\rangle - |4\rangle x_1 |1\rangle}{\langle 14 \rangle}. \quad (4.5.43)$$

The complex point x_{14} is null-separated from x_1, x_2, x_4 and x_5 ; the second point sharing this property is its parity conjugate which will be described shortly. These complex points play an important role in the story, and it is most convenient to discuss them on an equal footing with the rest of the points by working directly with momentum-twistor space integrands.

Notably, unlike standard scalar integrals, this pentagon integral is *chiral*. Like any pentagon integral, it has 5 quadruple cuts and twice as many leading singularities. But

unlike a generic pentagon integral, with this special numerator, half of the leading singularities vanish, and the others are all equal up to sign—hence, we say that this integral has “unit leading singularities”. All of the local integrals we consider have this quite remarkable feature.

Local momentum-twistor space integrals can be drawn in exactly the same way as familiar planar integrals in x -space; we introduce a new bit of notation to denote the numerator factors. The pentagon integral we just discussed is drawn as,



$$(4.5.44)$$

where the dashed line connecting $(1, 4)$ denotes the numerator factor $\langle AB 14 \rangle$. We will also have recourse to use the parity conjugates of these lines. The point Z_i in momentum twistor space is naturally paired with its projective-dual plane $W_i = (i-1 \ i \ i+1)$, and the parity conjugate of a line (ij) is the line which is the intersection of the corresponding planes $(\overline{ij}) \equiv (i-1 \ i \ i+1) \cap (j-1 \ j \ j+1)$. The numerator factor,

$$\langle AB \overline{ij} \rangle \equiv \langle A \ i-1 \ i \ i+1 \rangle \langle B \ j-1 \ j \ j+1 \rangle - \langle B \ i-1 \ i \ i+1 \rangle \langle A \ j-1 \ j \ j+1 \rangle \quad (4.5.45)$$

will be denoted by a wavy-line connecting i, j .

With this notation we can nicely write the integrand for n -particle 1-loop MHV amplitudes as

$$\frac{1}{n} \left(\begin{array}{c} \begin{array}{c} n \\ \vdots \\ i+1 \\ \vdots \\ i \\ \vdots \\ 3 \end{array} \begin{array}{c} \bullet \\ \vdots \\ \bullet \\ \vdots \\ \bullet \\ \vdots \\ \bullet \end{array} \begin{array}{c} \bullet \\ \vdots \\ \bullet \\ \vdots \\ \bullet \\ \vdots \\ \bullet \end{array} \begin{array}{c} 1 \\ \vdots \\ 2 \end{array} \\ \langle n \ 1 \ 2 \ 3 \rangle \langle 1 \ 2 \ i \ i+1 \rangle \\ 2 < i < n \end{array} + \begin{array}{c} \begin{array}{c} j+1 \\ \vdots \\ 1 \\ \vdots \\ j \\ \vdots \\ j-1 \\ \vdots \\ i \\ \vdots \\ i-1 \end{array} \begin{array}{c} \bullet \\ \vdots \\ \bullet \\ \vdots \\ \bullet \\ \vdots \\ \bullet \end{array} \begin{array}{c} \bullet \\ \vdots \\ \bullet \\ \vdots \\ \bullet \\ \vdots \\ \bullet \end{array} \begin{array}{c} 2 \\ \vdots \\ 3 \end{array} \\ \langle 2 \ j \ i-1 \ i \rangle \\ \times \langle AB \ (123) \cap (j-1 \ j \ j+1) \rangle \\ 3 < i < j \leq n \end{array} + \text{cyclic} \right). \quad (4.5.46)$$

In this expression we sum over all cyclic integrands, including duplicates, which is related to the presence of the $1/n$ pre-factor.

For definiteness, we have indicated the numerator factor beneath the corresponding picture. Recall the familiar form of the MHV amplitude as a sum over all 2-mass easy boxes; it is amusing that in our form the only boxes are 2-mass hard. The algorithm by which this form was deduced will be explained shortly.

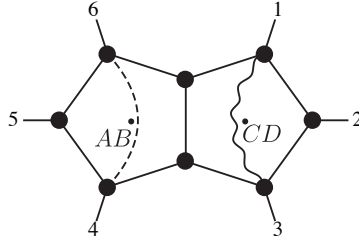
We pause to point out that the full integrand for some MHV amplitudes have been computed in the literature, in the context of using the leading singularity method to determine the integrand [97]. A peculiarity in these papers was that the set of integrals that were used to match all the leading singularities did not appear to be manifestly dual conformal invariant—which is particularly ironic, given that the leading singularities themselves are fully Yangian-invariant! This led some authors to the conclusion that the parity-odd parts of the amplitude are somehow irrelevant, since they not only integrate to zero on the real contour but are also not dual conformal invariant. Of course, nothing could be further from the truth: we have seen very clearly that the *full* integrand is determined recursively and exhibits the Yangian symmetry of the theory; the decomposition into parity even and odd parts is artificial. The problem is quite simple, the basis of scalar integrals has only parity even elements! Therefore, one is trying to model the full integrand with a very inappropriate basis.

From the momentum-twistor viewpoint, the source of the previous difficulties can be seen quite explicitly. We have seen that all 1-loop integrals can be reduced to pentagons, but these are *tensor* pentagons, *i.e.* with factors of (AB) in the numerator. Now, it *is* possible to further reduce a pentagon with numerator $\langle ABY \rangle$, with Y corresponding to a real line or not, to a scalar pentagon integral, by expanding Y in a basis of the 5 bitwistors appearing in the denominators, together with the infinity twistor I_∞ . But this breaks manifest dual conformal invariance! Thus the integrands obtained in [95, 97, 99] are indeed dual conformal invariant, but the symmetry was obscured by insistence to use scalar integrals.

Let's give an example of an interesting two-loop integrand using our notation:

$$\frac{\langle 1345 \rangle \langle 5613 \rangle \langle AB46 \rangle \langle CD(234) \cap (612) \rangle}{\langle CD61 \rangle \langle CD12 \rangle \langle CD23 \rangle \langle CD34 \rangle \langle ABCD \rangle \langle AB34 \rangle \langle AB45 \rangle \langle AB56 \rangle \langle AB61 \rangle} \quad (4.5.47)$$

which we draw as



At two-loops, there are generally 4 solutions to cutting any eight propagators, and so this integral has $9 \times 4 = 36$ different (non-composite) leading singularities. However, the integral is maximally chiral: putting any choice of eight propagators on shell will have only *one* solution with a non-vanishing residue. Moreover, the non-vanishing residues are equal up to a sign. This non-trivial fact can be understood as following from the global residue theorem applied to the integral. All the tensor integrals we write in this chapter are *chiral* in this sense, and the overall normalization of each has been chosen so that all its non-vanishing leading singularities are equal to ± 1 .

These chiral momentum-twistor integrals have another remarkable feature: they are less IR-divergent than generic loop integrals; indeed, many of them are completely IR-finite. Infrared divergences arise when the loop momenta become collinear with the external momenta p_j . In the dual co-ordinate space, this happens when a loop-integration variable x lies on the line connecting x_j and x_{j+1} . In momentum-twistor space, this corresponds to configurations where the associated line (AB) passes through the point Z_j while lying in the plane $(j-1 \ j \ j+1)$. An integral is IR-finite if the numerator factors have a zero in the dangerous configurations. There are an infinite class of IR-finite integrals at any loop order; for instance, it is easy to see that the two-loop example above is IR-finite. Further discussion of these objects and their role in determining IR-finite parts of amplitudes like the remainder [81] and ratio [106] functions will be carried out in [35]. Of course we expect that IR finite quantities, such as the ratio function, are manifestly finite already at the level of the integrand.

It is interesting that the naïvely “hardest” multi-loop integrands can be reduced to finite integrals plus simpler integrals. Consider for instance a general double pentagon integrand for six particles, of the form

$$\frac{\langle AB Y_1 \rangle \langle CD Y_2 \rangle}{\langle CD 61 \rangle \langle CD 12 \rangle \langle CD 23 \rangle \langle CD 34 \rangle \langle AB CD \rangle \langle AB 34 \rangle \langle AB 45 \rangle \langle AB 56 \rangle \langle AB 61 \rangle}. \quad (4.5.48)$$

We can expand Y_1 in terms of the 6 bitwistors $(Z_3 Z_4), (Z_4 Z_5), (Z_5 Z_6), (Z_6 Z_1)$ as well

as the bitwistors corresponding to (46) and its parity conjugate ($\overline{46}$). Similarly we can expand Y_2 in terms of $(Z_1Z_2), (Z_2Z_3), (Z_3Z_4), (Z_6Z_1)$ as well as (31) and ($\overline{31}$). Doing this reduces the integral to finite double-pentagon integrals, plus simpler pentagon-box and double-box integrals.

Finally, let us describe the general algorithm which we used to find local forms of the loop integrands. The first step is to construct an algebraic basis of dual conformal-invariant integrals, over which the integrand is to be expanded. It turns out, quite remarkably, that for at least 1- and 2-loops an (over-complete) algebraic basis can be constructed which contains exclusively integrals with unit leading singularities, in the sense just defined. We have explicitly constructed such a bases at 1- and 2-loops and arbitrary n [35]. The second step is to match the integrand as generated by equation (4.4.29) with a linear combination of the basis integrals. Since the loop integrand is a well-defined function of external momenta and loop momenta, this can be done by simply evaluating it at sufficiently many random points. Numerical evaluation of the integrand is itself quite fast. Finally, this procedure is greatly facilitated by the fact that, when using our particular integral basis, the coefficients are guaranteed to be pure numbers (or multiple of leading singularities, for arbitrary N^k MHV), as opposed to arbitrary rational functions of the external momenta.

4.6 Multi-Loop Examples

The recursion relation for loops gives a completely systematic way of determining the integrand for amplitudes with any (n, k, ℓ) . All the required operations are completely algebraic and can be easily automated. In this section we use the recursion relation to present a number of multi-loop results.

As we have stressed repeatedly, the individual terms in the BCFW expansion of the loop integrand have spurious poles and are also not manifestly cyclically-invariant; thus as a very strong consistency check on our results, necessary for a local form to exist, we verify that the integrand is free of all spurious poles: the only poles in the integrand should be of the form $\langle i-1 \ i \ j-1 \ j \rangle, \langle (AB)_\ell \ j-1 \ j \rangle, \langle (AB)_{\ell_1} \ (AB)_{\ell_2} \rangle$. We also explicitly check cyclic-invariance. Recall that the absence of spurious poles and cyclicity guarantees that all single-cuts of the amplitude are reproduced, and thus *all* cuts are automatically

correctly matched. While preparing this chapter we have explicitly checked that our recursive determination of the integrand passes these checks up to 14 point N^4 MHV amplitudes at 1-loop, 25-point MHV amplitudes at 2-loops, 8-point NMHV amplitudes at 2-loops, and 5-point MHV amplitude at 3-loops.

We can expand the integral in a local basis of chiral momentum-space integrals with unit leading singularities using the algorithm briefly described in the previous section. While the BCFW form of the integrand is almost always more concise than the local form, the local form is more familiar, so we will present the results in this way. Indeed, the (modestly) non-trivial work here is only in determining the natural basis for local integrands. While this is a straightforward exercise using momentum-twistor machinery, the result is non-trivial, yielding a canonical basis of multi-loop integrals, which we have constructed explicitly for all n up to 2-loops. In order to present a tree-loop result, we also found the 5pt basis at three-loops, deferring a complete discussion to [35]. Given the basis of local integrals with unit leading singularities, generating the integrand and finding its expansion in the basis is not difficult. The natural basis is over-complete and so the results can be expressed in a number of equivalent forms. We will choose the forms that seem canonical and reveal patterns. As we will see, somewhat surprisingly, the local forms are also often remarkably simple.

I. All 2-Loop MHV Amplitudes

The two-loop amplitude for 4- and 5-particles is given by, respectively,

$$\begin{array}{c}
 \begin{array}{ccc}
 4 & & 1 \\
 \bullet & \text{---} & \bullet \\
 | & & | \\
 \bullet & \text{---} & \bullet \\
 3 & & 2
 \end{array} \\
 \langle 2341 \rangle \langle 3412 \rangle \langle 4123 \rangle
 \end{array}
 + \text{cyclic} \quad (4.6.49)$$

(no repeat)

and

$$\begin{aligned}
 & \begin{array}{c} \text{Diagram 1: Double box with external legs 1, 2, 3, 4, 5} \\ \langle 2345 \rangle \langle 5123 \rangle \langle 3412 \rangle \end{array} + \begin{array}{c} \text{Diagram 2: Double box with a wavy line and external legs 1, 2, 3, 4, 5} \\ \langle 3451 \rangle \langle 4513 \rangle \end{array} + \text{cyclic} \\
 & \hspace{15em} \text{(no repeat)} \hspace{1em} (4.6.50) \\
 & \hspace{15em} \times \langle AB(512) \cap (234) \rangle
 \end{aligned}$$

while the 6-particle amplitude is

$$\begin{aligned}
 & \begin{array}{c} \text{Diagram 1: Double box with external legs 1, 2, 3, 4, 5, 6} \\ \langle 2345 \rangle \langle 6123 \rangle \langle 3412 \rangle \end{array} + \begin{array}{c} \text{Diagram 2: Double box with a wavy line and external legs 1, 2, 3, 4, 5, 6} \\ \langle 3456 \rangle \langle 4563 \rangle \end{array} + \begin{array}{c} \text{Diagram 3: Double box with a wavy line and external legs 1, 2, 3, 4, 5, 6} \\ \langle 2345 \rangle \langle 3462 \rangle \end{array} + \begin{array}{c} \text{Diagram 4: Double box with a wavy line and external legs 1, 2, 3, 4, 5, 6} \\ \langle 3456 \rangle \langle 4562 \rangle \end{array} \\
 & \hspace{15em} \times \langle AB(561) \cap (234) \rangle \quad \times \langle AB(561) \cap (123) \rangle \quad \times \langle AB(561) \cap (123) \rangle \\
 & \hspace{15em} (4.6.51) \\
 & + \begin{array}{c} \text{Diagram 5: Double box with external legs 1, 2, 3, 4, 5, 6} \\ \langle 3456 \rangle \langle 6123 \rangle \langle 4512 \rangle \end{array} + \begin{array}{c} \text{Diagram 6: Double box with two wavy lines and external legs 1, 2, 3, 4, 5, 6} \\ \langle 6235 \rangle \end{array} + \text{cyclic} \\
 & \hspace{15em} \text{(no repeat)} \\
 & \hspace{15em} \times \langle AB(234) \cap (456) \rangle \\
 & \hspace{15em} \times \langle CD(561) \cap (123) \rangle
 \end{aligned}$$

To be completely explicit, we have written the numerator factors accompanying each given term under its corresponding picture.

What about higher-points? The parity-even part of the integrand has been computed in [16], though the expressions are lengthy and do not expose a discernible pattern. However, looking at the *full* (non-parity invariant) integrand for 4-, 5- and 6-particles in momentum-twistor space reveals a clear pattern: the structure looks like the “square” of the 1-loop objects, with double-box, pentagon-box and double-pentagon topologies.

This motivates a simple conjecture for all 2-loop MHV amplitudes:

$$\begin{aligned}
 & \begin{array}{c} \text{Diagram 1: A square with two internal vertical lines. External legs are labeled } i+1, 1, i, 2. \end{array} + \begin{array}{c} \text{Diagram 2: A square with two internal vertical lines and a wavy line connecting the top-right and bottom-right vertices. External legs are labeled } i, j, i-1, j+1, i-1, 1, i-1, 2. \end{array} + \begin{array}{c} \text{Diagram 3: A square with two internal vertical lines and two wavy lines connecting the top-left to top-right and bottom-left to bottom-right vertices. External legs are labeled } j-1, j, k, i+1, i, 2, k+1, 1. \end{array} \\
 & \langle n \ 1 \ 2 \ 3 \rangle \times \langle 2 \ j \ i-1 \ i \rangle \langle i-2 \ i-1 \ i \ i+1 \rangle \langle 2 \ i \ j \ k \rangle \\
 & \langle 1 \ 2 \ i \ i+1 \rangle \langle i-1 \ i \ i+1 \ i+2 \rangle \times \langle AB \ (123) \cap (j-1 \ j \ j+1) \rangle \times \langle AB \ (123) \cap (k-1 \ k \ k+1) \rangle \\
 & \times \langle CD \ (i-1 \ i \ i+1) \cap (j-1 \ j \ j+1) \rangle \\
 & 2 < i < n \qquad 3 < i < j \leq n \qquad 2 < i < j-1 < k-1 < n
 \end{aligned} \tag{4.6.52}$$

We checked numerically that this matches the 2-loop MHV integrand as calculated by BCFW directly. Because the recursion relations are easily automated, this can be verified for any number of particles. We have checked this explicitly for up to 26 particles. It is worth emphasizing that independent of verifying the local-ansatz, the cancellation of spurious poles (and propagators) is a particularly strong consistency check for the recursion relations. For instance, for the 26-point 2-loop MHV amplitude, there are exactly 99,434 terms in the BCFW recursion, each riddled with spurious poles that cancel in the sum. Even a single sign-mistake would have spoiled this miracle.

It is interesting to note that the naïvely “hardest” integrals that appear here—the double pentagons—have a numerator which renders them completely finite.

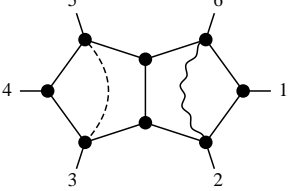
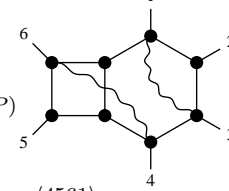
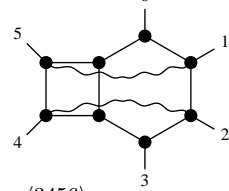
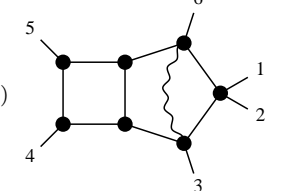
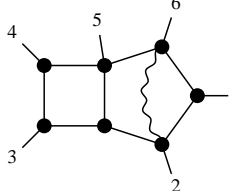
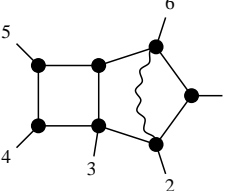
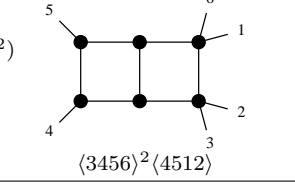
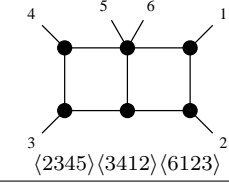
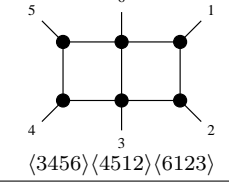
II. All 2-Loop NMHV Amplitudes

Although structurally identical to the 2-loop 5-particle MHV amplitude, it is worth writing explicitly the 2-loop 5-particle NMHV amplitude; it is,

$$[1 \ 2 \ 3 \ 4 \ 5] \left(\begin{array}{c} \text{Diagram 1: A square with two internal vertical lines. External legs are labeled } 4, 5, 1, 3, 2. \\ \langle 2345 \rangle \langle 5123 \rangle \langle 3412 \rangle \\ \text{Diagram 2: A square with two internal vertical lines and a dashed line connecting the top-right and bottom-right vertices. External legs are labeled } 5, 1, 2, 4, 3. \\ \langle 2345 \rangle \langle 3451 \rangle \langle 4512 \rangle \\ \times \langle AB \ 31 \rangle \\ \text{cyclic (no repeat)} \end{array} \right) \tag{4.6.53}$$

Notice how this answer highlights the role played by parity: equations (4.6.53) and (4.6.50) differ only by the parity of the numerator in the tensor-integral—and one can be

Table 4.1: Coefficients of residue (1) = [23456]. Here, “ g ” rotates each figure by $g : i \mapsto i+1$, and P exchanges wavy- and dashed-lines (together with each figure’s corresponding normalization).

<p>1</p>  <p>$\langle 6234 \rangle \langle 6245 \rangle$ $\times \langle AB \ 53 \rangle \langle CD \ (123) \cap (561) \rangle$</p>	<p>$1 + g^3$ $-g(1-g)(1-P)$</p>  <p>$\langle 4561 \rangle$ $\times \langle AB \ (345) \cap (561) \rangle$ $\times \langle AB \ (612) \cap (234) \rangle$</p>	<p>$(1 + g^3 P)$</p>  <p>$\langle 3456 \rangle$ $\times \langle AB \ (123) \cap (345) \rangle$ $\times \langle AB \ (456) \cap (612) \rangle$</p>
<p>$(1 + g^3 P)$</p>  <p>$\langle 3456 \rangle \langle 4563 \rangle$ $\times \langle AB \ (561) \cap (234) \rangle$</p>	<p>$-(1 + g^3 P)$</p>  <p>$\langle 2345 \rangle \langle 3462 \rangle$ $\times \langle AB \ (561) \cap (123) \rangle$</p>	<p>$(1 + g^3 P)$ $\times (1 + g - g^3)$</p>  <p>$\langle 3456 \rangle \langle 4562 \rangle$ $\times \langle AB \ (561) \cap (123) \rangle$</p>
<p>$(1 - g + g^2)$</p>  <p>$\langle 3456 \rangle^2 \langle 4512 \rangle$</p>	<p>$(1 + g^2 + g^4)$</p>  <p>$\langle 2345 \rangle \langle 3412 \rangle \langle 6123 \rangle$</p>	<p>$\frac{1}{2} (1 + g^2 + g^4)$</p>  <p>$\langle 3456 \rangle \langle 4512 \rangle \langle 6123 \rangle$</p>

obtained from the other simply by exchanging wavy- for dashed-lines. Next we present the 6-particle 2-loop NMHV amplitude, written in the manifestly-cyclic form,

$$(1)I_1 + \text{cyclic}, \quad (4.6.54)$$

where (1) is the Grassmannian residue given by the R -invariant [23456] written explicitly in equation (4.2.6). Below, we show the coefficient I_1 of residue (1).

We next move to the 7-particle NMHV amplitude, which will be presented in the form,

$$[(7)(1)I_{7,1} + \text{cyclic}] + [(7)(2)I_{7,2} + \text{cyclic}] + [(7)(3)I_{7,3} + \text{cyclic}] \quad (4.6.55)$$

where $(i)(j)$ is the Grassmannian residue given by the R -invariant defined by the complement of $\{i, j\}$ in $\{1, 2, \dots, 7\}$. The expressions for $I_{7,1}, I_{7,2}, I_{7,3}$ are given in appendix D.

III. All 3-Loop MHV Amplitudes

The four-point three-loop amplitude is given by the cyclic-sum of the following two classes of integrands:

$$\begin{aligned}
 & \begin{array}{c} \text{Diagram 1: A 2x4 grid of vertices with external lines 1, 2, 3, 4.} \\ \langle 2341 \rangle^3 \langle 3412 \rangle \end{array} + \begin{array}{c} \text{Diagram 2: A 2x4 grid with a wavy line connecting the top two vertices of the second and third columns.} \\ \langle 2341 \rangle \langle 3412 \rangle \\ \times \langle AB(412) \cap (123) \rangle \end{array} + \text{cyclic} \\
 & \hspace{15em} \text{(no repeat)} \quad (4.6.56)
 \end{aligned}$$

Although perhaps visually unfamiliar, the second integral above is commonly referred to as the “tennis-court” because of the way it is usually drawn. We have drawn it the way we have to highlight the presence of the pentagon sub-integral and the role played by the tensor-integral’s numerator (which should be read as connecting to vertices “1” and “2”).

Finally, we give the integrals contributing to the full 3-loop MHV amplitude for 5 particles. It is given by the following cyclic-sum of the integrands,

$$\begin{aligned}
 & \begin{array}{c} \text{Diagram 1: 2x4 grid with wavy line} \\ \langle 3451 \rangle^3 \\ \times \langle AB(234) \cap (512) \rangle \end{array} + \begin{array}{c} \text{Diagram 2: 2x4 grid with wavy line} \\ \langle 5123 \rangle \langle 4512 \rangle \langle 3451 \rangle \\ \times \langle AB(123) \cap (345) \rangle \end{array} + \begin{array}{c} \text{Diagram 3: 2x4 grid with wavy line} \\ \langle 4512 \rangle^2 \\ \times \langle AB(345) \cap (123) \rangle \end{array} + \begin{array}{c} \text{Diagram 4: 2x4 grid with wavy line} \\ \langle 4512 \rangle \\ \times \langle AB(451) \cap (512) \rangle \\ \times \langle AB(345) \cap (123) \rangle \end{array} \\
 & (1+r) \left(\begin{array}{c} \text{Diagram 5: 2x4 grid with wavy line} \\ \langle 5123 \rangle \langle 4512 \rangle \langle 3451 \rangle^2 \\ \times \langle AB(123) \cap (451) \rangle \end{array} + \begin{array}{c} \text{Diagram 6: 2x4 grid with wavy line} \\ \langle 5123 \rangle \langle 3451 \rangle \langle 2345 \rangle \\ \times \langle AB(123) \cap (451) \rangle \end{array} + \begin{array}{c} \text{Diagram 7: 2x4 grid with wavy line} \\ \langle 3451 \rangle \langle 4512 \rangle \langle 1234 \rangle / \langle 5123 \rangle \\ \times \langle AB(345) \cap (512) \rangle \end{array} + \begin{array}{c} \text{Diagram 8: 2x4 grid with wavy line} \\ \langle 2345 \rangle \langle 3451 \rangle / \langle 4512 \rangle \\ \times \langle AB(123) \cap (451) \rangle \\ \times \langle CD(234) \cap (512) \rangle \end{array} \right);
 \end{aligned}$$

here, r is the reflection operation that maps $i \mapsto (6 - i)$. Notice that deriving this three-loop amplitude using the loop-level recursion requires both the 1-loop 9-particle N^2 MHV integrand, and the 2-loop 7-particle NMHV integrand; and so the success of getting a manifestly-cyclic and spurious-pole-free, local object is an indirect check of the validity of the whole structure at lower-loops and higher points.

We conclude this quick tour of some simple multi-loop integrands by stressing again a remarkable feature of all these results. The integrals that appear are special objects with unit leading singularities—they are thus the most natural basis of local integrals with which to match the singularities of the theory. As a consequence the coefficients are also simple objects: “ ± 1 ” for MHV amplitudes, and Grassmannian residues with integer coefficients for more general amplitudes. These objects should be thought of as the correct building blocks for the local integrand, just as the BCFW terms provide the building blocks for the integrand in Yangian-invariant form. As we will discuss below, it is also likely that carrying out the integration will yield “simple” results for these classes of integrals.

4.7 Outlook

The loop integrand for scattering amplitudes is a well-defined object for any gauge theory in the planar limit, and in this chapter we have given an explicit recursive prescription for computing it to any loop order in $\mathcal{N} = 4$ SYM, in a way which manifests the full Yangian-invariance of the theory. This provides a complete definition of perturbative scattering amplitudes in planar $\mathcal{N} = 4$ SYM, with no reference to the Lagrangian, gauge redundancies or other off-shell notions. Along the way, we have also seen a new physical picture for how loops can arise purely from on-shell data, associated with removing pairs of particles in a naturally “entangled” way. From this vantage point, a number of directions for future work immediately suggest themselves.

I. The Origin of Loops

A few years ago, the tree-level BCFW recursion relations sat at an interesting cross-roads between the usual formulation of field theory, where space-time locality is manifest, and a hoped for dual description, where space-time should be emergent. On the one hand, the recursion relations were directly derived from field theory—without the field-theoretic motivation, it was hard to imagine the motivation for gluing lower-point objects together in the prescribed way. On the other hand, the presentation of the amplitude was very different from anything normally seen in field theory. The amplitudes could be presented in many different forms, with remarkable identities guaranteeing their equivalence. The

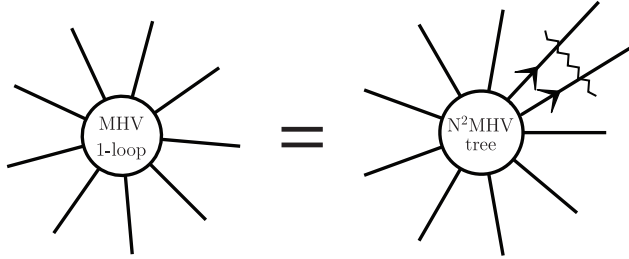
simplicity of the answers resulted directly from the presence of non-local poles. These properties, together with the dual super-conformal invariance of all terms in the BCFW expansions, strongly motivated the search for a dual theory which would make these features obvious, and which would furthermore give an intrinsic definition of the tree amplitudes on its own turf.

The Grassmannian duality for leading singularities provides this dual understanding of tree amplitudes in a satisfying way. The Yangian symmetry is manifest (for all leading singularities and not just tree amplitudes). The amplitude can be presented in many forms since it is a contour integral, with many representatives for a given homology class. The remarkable identities guaranteeing cyclic-invariance (together with important physical properties at loop-level) indeed find a new interpretation as higher-dimensional residue theorems. And finally, giving the contour integral over the Grassmannian a “particle interpretation” poses a natural question, intrinsic to the Grassmannian picture, whose answer yields the tree amplitude, along the way exposing a (still quite mysterious) connection with twistor string theory. We strongly suspect that a generalization of this picture exists that extends the duality to only to incorporate loop amplitudes but also explain why loops must be computed to begin with.

Our extension of BCFW to all loop orders puts loop amplitudes in the same position at the cross-roads between field theory and a sought-after dual description that tree amplitudes occupied a few years ago. This should set the stage for fully exposing the dual picture, and we have already made some inroads to uncovering its structure. For instance we saw that the remarkable identities guaranteeing cyclic-invariance of the MHV 1-loop amplitude indeed have an origin as a residue theorem in a new Grassmannian integral closely associated to the “master” integral computing leading singularities/Yangian-invariants. The nature of the “seed” for loops, arising from removing particles, is also clearly intimately related to the particle interpretation, which has already played a central role in the emergence of locality at tree-level.

Along these lines, here we give another presentation of the 1-loop MHV amplitudes, which differs from the form we obtained using the recursion relation. Consider the tree-level N^2 MHV amplitude $M_{n,k=2}(\mathcal{Z}_1, \dots, \mathcal{Z}_n, \mathcal{Z}_A, \mathcal{Z}_B)$. The 1-loop MHV amplitude arises

directly from the entangled removal of A and B :



Here it is easy to see, using the BCFW form of the tree amplitude, that there is a unique GL_2 -contour of integration associated with each term. This formula differs term-by-term from the BCFW form of this amplitude. We can however recognize all the terms as residues of the same auxiliary Grassmannian integral in equation (4.4.38), and we have shown that the equivalence to the BCFW form follows from a residue theorem. While this formula does not directly generalize for other amplitudes, its form is certainly suggestive.

Progress on all these questions would likely be accelerated by finding an explicit solution to the recursion relation for all (n, k, ℓ) , generalizing the explicit solution already known for tree-amplitudes [50].

As a final comment, our analysis of loops in this chapter has been greatly aided by working in momentum-twistor space; these variables allow us to recognize loop integrals in their familiar momentum-space setting. However, given that all the elements in the recursion relation were described in manifestly Yangian-invariant ways, it must be possible to translate these results into ordinary twistor space. It is likely that the twistor-space formulation will be most fundamental, amongst other things it could offer a natural understanding of non-planar loop amplitudes as well.

The results of this chapter also give a renewed hope for extracting loop-information from twistor-string theory. As we have seen, loop amplitudes can easily hide in plain sight in subtle ways, masquerading as a formal way of representing “1” in terms of IR-divergent integrals in $(3, 1)$ -signature! It is likely that a deeper understanding of the contours associated with the “Hodges diagrams” [17, 107], already for twistor-space tree-amplitudes in $(3, 1)$ -signature, will be important to make progress here.

II. Simplicity of Integrals and IR-Anomalies

Putting aside these highbrow issues, we are confronted with a much more urgent question: does our understanding of the integrand help us to carry out the integrations to obtain the physical amplitudes? Are the symmetries of the integrand of any use?

In fact the manifestly Yangian-invariant way of presenting the integrand *does* strongly suggest that the integrals themselves will be “simple”. The “super” part of super-dual conformal invariance is already an extremely powerful constraint. Consider MHV amplitudes for simplicity. The statement of super-dual conformal invariance is

$$\sum_a \eta_a^K \frac{\partial}{\partial Z_a^J} M_{\text{MHV}} = 0 \rightarrow \frac{\partial}{\partial Z_a^J} M_{\text{MHV}} = 0 \text{ for all } a, \quad (4.7.57)$$

where we use the fact that the MHV amplitude has no η_a dependence. Thus, the only super-dual conformally invariant amplitude is forced to be a constant! This reflects the well-known fact that the only Yangian invariant with $k = 0$ is the MHV tree amplitude (=1 in momentum-twistor space). Now, we have expressed the integrand for the MHV amplitude in a manifestly super-dual conformal (indeed Yangian)-invariant way. Consider for instance the 1-loop amplitude, which has the form

$$M_{\text{MHV}} = \int d^{3|4} \mathcal{Z}_A d^{3|4} \mathcal{Z}_B F(\mathcal{Z}_A, \mathcal{Z}_B; \mathcal{Z}_a), \quad (4.7.58)$$

with an entangled contour of integration for $\mathcal{Z}_{A,B}$; we suppress the explicit expression for F . The statement of super-dual conformal invariance is perfectly well-defined at the level of the integrand, which turns into a total derivative:

$$\sum_a \eta_a^K \frac{\partial}{\partial Z_a^J} M_{\text{MHV}} = \int d^{3|4} \mathcal{Z}_A d^{3|4} \mathcal{Z}_B \left(\eta_A^K \frac{\partial}{\partial Z_A^J} + \eta_B^K \frac{\partial}{\partial Z_B^J} \right) F. \quad (4.7.59)$$

After doing the $\eta_{A,B}$ and GL_2 -integrals, we have

$$\frac{\partial}{\partial Z_a^J} M_{\text{MHV}} = \int \frac{d^4 Z_A d^4 Z_B}{\text{vol}(GL_2)} \left(\frac{\partial}{\partial Z_A^J} G_A^a + \frac{\partial}{\partial Z_B^J} G_B^a \right), \quad (4.7.60)$$

where we suppress the explicit forms of $G_{A,B}^a$. We see that super-dual conformal-invariance continues to be manifest at the level of the Bosonic loop integrand in the dual co-ordinate space, also at all loop orders.

This symmetry therefore guarantees that no matter how complicated the integrand looks, on any contour of integration where the integral is completely well-defined, it can only integrate to a constant, “1”! The integral is not “1” *only* because we choose a

contour of integration over lines (AB) corresponding to real $(3, 1)$ -signature points in dual spacetime, and this integral is IR-divergent. We see that IR-divergences are not an annoying side-feature of loop amplitudes, they are the sole reason these amplitudes are non-trivial; in this Yangian-invariant form, the loop amplitudes are telling us “I diverge, therefore I am”¹⁰. This is a powerful statement that should be turned into an engine to simplify the computation of the loop integrals. Due to the IR-divergences, the Yangian generators will not quite annihilate the loop amplitude, but they should localize the integral to the IR-divergent regions of loop momentum-space collinear to the external particles. In the dual co-ordinate space, this is the region localized to the edges of the null-polygonal Wilson loop. It seems likely that these IR-anomalies fully control the structure of the amplitude. Amongst other things, they must lie behind the astonishing simplicity recently uncovered in the structure of the remainder function for the 2-loop, 6-particle MHV amplitude [108]. In the same line of thought, it is conceivable that there is a very direct link between the Yangian structure we uncovered and the very beautiful connections made at strong coupling with integrable systems, Y-systems, TBA equations and the Yang-Yang functional [109, 110]. Already these developments have allowed a bridge to weak coupling by computing sub-leading corrections to collinear limits [111–113].

Having said all of this, there is a very important issue that must be addressed to make progress in directly computing these Yangian-“invariant” but non-local integrals. The question is of course how to handle IR-regularization for these objects. Dimensional regularization has long been the preferred method for regulating IR-divergences in gauge theories, but it does particularly violent damage to the structure of the integrand, and is not useful for our purposes. Fortunately, there is a better regulator, both conceptually and computationally. Physically, the IR-divergences are removed by moving out on the Coulomb branch [94]. This gives a beautifully simple way to regulate the integrals in momentum-twistor space which is also useful for practical computations [114, 115]. With the loop integrand written in local form, one simply deforms the local propagators as $\langle AB \ j-1 \ j \rangle \mapsto \langle AB \ j-1 \ j \rangle + m^2 \langle AB \rangle \langle j-1 \ j \rangle$. The physics is always four dimensional. The ambiguities in this regulator occur at an irrelevant level $\mathcal{O}(m^2)(\log(m^2))^p$. In particular there are no issues with the notorious “ μ -terms” in dimensional regularization, and we

¹⁰We thank Peter Goddard for this remark.

don't encounter the ubiquitous ϵ/ϵ effects either. This is clearly the physically correct regularization for our set-up.

How should we use this regularization to compute the non-local integrals of interest? One can glibly regulate all 4-brackets $\langle AB xy \rangle \mapsto \langle AB xy \rangle + m^2 \langle AB \rangle \langle xy \rangle$, but this is not physically correct: the regularization of the local propagators is reflecting the (local!) masses induced by Higgsing; and so it is not clear how the non-local propagators should be regularized. Indeed, we have checked that for the 1-loop MHV amplitudes, this very naïve regularization of the integrals does not produce the standard result. Of course, since the Yangian invariant form of the full amplitude can be expanded in terms of local integrals, we can in principle work backwards to see how the correct local regulator affects the non-local integrand; the question is whether there is a sensible way of computing these non-local integrals directly. We intend to return to these questions in near future.

We have emphasized that the Yangian-invariant presentation of the loop integrand strongly suggests that the integrals should be simple. But as we have seen in a number of examples, even the local forms of the integrand, when written in terms of the natural chiral basis of momentum-twistor space integrals with unit leading singularities, look surprisingly elegant. In fact, these integrals with unit leading singularities should also be “simple”. The reason is precisely that their leading singularities are “1” or “0”; these are the only possible values of the integrals on any closed contour of integration, independent of the kinematic variables. This means that *e.g.* $\partial/\partial Z_a^I$ acting on these integrals should also be a total derivative with respect to the loop variables, and that they too should be localized to regions with collinear singularities. Since these are local integrals their regularization is well defined. Indeed, as we pointed out in our multi-loop examples, the naïvely “hardest” integrals are even IR-finite. The integrals for our form of the two-loop 6-point MHV amplitude have been computed analytically for certain cross-ratios by [87], passing all non-trivial checks. The simplicity of these partial results strongly supports the idea that the full amplitude computed with these integrals are also simple.

III. Other Planar Theories

We end by stressing that many of the ideas in this chapter are likely to generalize beyond the very special case of $\mathcal{N} = 4$ SYM. Since the integrand is well-defined in any planar theory, one can try to determine it with recursion relations just as we have done for $\mathcal{N} = 4$

SYM. In [91], it was argued that the single-cuts of the 1-loop amplitude are well-defined for any theory with at least $\mathcal{N} = 1$ SUSY (or $\mathcal{N} = 2$ in the presence of massive particles), so the BCFW recursion determines amplitudes at least up to 1-loop in these theories too, with or without maximal SUSY and Yangian-invariance. In non-supersymmetric theories, further progress on these questions will require a better understanding of single-cuts. One difficulty is that the naïve forward limit of tree amplitudes is ill-defined. It is plausible that this is closely related to presence of rational terms in 1-loop amplitudes, which have a beautiful and fascinating structure which is strongly suggestive of a deeper origin.

Chapter 5 *Remarkable Simplicity for Loop Amplitudes in Planar $\mathcal{N} = 4$*

5.1 Invitation to Local Loop Integrals and Integrands

As described in Chapter 4 the *integrand* for scattering amplitudes in planar theories is a well-defined, rational function of external- and loop-momenta at all orders of perturbation theory [15]. Recently, an explicit recursion for the integrand of planar scattering amplitudes in $\mathcal{N} = 4$ SYM was presented in Chapter 4, generalizing the BCFW recursion for tree amplitudes [7, 31]. The integrand is most naturally presented in momentum-twistor space. All the objects appearing in the recursion relation have simple interpretations in terms of canonical operations on Yangian-invariants derived from the Grassmannian integral [10], making the Yangian invariance of the theory (up to total derivatives) manifest at the level of the integrand. It has also been recently realized that the integrand has a beautiful dual interpretation as a natural supersymmetric Wilson loop, resolving a long-standing open problem [116, 117]. This proposal has been checked to satisfy the all-loop recursion relation at the level of the integrand [116], providing a proof of the duality between scattering amplitudes and Wilson-loops [118].

The recursion relation gives a complete definition for the integrand, making no explicit reference to spacetime notions either in the usual or dual spacetimes. The words “spacetime”, “Lagrangian”, “path integral” and “gauge symmetry” make no appearance. A reflection of this fact is that, as familiar from the BCFW computation of tree amplitudes, individual terms in the integrand are riddled with non-local poles that cancel in the sum. But also familiar from BCFW at tree-level, the recursion relation is a very powerful calculational tool, and has allowed us to gather a huge amount of “data” about the properties of multi-loop amplitudes.

In this chapter we report on a remarkable property of the loop integrand revealed by examining this “data”, amplifying a theme already stressed in Chapter 4. Loop

integrands take an amazingly simple form *when expressed in a manifestly local way*. This is surprising, since the enormous complexity of Feynman diagrams is inexorably tied to locality, while by contrast, the great simplicity of BCFW recursion is inexorably tied to the presence of non-local poles. What we are finding is a *new* local form of the integrand—certainly not following from Feynman diagrams!—which is even simpler than the forms obtained from BCFW recursion.

This great simplicity is apparent only when the integrand is written in momentum-twistor space, using a special set of objects that are almost completely *chiral*, and have *unit leading singularities*. For instance, all 2-loop MHV amplitudes are given as a sum over a single type of object,

$$\mathcal{A}_{\text{MHV}}^{2\text{-loop}} = \frac{1}{2} \sum_{i < j < k < l < i} \text{Diagram} \quad (5.1.1)$$

This result was already presented (albeit in a slightly more clumsy form) in Chapter 4. We will describe these objects in much more detail in the body of this Chapter; here, it suffices to say that these are simple double-pentagon integrals with a special tensor-numerator structure which is indicated by the wavy lines, and that the notation ‘ $i < j < \dots < k < i$ ’ in the summand should be understood as the sum of all cyclically-ordered sets of labels i, j, \dots, k for each $i \in \{1, \dots, n\}$.

All 2-loop NMHV amplitudes are also associated with similar integrands; indeed, the n -point NMHV scattering amplitude’s integrand is simply given by,

$$\mathcal{A}_{\text{NMHV}}^{2\text{-loop}} = \sum_{\substack{i < j < l < m \leq k < i \\ i < j < k < l < m \leq i \\ i \leq l < m \leq j < k < i}} \text{Diagram} \times [i, j, j+1, k, k+1] + \frac{1}{2} \sum_{i < j < k < l < i} \text{Diagram} \times \left\{ \begin{array}{l} \mathcal{A}_{\text{NMHV}}^{\text{tree}}(j, \dots, k; l, \dots, i) \\ + \mathcal{A}_{\text{NMHV}}^{\text{tree}}(i, \dots, j) \\ + \mathcal{A}_{\text{NMHV}}^{\text{tree}}(k, \dots, l) \end{array} \right\} \quad (5.1.2)$$

Here, $[i j k l m]$ denotes the familiar dual-superconformal invariant of five particles,

$$[i j k l m] \equiv \frac{\delta^{0|4} (\langle j k l m \rangle \eta_i + \langle k l m i \rangle \eta_j + \langle l m i j \rangle \eta_k + \langle m i j k \rangle \eta_l + \langle i j k l \rangle \eta_m)}{\langle i j k l \rangle \langle j k l m \rangle \langle k l m i \rangle \langle l m i j \rangle \langle m i j k \rangle}. \quad (5.1.3)$$

This result dramatically simplifies the way this result was presented in Chapter 4 for the 6- and 7-particle 2-loop NMHV integrands.

Finally, all 3-loop MHV amplitude integrands are given by a sum over the same types of objects,

$$\mathcal{A}_{\text{MHV}}^{3\text{-loop}} = \frac{1}{3} \sum_{\substack{i_1 \leq i_2 < j_1 \leq \\ \leq j_2 < k_1 \leq k_2 < i_1}} \text{Diagram 1} + \frac{1}{2} \sum_{\substack{i_1 \leq j_1 < k_1 < \\ < k_2 \leq j_2 < i_2 < i_1}} \text{Diagram 2}$$

These explicitly-local, manifestly cyclic results for all 2-loop NMHV and 3-loop MHV amplitudes are new, and stunningly-simple—even simpler than the form produced by the loop-level recursion formula.

As we will see, these extremely simple expressions are very closely related to the leading singularity structure of the theory. The reason for the dramatic simplicity of these results relative to the ones presented in Chapter 4 is that there, each integrand was straightforwardly expanded in terms of a fixed basis of chiral integrals with unit leading singularities, while here we are tailoring the objects that appear directly to the amplitude. The structures are motivated by matching a particularly simple set of leading singularities of the theory; this is made possible only by using chiral integrands with unit leading singularities, which is why these objects play such a crucial role in the story. What is remarkable is that matching only a small subset of leading singularities in this way suffices to determine the full result. Of course, we confirm this not by laboriously matching all leading singularities, but rather by directly checking the conjectured local forms against what we obtain from the all-loop recursion relation.

We do not yet have a satisfactory understanding for the origin of this amazing simplicity. Certainly, these expressions differ from the BCFW form in that they are not term-by-term Yangian invariant. This suggests the existence of a deeper theory for the integrand that will directly produce these new local forms, allowing a more direct understanding of the emergence of local spacetime physics. We strongly suspect that it is *this*

formulation that will also help explain the amazing simplicity [13] seen in the *integrals* yielding the physical amplitudes, and also form the point of contact with the remarkable integrable structures of $\mathcal{N} = 4$ SYM—Y-systems and Yang-Yang equations—seen at strong coupling and also in some collinear limits [110, 111, 119].

In Chapter 6, a geometric picture for scattering amplitudes is advanced, building on a beautiful paper of Hodges [20], which may shed some light on the origin of these new local expressions. Hodges interpreted NMHV tree amplitudes as the volume of certain polytopes in momentum-twistor space, and showed that a natural class of triangulations of this polytope correspond to different BCFW representations of the amplitude. In Chapter 6, it is shown that at an even simpler triangulation of the same polytope is possible, yielding a new, manifestly-local formula for NMHV tree-amplitudes. Also in Chapter 6, a completely analogous ‘polytope’ formulation is presented for all 1-loop MHV amplitudes. Again, one natural set of triangulations leads to the BCFW form of the integrand, while even simpler triangulations directly lead to a number of new, manifestly local forms for the integrand. While this polytope picture has not yet been generalized beyond these most elementary cases of NMHV tree and MHV 1-loop amplitudes, the extremely simple local forms for higher loop amplitudes we present in this chapter strongly encourages the thought that an appropriate extension of this idea must be possible.

We should stress that when we say our results for the integrand are “manifestly local”, we mean that the poles involving the loop integration variables are local. Of course the integrand should be “ultralocal”, that is, the poles involving both the loop integration variables as well as the external momenta must be local. The MHV integrands we present trivially have this property, but for NMHV amplitudes, our expressions involve the standard R -invariants which have spurious poles as function of the external particle momenta. Given the beautiful, local form of the NMHV tree amplitude obtained from the polytope picture [13], it is quite likely that there is an even nicer representation of loop amplitudes which are not only local but ultralocal. This fascinating possibility certainly merits further exploration, but is beyond the scope of the present Chapter.

We close this invitation with an outline for the rest of the paper. We begin with a pedagogical introduction to some of the foundations of the subject in section 5.2 starting with a review of momentum-twistors and some of the associated projective geometry in \mathbb{CP}^3 . We also discuss how planar loop integrals are written in momentum-twistor space;

while our focus in this Chapter is on $\mathcal{N} = 4$ SYM, we expect that the momentum-twistor representation of loop amplitudes will be extremely useful for *any* planar theory. We discuss the way that momentum-twistors make integral reduction trivial, and illustrate this by showing how the 1-loop integrand can be reduced to a sum over pentagon integrals. Finally we discuss leading singularities at 1-loop and beyond in momentum-twistor language. The standard exercise of determining quadruple-cuts in momentum space is mapped in momentum-twistor language to a simple, beautiful and classic problem in enumerative geometry first posed by Schubert in the 1870’s, and we discuss the solution of these “Schubert problems” in detail.

In section 5.3 we introduce chiral integrals with unit leading singularities which play a central role in our story. We illustrate how they work starting with the simplest case of 1-loop MHV amplitudes.

In section 5.4, we discuss another feature of chiral integrals with unit leading singularities—generic integrals of this form are manifestly infrared finite, and can be used to express finite objects related to scattering amplitudes, such as the ratio function [8].

In section 5.5, we construct a basis for all 1-loop integrands, whose building blocks are not the familiar boxes or even pentagons, but a natural set of chiral octagons with unit leading singularities. We also compute the finite 1-loop integrals explicitly, and use these results to give a simple formula for the NMHV ratio-function at 1-loop, for any number of particles.

In section 5.6, we discuss multi-loop amplitudes. We describe our heuristic strategy for using leading singularities to tailor momentum-twistor integrals to the amplitude, and show how this works for the 1-loop MHV amplitude, reproducing one of the local forms first derived using the polytope picture of Chapter 6. We also discuss the 1-loop NMHV amplitudes in the same way. We then extend these methods to two loops and beyond, and show how to “glue” the 1-loop expressions together to produce natural conjectures for all 2- and 3-loop MHV amplitudes, as well all 2-loop NMHV amplitudes. These conjectures are verified by comparing with the integrand derived from the all-loop recursion relation.

A number of appendices discuss various technical points needed in the body of this Chapter, including a detailed discussion of the 2-loop NMHV and 3-loop MHV integrands.

5.2 Foundations

In theories with massless particles, a well-known and convenient way of trivializing the constraint $p_a^2 = 0$ for each particle is to introduce a pair of spinors $\lambda^{(a)}$ and $\tilde{\lambda}^{(a)}$, replacing $p_a^\mu \mapsto (p_a)_{\alpha\dot{\alpha}} \equiv p_a^\mu (\sigma_\mu)_{\alpha\dot{\alpha}} \equiv \lambda_\alpha^{(a)} \tilde{\lambda}_{\dot{\alpha}}^{(a)}$. Of course, this map is not invertible, as any rescaling $\{\lambda, \tilde{\lambda}\} \rightarrow \{t\lambda, t^{-1}\tilde{\lambda}\}$ leaves p invariant. This reflects that these variables come with a new source of redundancy; in the case of particles with spin, this redundancy is quite welcomed as it allows the construction of functions that transform with fixed projective weights as S-matrix elements under Lorentz transformations. This is all well-known under the name of the *spinor-helicity formalism* [120–124].

Amplitudes are supported on momenta that satisfy momentum conservation. Clearly, it would be convenient to find variables where this constraint, $\sum_a p_a = 0$, is trivial. In planar theories, where color ordering is available, there is a natural way to achieve this, by choosing instead to express the external momenta in terms of what are known as dual-space coordinates, writing $p_a \equiv x_a - x_{a-1}$, [47].

To see the role played by planarity, consider the standard decomposition of scattering amplitudes according to the overall color structure, keeping only the leading color part:

$$A_n = \text{Tr}(T^{a_1} T^{a_2} \dots T^{a_n}) \mathcal{A}_n(1, 2, \dots, n) + \text{permutations}; \quad (5.2.4)$$

here, each *partial amplitude* $\mathcal{A}_n(1, 2, \dots, n)$ can be expanded in perturbation theory, and we denote the L -loop contribution by $\mathcal{A}_n^{L\text{-loop}}$. Partial amplitudes are computed by summing over Feynman diagrams with a given color-ordering structure.

In this chapter we only consider the planar sector of the theory, and therefore $\mathcal{A}_n^{L\text{-loop}}$ will always refer to the leading-color, partial amplitude in the planar limit.

Restricted to a particular partial amplitude, say, $\mathcal{A}_n(1, 2, \dots, n)$, each momenta can be expressed as the difference of two “spacetime” points. More precisely, we make the identification $p_a \equiv x_a - x_{a-1}$, with $p_1 = x_1 - x_n$. It is clear that momenta obtained in this way automatically satisfy $\sum_a p_a = 0$ —and the redundancy introduced in this case is a translation $x_a \rightarrow x_a + y$ by any fixed vector y .

Now, the only poles that can occur in $\mathcal{A}_n(1, 2, \dots, n)$ are of the form $\sum_{m=a}^b p_m$, *i.e.*, only the sum over consecutive momenta can appear. In the dual variables these become

$\sum_{m=a+1}^b p_m = x_a - x_b$. The same kind of simplifications happen in planar Feynman diagrams to all orders in perturbation theory as we will describe.

Now we have the variables $\{\lambda, \tilde{\lambda}\}$ which make the null condition trivial while ignoring momentum conservation, while the dual-space variables do the opposite. It is perfectly natural to wonder if there exists any way to combine these two constructions which makes both the null-condition and momentum conservation trivial. It turns out that such a set of variables does exist: they are known as *momentum-twistors* and were introduced by Hodges in [20].

The standard twistor construction developed in the 1960's [125] starts by making a connection between points in an auxiliary space—twistor-space—and null rays in spacetime. Likewise, a complex line in twistor space is related to a point in spacetime. The key formula is called the *incidence relation*, according to which a point x in spacetime corresponds to set of twistors $Z = (\lambda, \mu)$ which satisfy

$$\mu_{\dot{\alpha}} = x_{\alpha\dot{\alpha}}\lambda^{\alpha}. \quad (5.2.5)$$

Twistors satisfying this relation form a projective line in \mathbb{CP}^3 . Even though Z has the components of a point in \mathbb{C}^4 , the incidence relation cannot distinguish Z from tZ , and therefore the space is projectivized.

In order to specify a line in twistor space—and therefore a point in spacetime—all that is needed is a pair of twistors, say Z_A and Z_B , that belong to the line. Given the twistors, the line or spacetime point is found by solving the four equations coming from imposing the incidence relation for Z_A and Z_B with x . It is easy to check that the solution is,

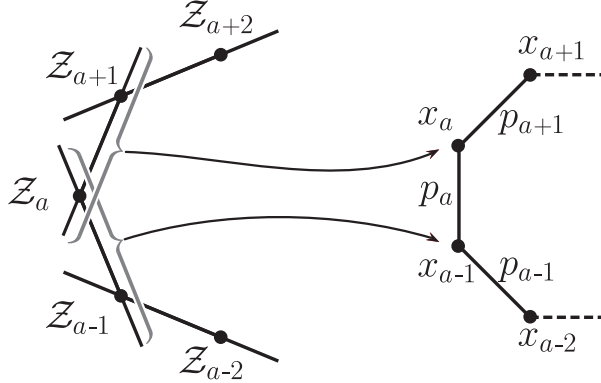
$$x_{\alpha\dot{\alpha}} = \frac{\lambda_{A,\alpha}\mu_{B,\dot{\alpha}}}{\langle\lambda_A\lambda_B\rangle} + \frac{\lambda_{B,\alpha}\mu_{A,\dot{\alpha}}}{\langle\lambda_B\lambda_A\rangle}. \quad (5.2.6)$$

(Here, we have made use of the familiar Lorentz-invariant contraction of two spinors $\langle\lambda_A\lambda_B\rangle \equiv \epsilon_{\alpha\beta}\lambda_A^{\alpha}\lambda_B^{\beta}$).

Hodges' construction starts with any set of n twistors $\{Z_1, \dots, Z_n\}$. Using the association $x_a \leftrightarrow (Z_a, Z_{a+1})$, n spacetime points are defined. Quite nicely, it is trivial that $p_a^2 = (x_a - x_{a-1})^2 = 0$ because the corresponding lines, or (\mathbb{CP}^1 s), intersect. This is illustrated in Figure 5.1.

Given the importance of this latter fact, it is worth giving it a slightly more detailed discussion than we have so far. If two lines in twistor-space intersect, *i.e.* share a twistor

Figure 5.1: Defining the connections between momentum-twistors, dual-coordinates, and cyclically-ordered external four-momenta



Z_{int} , then the corresponding spacetime points, say x and y , associated with the lines are null-separated. To see this, take the difference of the incidence relations for Z_{int} ,

$$\mu_{\dot{\alpha}}^{\text{int}} = x_{\alpha\dot{\alpha}}\lambda_{\text{int}}^{\alpha}, \quad \mu_{\dot{\alpha}}^{\text{int}} = y_{\alpha\dot{\alpha}}\lambda_{\text{int}}^{\alpha},$$

to get

$$(x - y)_{\alpha\dot{\alpha}}\lambda_{\text{int}}^{\alpha} = 0;$$

which means that the 2×2 -matrix $(x - y)$ has a non-vanishing null eigenvector, *i.e.* $\lambda_{\text{int}}^{\alpha}$, and therefore the determinant of $(x - y)$ vanishes. But the determinant is proportional to $(x - y)^2$ when x and y are taken as vectors; and therefore x and y are null separated.

As useful background for the rest of the Chapter let us discuss the null-separation condition, which is a conformally invariant statement, in twistor space. Consider again two generic spacetime points x and y and choose two representatives of the lines associated to them in twistor space, say, (Z_A, Z_B) and (Z_C, Z_D) . Treating each twistor as a vector in \mathbb{C}^4 there is a natural SL_4 (conformal) invariant that can be constructed. This is done by contracting all four twistors with the completely antisymmetric tensor ϵ_{IJKL} to produce

$$\langle Z_A Z_B Z_C Z_D \rangle = \epsilon_{IJKL} Z_A^I Z_B^J Z_C^K Z_D^L. \quad (5.2.7)$$

Clearly, this conformally-invariant quantity must encode information about how x and y are causally related. The Lorentz invariant separation $(x - y)^2$ is not conformally-invariant because it is not a cross ratio. However, the way to relate the two quantities is simple

$$(x - y)^2 = \frac{\langle Z_A Z_B Z_C Z_D \rangle}{\langle \lambda_A \lambda_B \rangle \langle \lambda_C \lambda_D \rangle}. \quad (5.2.8)$$

This relation is consistent with our earlier finding that if the points x and y are null-separated, then the twistors Z_A, Z_B, Z_C and Z_D , are coplanar as points in \mathbb{CP}^3 . In other words, the two complex lines intersect.

When twistors are used to produce a configuration of points in spacetime which are pairwise null separated and then used to build momenta, the corresponding twistor space is called *momentum-twistor space* [20].

This twistor construction is in fact slightly more involved when one is interested in *real* slices of spacetime. In our discussion so far, we have been assuming that momenta are complex and hence the dual spacetime is complexified. This is useful for *e.g.* defining the usual unitarity cuts of loop amplitudes. In this chapter, the complex version suffices and we refer the interested reader to [20, 92].

A related construction is called dual momentum twistor space. Here ‘dual’ refers to the usual geometric—‘Poincaré’—dual of a space. In other words, the dual space is the space of planes in \mathbb{CP}^3 . Points in the new space which is also a \mathbb{CP}^3 are denoted by W_I . The construction maps points to planes and lines to lines. In Hodges’ construction [20], there is a natural definition of dual points associated to the planes defined by consecutive lines of the polygon in momentum twistor space of Figure A.5.

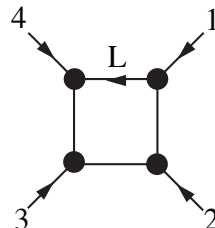
The construction defines a dual polygon by introducing dual momentum twistors W_a defined by

$$(W_a)_I = \frac{\epsilon_{IJKL} Z_{a-1}^J Z_a^K Z_{a+1}^L}{\langle \lambda_{a-1} \lambda_a \rangle \langle \lambda_a \lambda_{a+1} \rangle}. \quad (5.2.9)$$

This definition is made so that W_a contains $\tilde{\lambda}_a$ as two of its components.

I. Loop Integrals

The focus of this chapter is loop integrands and integrals. Here too, it is well known that in planar theories, loop integrals are very naturally expressed in terms of dual spacetime coordinates. Consider a very simple 1-loop integral, known as a zero mass integral,



The diagram shows a square loop with four vertices. External momenta are labeled 1, 2, 3, and 4. Momenta 1 and 2 are outgoing from the top-right and bottom-right vertices respectively. Momenta 3 and 4 are incoming to the bottom-left and top-left vertices respectively. The loop momentum is labeled L and flows clockwise from the top-left vertex to the top-right vertex.

$$= \int d^4 L \frac{N}{L^2 (L - p_1)^2 (L - p_1 - p_2)^2 (L - p_1 - p_2 - p_3)^2} \quad (5.2.10)$$

where the external momentum at each of the four vertices is null (hence the name) and $N = (p_1 + p_2)^2(p_2 + p_3)^2$ is a convenient normalization factor. Momentum conservation gives $p_4 = -p_1 - p_2 - p_3$; and introducing the dual-coordinates $p_a = x_a - x_{a-1}$, it is easy to see that the unique choice of L that makes translation invariance (in x -space) manifest is $L = x - x_4$. The integral becomes [47]

$$= \int d^4x \frac{N}{(x - x_1)^2(x - x_2)^2(x - x_3)^2(x - x_4)^2}, \quad (5.2.11)$$

where $N = (x_1 - x_3)^2(x_2 - x_4)^2$. Imposing translation-invariance gives rise to the same integral in x -space regardless of the original definition of L in the loop diagram. In other words, a different propagator could have been chosen to be L and the form (5.2.11) would still be the same. This uniqueness plays a crucial role in the definition of the integrand of the theory.

Integrating over all points x in spacetime is the same as integrating over all \mathbb{CP}^1 's in \mathbb{CP}^3 . As before, each line in twistor space can be represented by a pair of twistors $x \leftrightarrow (Z_A, Z_B)$. Clearly, any $GL_2(\mathbb{C})$ transformation on the A, B “indices” leaves the line invariant. Therefore the integral over spacetime is the same as the integral over the pairs (Z_A, Z_B) modulo GL_2 . This is nothing but the Grassmannian $G(2, 4)$ which can be parameterized by a 2×4 matrix

$$\begin{pmatrix} Z_A^1 & Z_A^2 & Z_A^3 & Z_A^4 \\ Z_B^1 & Z_B^2 & Z_B^3 & Z_B^4 \end{pmatrix} = \begin{pmatrix} \lambda_A^1 & \lambda_A^2 & \mu_A^1 & \mu_A^2 \\ \lambda_B^1 & \lambda_B^2 & \mu_B^1 & \mu_B^2 \end{pmatrix}. \quad (5.2.12)$$

We can immediately write a measure which is GL_2 -invariant by integrating over all Z_A 's and Z_B 's together with a combination of 2×2 minors of the matrix (5.2.12) with total weight -4 . It turns out that the precise measure that corresponds to a d^4x integration is

$$\int d^4x \Leftrightarrow \int \frac{d^4Z_A d^4Z_B}{\text{vol}(GL_2) \times \langle \lambda_A \lambda_B \rangle^4}, \quad (5.2.13)$$

where $\langle \lambda_A \lambda_B \rangle$ is the $(1 \ 2)$ minor of (5.2.12)—the determinant of the first two columns of the 2×4 matrix (5.2.12). In the twistor literature this is written as $\langle \lambda_A \lambda_B \rangle = \langle Z_A Z_B I_\infty \rangle$

where $(I_\infty)^{KL}$ is the infinity twistor which is block diagonal with the only nonzero diagonal element equal to ϵ_{ab} . I_∞ is called the infinity twistor because it corresponds to a choice of the point at infinity in spacetime and therefore a line in twistor space. Its presence therefore breaks conformal invariance. This is not surprising as the measure d^4x ‘knows about’ the metric in spacetime.

Since the integration over lines will appear in many different contexts in this chapter we introduce a special notation for it. Let’s define

$$\int_{(AB)} \Leftrightarrow \int \frac{d^4 Z_A d^4 Z_B}{\text{vol}(GL_2)}. \quad (5.2.14)$$

The reason we have not included the factor $\langle \lambda_A \lambda_B \rangle^4$ in the definition is that in this chapter we mostly deal with $\mathcal{N} = 4$ SYM and in its integrand factors with infinity twistors cancel.

Going back to the loop integral in x -space (5.2.11), one can introduce the four momentum twistors in Hodges’ construction $\{Z_1, Z_2, Z_3, Z_4\}$ to describe the external particles. Using the relation between the Lorentz invariant separations and momentum twistor invariants in (5.2.8), the integral (5.2.11) becomes

$$\int_{(AB)} \frac{\langle 1234 \rangle^2}{\langle AB 12 \rangle \langle AB 23 \rangle \langle AB 34 \rangle \langle AB 41 \rangle}. \quad (5.2.15)$$

where $\langle ijkl \rangle$ stands for the determinant of the 4×4 matrix with columns given by four twistors Z_i, Z_j, Z_j, Z_k defined in (5.2.7).

One of the remarkable facts about (5.2.15) is that all factors involving the infinity twistor have disappeared. This means that the integral is formally conformal invariant under the conformal group that acts on the dual spacetime. This is why it is said to be *dual conformally invariant* (DCI).

Clearly, if we had started with a triangle integral then the factor $\langle Z_1 I Z_2 \rangle = \langle \lambda_1 \lambda_2 \rangle$ would not have canceled and would have remained with power one in the denominator as if it were a propagator. Indeed, this viewpoint trivializes the surprising connections made in the past between the explicit form of triangle and box integrals. In other words, one can think of a triangle integral as a box where one of the points is at infinity.

Once again, a careful definition of the contour which should correspond to only points in a real slice of complexified spacetime is not needed in this chapter. It suffices to say

that on the physical contour, the integrals can have infrared divergences (IR). This is the reason why we said that the integral was ‘formally’ DCI. We postpone a more detailed discussion of IR-divergences to section 5.4.

The purpose of this section is to show how momentum twistors are the most natural set of variables to work with loop amplitudes in planar theories. In order to do this we will first show how many familiar results can be translated into momentum twistors. Not infrequently, momentum twistors will completely clarify physics points which have been misunderstood in the literature.

Integral Reduction at 1-Loop Level

In a general theory, 1-loop integral reduction techniques allow scattering amplitudes to be expressed as linear combinations of a basic set of scalar integrals¹. The integrals have the topology of bubbles, triangles or boxes.

Let us start this section by translating each of the integrals in the standard basis into momentum twistor language. Their corresponding form in momentum twistor space is

$$\begin{aligned}
 I_{\text{Box}} &= \begin{array}{c} \begin{array}{ccc} & i & i+1 \\ & \bullet & \bullet \\ \begin{array}{c} l+1 \\ \vdots \\ l \end{array} & \begin{array}{c} \vdots \\ \vdots \end{array} & \begin{array}{c} \vdots \\ \vdots \end{array} \\ & \begin{array}{ccc} & j & \\ & \bullet & \bullet \\ & \begin{array}{c} \vdots \\ \vdots \end{array} & \begin{array}{c} \vdots \\ \vdots \end{array} \\ & \begin{array}{ccc} & k+1 & k \end{array} \end{array} \\ &= \int_{(AB)} \frac{\langle i \ i+1 \rangle \langle j \ j+1 \rangle \langle k \ k+1 \rangle \langle l \ l+1 \rangle}{\langle AB \ i \ i+1 \rangle \langle AB \ j \ j+1 \rangle \langle AB \ k \ k+1 \rangle \langle AB \ l \ l+1 \rangle}; \\
 I_{\text{Triangle}} &= \begin{array}{c} \begin{array}{ccc} & i+1 & j \\ & \bullet & \bullet \\ \begin{array}{c} i \\ \vdots \\ i+1 \end{array} & \begin{array}{c} \vdots \\ \vdots \end{array} & \begin{array}{c} \vdots \\ \vdots \end{array} \\ & \begin{array}{ccc} & j+1 & \\ & \bullet & \bullet \\ & \begin{array}{c} \vdots \\ \vdots \end{array} & \begin{array}{c} \vdots \\ \vdots \end{array} \\ & \begin{array}{ccc} & k+1 & k \end{array} \end{array} \\ &= \int_{(AB)} \frac{1}{\langle AB \rangle} \frac{\langle i \ i+1 \rangle \langle j \ j+1 \rangle \langle k \ k+1 \rangle}{\langle AB \ i \ i+1 \rangle \langle AB \ j \ j+1 \rangle \langle AB \ k \ k+1 \rangle}; \\
 I_{\text{Bubble}} &= \begin{array}{c} \begin{array}{ccc} & i & i+1 \\ & \bullet & \bullet \\ \begin{array}{c} i \\ \vdots \\ j+1 \end{array} & \begin{array}{c} \vdots \\ \vdots \end{array} & \begin{array}{c} \vdots \\ \vdots \end{array} \\ & \begin{array}{ccc} & j & \\ & \bullet & \bullet \\ & \begin{array}{c} \vdots \\ \vdots \end{array} & \begin{array}{c} \vdots \\ \vdots \end{array} \\ & \begin{array}{ccc} & j+1 & j \end{array} \end{array} \\ &= \int_{(AB)} \frac{1}{\langle AB \rangle^2} \frac{\langle i \ i+1 \rangle \langle j \ j+1 \rangle}{\langle AB \ i \ i+1 \rangle \langle AB \ j \ j+1 \rangle}.
 \end{aligned} \tag{5.2.16}$$

Note that here we have translated the plain scalar integrals without any normalization factors. Once again, only boxes are dual conformal invariant except for an overall factor which only depends on the external data. This factor involving 2-brackets and hence the

¹This is true in theories with no rational terms or in general theories for what is known as the cut-constructible part of them. See [126] for more details. In $\mathcal{N} = 4$ SYM rational terms are absent. This is why we do not elaborate more on this point.

infinity twistor can always be removed by a proper normalization as done in the zero-mass example (5.2.15). Scalar boxes in momentum twistor space have also been recently studied in [92, 93].

A well known fact about $\mathcal{N} = 4$ SYM is that at 1-loop level, bubbles and triangles are absent and all one needs are scalar box integrals. However, as we will see, this point of view is not the most natural one and actually turns out to be misleading.

In order to understand this point, one needs to review the reduction procedures used to reach this conclusion. Before doing that let us mention some useful facts about momentum twistors.

In loop integrals, combinations of momentum twistors of the form $Z_A^I Z_B^J$ make an appearance in every expression (where the brackets mean that the indices are anti-symmetrized), reflecting the fact that it is the *line* (AB) that is being integrated-over, and not the individual twistors Z_A and Z_B .

These two-index objects are a class of more general ones called bitwistors. A generic bitwistor is a rank-two antisymmetric tensor Y^{IJ} . Given two bitwistors, Y and \tilde{Y} , the conformally-invariant inner-product is given by $\langle Y \tilde{Y} \rangle = \epsilon_{IJKL} Y^{IJ} \tilde{Y}^{KL}$. A bitwistor which can be written in terms of two twistors as $Z_A^I Z_B^J$ is called *simple*. It is easy to show that a bitwistor is simple if and only if $Y^2 = 0$ with the product defined as above.

The reason for discussing bitwistors is that they provide a very natural integral reduction procedure. The procedure can be applied to integrals at any loop order but in this section we concentrate on only 1-loop integrals. The procedure we are about to present is in part the momentum twistor analog of the one introduced by van-Neerven and Vermaseren in [105].

At 1-loop one starts with general Feynman integrals of the form

$$T_{\mu_1 \dots \mu_m} \int d^4 L \frac{L^{\mu_1} \dots L^{\mu_m}}{\prod_{i=1}^n (L - P_i)^2} \quad (5.2.17)$$

where the tensor T is made out of polarization vectors, momenta of external particles and the spacetime metric.

By Lorentz invariance, it is clear that one can decompose integrals of this type as linear combinations of momentum twistor tensor integrals of the form

$$\int_{(AB)} \frac{1}{\langle AB I_\infty \rangle^{4-(n-m)}} \frac{\langle AB Y_1 \rangle \langle AB Y_2 \rangle \dots \langle AB Y_m \rangle}{\langle AB 12 \rangle \langle AB 23 \rangle \dots \langle AB n-1 n \rangle \langle AB n 1 \rangle} \quad (5.2.18)$$

where Y_a are generic bitwistors.

The reduction procedure relies on the fact that a generic bitwistor has six degrees of freedom and can therefore be expanded in a basis of any six independent bitwistors. To reduce the integrals in (5.2.18) simply choose any six of the bitwistors that appear in the denominator, say, $Z_1Z_2, Z_2Z_3, \dots, Z_6Z_7$ and expand any of the bitwistors in the numerator as

$$(Y_j)^{IJ} = \alpha_1 Z_1^I Z_2^J + \alpha_2 Z_2^I Z_3^J + \dots + \alpha_6 Z_6^I Z_7^J. \quad (5.2.19)$$

The coefficients can be found by contracting with enough bitwistors to get six independent equations. More explicitly, one can consider equations of the form

$$\langle Z_2 Z_3 Y_j \rangle = \alpha_4 \langle 2345 \rangle + \alpha_5 \langle 2356 \rangle + \alpha_6 \langle 2367 \rangle.$$

and solve for the α 's. Once this is done, the factor $\langle AB Y_j \rangle$ becomes a linear-combination of factors in the denominator, thus reducing the degree of the denominator and numerator by one.

The integral in (5.2.18) is for a general quantum field theory with a planar sector. One can continue with the integral procedure in this case but it will take us too far away from the main line of this Chapter. Therefore we concentrate directly on $\mathcal{N} = 4$ SYM. In $\mathcal{N} = 4$ SYM it has been known since the 1990's [75] that all integrals satisfy $n - m = 4$. In modern language, this means that the integrals are dual conformally-invariant as discussed in the simple example of the all massless box integral (5.2.15).

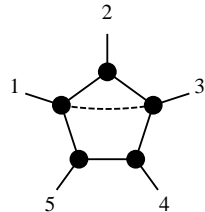
Iterating the reduction procedure, we can write the any amplitude as a sum over pentagons and boxes. But as far as we have seen, the reduction procedure we have described so far does not reduce the pentagons any further. Notice that the pentagons we have described here are not *scalar* pentagons, but *tensor* pentagons—and they are *manifestly* DCI. However, one is always free to choose a basis of bitwistors including $Y = I_\infty$ to obtain scalar pentagons, but only at the cost of manifest dual conformal invariance.

But doesn't the reduction procedure of van-Neerven and Vermaseren, when applied to $\mathcal{N} = 4$ SYM, allow for a reduction all the way down to only scalar boxes? One might wonder why our analysis so far does not generate this familiar 'box-expansion'. The answer is that the reduction to box-integrals is *not valid at the level of the integrand*—only the reduction to boxes *and pentagons* (scalar or otherwise) is valid at the level

of the integrand. In order to obtain the all-too familiar box-expansion, it is necessary to parity-symmetrize the integrand—a step that is only justified when integrated on a parity-invariant contour, and one which does violence to the highly *chiral* loop-integrands of a quantum field theory such as $\mathcal{N} = 4$ SYM.

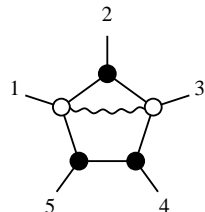
Here, we should briefly clarify a point which has been unnecessarily confused in the literature on $\mathcal{N} = 4$. Because *integrand*-level reduction must terminate with boxes *and* pentagons, and box-integrals are both manifestly parity-even and DCI while *scalar* pentagons—which have a factor of $\langle AB I_\infty \rangle$ in the numerator—are not DCI, the corrections to the box-expansion needed to match the full integrand of $\mathcal{N} = 4$ were first expressed in terms of parity-odd combinations of scalar pentagons. This led some researchers to suppose that there was some connection between DCI and parity. There is of course no such connection: as evidenced by the extension of BCFW to all-loop orders, the full $\mathcal{N} = 4$ loop-integrand is DCI.

Especially for theories such as $\mathcal{N} = 4$ which are DCI, one should strictly avoid parity-symmetrization at one-loop or higher. Although scalar pentagon integrals are quite familiar, *chiral* pentagons are slightly novel—although they have already played an important role in the literature (see e.g. [15, 127]). The first appearance of pentagon integrals occurs for five particles, and there are essentially two possibilities that arise:



$$\iff \int_{(AB)} \frac{\langle ABY \rangle \times \langle 2345 \rangle \langle 4512 \rangle}{\langle AB12 \rangle \langle AB23 \rangle \langle AB34 \rangle \langle AB45 \rangle \langle AB51 \rangle}, \quad (5.2.20)$$

where $\langle 2345 \rangle \langle 4512 \rangle$ in the numerator is for normalization² and the bitwistor Y is simply $Z_1 Z_3$ (this is indicated by the dashed-line in the associated figure); and,



$$\iff \int_{(AB)} \frac{\langle AB\tilde{Y} \rangle \times \langle 3451 \rangle}{\langle AB12 \rangle \langle AB23 \rangle \langle AB34 \rangle \langle AB45 \rangle \langle AB51 \rangle}, \quad (5.2.21)$$

²We will see that this normalization follows from the requirement that the integral have *unit leading-singularities*, and its sign is fixed by parity relative to the ‘wavy-line’ pentagon drawn below it. In fact, as we will describe in section 5.3, the dashed-line in the figure dictates both the bitwistor $Y \equiv Z_1 Z_3$ and the normalization of the integral.

where the factor $\langle 3451 \rangle$ in the numerator is for normalization, and the bitwistor $\tilde{Y} \equiv \langle (512) \cap (234) \rangle$ is the line in twistor-space which lies along the intersection of the planes spanned by twistors (Z_5, Z_1, Z_2) and (Z_2, Z_3, Z_4) —which is indicated in the figure by the ‘wavy-line’. As the first of many such examples, it is useful to write-out \tilde{Y} explicitly:

$$\begin{aligned} \tilde{Y} &\equiv (512) \cap (234) = Z_5 Z_1 \langle 2234 \rangle + Z_1 Z_2 \langle 5234 \rangle + Z_2 Z_5 \langle 1234 \rangle, \\ &= 0 + Z_1 Z_2 \langle 5234 \rangle + Z_2 Z_5 \langle 1234 \rangle, \end{aligned} \tag{5.2.22}$$

where we have used the fact that $\langle 2234 \rangle = 0$. (The translation between statements such as ‘the line along the intersection of two planes’ and explicit representative formulae such as the above will be explained in more detail below; here, we merely quote the result in a way from which we hope it will be easy to guess the general case.)

These two integrals are examples of a very important class of integrals that we call *chiral integrals with unit leading singularities*, or *pure integrals*. In each case, the bitwistor appearing in the numerator (together with the integrand’s normalization) is completely specified by the dashed- or wavy-line in the corresponding figure. We will explain many of the important features of these integrals together with the way their graphical representations in more detail in section 5.3. It is worth noting in passing, however, that the two integrals are parity conjugates of one another, and special twistors Y and \tilde{Y} represent the two lines in twistor-space which simultaneously intersect the four lines (51), (12), (23), and (34); this means that $\langle Y 51 \rangle = \langle Y 12 \rangle = \langle Y 23 \rangle = \langle Y 34 \rangle = 0$, and similarly for \tilde{Y} . Because of this, they represent the two isolated points in (AB) -space for which these four propagators go on-shell.

Before moving-on to discuss loop integrands, we should emphasize that because the primary focus of this chapter is the loop *integrand*—the sum of all the Feynman diagrams, as a rational function—there is nothing to say about the regulation of IR-divergent integrals such as the zero-mass box integral and the pentagons integrals given above. The only *integrals* we will evaluate explicitly are all *manifestly* finite (in a precise sense which will be described in section 5.4), and hence are well-defined without any regulator. However, it is important to mention that IR-divergent integrals can also easily be regulated and evaluated. In fact, the most natural way to add a regulator is also a very physical one, given by moving out on the Coulomb branch [94] of the theory.

II. The Loop Integrand

A simple but far-reaching consequence of writing each Feynman integral in a loop amplitude using the dual variables is that one can meaningfully combine all integrals appearing in a particular amplitude under the same integral sign. This leads to the concept of *the loop integrand* [15]. We stress again that planarity and the use of dual variables plays a crucial role in making this possible—for a general theory, there is no natural origin of loop momentum space and therefore no canonical way of combining all Feynman diagrams under a common loop integral.

It is easy to characterize the structure of the n particle 1-loop integrand for $\mathcal{N} = 4$ SYM using momentum-twistor space integrals. All the terms in the integrand can be combined defining a universal denominator containing all n physical propagators of the form $\langle AB a a+1 \rangle$. If a particular Feynman diagram has fewer propagators, then the numerator is chosen so as to cancel the extra propagators. The loop amplitude is given as an an integral over a single rational function,

$$\mathcal{A}_n = \int_{(AB)} \frac{\sum_i c_i \langle AB Y_1^i \rangle \langle AB Y_2^i \rangle \dots \langle AB Y_{n-4}^i \rangle}{\langle AB 12 \rangle \langle AB 23 \rangle \dots \langle AB n-1 n \rangle \langle AB n 1 \rangle} \quad (5.2.23)$$

where \mathcal{A}_n is the full 1-loop partial amplitude. This formula is already written using the simplifications that arise in $\mathcal{N} = 4$ SYM, in other words, it is manifestly DCI. However, the integrand exists in any planar theory: for a theory which is not DCI, (5.2.23) would necessarily contain also terms with powers of $\langle AB I_\infty \rangle$.

At higher loops, say L loops, scattering amplitudes are given as linear combination of integrals of the form

$$\int \prod_{i=1}^L d^4 \ell_i \frac{\prod_{j=1}^L N(\ell_j)}{\prod_{k=1}^L P(\ell_k)} \times \frac{1}{R(\ell_1, \dots, \ell_L)}, \quad (5.2.24)$$

where N, P , and R are products of Lorentz invariants constructed out of Feynman propagators and which depend on the variables shown and on the external momenta. Written in this form, there is clearly a large amount of redundancy in the definitions of the internal loop momenta.

Since we are dealing with only planar integrals, for each Feynman diagram there exists a dual diagram (the standard dual graph of a planar graph). Consider for example the

where ‘ (AB, CD) ’ implies that the integration measure carries with it a factor of $1/2$ from the symmetrization of $(AB) \leftrightarrow (CD)$. We should mention here that for 3-loops, we will use (Z_E, Z_F) to denote the line corresponding to y_3 —but of course, a convention such as that of associating (Z_{A_m}, Z_{B_m}) with y_m would be increasingly preferable at high-loop order.

Before we leave the topic of *the* loop-integrand in general, we should mention that the form of the integrand obtained via BCFW as described in Chapter 4 makes it completely manifest that the loop-integrands in $\mathcal{N} = 4$ enjoy the full Yangian symmetry of the theory. (Of course, the choice of an integration contour which introduces IR-divergences, such as the physical contour, breaks this symmetry.)

However, just as with the BCFW recursion relations at tree level, the formulae obtained from the recursion do not enjoy manifest locality or manifest cyclic invariance. The restriction that we impose throughout this work, however, is that loop-integrand be expanded in a way which makes use of only planar, local propagators. As we have stressed a number of times, we will find amazingly simple, manifestly cyclically symmetric and local expressions for multi-loop amplitudes, that are significantly simpler and more beautiful than their BCFW counterparts! Taken together with the parallel results presented in Chapter 6, this strongly suggests the existence of a formulation for scattering amplitudes directly yielding these remarkable local forms.

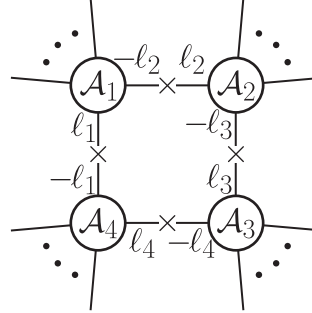
The local formulae presented in this chapter are very closely related to and influenced by the concept of the *leading singularities* of scattering amplitudes, which we proceed to presently describe.

III. Leading Singularities

Definition

The concept of leading singularities was introduced in the 1960’s in the context of massive scalar theories [128]. More recently, in 2004, the same concept was modified to accommodate massless particles and this was exploited for Yang-Mills in [129]. The original definition of ‘leading-singularity’ refers to a discontinuity of a scattering amplitude across a singularity of the highest possible co-dimension. At 1-loop, for example, leading singularity discontinuities are computed using a generalization of a unitarity cut, but where

four propagators are cut instead of two. Using \mathcal{A}_i for $i = 1, \dots, 4$ to denote the four partial amplitudes, each with their associated momentum-conserving δ -function, one has what can be called leading-singularity discontinuity,



(5.2.27)

$$\begin{aligned}
 &= \int \prod_{r=1}^4 d^4 \tilde{\eta}_r d^4 \ell_r \delta(\ell_r^2) \mathcal{A}_1(\{\ell_1, \tilde{\eta}_1\}, \{-\ell_2, \tilde{\eta}_2\}, \dots) \times \mathcal{A}_2(\{\ell_2, \tilde{\eta}_2\}, \{-\ell_3, \tilde{\eta}_3\}, \dots) \\
 &\quad \times \mathcal{A}_3(\{\ell_3, \tilde{\eta}_3\}, \{-\ell_4, \tilde{\eta}_4\}, \dots) \times \mathcal{A}_4(\{\ell_4, \tilde{\eta}_4\}, \{-\ell_1, \tilde{\eta}_1\}, \dots).
 \end{aligned}$$

Here, the integrations over the internal loop momenta are there only to remind us that we are to sum-over all solutions to the conditions imposed by the δ -functions, and the integral over the Grassmann coordinate $\tilde{\eta}_i$ of each internal particle ℓ_i is there to remind us that we are to sum-over the exchange of all possible internal particles—which in the case of $\mathcal{N} = 4$ means the full super-multiplet.³

This point of view of leading-singularities has been very useful and allows a complete determination of 1-loop amplitudes in $\mathcal{N} = 4$ and in $\mathcal{N} = 8$ supergravity amplitudes when thought of as linear combinations of scalar box integrals with rational coefficients. The rational coefficients can be computed using the notion of generalized unitarity. Clearly, the notion of discontinuities is not related to the existence of an integrand and this is the reason it works in $\mathcal{N} = 8$, supergravity where an analog of ‘the integrand’—which requires a way to combine integrals with different cyclic orderings—has not yet been found.

As mentioned in our discussion of reduction procedures in $\mathcal{N} = 4$ SYM, the expansion in terms of boxes cannot give the physical integrand. The physical integrand is defined as that which coincides with the one from Feynman diagrams, prior any to reduction

³Here, we are using an on-shell superspace formalism which allows us to talk about all particles in the same super-multiplet as a single 1-particle state. We assume familiarity with this concept, but for careful definitions, more references and applications see [72].

techniques, as rational functions—and, as we will see, the Feynman diagrams of $\mathcal{N} = 4$ in a given R -charge sector are *chiral*.

Once we think about the integrand as being the object we are after, we can try to model it by using some appropriate basis of functions, dictated by a general reduction procedure. Clearly, the set of all DCI tensor pentagons and boxes should be enough. Nevertheless, we will find that such a basis would still possess many of the unattractive features of the box-expansion, and so we will introduce much more refined choice in section 5.5.

The importance of dealing with a specific rational function is that we can integrate it on *any* choice of contour we'd like—not just the real-contour which defines the Feynman integral. This allows us to define a more refined notion of a leading-singularity—the previous notion, motivated by generalized unitarity, is much coarser version of the one we will use now. In [97], this more refined notion was introduced, and it was used to match the full $\mathcal{N} = 4$ integrand for several 1-loop and 2-loop examples. However, in [97] the deep reason for why the idea was working, *i.e.*, the existence of the integrand, was not appreciated.

Whether written in ordinary momentum space, using dual-coordinates, or using momentum-twistors, loop integrals can be thought of as complex contour integrals on \mathbb{C}^4 with the choice of contour corresponding to \mathbb{R}^4 —the real-slice. However, this choice of contour is known to break many of the symmetries of the theory, and is littered with IR-divergences, etc. that can be the source of confusion. From various viewpoints, the most natural contours would instead be those which compute the *residues* of the integrand. These are always finite, are often vanishing, and make manifest the full Yangian symmetry of the theory. We refer the reader to [65] for a mathematical definition of residues in several complex variables; here we hope the reader will find the definitions a natural generalization of the one-dimensional residues with which everyone is familiar.

Let us present the definition using x variables first. Consider a contour of integrations with the topology of a $T^4 = (S^1)^4$. In order to compute a particular residue one has to choose four propagators $(x - x_{a_i})^2$, with $i = 1, \dots, 4$ and integrate over the T^4 , defined by $|(x - x_{a_i})| = \epsilon_i$ where ϵ_i are small positive real numbers near one of the solutions. The circles, S^1 are parametrized by the phases and are given a particular orientation.

The definition of a multidimensional residue is very natural if one defines variables

$u_i = (x - x_{a_i})^2$. Performing the change of variables the integral becomes

$$\int \prod_{i=1}^4 \frac{du_i}{u_i} \times \frac{1}{J} \times \{\text{The rest of the integrand}\} \quad (5.2.28)$$

where now the contour becomes small circles around $u_i = 0$. J is the Jacobian of the change of variables. The residue is then the Jacobian times the rest of the integrand evaluated at $u_i = 0$. The Jacobian

$$J = \det \left(\frac{\partial(u_1, u_2, u_3, u_4)}{\partial(x_1, x_2, x_3, x_4)} \right), \quad (5.2.29)$$

is clearly antisymmetric in the order of the columns. Different orderings can differ by a sign and this is related to the orientation of the contour. These signs are important when discussing the generalization of residue theorems to the multidimensional case, which will play an important role momentarily.

From now on we call each individual residue a *leading-singularity*. As before, these are given by the product of four on-shell tree amplitudes as shown in Figure 5.2. The reason for the appearance of the tree amplitudes is that the residue of the poles is computed where the four propagators vanish and therefore internal particles can be taken on-shell.

Leading singularities at higher loop-level can also be defined as residues of a complex, multidimensional integral over \mathbb{C}^{4L} where L is the loop order. This means that in order to define a residue one has to define a T^{4L} torus as a contour of integration. Naively, residues can only be defined for integrals with at least $4L$ propagators. However, noticing that propagators are quadratic in the loop-momentum, one can define *composite leading singularities* which involve less than $4L$ propagators as done in [10, 97, 98], using the

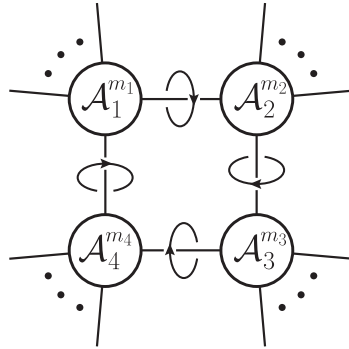


Figure 5.2: A ‘quad-cut’ one-loop leading-singularity viewed as a T^4 contour-integral which ‘encircles’ the point in \mathbb{C}^4 where four-propagators are made on-shell.

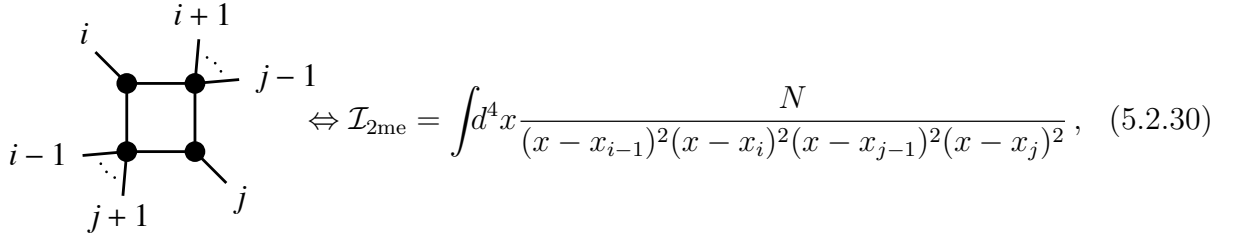
self-intersection of curves defined by the on-shell condition to define isolated points in \mathbb{C}^4 about which the T^{4L} contour should ‘encircle.’

We will not discuss composite leading singularities in detail here simply because we will present evidence that when a special set of integrals, we call *chiral integrals with unit leading-singularities*, are used, matching non-composite leading-singularities appears to suffice to fix the entire amplitude. Moreover, we will see that only a very small subset of non-composite leading-singularities need to be considered to accomplish this.

Chirality of Leading Singularities

It turns out that for nonsingular external momenta, there are exactly two solutions to the equations $(x - x_{a_i})^2 = 0$, with $i = 1, \dots, 4$, and therefore two residues of each choice of four propagators. (This has a beautiful geometric interpretation in momentum twistors as we will see shortly.) This means that for an n -particle amplitude, there are $2\binom{n}{4}$ (non-composite) one-loop leading-singularities.

Consider any box integral, say, an integral with two massless legs and two massive, known as the ‘two-mass-easy’ integral:



where N is just some normalization that need not concern us presently. The equations

$$(x - x_{i-1})^2 = (x - x_i)^2 = (x - x_{j-1})^2 = (x - x_j)^2 = 0$$

have two solutions, and therefore a residue can be computed for each such point separately. We’ll soon see that these two solutions are easily found and differentiated when written with momentum-twistor variables; but for now, let us suppose the two solutions have been found, and denote the corresponding contours T_1^4 and T_2^4 .

A very important tool that will make an appearance many times is multidimensional analogue of Cauchy’s theorem, called the *Global Residue Theorem* (GRT). The GRT states that—given a suitable condition at infinity—the sum over all the residues of a

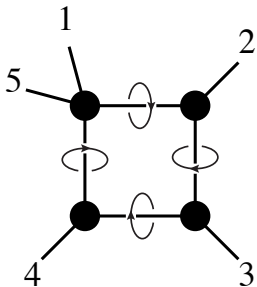
given rational function vanishes (see chapter 6 of [65]). This means, in the present case, that

$$\text{res}_{T_1^4}(\mathcal{I}_{2\text{me}}) + \text{res}_{T_2^4}(\mathcal{I}_{2\text{me}}) = 0 \quad (5.2.31)$$

Moreover, we can choose the normalization N is such that, say $\text{res}_{T_1^4}(\mathcal{I}_{2\text{me}}) = 1$. Such a choice is possible for all box integrals, following from the simple fact that all box-integrals—having only four propagators—must have residues which are proportional equal and opposite. We refer to this fact by saying that scalar box integrals are *not chiral*. The use of the word chiral is justified by the fact that the locations of the leading singularities, as points in \mathbb{C}^4 , are mapped into each other by parity—which is just complex conjugation. And so the corresponding contours are mapped into each other up to orientation by parity. If use $(T_1^4)^*$ to denote the parity conjugate contour of T_1^4 , then $\text{res}_{(T_1^4)^*} = -\text{res}_{T_1^4}$ and the GRT implies that

$$\text{res}_{T_1^4}(\mathcal{I}_{2\text{me}}) = \text{res}_{(T_1^4)^*}(\mathcal{I}_{2\text{me}}). \quad (5.2.32)$$

Let us now consider the leading-singularities of the one-loop integrands of $\mathcal{N} = 4$ Yang-Mills. We'll see that, as scattering amplitudes of $\mathcal{N} = 4$ in a given R -charge sector are chiral, so are the one-loop leading-singularities of field theory! In other words, the two residues associated with the two solutions of cutting four-propagators are *not* the same. Let us see this in an example. The simplest possible example is the five-particle MHV amplitude⁴. Let us consider taking the leading singularities of the field-theory integrand which encircles the point in \mathbb{C}^4 where the following four propagators go on-shell:



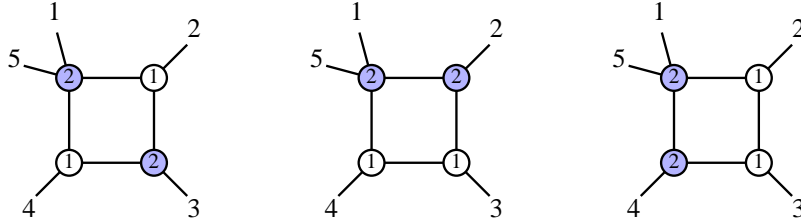
$$\iff (x - x_1)^2 = (x - x_2)^2 = (x - x_3)^2 = (x - x_4)^2 = 0. \quad (5.2.33)$$

It was noticed already in [129] that on one solution $\mathcal{N} = 4$ SYM gives the tree amplitude, A_5^{tree} , while it vanishes on the second.

⁴The only DCI object for four-particles is the zero-mass box integral. This is why both leading singularities are equal to the tree amplitude.

The vanishing of leading singularities can be understood from pure supersymmetry. Consider an amplitude in the R -charge sector m . Recall the N^{m-2} MHV classification of amplitudes in $\mathcal{N} = 4$: under a rescaling of all $\tilde{\eta}_a$ variables by $t\tilde{\eta}_a$, an N^{m-2} MHV amplitude picks up a factor of t^{4m} . From the definition of leading singularities as the product of tree amplitudes connected by internal on-shell states we see that every internal line contributes (-1) to the R -charge counting coming from the integration over $\tilde{\eta}$ variables. At 1-loop, we have four tree-amplitudes and four propagators. If the R -charge of each tree-amplitude is m_i (see Figure 5.2), then the R -charge of the leading singularity is $m_1 + m_2 + m_3 + m_4 - 4$.

Returning to the five-particle example, because we are interested in a one-loop MHV amplitude, all its leading-singularities must have $m = 2$. The four-particle vertex (in the upper-left of the figure above) can only have $m_1 = 2$ and therefore the three-particle vertices have to satisfy $m_2 + m_3 + m_4 = 4$. Since the possible values for m for a three-particle amplitude are 1 and 2, two vertices must have $m = 1$ and one must have $m = 2$. This leaves only the possibilities shown below:



Of these three possible leading-singularities of field theory, it turns out that the first one is equal to the five-point MHV tree-amplitude, and the latter two vanish for generic external momenta. In fact, whenever one is considering a leading singularity which involves 3-particle vertices, some very simple and powerful rules prove very useful: 1. any leading singularity involving adjacent three-particle vertices with the same R -charge will vanish for generic external momenta (momentum conservation in this case, requires that the external particles attached to these vertices must be collinear); and 2. leading singularities involving three-particle amplitudes are almost always *chiral*—the only exception being the four-particle amplitude.

In the case of the five particle example under consideration, we see that the residue from the contour encircling one of the two solutions to the quad-cut equations in (5.2.33) is equal to $\mathcal{A}_{5,\text{MHV}}^{\text{tree}}$, while the conjugate contour integral vanishes. We will explore this in more detail once we introduce the geometric point of view.

Dual Formulation of Leading Singularities

In the rest of the Chapter, we will make much use of the fact that leading-singularities satisfy many relations. These relations can be seen as resulting from residue theorems of the integrals which compute them. As a final comment before exploring the connection between leading singularities and the classic enumerative problems in the projective geometry of momentum twistor space let us briefly introduce the Grassmannian formulation.

In [10], leading singularities were proposed as completely IR-finite quantities that were likely to contain all the information needed to compute the S-Matrix of $\mathcal{N} = 4$ SYM. Moreover, it was conjectured that all leading singularities of the theory, which can be obtained to arbitrarily higher loop order, are computed by a contour integral over a Grassmannian manifold⁵ $G(m, n)$ called $\mathcal{L}_{m,n}$. Here m determines the R -charge sector of the theory under consideration.

The integral was first presented in twistor space

$$\mathcal{L}_{m,n}(\mathcal{W}_a) = \int \frac{d^{nm} C_{\alpha a}}{\text{vol}(GL_m)} \frac{\prod_{\alpha=1}^m \delta^{4|4}(\sum_{a=1}^n C_{\alpha a} \mathcal{W}_a)}{(1\ 2 \cdots m)(2\ 3 \cdots m+1) \cdots (n\ 1 \cdots m-1)}. \quad (5.2.34)$$

In this presentation, residues of this integral are manifestly superconformal invariant (that is, superconformally-invariant in ordinary spacetime). Here we have introduced the concept of dual super twistor space $W = (\tilde{\lambda}, \mu, \tilde{\eta})$. This particular space will not play a significant role in this work, so we refer the interested reader to [10, 17] for more details.

This formula can be transformed to momentum-space and then to momentum-twistor space. Very remarkably, the formula in momentum-twistor space also turns out to be an integral over a Grassmannian, with the MHV-tree-amplitude arising as the Jacobian from the change of variables. Specifically,

$$\mathcal{L}_{m,n}|_{\text{momentum-space}}(\lambda, \tilde{\lambda}, \tilde{\eta}) = \mathcal{L}_{2,n} \times \mathcal{R}_{k,n}, \quad (5.2.35)$$

where $k = m - 2$ and

$$\mathcal{R}_{k,n}(\mathcal{Z}_a) = \int \frac{d^{nk} D_{\alpha a}}{\text{vol}(GL_k)} \frac{\prod_{\alpha=1}^k \delta^{4|4}(\sum_{a=1}^n D_{\alpha a} \mathcal{Z}_a)}{(1\ 2 \cdots k)(2\ 3 \cdots k+1) \cdots (n\ 1 \cdots k-1)}. \quad (5.2.36)$$

⁵The Grassmannian $G(m, n)$, a natural generalization of ordinary projective space, is the space of m -dimensional planes in n -dimensions. Each point in $G(m, n)$ can be represented by the m n -vectors which span the plane, modulo a GL_m redundancy.

This representation in momentum twistor space makes *dual* superconformal invariance manifest [18, 19]. With some more effort one can prove that residues of this formula are also invariant under level one generators of the Yangian of the dual superconformal algebra and hence invariant under the whole Yangian [11]. The level one generators are nothing but the superconformal generators when passed through $\mathcal{L}_{2,n}$.

It has now been proven that all leading singularities are Yangian invariant and that all Yangian invariants are residues of the integral (5.2.36). From the physical point of view the problem has been solved. It might also be interesting to go further and prove that all residues of (5.2.36) correspond to some leading singularity but we will not discuss this issue any further.

Momentum Twistors and Schubert Problems

Statements like the number of solutions to setting four propagators to zero is two are non-obvious from the dual space x point of view. In terms of momentum twistors, this statement turns out to be a simple, classic problem of the enumerative geometry of \mathbb{CP}^3 , solved by Schubert in the 1870's [130, 131].

Recall that an n -particle 1-loop amplitude can be written as

$$\mathcal{A}_n = \int_{(AB)} \frac{\sum_i c_i \langle AB Y_1^i \rangle \langle AB Y_2^i \rangle \cdots \langle AB Y_{n-4}^i \rangle}{\langle AB 12 \rangle \langle AB 23 \rangle \cdots \langle AB n-1 n \rangle \langle AB n 1 \rangle}. \quad (5.2.37)$$

Each one-loop leading-singularity is associated with a *point* in the space of loop-momenta for which some choice of four propagators simultaneously become on-shell,

$$\begin{array}{ccc} i & i+1 & \\ \bullet & \bullet & \\ \vdots & \vdots & \\ l+1 & & j \\ \circ & \circ & \\ \vdots & \vdots & \\ l & & j+1 \\ \bullet & \bullet & \\ \vdots & \vdots & \\ k+1 & k & \end{array} \iff \langle AB i i+1 \rangle = \langle AB j j+1 \rangle = \langle AB k k+1 \rangle = \langle AB l l+1 \rangle = 0;$$

Because the loop momentum is represented in momentum-twistors as the *line* (AB) , the solution to these four equations should correspond to a particular configuration for the line (AB) . We will see that for all leading-singularities which involve a three-particle vertex (a ‘massless leg’), the two solutions to four equations above are cleanly distinguished geometrically, allowing for a richly-chiral description of the integrand.

Before describing the full problem of putting four propagators on-shell, let us briefly consider the geometric significance of having a single factor, say $\langle ABii+1 \rangle$, vanish. Recall that the four-bracket $\langle \cdot \cdot \cdot \cdot \rangle$ is nothing but the determinant of the 4×4 matrix of components of its four momentum-twistor arguments (viewed as elements of \mathbb{C}^4). As such, $\langle ABii+1 \rangle = 0$ if and only if the vectors Z_A, Z_B, Z_i, Z_{i+1} are *not* linearly independent, implying the existence of some linear relation among the four twistors of the form $\alpha_A Z_A + \alpha_B Z_B + \alpha_i Z_i + \alpha_{i+1} Z_{i+1} = 0$. Trivially rearranging we see that

$$\alpha_A Z_A + \alpha_B Z_B = -(\alpha_i Z_i + \alpha_{i+1} Z_{i+1}), \quad (5.2.38)$$

which we may read as saying there is a point on the line spanned by Z_A, Z_B —namely $(\alpha_A Z_A + \alpha_B Z_B)$ —which lies along the line spanned by Z_i, Z_{i+1} . Which is to say, the lines (AB) and $(Z_i Z_{i+1})$ *intersect*; and because two intersecting lines describe a plane, we say that the four points Z_A, Z_B, Z_i, Z_{i+1} are *coplanar*.

Therefore, the problem of finding the particular lines (AB) for which four propagators simultaneously vanish is equivalent to finding the set of lines in \mathbb{CP}^3 which simultaneously intersect four given lines (which are presumed fixed by the external data). The number of solutions to this problem is one of the classic examples of the enumerative geometry developed by Schubert in the 1870’s. For this reason we call these problems *Schubert problems*.

The answer to the number of lines which intersect a given four turns out to be remarkably robust: provided the four lines are sufficiently generic, there are always 2 solutions, and an infinite number otherwise.⁶ (An example of a *non-generic* configuration would be one for which three or more of the lines were coplanar; these are never found for generic external momenta.)

Schubert derived the number of such solutions with an argument that is deceptively simple. The idea is to consider a particular configuration where it is easy to count the number of solutions. Schubert intuited that the answers to such enumerative questions should be topological in nature, and therefore should not depend on the particular configuration in question. Therefore, one can analyze the most convenient possible configuration (for which the number of solutions is not infinite) and the answer found for

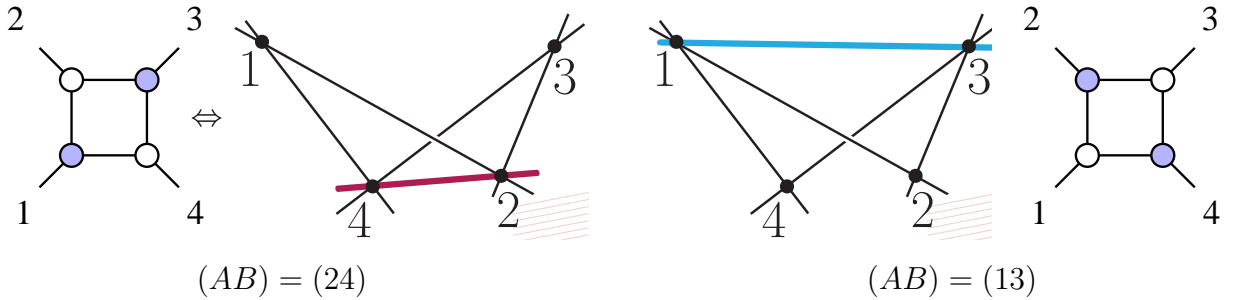
⁶To be precise, we must count solutions with multiplicity; however, for a generic set of lines in the problem, the 2 solutions will always be distinct.

that case, should be the answer in general. Said another way, the number of solutions to a given Schubert problem should not change when a particular special configuration is smoothly moved into a more general position.

Perhaps the easiest configuration for which we can count the number of solutions to the Schubert problem of finding the lines (AB) that intersect four given lines in \mathbb{CP}^3 is the *zero-mass* configuration; it is so-called because it is the configuration which corresponds to the box integral with *zero* of its four corners massive,

$$\begin{array}{ccc}
 \begin{array}{c} 2 \\ \bullet \\ \diagup \quad \diagdown \\ \bullet \quad \bullet \\ \diagdown \quad \diagup \\ \bullet \\ 1 \quad 4 \end{array} & \iff & \int_{(AB)} \frac{\langle 1234 \rangle \langle 2341 \rangle}{\langle AB 12 \rangle \langle AB 23 \rangle \langle AB 34 \rangle \langle AB 41 \rangle}, \\
 \end{array}$$

which is an integral we have seen before. Explicitly, we would like to find all the lines (AB) which intersect all the four lines (12) , (23) , (34) , and (41) . This problem is indeed easy to solve, and the two solutions are drawn below.



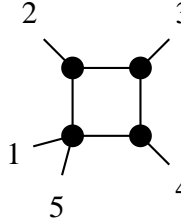
Clearly, because $(12) \cap (23) \supset Z_2$ and $(34) \cap (41) \supset Z_4$, the line $(AB) = (24)$ intersects all four lines, as desired; this is drawn in red above. The same argument also applies to the second solution, the line $(AB) = (13)$, drawn in blue above. Also in this figure, we have indicated which leading-singularities have non-vanishing support on the corresponding (complex) point in the space of loop-momenta which corresponds to the particular line (AB) . As explained above, each three-particle MHV ($m = 2$)—colored blue in the figure above—or $\overline{\text{MHV}}$ ($m = 1$)—colored white—vertex of a leading singularity vanishes for every leading-singularity, and so which of the 2 three-particle amplitudes is non-vanishing for this value of the loop-momentum determines the chirality of the contour.

As a convenient way to gain some intuition about momentum-twistor geometry that will prove useful in the rest of this chapter and to establish some of the notation that

will be ubiquitous throughout, we will study each of the 1-loop Schubert problems in turn.

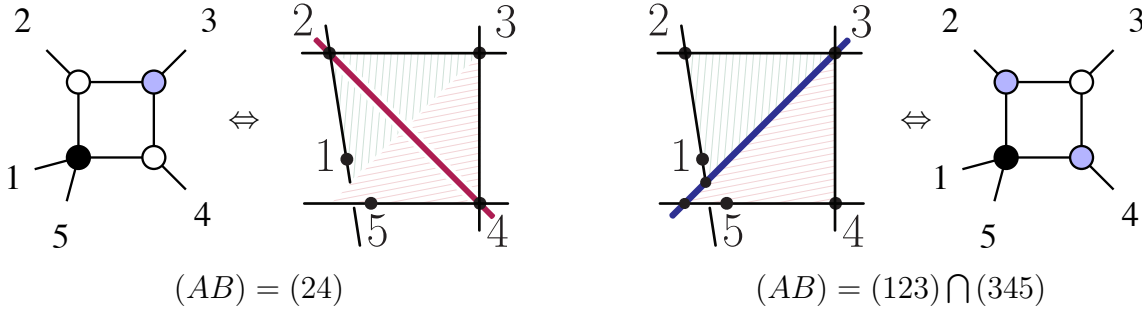
One-Mass Schubert Problem:

A ‘one-mass’ 1-loop leading singularity is one for which three of the four legs are massless, and is associated with the following archetypical box-integral:



$$\int_{(AB)} \frac{\langle 12\ 34 \rangle \langle 23\ 45 \rangle}{\langle AB\ 12 \rangle \langle AB\ 23 \rangle \langle AB\ 34 \rangle \langle AB\ 45 \rangle} . \quad (5.2.39)$$

In momentum-twistor space, the leading-singularities of this integral are associated with the lines (AB) which intersect the four lines (12) , (23) , (34) , and (45) . Considering the configuration of lines, it is not hard to find the two configurations which solve this Schubert problem:



As before, because $(12) \cap (23) \supset Z_2$ and $(34) \cap (45) \supset Z_4$, the line $(AB) = (24)$ intersects all four lines. The second solution, however, is new. This solution is drawn in blue in the figure above, and represents the line of the intersection of the planes spanned by $(Z_1, Z_2, Z_3) \equiv (123)$ and $(Z_3, Z_4, Z_5) \equiv (345)$. Although geometrically clear, it is worthwhile to recall that any generic line in the plane (123) will intersect the lines (12) , (23) , and (31) , and any generic line in the plane (345) will intersect the lines (34) , (45) , and (53) . Therefore, the line $(AB) = (123) \cap (345)$ will intersect all four lines, as required.

Similar to the case discussed in the context of the pentagon with a ‘wavy-line’ numerator (5.2.21), the line $(123) \cap (345)$ can easily be expanded in terms of ordinary bitwistors as: $(23)\langle 1\ 345 \rangle + (31)\langle 2\ 345 \rangle$. This follows from a more general rule which review presently.

On the Intersection of Planes in Twistor-Space

In general, the intersection of the planes $(abc) \cap (def)$ can be canonically expanded in either of the following ways:

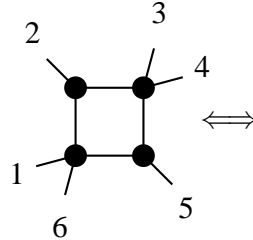
$$\begin{aligned} (abc) \cap (def) &= Z_a Z_b \langle c d e f \rangle + Z_b Z_c \langle a d e f \rangle + Z_c Z_a \langle b d e f \rangle; \\ &= \langle a b c d \rangle Z_e Z_f + \langle a b c f \rangle Z_d Z_e + \langle a b c e \rangle Z_f Z_d. \end{aligned} \tag{5.2.40}$$

Alternatively, when expanding a four-bracket of the form $\langle xy (abc) \cap (def) \rangle$, the manifest dependence on the two planes can be preserved at the cost of breaking the manifest dependence on the line (xy) , as follows:

$$\langle xy (abc) \cap (def) \rangle = \langle x a b c \rangle \langle y d e f \rangle - \langle y a b c \rangle \langle x d e f \rangle. \tag{5.2.41}$$

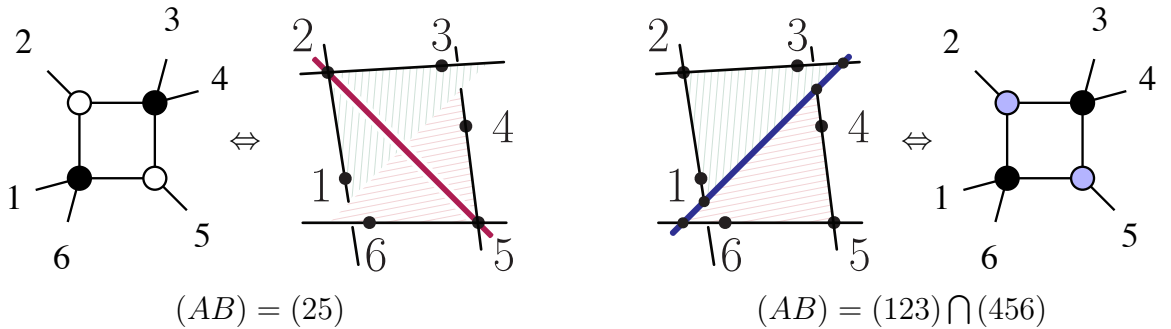
Two-Mass-Easy Schubert Problem

The two-mass-easy Schubert problem is associated with the following one-loop archetypical box-integral,



$$\int_{(AB)} \frac{\langle 1235 \rangle \langle 2345 \rangle}{\langle AB 12 \rangle \langle AB 23 \rangle \langle AB 45 \rangle \langle AB 56 \rangle}, \tag{5.2.42}$$

which has leading singularities supported on the configuration (AB) which intersect all four of the lines (12) , (23) , (45) , and (56) . The two solutions are essentially the same as for the one-mass Schubert problem, and are illustrated in the Figure below:



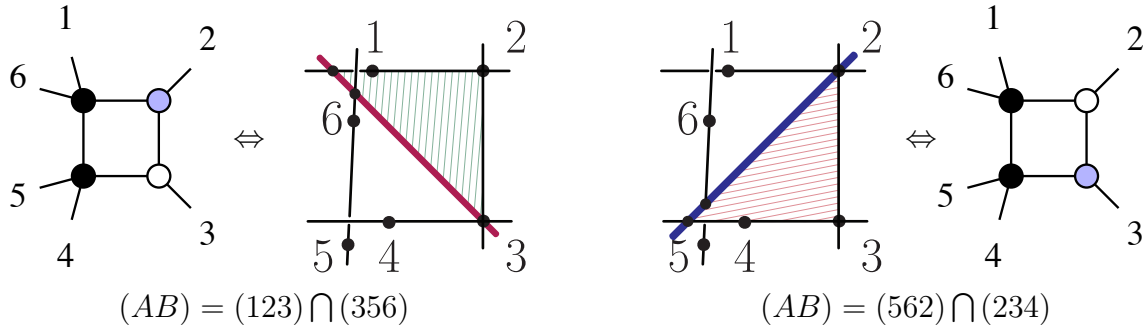
Once again, there is a very easy solution, in this case the line $(AB) = (25)$ which obviously intersects the four lines. And using the same reasoning as in the one-mass Schubert problem, it is easy to see that the second solution is simply the intersection of the planes $(123) \cap (456)$.

Two-Mass-Hard Schubert Problem

The two-mass-hard Schubert problem differs from the two-mass easy problem in that the two massless corners are adjacent—making the Schubert problem slightly less ‘easy’ (which at least partially justifies the name). It is associated with the following archetypical one-loop integral,

$$\int_{(AB)} \frac{\langle 12\ 34 \rangle \langle 23\ 56 \rangle}{\langle AB\ 12 \rangle \langle AB\ 23 \rangle \langle AB\ 34 \rangle \langle AB\ 56 \rangle}, \quad (5.2.43)$$

and has leading singularities supported where the line (AB) intersects the four lines (12) , (23) , (34) , and (56) . The two solutions are shown in the Figure below:



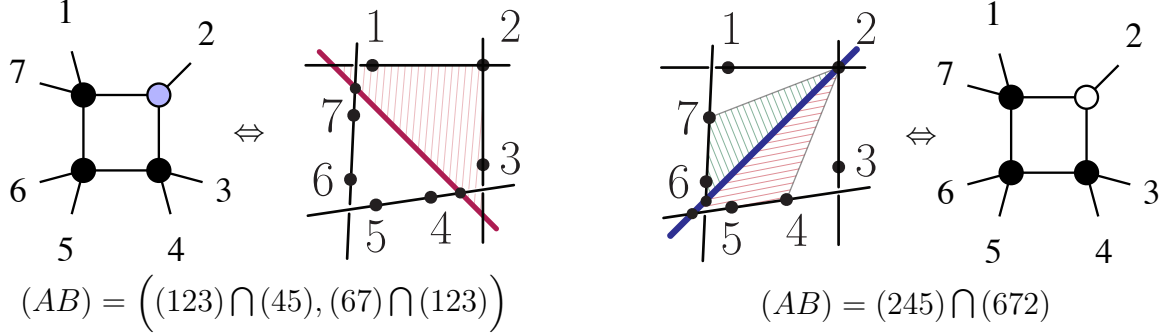
Let us briefly discuss the first of the two solutions. Here, the line $(AB) = (123) \cap (356)$ intersects the lines (23) , (34) trivially because $Z_3 \subset (123) \cap (356)$, and it intersects the lines (12) and (56) because any generic line in the plane (123) intersects (12) , and any generic line in the plane (356) intersects (56) .

Three-Mass Schubert Problem

The last Schubert problem that involves a massless corner is known as the ‘three-mass’ problem, and is associated with the following archetypical one-loop integral:

$$\int_{(AB)} \frac{\langle 1\ (245) \cap (672)\ 3 \rangle}{\langle AB\ 12 \rangle \langle AB\ 23 \rangle \langle AB\ 34 \rangle \langle AB\ 45 \rangle}. \quad (5.2.44)$$

This integral is the most general one which involves a massless corner, and supports leading singularities where the line (AB) intersects the four lines (12) , (23) , (45) , and (67) . The two solutions are indicated in the Figure below.



Here, the notation $'(ab) \cap (cde)'$ has been used to indicate the *point* in twistor-space where the line (ab) intersects the plane (cde) . We will discuss the expansion of such geometrically-defined objects more generally at the end of this subsection; for now, let us merely quote the result:

$$(ab) \cap (cde) \equiv Z_a \langle bcde \rangle + Z_b \langle cdea \rangle = - \left(Z_c \langle deab \rangle + Z_d \langle eabc \rangle + Z_e \langle abcd \rangle \right);$$

and similarly,

$$(cde) \cap (ab) \equiv Z_c \langle deab \rangle + Z_d \langle eabc \rangle + Z_e \langle abcd \rangle = - \left(Z_a \langle bcde \rangle + Z_b \langle cdea \rangle \right);$$

so that $(ab) \cap (cde) = -(cde) \cap (ab)$.

On Schouten-Identities and Projective Geometry

Perhaps the single most useful identity for momentum-twistor geometry is known as *'the five-term identity:'* any arbitrary set of five twistors $\{Z_a, Z_b, Z_c, Z_d, Z_e\}$ will satisfy the following identity,

$$Z_a \langle bcde \rangle + Z_b \langle cdea \rangle + Z_c \langle deab \rangle + Z_d \langle eabc \rangle + Z_e \langle abcd \rangle = 0. \quad (5.2.45)$$

This identity merely reflects the general solution to a homogeneous, linear system of equations in four-variables, and as such, has analogues in any number of dimensions. For example, in two dimensions, we have that for any $\{\lambda_a, \lambda_b, \lambda_c\} \subset \mathbb{C}^2$, there is an identity

$$\lambda_a \langle bc \rangle + \lambda_b \langle ca \rangle + \lambda_c \langle ab \rangle = 0, \quad (5.2.46)$$

where we have naturally extended the definition of ‘ $\langle \cdot \cdot \rangle$ ’ to be the determinant of the components of the corresponding two-vectors. This two-dimensional identity represents the general solution to a homogeneous, linear system of equations in 2 unknowns, and by contracting it with a fourth two-vector λ_d , we obtain the familiar ‘Schouten identity:’

$$\langle da \rangle \langle bc \rangle + \langle db \rangle \langle ca \rangle + \langle dc \rangle \langle ab \rangle = 0. \quad (5.2.47)$$

This familiar identity of course has an analogue descending from equation (5.2.45). By contracting equation (5.2.45) with any arbitrary plane (fgh) , we find the following 5-term identity which we will therefore call ‘a Schouten identity:’

$$\langle fgha \rangle \langle bcde \rangle + \langle fghb \rangle \langle cdea \rangle + \langle fghc \rangle \langle deab \rangle + \langle fghd \rangle \langle eabc \rangle + \langle fghe \rangle \langle abcd \rangle = 0.$$

In addition to being quite useful for simplifying formulae, equation (5.2.45) can be trivially re-arranged to yield the solutions to some of the most often-encountered problems in momentum-twistor geometry:

1. the expansion of any arbitrary twistor Z_a into a basis composed of any four linearly-independent twistors $\{Z_b, Z_c, Z_d, Z_e\}$:

$$Z_a \langle bcde \rangle = -\left(Z_b \langle cdea \rangle + Z_c \langle deab \rangle + Z_d \langle eabc \rangle + Z_e \langle abcd \rangle \right);$$

2. the point along the line (ab) which intersects the plane (cde) :

$$(ab) \cap (cde) \equiv Z_a \langle bcde \rangle + Z_b \langle cdea \rangle = -\left(Z_c \langle deab \rangle + Z_d \langle eabc \rangle + Z_e \langle abcd \rangle \right);$$

3. the point on the plane (abc) which intersects the line (de) :

$$(abc) \cap (de) \equiv Z_a \langle bcde \rangle + Z_b \langle cdea \rangle + Z_c \langle deab \rangle = -\left(Z_d \langle eabc \rangle + Z_e \langle abcd \rangle \right);$$

and so-on.

Matching All Leading Singularities

We close this introductory section to momentum twistor integrals and leading singularities with a physical point. We have seen that the leading singularities of $\mathcal{N} = 4$ SYM are chiral while those of scalar boxes are non-chiral. This means that if we want to construct the integrand of the theory it is impossible to do it using scalar boxes. Momentum twistors already give the solution to this problem. Since leading singularities are Yangian invariant and in particular dual conformal invariant (DCI), one should use the reduction procedure to go down to tensor pentagons and boxes and not any further. Even going down to scalar pentagons would be doing something brutal to the manifestly DCI structure of the amplitudes.

In the rest of the Chapter, we will find that by using a special class of integrals known as *chiral unit leading singularity* integrals, the full integrand of scattering amplitudes can be reproduced yielding to stunningly simple forms.

5.3 Chiral Integrals with Unit Leading Singularities

Given the success of the recently introduced recursion relations for the construction of the integrand to all orders in perturbation theory described in Chapter 4, it is clear that the physical integrand is the important object to obtain.

In the previous section we showed that the usual constructions of, say, one-loop amplitudes in $\mathcal{N} = 4$ SYM as a linear combination of scalar boxes cannot possibly be the physical integrand. Of course, the answer obtained from scalar boxes gives the same integrals as the one originally defined from Feynman diagrams. However, as we will see, insisting in obtaining the physical integral leads to stunningly simple formulas for one and higher loop amplitudes. These new formulas are possible thanks to the use of a new suit of integrals with very special properties. These are *chiral integrals with unit leading singularities*.

I. Integrals with Unit Leading Singularities, or *Pure Integrals*

Let us start by given a definition of integrals with unit leading singularities. As we will see, it is appropriate to call these *pure integrals*.

Consider a particular DCI L -loop integral and compute all possible residues. If all non-vanishing residues are the same up to a sign then the integral can be normalized so that all residues are ± 1 or 0. When this is done, the integral is said to have *unit leading singularities* or to be a *pure integral*.

We already encountered examples of pure integrals in the previous section. The zero mass box (5.2.15), the general scalar box (5.2.16) (properly normalized), and the pentagon integrals in (5.2.20) and (5.2.21).

Using the global residue theorem, we proved in section 2 that boxes are pure integrals. However, it is not obvious that the pentagons in (5.2.20) and (5.2.21) satisfy the requirement.

Consider first pentagons of the first class

$$\int_{(AB)} \frac{\langle AB 13 \rangle N}{\langle AB 12 \rangle \langle AB 23 \rangle \langle AB 34 \rangle \langle AB 45 \rangle \langle AB 51 \rangle} \quad (5.3.48)$$

where $N = \langle 12 45 \rangle \langle 23 45 \rangle$.

In order to see that all non-vanishing leading singularities are equal up to a sign let us use a global residue theorem. In section 2 we gave a very imprecise definition of the global residue theorem (GRT) which was enough for the purposes of that section. Here we have to be more precise. The GRT states that given a choice of a map $f : \mathbb{C}^4 \rightarrow \mathbb{C}^4$ made from polynomial factors in the denominator, the sum over all the residues associated with the zeroes of the map vanishes.

In the present case, consider the map given by $f = (f_1, f_2, f_3, f_4)$ where

$$f_1 = \langle AB 12 \rangle, \quad f_2 = \langle AB 23 \rangle, \quad f_3 = \langle AB 34 \rangle, \quad f_4 = \langle AB 45 \rangle \langle AB 51 \rangle.$$

It is easy to see that the map f has four zeroes (see section 2 for more details). The GRT assures that the sum over the four residues vanishes. How can we prove that residues are equal if the GRT only gives relations among four residues?

The answer has to do with our choice of numerator. Consider the value of $\langle AB 13 \rangle$ on

the four zeroes. Each zero is a line which is the solution to some Schubert problem⁷. The four solutions are the lines (24), $(123) \cap (345)$, (13) and $(512) \cap (234)$ (see the end of the section or section 2 for the notation). It is a simple exercise to show that $\langle AB 13 \rangle$ vanishes on the second and third solutions and it is non zero on the first and fourth. This means that the GRT implies that two leading singularities are equal and opposite in sign. The first is one of the two solutions to $\langle AB 12 \rangle = \langle AB 23 \rangle = \langle AB 34 \rangle = \langle AB 45 \rangle = 0$ while the fourth is one of the two solutions to $\langle AB 12 \rangle = \langle AB 23 \rangle = \langle AB 34 \rangle = \langle AB 51 \rangle = 0$. Let us denote these non-vanishing residues by $r_{(12),(23),(34),(45)}$ and $r_{(12),(23),(34),(51)}$ respectively. Therefore the GRT states that

$$(0 + r_{(12),(23),(34),(45)}) + (r_{(12),(23),(34),(51)} + 0) = 0$$

which implies the equality of the residues up a sign.

The pentagon integral has 10 leading singularities. This means that more work is needed to show that it has unit leading singularity. Consider a GRT associated to the map

$$f_1 = \langle AB 12 \rangle \langle AB 51 \rangle, f_2 = \langle AB 23 \rangle, f_3 = \langle AB 34 \rangle, f_4 = \langle AB 45 \rangle.$$

Once again, there are four zeroes of this map. Two of them are shared with the map we constructed before, *i.e.*, (24) and $(123) \cap (345)$. The two new solutions are (35) and $(234) \cap (451)$. As before, the numerator vanishes on $(123) \cap (345)$. Very nicely, it also vanishes on (35). We can denote by $r_{(12),(23),(34),(45)}$ and $r_{(51),(23),(34),(45)}$ the corresponding non-zero residues. Therefore the GRT gives

$$(0 + r_{(12),(23),(34),(45)}) + (r_{(51),(23),(34),(45)} + 0) = 0$$

This means that the GRT sets equal the non vanishing leading singularity in $\langle AB 51 \rangle = \langle AB 23 \rangle = \langle AB 34 \rangle = \langle AB 45 \rangle = 0$ with the ones we found before.

This procedure can be continued three more times by shifting the labels in the map by one. We leave it as an exercise for the reader to verify that in every case, the numerator vanishes on one solution implying that the GRT sets all non-zero leading singularities to be the same.

⁷A Schubert problem was defined in section 2 as the projective geometry problem of finding lines that intersect four given lines which can be in special configurations called one-mass, two-mass-easy, two-mass-hard, and three-mass, as well as in generic positions which we call four-mass configurations.

In order to compute the normalization and also to show how the GRT makes obvious statements that require computations to be verified, even in this trivial case, let us compute explicitly the two residues in the first GRT discussed above.

Consider the ones in the first step. In other words, let's evaluate the residue on the solution (24) to the system $\langle AB 12 \rangle = \langle AB 23 \rangle = \langle AB 34 \rangle = \langle AB 45 \rangle = 0$. The residue is given by

$$N \frac{\langle 2413 \rangle}{\langle 2451 \rangle (\langle 1234 \rangle \langle 2345 \rangle)} \quad (5.3.49)$$

Here the terms in parenthesis are the Jacobian in the residue computation. A geometric way to see that the Jacobian has to contain the factors $\langle 1234 \rangle$ and $\langle 2345 \rangle$ is that on the special configurations where either one of them vanishes, the number of solutions to the Schubert problem becomes infinite. For example, consider the configuration where $\langle 1234 \rangle = 0$. In this case, any line on the plane (123) which passes through Z_4 solves the Schubert problem. Using the scaling of each momentum twistor, the Jacobian must be what we found. It might be instructive to see the full computation of the Jacobian using momentum twistors. This is carried out in detail in appendix E.

In order to have a properly normalized integral we require (5.3.49) to be equal to one. This means that $N = \langle 5124 \rangle \langle 2345 \rangle$ which is the factor first given in section 2 in (5.2.20).

Consider now the residue coming from the second Schubert problem, $\langle AB 12 \rangle = \langle AB 23 \rangle = \langle AB 34 \rangle = \langle AB 51 \rangle = 0$. The non-zero residue is associated with the solution $(512) \cap (234)$. This is a one-mass Schubert problem and one explicit form of Z_A and Z_B was given in section 2. Let us use $Z_A = Z_2$ and $Z_B = -\langle 1234 \rangle Z_5 + \langle 5234 \rangle Z_1$ and compute the residue. The Jacobian is the same as before but with labels shifted back by one. The residue is then

$$N \frac{\langle 1234 \rangle \langle 2513 \rangle}{\langle 2345 \rangle \langle 5124 \rangle (\langle 1234 \rangle \langle 2513 \rangle)}. \quad (5.3.50)$$

Using the normalization derived above this quantity equals one as expected.

In section 2 we also presented a second pentagon integral which differs from the first one only in the choice of numerator. We leave it as an exercise for the reader to repeat the analysis done here and show that with the new numerator this is a pure integral⁸.

⁸Of course, one could simply translate the whole problem into dual momentum twistor space to find exactly the same integral as before. However, it is still an instructive exercise to do it in momentum twistor space.

Let us rewrite the integral here with the numerator given in geometric form

$$\int_{(AB)} \tilde{N} \frac{\langle AB (512) \cap (234) \rangle}{\langle AB 12 \rangle \langle AB 23 \rangle \langle AB 34 \rangle \langle AB 45 \rangle \langle AB 51 \rangle}. \quad (5.3.51)$$

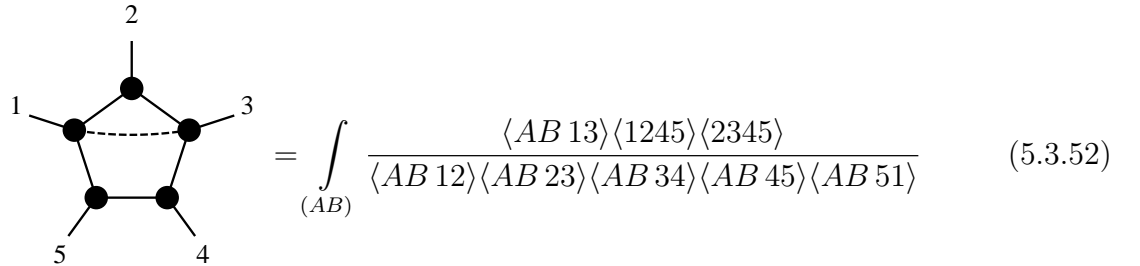
Now it should be obvious that the comment made in section 2 is true. The special numerators are made from lines, (13) and $(512) \cap (234)$, which are the two solutions to a Schubert problem.

In section 4 we study a less trivial example; a hexagon integral where the special choice of numerator also allows the use of the GRT to show that all non-vanishing residues are equal. In the hexagon case, checking the statement that all residues are equal algebraically requires many applications of 4-bracket Schouten identities.

Basic Diagrammatic Notation

We find it convenient to introduce a diagrammatic representation for numerators. Note that with our definition of dual variables $p_a = x_a - x_{a-1}$ and of momentum twistors $x_a \leftrightarrow (Z_a, Z_{a+1})$, there is a natural diagrammatic relation between loop integrals and momentum twistor configurations. Consider a general one-loop amplitude as a polygon with n -sides. Attached to each vertex there is some momentum p_a . In momentum twistor space, we also have an n -sided polygon and attached to each vertex there is a momentum twistor Z_a . Following the intuitive correspondence between the two diagrams we are led to denote denominators (propagators) as lines connecting points depending on their geometric configuration. These are denoted by solid lines. In order to distinguish numerators, we also introduce dashed and wavy lines.

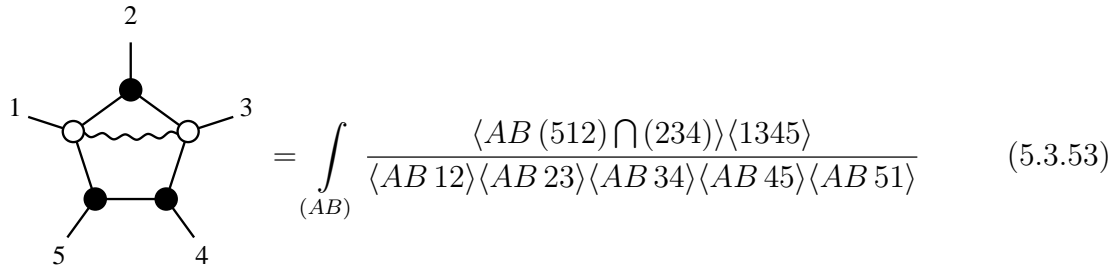
Dashed lines: Numerators which correspond to factors of the form $\langle AB ef \rangle$, where (ef) represents a line in momentum twistor space specified by two momentum twistors Z_e and Z_f is represented by a dashed line connecting points e and f as in



$$= \int_{(AB)} \frac{\langle AB 13 \rangle \langle 1245 \rangle \langle 2345 \rangle}{\langle AB 12 \rangle \langle AB 23 \rangle \langle AB 34 \rangle \langle AB 45 \rangle \langle AB 51 \rangle} \quad (5.3.52)$$

Wavy lines: We also allow points to represent dual twistors. In this case the second class of numerators constructed as intersection of planes can also be represented by a line

connecting two points. In order to distinguish this from the previous case we use wavy lines. In the example where the numerator corresponds to the line $(512) \cap (234)$ or in dual twistor terminology to the point $(13)_W$, one has



$$= \int_{(AB)} \frac{\langle AB (512) \cap (234) \rangle \langle 1345 \rangle}{\langle AB 12 \rangle \langle AB 23 \rangle \langle AB 34 \rangle \langle AB 45 \rangle \langle AB 51 \rangle} \quad (5.3.53)$$

II. Chiral Integrals

From the discussion of the pentagons, it is clear that there is a striking difference between a pentagon with a special numerator and plain scalar box integrals. Even though both kind of objects can be made pure integrals, each Schubert problem in the case of the pentagon has a single non-vanishing residue while in the boxes both solutions give rise to a residue.

When an integral has the property that the residues associated to at least one of its Schubert problems are not the same, we say that the integral is *chiral*. The reason for the terminology comes from the fact that the two contours associated to a given Schubert problem are exchanged under parity (see section 2 for more details). This means that one can have chiral, pure, or chiral and pure integrals.

At one-loop, one can have an even more especial class of integrals. When an integral has a numerator where at most one of the solutions to each Schubert problem gives a non-zero residue then we say that the integral is *completely chiral*.

Let us give two more examples in this section. The first is the most general class of chiral pure pentagon integrals. This is an integral where only two of the five legs needs to be massless. Moreover, it is clear that in order to write a special numerator the two massless legs cannot be adjacent. The claim is that the following family of integrals is

(completely) chiral and pure.

$$\int_{(AB)} \frac{\langle AB (i-1 i i+1) \cap (j-1 j j+1) \rangle \langle i j k k+1 \rangle}{\langle AB i-1 i \rangle \langle AB i i+1 \rangle \langle AB j-1 j \rangle \langle AB j j+1 \rangle \langle AB k k+1 \rangle} \quad (5.3.54)$$

In this case, the GRT can also be applied to show that all residues are the same. In order to show that the normalization gives unit leading singularities, identities of the form discussed at the end of this section are needed.

Next, let us give a six-point two-loop example. Consider the following integral

$$= \left\{ \frac{\langle AB (i-1 i i+1) \cap (j-1 j j+1) \rangle \langle i j k l \rangle}{\langle AB i-1 i \rangle \langle AB i i+1 \rangle \langle AB j-1 j \rangle \langle AB j j+1 \rangle \langle AB CD \rangle} \times \frac{\langle CD (k-1 k k+1) \cap (l-1 l l+1) \rangle}{\langle CD k-1 k \rangle \langle CD k k+1 \rangle \langle CD l-1 l \rangle \langle CD ll+1 \rangle} \right\}$$

This integral has the structure of two of the general pentagon integrals joined by the all massive edge. Consider a residue of the full integral over \mathbb{C}^8 which computes a residue of the pentagon on the left. The contour integral in Z_A and Z_B is the same as before except that the normalization is different and therefore the residue is not equal to one. The residue must then be the ration of the two normalizations, *i.e.*, $\langle i j k l \rangle / \langle i j CD \rangle$. Plugging this in the integral over Z_C and Z_D we now find a properly normalized integral and therefore the remaining part of residue computation gives one.

One might be tempted at this point to think that all completely chiral integrals are pure. In section 4, we describe in detail the example of a hexagon with a wavy line and a dashed line in the numerator. This integral is in fact completely chiral but it is not pure.

III. Evaluation of Pure Integrals

Evaluating integrals explicitly can be very hard and many techniques have been developed for this purpose. At one-loop, all integrals appearing in the standard reduction techniques are known analytically. At higher loops, very few examples have been evaluated analytically. Many of our chiral pure integrals turn out to be completely IR finite and therefore their evaluation can be made directly four dimensions without any regulators.

Consider the family of pentagon integrals discussed above. The evaluation of the integrals for generic j and k gives

$$\begin{aligned}
 I_5(i, j, k) &= \int_{(AB)} \frac{\langle AB (i-1 i i+1) \cap (j-1 j j+1) \rangle \langle i j k k+1 \rangle}{\langle AB i-1 i \rangle \langle AB i i+1 \rangle \langle AB j-1 j \rangle \langle AB j j+1 \rangle \langle AB k k+1 \rangle}, \quad (5.3.55) \\
 &= \log(u_{j,k,i-1,j-1}) \log(u_{k,i-1,i,j}) + \text{Li}_2(1 - u_{j,k,i-1,j-1}) + \text{Li}_2(1 - u_{k,i-1,i,j}) \\
 &\quad - \text{Li}_2(1 - u_{j,k,i,j-1}) - \text{Li}_2(1 - u_{i,j-1,k,i-1}) + \text{Li}_2(1 - u_{i,j-1,j,i-1})
 \end{aligned}$$

where

$$u_{i,j,k,l} \equiv \frac{\langle i i+1 j j+1 \rangle \langle k k+1 l l+1 \rangle}{\langle l l+1 j j+1 \rangle \langle k k+1 i i+1 \rangle} \quad (5.3.56)$$

For special values of j and k the integral becomes IR-divergent and a regulator is needed.

We postpone this discussion to section 4.

The reason for presenting the explicit form of the pentagon integrals is to note a general fact about pure integrals: The explicit evaluation of the integrals must be a linear combination of functions known as iterated integrals, such as polylogarithms, all with coefficient one.

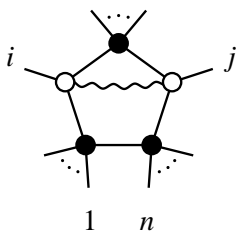
It is striking that the coefficients do not depend on kinematic invariants but this is a consequence of having unit leading singularities. This is the motivation for the terminology: pure integrals. Roughly speaking, the coefficients of the different polylogarithms are the leading singularities of the integrals. Having a pure integral ensures that no coefficient can depend on kinematical invariants.

Once again, the hexagon with a wavy and a dashed line in the numerator given in section 4 will be an example of a completely chiral and IR finite integral which is not pure and its evaluation gives products of logarithms with different coefficients that depend on kinematic invariants.

IV. Example: 1-Loop MHV Amplitudes

Up until now we have been studying integrals individually. This is a good point to actually use them to determine the full physical integral of the simplest set of amplitudes. These are one-loop MHV amplitudes. Historically, one-loop MHV amplitudes were the very first set of amplitudes to be computed for all n as a linear combination of scalar box integrals [75]. It was found that the answer is very simple; an overall prefactor, proportional to the tree-level amplitude, and a sum over all one-mass and two-mass-easy box integrals with coefficient one, when properly normalized. In our modern terminology, the normalization was such that only pure integrals appear. It was realized that this form of the amplitude was not equivalent to the Feynman diagram amplitude as an expansion in the dimensional regularization parameter but it differs from it only at $\mathcal{O}(\epsilon)$. In our language this is nothing but the fact that an expansion in terms of box integrals cannot possibly reproduce the physical integrand of the theory as stressed a number of times already.

Now that we have a set of chiral pure integrals, the natural question is how much more complicated the amplitude will look like if written in a form that matches the physical integrand. It turns out that the full integrand is stunningly simple

$$\mathcal{A}_{\text{MHV}}^{1\text{-loop}} = \sum_{i < j} \langle AB n 1 \rangle \quad (5.3.57)$$


where the propagator $\langle AB n 1 \rangle$ is present in all terms. Note that not all integrals in the sum are chiral pure integrals. There are boundary terms which are box integrals. Consider for example $j = i + 1$. In this case the numerator cancels one of the propagators leaving us with the box. We give no derivation for this formula here and postpone a more detailed discussion to section 6. A final comment, even though the line $(n1)$ seems especial, the amplitude is cyclic as it should be!

5.4 Finite Integrals

We have seen that the chiral integrals with unit leading singularities, naturally written in momentum-twistor space, provide a natural basis of objects to express the loop integrand. In this section we will see that they have another beautiful property—most such integrals are manifestly infrared finite.

Let us begin by illustrating with a simple example. Consider a general 1-loop integral for 6 particles, which we can write as

$$\int_{(AB)} \frac{\langle ABX \rangle \langle ABY \rangle}{\langle AB12 \rangle \langle AB23 \rangle \cdots \langle AB61 \rangle}. \quad (5.4.58)$$

Here X, Y are generic bitwistors. Of course, like almost all generic integrals with massless external legs, this integral is infrared divergent. Recall that the infrared divergences arise when the loop momentum l become collinear to a massless external momentum p_a , *i.e.* when $l \cdot p_a \rightarrow 0$. The extra soft logarithmic divergence can be thought of as an even more special case of this situation, where the loop momentum becomes collinear to two consecutive momenta so that $l \cdot p_a, l \cdot p_{a+1} \rightarrow 0$. In the dual co-ordinate space, the collinear divergence arises when the loop integration point x approaches one of the edges of the Wilson loop, connecting x_a with x_{a+1} , and of course the extra soft divergence occurs when x gets close to both the lines $(x_{a-1} x_a)$ as well as $(x_a x_{a+1})$, that is when it is close to the point x_a itself. But again the IR-divergence is fundamentally a collinear one, with the soft divergence being thought of as “double-collinear”.

We can finally describe these IR-divergent regions in momentum-twistor language. The collinear divergence associated with $l \cdot p_a \rightarrow 0$ corresponds to the region where the line (AB) in momentum twistor space, associated to the loop integration point, passes through Z_a while lying in the plane $(Z_{a-1} Z_a Z_{a+1})$. Note that this region is quite nicely parity invariant. Recall that in momentum-twistor variables, parity is just the poincare duality, and exchanges the point Z_a^I with the plane $W_{aI} = (Z_{a-1} Z_a Z_{a+1})_I$ naturally paired with Z_a . Thus, the condition is that the line $(AB)^{IJ}$ passes through Z_a^I , and also that the dual line $(AB)_{IJ}$ passes through W_{aI} .

While a generic integral will indeed be IR-divergent, we see a simple way of getting completely IR finite integrals. If the bitwistors X, Y are chosen to have a zero in all the dangerous IR-divergent configurations, then the integrals will be finite. This is very

simple to achieve. For instance, let us choose $X = (13)$ and $Y = (46)$; we can write out the integral again as,

$$= \int_{(AB)} \frac{\langle AB 13 \rangle \langle AB 46 \rangle \langle 5 6 1 2 \rangle \langle 2 3 4 5 \rangle}{\langle AB 12 \rangle \langle AB 23 \rangle \langle AB 34 \rangle \langle AB 45 \rangle \langle AB 56 \rangle \langle AB 61 \rangle} \quad (5.4.59)$$

Let us check that the numerator has a zero in all the IR-divergent regions. Consider first collinearity with p_3 . We need to see what the numerator does when (AB) passes through Z_3 while lying in the plane (234) . However, the numerator factor $\langle AB 13 \rangle$ vanishes simply if (AB) passes through 1 or 3, regardless of whether or not it also happens to lie in the plane (234) . In this way, we can see that the collinear divergences with 1, 3, 4, 6 are all killed by the numerator. Next, consider what happens when (AB) passes through 2, lying in the plane (123) . Since (AB) lies in (123) , it necessarily intersects the line (13) , and therefore, $\langle AB 13 \rangle = 0$, regardless of whether or not (AB) also happens to pass through 2. A completely analogous argument holds for the collinear divergence associated with particle 5.

Thus we see that with this numerator, *all* the regions with collinear divergences are killed by the numerator factors, and the integral is completely IR-finite! There are other choices for X, Y that will do the same job; our argument above also holds if one or both of the numerator factors $(13), (46)$ were replaced by their parity-conjugates, $(612) \cap (234)$ and $(345) \cap (561)$, respectively—changing one or more of the dashed-lines in (5.4.59) to wavy-lines.

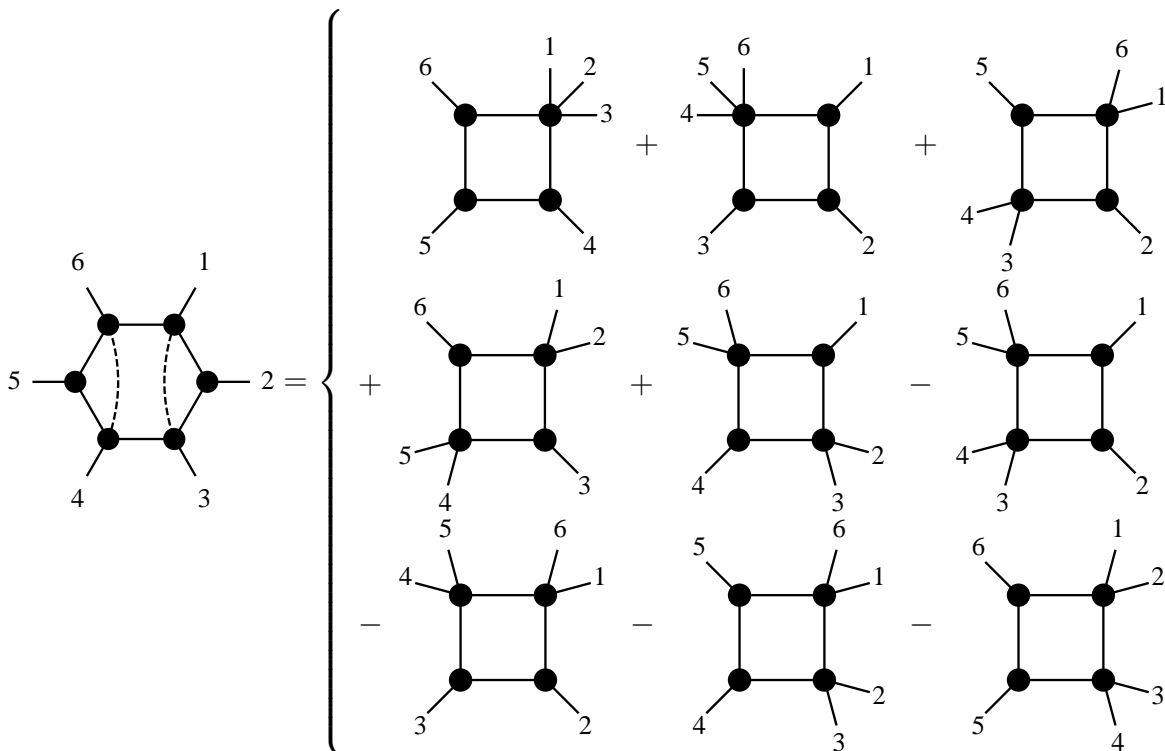
Now, these finite integrals are clearly chiral. And when the two numerators are of the same kind, they have, quite nicely and non-trivially, unit leading singularities. As usual, verifying by direct computation requires manipulating non-trivial sequences of 4-bracket Schouten identities, but the result follows much more transparently from an application of the global residue theorem to this integral. Consider for instance the GRT following from choosing $f_1 = \langle AB 34 \rangle, f_2 = \langle AB 45 \rangle, f_3 = \langle AB 56 \rangle$ and $f_4 = \langle AB 61 \rangle \langle AB 12 \rangle \langle AB 23 \rangle$. We have three different Schubert problems to consider, with the lines $(34), (45), (56)$ combined with $(61), (12), (23)$. Consider first the Schubert problem with the four lines $(34), (45), (56), (61)$. This is a one-mass configuration, and it is easy to see that the nu-

erator kills the solution where (AB) is the line (46), only leaving the solution passing through 5. Let us call this non-vanishing residue $r_{(34),(45),(56),(61)}$. Similarly, for the Schubert problem with lines (34), (45), (56) and (12), the numerator kills the solution passing through 4 while leaving the one passing through 5; we can call this single non-vanishing residue $r_{(34),(45),(56),(12)}$. Finally, for the Schubert problem with lines (34), (45), (56), (23), we can see that *both* solutions—the line 35 as well the line passing through 4—are killed by the numerator, so both of these residues vanish. The GRT then tells us that

$$\begin{aligned} (0 + r_{(34),(45),(56),(61)}) + (0 + r_{(34),(45),(56),(12)}) + (0 + 0) &= 0 \\ \rightarrow r_{(34),(45),(56),(61)} &= -r_{(34),(45),(56),(12)} \end{aligned} \tag{5.4.60}$$

It is possible to repeat this argument for other GRT's, finding a sequence of 2-term identities relating *all* the non-vanishing residues, showing that the integral is not only chiral but has *unit* leading singularities. Thus, we see in this instance something that can be checked also to be true for all other residues: the integral is completely chiral; at most one of the two solutions to each Schubert problem are non-vanishing, and sometimes both vanish.

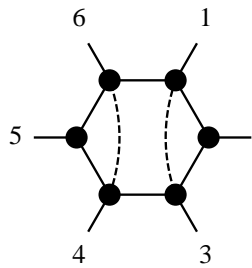
Given that this integral has unit leading singularities, it is instructive to expand it in terms of boxes, which will then also have unit coefficients. This simple, finite momentum-twistor integral in fact expands into the sum of nine boxes:



The seemingly complicated combinations of a large number of boxes have been encountered before in the computation of finite 1-loop objects, such as the NMHV ratio function [8, 48, 86, 106] —the ratio function for the full superamplitude is simply defined to be

$$\mathcal{R}_{n,k}^{1\text{-loop}} = \mathcal{A}_{n,k}^{1\text{-loop}} - \mathcal{A}_{n,k}^{\text{tree}} \cdot \mathcal{A}_{n,k=2}^{1\text{-loop}}. \quad (5.4.61)$$

Note that in the box expansion, every integral is individually IR-divergent, the IR-divergences only canceling in the sum. Moreover, the boxes themselves are not dual conformal invariant—again, only become dual conformal invariant in the sum. But since the hexagon in which we are interested is manifestly finite and dual conformal invariant⁹, we can evaluate it directly—for example, using Feynman parameterization directly without any regularization. A straightforward computation shows,



$$= \text{Li}_2(1 - u_1) + \text{Li}_2(1 - u_2) + \text{Li}_2(1 - u_3) + \log(u_3)\log(u_1) - \frac{\pi^2}{3}, \quad (5.4.62)$$

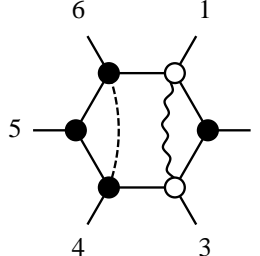
where the u_i are the familiar six-point cross-ratios:

$$u_1 \equiv \frac{\langle 12\ 34 \rangle \langle 45\ 61 \rangle}{\langle 12\ 45 \rangle \langle 34\ 61 \rangle}, \quad u_2 \equiv \frac{\langle 23\ 45 \rangle \langle 56\ 12 \rangle}{\langle 23\ 56 \rangle \langle 45\ 12 \rangle}, \quad \text{and} \quad u_3 \equiv \frac{\langle 34\ 56 \rangle \langle 61\ 23 \rangle}{\langle 34\ 61 \rangle \langle 56\ 23 \rangle}. \quad (5.4.63)$$

It is easy to find examples of integrals which are finite and chiral, but which do not have unit leading singularities. For example, changing one the ‘dashed-line’ numerator factor $\langle AB\ 13 \rangle$ in the integral above to a ‘wavy-line’ $\langle AB\ (612) \cap (234) \rangle$ will leave the integral finite and chiral, but spoil the equality of its leading singularities. Indeed, as it is also finite and dual-conformally invariant, the ‘mixed’ hexagon integral can also be

⁹In the literature on ratio functions, some authors have found what were claimed to be “finite” combinations of boxes that did *not* end up being dual-conformal invariant. In every case, the combinations of boxes in question were not honestly IR-finite: the divergences from different regions of the integration contour canceling between each-other. Such a cancellation is highly regulator-dependent, and is not very meaningful.

evaluated without any regularization, and one finds that,



$$= \int_{(AB)} \frac{\langle AB (612) \cap (234) \rangle \langle AB 46 \rangle}{\langle AB 12 \rangle \langle AB 23 \rangle \langle AB 34 \rangle \langle AB 45 \rangle \langle AB 56 \rangle \langle AB 61 \rangle}$$

$$= \left(\frac{\langle 1234 \rangle}{\langle 1345 \rangle \langle 1235 \rangle} \right) \log(u_1) \log(u_2) + \left(\frac{\langle 6134 \rangle}{\langle 1345 \rangle \langle 5613 \rangle} \right) \log(u_3) \log(u_1)$$

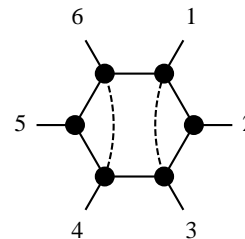
$$+ \left(\frac{\langle 6123 \rangle}{\langle 1235 \rangle \langle 3561 \rangle} \right) \log(u_2) \log(u_3).$$

In order for GRTs to yield the two-term identities necessary to guarantee that all the leading singularities are equal up-to a sign, the numerator must force vanishing residues for all but two Schubert problems. In the case of the ‘mixed-numerator’ hexagon integral, for example, GRTs can only be used to show that the coefficients of the logarithms sum to zero:

$$\left(\frac{\langle 1234 \rangle}{\langle 1345 \rangle \langle 1235 \rangle} \right) + \left(\frac{\langle 6134 \rangle}{\langle 1345 \rangle \langle 5613 \rangle} \right) + \left(\frac{\langle 6123 \rangle}{\langle 1235 \rangle \langle 3561 \rangle} \right) = 0. \quad (5.4.64)$$

It is clear that these chiral momentum-twistor integrals with unit leading singularities give us the simplest and most transparent way of talking about finite integrals.

Just as a trivial example, the 6-point NMHV ratio function, which is typically written in terms of all 15 six-point box-integrals, with many R -invariants as coefficients, is given simply by



$$\mathcal{R}_{\text{NMHV}}^{1\text{-loop}} \underset{\substack{\text{post-} \\ \text{integration}}}{=} (1 + g + g^2) \left\{ \begin{array}{l} \text{Diagram} \\ \times ([23456] - [34561] + [45612]) \end{array} \right\}, \quad (5.4.65)$$

where $g : i \mapsto i+1$ acts on both the integrand and its coefficient. Also recall the definition of the R -invariants given in section 1,

$$[abcde] = \frac{\delta^{0|4}(\eta_a \langle bcde \rangle + \eta_b \langle cdea \rangle + \eta_c \langle deab \rangle + \eta_d \langle eabc \rangle + \eta_e \langle abc d \rangle)}{\langle abcd \rangle \langle bcde \rangle \langle cdea \rangle \langle deab \rangle \langle eabc \rangle}. \quad (5.4.66)$$

5.5 1-Loop Integrands, Integrals, and Amplitudes

As described in section I., one can use elementary tensor-reduction to express any 1-loop integrand in $\mathcal{N} = 4$ in terms of pentagon and box integrands. These of course would form a complete basis for any 1-loop integrand in $\mathcal{N} = 4$ SYM. However, such a basis would necessarily include many integrands which are *non-chiral* (including all boxes), and which have *non-uniform* leading singularities; moreover, such a basis would allow for linear combinations of IR-divergent integrals to be ultimately IR-finite and non-vanishing. But we saw in the last section that there are integrands—pentagons and hexagons with ‘magic’ numerators—which avoid all of these shortcomings, and these integrands closely mirror the leading singularities of MHV-amplitudes, suggesting that they may be well-suited to express amplitudes more generally.

It is therefore natural to wonder if there exists a complete basis of 1-loop integrands involving only chiral, manifestly dual-conformally invariant integrands with unit leading-singularities, and for which no non-vanishing linear-combination of IR-divergent integrands is IR-finite. We’ll see momentarily that the answer is affirmative, and extremely beautiful.

Before trying to construct such a basis, however, we can gain some intuition about what to expect by assessing its size—that is, finding the dimension of the space of planar, 1-loop integrands. Recall that every n -point 1-loop planar integral can be written in the form

$$\int_{(AB)} \frac{\langle AB Y_1 \rangle \cdots \langle AB Y_{n-4} \rangle}{\langle AB 1 2 \rangle \langle AB 2 3 \rangle \langle AB 3 4 \rangle \cdots \langle AB n-1 n \rangle \langle AB n 1 \rangle}. \quad (5.5.67)$$

When $n = 5$, the space of 1-loop integrands is just the space of bitwistors Y , which is six-dimensional—which explains how the complete 5-point 1-loop integrand could be constructed in [97] through the introduction of a single pentagon integrand.

For $n = 6$, the most general integrand is a hexagon with $\langle AB Y_1 \rangle \langle AB Y_2 \rangle$ in the numerator. Now, each Y_i is a **6**-dimensional representation of SU_4 , and of course $\mathbf{6} \otimes \mathbf{6} = \mathbf{1} \oplus \mathbf{15} \oplus \mathbf{20}$. Ordinary multiplication being commutative, the antisymmetric part, the **15**-component, clearly vanishes. By expanding each Y_i into a basis of six simple bitwistors, it is easy to see that the trace component, **1**, also vanishes, as $\langle Y_i Y_i \rangle = 0$, when Y_i is

simple. Therefore, the space of 6-point 1-loop integrands is **20-dimensional**¹⁰.

More generally, it is not hard to see that the dimension, d , of 1-loop integrands is the same as the dimension of the space of symmetric $(n - 4)$ -fold symmetric, traceless tensors of $\mathbf{6}$'s of SU_4 , which is simply

$$d = \binom{n}{4} + \binom{n-1}{4} \quad (5.5.68)$$

Recall that box-integrands form a complete basis of parity-even integrands, and that there are precisely $\binom{n}{4}$ boxes, all of which are independent. Therefore, we may separate d in equation (5.5.68), according to $d = d_{\text{even}} + d_{\text{odd}}$ with $d_{\text{even}} = \binom{n}{4}$ and $d_{\text{odd}} = \binom{n-1}{4}$. Once we have a basis of integrands which makes parity manifest, this will allow us to count the number of relations satisfied by (parity-odd) integrands.

I. The Chiral Octagon: A Basis of 1-Loop Integrands

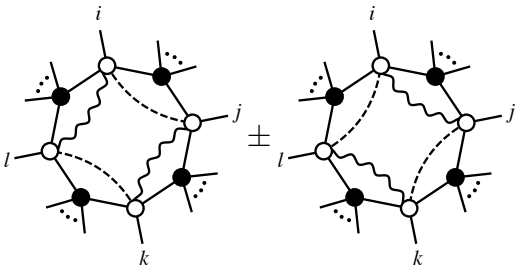
As we can see from equation (5.5.68), the number of independent integrands grows asymptotically like $\mathcal{O}(n^4)$. In contrast, the number of chiral pentagons grows only like $\mathcal{O}(n^2)$. It is not hard to see that the simplest class of chiral integrands which number $\mathcal{O}(n^4)$ are the chiral octagons. As we will see presently, it turns out that chiral octagon-integrands indeed form an (over)-complete basis for all 1-loop integrands that satisfies all the desired criteria listed above. The most general chiral octagon integral is given by,

$$I_8(i, j, k, l) \equiv \text{Diagram} \quad \text{for } i < j < k < l < i \quad (5.5.69)$$

$$= \int_{(AB)} \frac{\langle AB i j \rangle \langle AB(j-1 j j+1) \cap (k-1 k k+1) \rangle \langle AB k l \rangle \langle AB(l-1 l l+1) \cap (i-1 i i+1) \rangle}{\langle AB i-1 i \rangle \langle AB i i+1 \rangle \langle AB j-1 j \rangle \langle AB j j+1 \rangle \langle AB k-1 k \rangle \langle AB k k+1 \rangle \langle AB l-1 l \rangle \langle AB l l+1 \rangle}.$$

Notice that parity acts according to $\mathbb{P} : I_8(i, j, k, l) \mapsto I_8(j, k, l, i)$, making it trivial to define parity-even/parity-odd sectors:

¹⁰We thank Simon Caron-Huot for helpful discussions regarding this counting.

$$I_8^{\text{even/odd}}(i, j, k, l) \equiv I_8(i, j, k, l) \pm I_8(j, k, l, i) =$$


Notice that these octagon integrands are well-defined for any distinct set of indices $\{i, j, k, l\}$, including those for which the ‘octagon’ degenerates into lower-polygons. For example, when $l = k + 1$, the extra (duplicated) propagator in equation (5.5.69), $\langle AB k k+1 \rangle$ is cancelled by the dashed-line term $\langle AB k l \rangle \rightarrow \langle AB k k+1 \rangle$ in the numerator. A complete sampling of degenerate ‘octagons’ is illustrated in Figure 5.3. One important advantage of this presentation is that all but the most degenerate of the octagons are *manifestly* finite. Indeed, only the pentagons—octagons of the form $I_8(i, i+1, i+2, i+3, i+4)$ —and the lower hexagons in Figure 5.3—octagons of the form $I_8(i, i+1, i+2, j)$ —are IR-divergent. Specifically, we have the following separation into manifestly IR-finite and IR-divergent basis integrands.

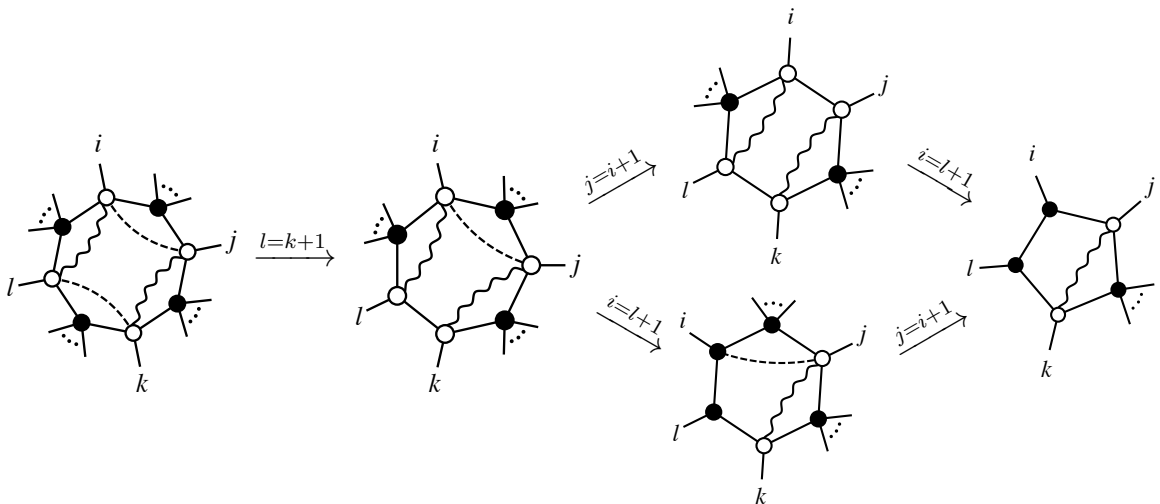
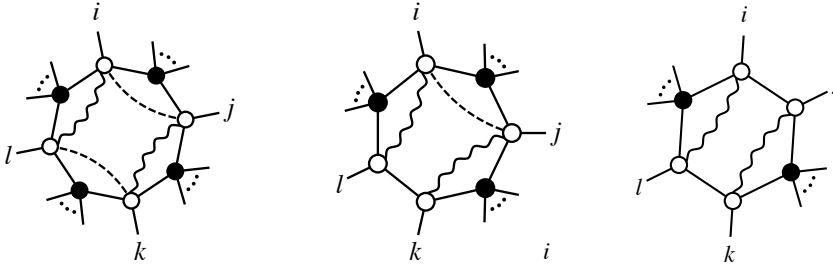
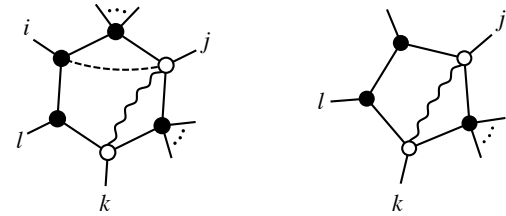


Figure 5.3: The possible degenerations of the general octagon integrand.

IR-finite: 

IR-divergent: 

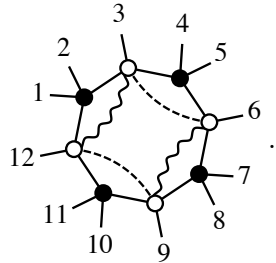
(5.5.70)

It is worth emphasizing that the only IR-finite combinations of IR-divergent integrals in this basis are parity-odd, which automatically vanish upon integration. Furthermore, as discussed above, because the criterion for local divergences in the region of integration is itself parity-invariant,¹¹ parity-odd combinations of integrands are in fact manifestly *locally finite*.

Parity-symmetrizing, and parity anti-symmetrizing, it is clear that there $\binom{n}{4}$ octagon integrands, evenly split between parity-odd and parity-even. As we described above, among the parity-odd combinations of integrands only $\binom{n-1}{4}$ are linearly-independent, so the octagon basis is strictly *over-complete*, but there are only non-trivial relations among integrands in the parity-odd sector.

II. Integration of Manifestly-Finite Octagons

It is not hard to directly evaluate the general octagon integral $I_8(i, j, k, l)$. Consider for example the case $I_8(3, 6, 9, 12)$ for which all indices are separated by at least 3,



(5.5.71)

Because of the numerator factors, the only non-vanishing leading singularities of this integral involve cutting at most one of each the pairs of lines $\{(23), (34)\}$, $\{(56), (67)\}$,

¹¹Recall that a local, IR-divergence develops in the region of integration when the line (AB) passes through a point Z_i while simultaneously lying on the plane $(Z_{i-1} Z_i Z_{i+1})$.

$\{(89), (9\ 10)\}$, and $\{(11\ 12), (12\ 1)\}$. Therefore, this integral's box-expansion is simply the (manifestly-finite) sum of 16 four-mass box integrals. One disadvantage with this presentation of the integral, however, is that the four-mass box integral logarithmically-diverges when any of its four massive corners becomes massless, and yet we saw above that the general octagon remains manifestly finite upon many such degenerations.

Because of this, we are motivated to replace the four-mass box function with a new function that is free of any divergences over the physical domain of cross ratios. Letting $\Delta_4(u, v)$ denote the familiar four-mass box integral¹²—a symmetric function in the two cross-ratios—then let us define the following ‘modified four-mass’ function

$$\tilde{\Delta}_4(i, j, k, l) \equiv \gamma \Delta_4(u_{i,j,k,l}, u_{j,k,l,i}) - \frac{1}{2} \log(u_{i,j,k,l}) \log(u_{j,k,l,i}), \quad (5.5.72)$$

where

$$\Delta_4(u, v) \equiv \text{Li}_2(1 - \alpha_+) - \text{Li}_2(1 - \alpha_-) + \frac{1}{2} \log(v) \log(\alpha_+/\alpha_-), \quad (5.5.73)$$

and

$$\gamma \equiv \frac{\sqrt{(1-u-v)^2 - 4uv}}{1-u-v}, \quad \text{and} \quad \alpha_{\pm} \equiv \frac{2u}{1+u-v \pm \sqrt{(1-u-v)^2 - 4uv}}; \quad (5.5.74)$$

here, we have used the four indices $\{i, j, k, l\}$ to signify the (generally time-like separated) spacetime points corresponding to the lines $(i\ i+1)$, $(j\ j+1)$, $(k\ k+1)$, and $(l\ l+1)$ in twistor space, which together define the cross-ratios

$$u_{i,j,k,l} \equiv \frac{\langle i\ i+1\ j\ j+1 \rangle \langle k\ k+1\ l\ l+1 \rangle}{\langle l\ l+1\ j\ j+1 \rangle \langle k\ k+1\ i\ i+1 \rangle} \quad \text{and} \quad u_{j,k,l,i} \equiv \frac{\langle j\ j+1\ k\ k+1 \rangle \langle l\ l+1\ i\ i+1 \rangle}{\langle i\ i+1\ k\ k+1 \rangle \langle l\ l+1\ j\ j+1 \rangle}. \quad (5.5.75)$$

The principle distinction between $\tilde{\Delta}_4(i, j, k, l)$ and the more familiar four-mass box function is that $\tilde{\Delta}_4(i, j, k, l)$ remains finite even when many of the spacetime points become null-separated (or even become identified). In particular,

$$\lim_{u_{i,j,k,l} \rightarrow 0} \left(\tilde{\Delta}_4(i, j, k, l) \right) = \text{Li}_2(1 - u_{j,k,l,i}) \quad \text{and} \quad \lim_{u_{j,k,l,i} \rightarrow 0} \left(\tilde{\Delta}_4(i, j, k, l) \right) = \text{Li}_2(1 - u_{i,j,k,l}). \quad (5.5.76)$$

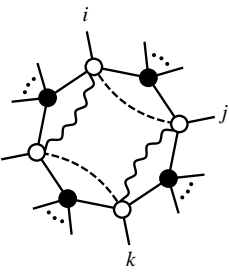
Of course, if we use $\tilde{\Delta}_4$'s to represent $I_8(3, 6, 9, 12)$, for example, then each four-mass box will contribute a ‘log-log’-term. It may be worried that this will greatly clutter the

¹²If we denote the massive, incoming four-momenta of the box by K_1, K_2, K_3 , and K_4 , and define the canonical Mandelstam variables $s \equiv (K_1 + K_2)^2$ and $t \equiv (K_2 + K_3)^2$, then we are using u and v to denote the cross ratios $K_1^2 K_3^2 / (st)$, and $K_2^2 K_4^2 / (st)$, respectively.

final expression, but this turns out to not be the case: taken together, these 16 additional ‘log-log’ terms combine into a single such term.

With this new function, the general octagon integral—together with all its degenerations—becomes extremely simple. Explicitly, the general octagon $I_8(i, j, k, l)$ integral is given

by,

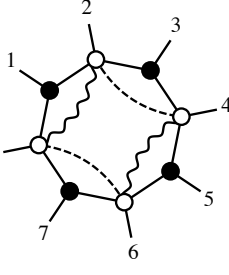


$$= \begin{cases} \log(u_{ik-1ki-1}) \log(u_{jl-1lj-1}) \\ +\tilde{\Delta}_4(i, j, k, l) & -\tilde{\Delta}_4(i, j, k, l-1) & -\tilde{\Delta}_4(i, j, k-1, l) & +\tilde{\Delta}_4(i, j, k-1, l-1) \\ -\tilde{\Delta}_4(i, j-1, k, l) & +\tilde{\Delta}_4(i, j-1, k, l-1) & +\tilde{\Delta}_4(i, j-1, k-1, l) & -\tilde{\Delta}_4(i, j-1, k-1, l-1) \\ -\tilde{\Delta}_4(i-1, j, k, l) & +\tilde{\Delta}_4(i-1, j, k, l-1) & +\tilde{\Delta}_4(i-1, j, k-1, l) & -\tilde{\Delta}_4(i-1, j, k-1, l-1) \\ +\tilde{\Delta}_4(i-1, j-1, k, l) & -\tilde{\Delta}_4(i-1, j-1, k, l-1) & -\tilde{\Delta}_4(i-1, j-1, k-1, l) & +\tilde{\Delta}_4(i-1, j-1, k-1, l-1) \end{cases}$$

Although admittedly lengthy, this expression can be considerably compressed in a way which helps illustrate the relative signs appearing in the formula above,

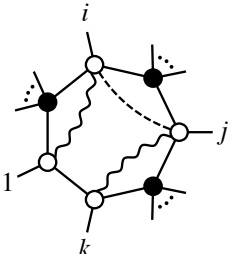
$$I_8(i, j, k, l) = \log(u_{ik-1ki-1}) \log(u_{jl-1lj-1}) + \sum_{\sigma_i \in \{1,0\}} (-1)^{(\sigma_1 + \sigma_2 + \sigma_3 + \sigma_4)} \tilde{\Delta}_4(i - \sigma_1, j - \sigma_2, k - \sigma_3, l - \sigma_4). \quad (5.5.77)$$

We can see how the modified four-mass function $\tilde{\Delta}_4(i, j, k, l)$ helps to make all of the octagon’s degenerations manifest by looking at a few examples explicitly. For example, consider the 8-point octagon $I_8(2, 4, 6, 8)$; in this case, only 20 of the 34 cross ratios which play a role in the general answer are non-vanishing, converting virtually all the generalized four-mass functions $\tilde{\Delta}_4$ ’s into Li_2 ’s.



$$= \begin{cases} \log(u_{2,5,6,1}) \log(u_{4,7,8,3}) \\ + \tilde{\Delta}_4(2, 4, 6, 8) - \text{Li}_2(1 - u_{4,6,7,2}) - \text{Li}_2(1 - u_{2,4,5,8}) + \text{Li}_2(1 - u_{2,4,5,7}) \\ - \text{Li}_2(1 - u_{8,2,3,6}) + \text{Li}_2(1 - u_{3,6,7,2}) + \text{Li}_2(1 - u_{8,2,3,5}) - \text{Li}_2(1 - u_{7,2,3,5}) \\ - \text{Li}_2(1 - u_{6,8,1,4}) + \text{Li}_2(1 - u_{4,6,7,1}) + \text{Li}_2(1 - u_{1,4,5,8}) - \text{Li}_2(1 - u_{1,4,5,7}) \\ + \text{Li}_2(1 - u_{6,8,1,3}) - \text{Li}_2(1 - u_{3,6,7,1}) - \text{Li}_2(1 - u_{5,8,1,3}) + \tilde{\Delta}_4(1, 3, 5, 7) \end{cases}$$

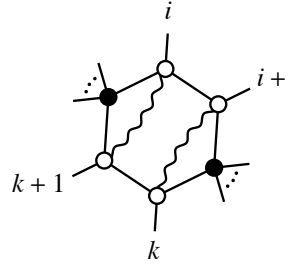
Even more simplification occurs for the degenerate ‘octagons.’ Consider for example the general finite heptagon integral, given by $I_8(i, j, k, k+1)$,



$$= \begin{cases} \log(u_{i,k-1,k,i-1}) \log(u_{j,k,k+1,j-1}) \\ + \text{Li}_2(1 - u_{j,k,k+1,i}) & -0 & -\tilde{\Delta}_4(i, j, k-1, k+1) & + \text{Li}_2(1 - u_{j,k-1,k,i}) \\ - \text{Li}_2(1 - u_{j-1,k,k+1,i}) & +0 & +\tilde{\Delta}_4(i, j-1, k-1, k+1) & - \text{Li}_2(1 - u_{j-1,k-1,k,i}) \\ - \text{Li}_2(1 - u_{j,k,k+1,i-1}) & +0 & +\tilde{\Delta}_4(i-1, j, k-1, k+1) & - \text{Li}_2(1 - u_{j,k-1,k,i-1}) \\ + \text{Li}_2(1 - u_{j-1,k,k+1,i-1}) & -0 & -\tilde{\Delta}_4(i-1, j-1, k-1, k+1) & + \text{Li}_2(1 - u_{j-1,k-1,k,i-1}) \end{cases}$$

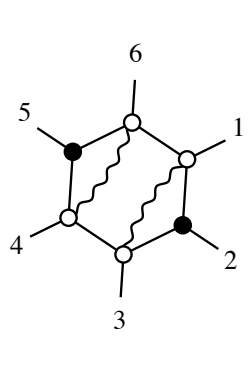
Here, because $\tilde{\Delta}_4(i, j, k, k) = \text{Li}_2(0) = 0$, four of the contributions vanish, and eight of the modified four-mass box functions simplify to simple Li_2 's.

The final class of finite, degenerate octagons are the hexagon integrals—octagons of the form $I_8(i, i + 1, k, k + 1)$,



$$= \begin{cases} \log(u_{i,k-1,k,i-1}) \log(u_{i+1,k,k+1,i}) \\ +\text{Li}_2(1 - u_{i+1,k,k+1,i}) & -0 & -\text{Li}_2(1 - u_{k+1,i,i+1,k-1}) & +\text{Li}_2(1 - u_{i+1,k-1,k,i}) \\ -0 & +0 & +0 & -0 \\ -\text{Li}_2(1 - u_{i+1,k,k+1,i-1}) & +0 & +\tilde{\Delta}_4(i-1, i+1, k-1, k+1) & -\text{Li}_2(1 - u_{i+1,k-1,k,i-1}) \\ +\text{Li}_2(1 - u_{i,k,k+1,i-1}) & -0 & -\text{Li}_2(1 - u_{k+1,i-1,i,k-1}) & +\text{Li}_2(1 - u_{i,k-1,k,i-1}) \end{cases}$$

Just as for the case of the 8-point octagon integral, the general hexagon integral simplifies considerably when potentially-massive corners become massless. As a final illustration, let us see how the general formula for the octagon given above directly yields the result quoted in section 5.4 for the 6-point hexagon integral which played such an important role in the 6-point NMHV ratio function:



$$= \begin{cases} \log(u_{3,5,6,2}) \log(u_{4,6,1,3}) \\ +\text{Li}_2(1 - u_{4,6,1,3}) & -0 & -\text{Li}_2(1) & +\text{Li}_2(1) \\ -0 & +0 & +0 & -0 \\ -\text{Li}_2(1) & +0 & +\text{Li}_2(1 - u_{2,4,5,1}) & -\text{Li}_2(1) \\ +\text{Li}_2(1) & -0 & -\text{Li}_2(1) & +\text{Li}_2(1 - u_{3,5,6,2}) \end{cases}$$

$$= \text{Li}_2(1 - u_{4,6,1,3}) + \text{Li}_2(1 - u_{2,4,5,1}) + \text{Li}_2(1 - u_{3,5,6,2}) + \log(u_{3,5,6,2}) \log(u_{4,6,1,3}) - 2\text{Li}_2(1).$$

III. Application: the NMHV 1-Loop Ratio Function

As should be clear from the previous subsection, any IR-finite object such as the ratio function will be *manifestly finite* when expanded in the basis of octagon integrands. Moreover, since the formula for the completely general octagon integral, equation (5.5.77), is free of discontinuities for all the IR-finite degenerations of the octagon, any finite 1-loop integrand expressed in the basis of octagons directly translates into a function that is manifestly dual-conformally invariant.

A very important, manifestly finite function associated with 1-loop scattering ampli-

tudes is the ratio function,

$$\mathcal{R}_{n,k}^{1\text{-loop}} = \mathcal{A}_{n,k}^{1\text{-loop}} - \mathcal{A}_{n,k}^{\text{tree}} \cdot \mathcal{A}_{n,k=2}^{1\text{-loop}}. \quad (5.5.78)$$

The most trivial example must be the 5-point 1-loop NMHV ratio function. Expanding into the basis of octagons, the integrand is easily seen to be given by

$$\mathcal{R}_{5,3,1} = [1, 2, 3, 4, 5] \left(\begin{array}{c} \text{Diagram 1} \\ \text{Diagram 2} \end{array} \right) + \text{cyclic}. \quad (5.5.79)$$

Being a parity-odd combination of pentagons, the ratio function is locally free of any divergences at the level of the integrand and is therefore manifestly finite—of course, being parity odd, it also vanishes upon integration.

A less trivial example, and one which we quoted in section 5.4, is the 6-point NMHV 1-loop ratio function. In section 5.4 only the parity-even contribution to the ratio function was described; the full integrand is given by,

$$\begin{aligned} \mathcal{R}_{6,3,1} = & \begin{array}{c} \text{Diagram 1} \\ \text{Diagram 2} \end{array} + \left(\begin{array}{c} \text{Diagram 3} \\ \text{Diagram 4} \end{array} \right) \\ & \times \frac{1}{2}([1, 2, 3, 4, 5] + [1, 2, 3, 5, 6] + [1, 2, 3, 6, 4]) \quad \times \frac{1}{6}[1, 2, 3, 4, 6] \\ & + \left(\begin{array}{c} \text{Diagram 5} \\ \text{Diagram 6} \end{array} \right) + \left(\begin{array}{c} \text{Diagram 7} \\ \text{Diagram 8} \end{array} \right) \\ & \times \frac{1}{6}([1, 2, 3, 4, 5] - [1, 3, 4, 5, 6]) \quad \times \frac{1}{6}([1, 2, 4, 5, 6] + [1, 3, 4, 5, 6]) \\ & + \text{cyclic}. \quad (5.5.80) \end{aligned}$$

Of course, only the first term in equation (5.5.80) is non-vanishing when integrated along a parity-invariant contour, reproducing the formula given in equation (5.4.65).

The general formula for the n -point NMHV 1-loop ratio function integrand nicely separates into a part which is parity-odd, and another which involves only manifestly

finite integrands. In order to best capture the ratio function succinctly, let us introduce one small bit of notation and define

$$[i, \{i+1, \dots, j\}, \{k, \dots, l\}] \equiv \sum_{J=\{i+1, i+2\}}^{\{j-1, j\}} \sum_{K=\{k, k+1\}}^{\{l, k\}} [i, J, K]; \quad (5.5.81)$$

for example,

$$\begin{aligned} [1, \{2, 3, 4\}, \{5, 6, 7\}] = & [1, 2, 3, 5, 6] + [1, 2, 3, 6, 7] + [1, 2, 3, 7, 5] \\ & + [1, 3, 4, 5, 6] + [1, 3, 4, 6, 7] + [1, 3, 4, 7, 5]. \end{aligned} \quad (5.5.82)$$

Notice that the two-index J ranges over all consecutive pairs between $i+1$ and j inclusively, while the two-index K *also* includes a non-consecutively-ordered ‘wrapping’ term. With this notation, it is very easy to write the n -point NMHV ratio function integrand:

$$\begin{aligned} \mathcal{R}_{n,3}^{1\text{-loop}} = & \frac{1}{2} \sum_{i < j < k < l < i} [i, \{i+1, \dots, j\}, \{k, \dots, l\}] I_8(i, j, k, l) \\ & - \frac{1}{n} \sum_{i < j < k < l < m < i} [i, j, k, l, m] I_8^{\text{odd}}(i, j, k, l). \end{aligned} \quad (5.5.83)$$

Notice that while the first term in equation (5.5.83) appears to include divergent ‘octagons’, only the finite octagons have non-vanishing coefficients. For five-particles, for example, the coefficient of the octagon $I_8(1, 3, 4, 5)$ from equation (5.5.83) would be $[1, \{2, 3\}, \{4, 5\}] = [1, 2, 3, 4, 5] + [1, 2, 3, 5, 4] = 0$.

Combining formula (5.5.83) with the analytic form of the general octagon integral given in equation (5.5.77) immediately yields a concise, analytic, manifestly dual-conformally invariant, and manifestly-cyclic form of the 1-loop ratio function for any n .

Let us close this section by given another explicit example. The 7-point NMHV 1-loop ratio function is straightforwardly found to be,

$$\mathcal{R}_{7,3}^{1\text{-loop}} = [1, \{2, 3\}, \{4, 5, 6\}] I_8(1, 3, 4, 6) + [1, \{2, 3\}, \{4, 5, 6, 7\}] I_8(1, 3, 4, 7) + \text{cyclic}, \quad (5.5.84)$$

where

$$\begin{aligned} I_8(1, 3, 4, 6) \equiv & \left\{ \begin{aligned} & \text{Li}_2(1 - u_{1,3,4,6}) + \text{Li}_2(1 - u_{2,4,5,1}) + \text{Li}_2(1 - u_{4,6,7,2}) + \text{Li}_2(1 - u_{7,2,3,5}) \\ & - \text{Li}_2(1 - u_{2,4,5,7}) - \text{Li}_2(1 - u_{3,6,7,2}) - \text{Li}_2(1 - u_{4,6,7,3}) - \text{Li}_2(1 - u_{6,1,2,4}) \\ & + \log(u_{1,3,4,7}) \log(u_{3,5,6,2}) \end{aligned} \right\}; \\ I_8(1, 3, 4, 7) \equiv & \left\{ \begin{aligned} & \log(u_{1,3,4,7}) \log(u_{3,6,7,2}) - \text{Li}_2(1) - \text{Li}_2(1 - u_{1,3,4,6}) - \text{Li}_2(1 - u_{4,6,7,2}) \\ & + \text{Li}_2(1 - u_{1,3,4,7}) + \text{Li}_2(1 - u_{3,6,7,2}) + \text{Li}_2(1 - u_{4,6,7,3}) + \text{Li}_2(1 - u_{6,1,2,4}) \end{aligned} \right\}. \end{aligned}$$

(Here, we have not neglected an overall factor of $\frac{1}{2}$: like in the case of the 6-point ratio function—the summand in equation (5.5.83) includes exactly two copies of each term; but this is not generally the case for higher- n).

5.6 Multiloop Amplitudes

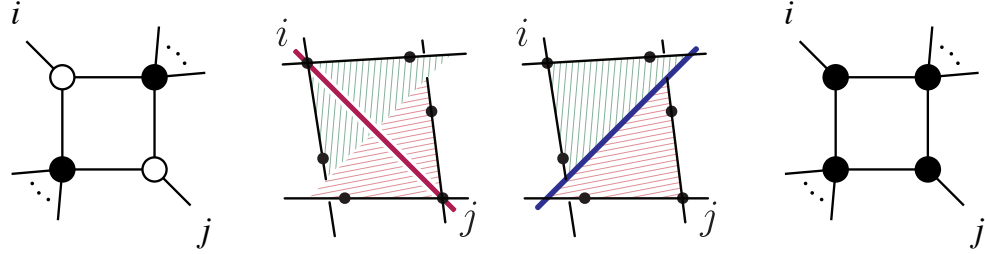
In this section, we introduce a new strategy for finding local representations of loop integrands. The idea is closely related to the leading singularity method, but the philosophy differs in some important ways. In particular we will *not* be guided by systematically trying to match all the leading singularities of the integrand. Instead, we will look at a simple subset of leading singularities defined for generic, large enough number of particles—no “composite” leading singularities will be considered. We will then find a natural set of pure integrals designed to match this subset of leading singularities. We will find that boldly summing over all such objects miraculously suffices to match the full integrand! In particular, while the pure integrals are motivated for a large-enough generic number of external particles, their degenerations nicely produce all the needed lower-point objects as well.

This method is heuristic—we do not yet have a deep understanding for why the miracles happen. However we have used this strategy successfully to find stunningly simple expressions for the integrands of all 2- and 3-loop MHV amplitudes as well as all 2-loop NMHV amplitudes, and have checked that the results are correct by comparing with the form obtained from the all-loop BCFW recursion.

We will begin by illustrating this strategy by going back to 1-loop integrands, which will motivate structures for 1-loop integrands different from the ones we encountered in section 3. For the MHV integrand, this new form coincides with one of “polytope representations” discussed in Chapter 6. We will then use this discussion as a springboard to our treatment of 2- and 3-loop integrands.

I. A New Form for the MHV 1-Loop Integrand

Let’s begin by going back to the MHV 1-loop integrand, and motivate a new form for it inspired by straightforwardly matching its leading singularities, associated with the familiar two-mass-easy colored diagrams



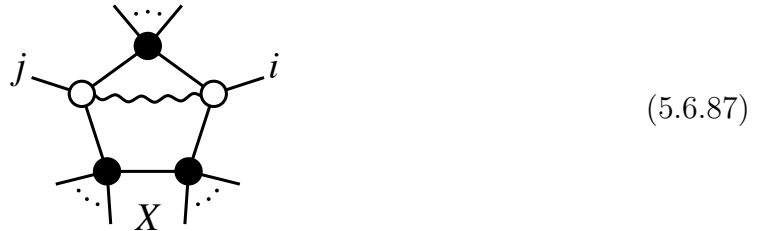
corresponding to cutting the propagators

$$\langle AB\ i-1\ i\rangle\langle AB\ i\ i+1\rangle\langle AB\ j-1\ j\rangle\langle AB\ j\ j+1\rangle \quad (5.6.85)$$

The amplitude has unit leading singularity for the first solution of the Schubert problem $(AB) = (ij)$, and vanishing leading singularity for the second solution where $(AB) = (i-1\ i\ i+1) \cap (j-1\ j\ j+1)$. We would like to build the integrand out of objects that have exactly this property. To beat a dead horse yet again—it is obvious that the two-mass-easy box does not do this job because it is not chiral. The easiest way to do this is to simply insert a factor in the numerator, $\langle AB\ (i-1\ i\ i+1) \cap (j-1\ j\ j+1)\rangle$, that kills the “wrong” leading singularity. For correct little-group weights, we add a factor $\langle AB\ X\rangle$ in the denominator, where X is an arbitrary bitwistor, and look at an object of the form

$$I_{i,j} = \frac{\langle AB\ (i-1\ i\ i+1) \cap (j-1\ j\ j+1)\rangle\langle X\ i\ j\rangle}{\langle AB\ i-1\ i\rangle\langle AB\ i\ i+1\rangle\langle AB\ j-1\ j\rangle\langle AB\ j\ j+1\rangle\langle AB\ X\rangle} \quad (5.6.86)$$

which is just the pentagon already familiar from section 2, where the local propagator $\langle AB\ n\ 1\rangle$ has been replaced by $\langle AB\ X\rangle$. We denote this graphically as



Note that there is in general no significance to the presence of the legs adjacent to X in this picture. We draw it in this way because in the special case where $X = (k\ k+1)$, the legs adjacent to X are identified with $k, k+1$.

Now consider the Schubert problems associated with cutting four physical propagators. By construction this object has vanishing leading singularities on the “wrong” solution, and can easily be seen to have unit leading singularity on the “right” one. Summing over all the indices $i < j$ —with $|i - j| \geq 2$ corresponding to the two-mass easy

colored graphs—produces an object matching all the physical leading singularities of the amplitude. Naïvely this should give us the integrand, but there is a catch: each term also has “spurious cuts” where $\langle AB X \rangle$ is one on the cut propogators. Indeed, the sum we just described does not match the integrand.

However some wonderful magic happens: the sum over *all* indices $i < j$, including a “boundary term” with $j = i+1$, which is not included in the sum over colored graphs, *does* reproduce the amplitude! We have

$$A_{\text{MHV}}^{1\text{-loop}} = \sum_{i < j} \frac{\langle AB (i-1 i i+1) \cap (j-1 j j+1) \rangle \langle X i j \rangle}{\langle AB X \rangle \langle AB i-1 i \rangle \langle AB i i+1 \rangle \langle AB j-1 j \rangle \langle AB j j+1 \rangle} \quad (5.6.88)$$

or written pictorially

$$A_{\text{MHV}}^{1\text{-loop}} = \sum_{i < j < i} \left\{ \begin{array}{c} \text{Diagram of a pentagon with vertices } j, i, X, \text{ and two unlabeled vertices.} \\ \text{The diagram is enclosed in large curly braces.} \end{array} \right\} . \quad (5.6.89)$$

This form is manifestly cyclic but has spurious $\langle AB X \rangle$ poles term-by-term. The sum is however independent of X . If we choose X to correspond to one of the external point $X = (k k+1)$, all the poles are manifestly physical but the formula is not manifestly cyclic invariant.

As mentioned above, this expression follows from a simple “polytope” interpretation described in Chapter 6. The local formula given in Chapter [15] is obtained by choosing $X = k k+1$, summing over all k and dividing by $1/n$. The similar expression in [116] corresponds to setting $X = I_\infty$ where I_∞ is infinity twistor.

Let us look at the “boundary term” where $j = i + 1$ in more detail—using $\langle i-1 i i+1 i+2 \rangle \langle AB i i+1 \rangle = \langle AB (i-1 i i+1) \cap (i i+1 i+2) \rangle$, we can see that it is just a (spurious) box

$$\frac{\langle i-1 i i+1 i+2 \rangle \langle X i i+1 \rangle}{\langle AB X \rangle \langle AB i-1 i \rangle \langle AB i i+1 \rangle \langle AB i+1 i+2 \rangle} \quad (5.6.90)$$

It is instructive to explicitly understand the purpose of this boundary term in this simple example, since the same phenomenon will occur in all the rest of our examples in this section. Let us return to our most naïve ansatz, summing only over the pentagons associated with the colored graphs. Each of the spurious cuts involving $\langle AB X \rangle$, such as

$$\langle AB X \rangle \langle AB i-1 i \rangle \langle AB i i+1 \rangle \langle AB j-1 j \rangle \quad (5.6.91)$$

is shared by two pentagons e.g. $I_{i,j-1}$ and $I_{i,j}$. For generic terms in the sum, these cuts cancel against each other in pairs. However, in the limiting cases when $j = i+2$ (or $j = i-2$) the quad-cut is shared by $I_{i,i+2}$ and $I_{i-1,i+1}$ but there is no cancellation between them because the non-vanishing leading singularities occur for two different solutions of the Schubert problems. The spurious box of (5.6.90) precisely has non-vanishing leading singularities for these two Schubert problems and completes the cancellation of all $\langle ABX \rangle$ poles, ensuring the full sum is independent of X . It is quite remarkable that the “new” object needed to fix the leading singularities and match the amplitude is simply a degeneration of the pentagon itself.

In our remaining examples, we will not delve into understanding the details of how all leading singularities match. We will instead take a class of leading singularities as a guide for the local integrals to consider, and sum over all the relevant objects, including boundary terms that do not directly correspond to any of the leading singularity pictures that motivated the construction of the objects to begin with. These formulae are then verified by comparing with the integrand as computed by BCFW recursion.

Let us finally note a very pretty property of equation (5.6.88): for generic X , all the pentagons in the double sum are manifestly manifestly IR finite. This ceases to be true if we make the special choice like $X = (12)$, since the diagrams with $i = 2$ or $j = n$ have an additional massless corner which is not controlled by the numerator.

$$\begin{array}{ccc}
 \begin{array}{c} 4 \quad i-1 \\ \vdots \\ 3 \quad \circ \quad i \\ \vdots \\ 2 \quad \bullet \quad \bullet \quad i+1 \\ \vdots \\ X \end{array} & \longrightarrow & \begin{array}{c} 4 \quad i-1 \\ \vdots \\ 3 \quad \circ \quad i \\ \vdots \\ 2 \quad \bullet \quad \bullet \quad i+1 \\ \vdots \\ 1 \end{array} \\
 & & X = (12)
 \end{array} \tag{5.6.92}$$

II. The 1-Loop NMHV Integrand, Revisited

We proceed to use the same strategy to determine a local expression for the NMHV 1-loop integrand, which will yield a quite different form than we obtained in section 3. We again start with the colored graphs for leading singularities. There are two of them for NMHV amplitudes:

$$(5.6.93)$$

Unlike the MHV case where the non-vanishing leading singularities were “1”, here the non-vanishing leading singularities are the R -invariants. The goal is to find objects with non-vanishing support on the same Schubert problems as the amplitude, and decorate these with the appropriate R -invariants to get a nice ansatz for the integrand.

The first colored graph correspond to 2-mass easy Schubert problems and have the same structure as the MHV case. The leading singularity is just the tree-level amplitude appearing in the upper-left corner of the figure, $\mathcal{A}_{\text{NMHV}}^{\text{tree}}(j, j+1, \dots, i-1, i)$. Thus we expect to have objects in the integrand of the form

$$\sum_{i < j < i} \left\{ \left(\text{Diagram with nodes } j, i, X \text{ and cut propagator } X \right) \times \mathcal{A}_{\text{NMHV}}^{\text{tree}}(j, j+1, \dots, i-1, i) \right\} \quad (5.6.94)$$

Finding an object matching the physical leading singularities of the second class of colored diagrams is a more interesting exercise. The cut propogators are

$$\langle AB \ i-1 \ i \rangle \langle AB \ i \ i+1 \rangle \langle AB \ j \ j+1 \rangle \langle AB \ k \ k+1 \rangle \quad (5.6.95)$$

The leading singularities vanish for the solution $(AB) = (i-1 \ i \ i+1) \cap (j \ j+1)(i-1 \ i \ i+1) \cap (k \ k+1)$, while for $(AB) = (i \ j \ j+1) \cap (i \ k \ k+1)$ the leading singularity is $[i, j, j+1, k, k+1]$.

Let us consider objects of the form

$$I_{i,j,k} \equiv \left(\text{Diagram with nodes } i, j, k \text{ and cut propagator } X \right) = \int_{(AB)} \frac{N(i, j, k)}{\langle AB \ X \rangle \langle AB \ i-1 \ i \rangle \langle AB \ i \ i+1 \rangle \langle AB \ j \ j+1 \rangle \langle AB \ k \ k+1 \rangle}$$

We are searching for a numerator supported on the same leading singularities as the amplitude. In addition it should also have unit leading singularity on all other spurious quad-cuts. The reason is that the spurious cuts must cancel in a sum over terms; since the integrals are multiplied by different R -invariants, the only way this can happen is

through residue theorem 6-term identities between the R -invariants. For instance the spurious quad-cut

$$\langle AB X \rangle \langle AB i i+1 \rangle \langle AB j j+1 \rangle \langle AB k k+1 \rangle \quad (5.6.96)$$

is shared by six different integrals $I_{i;j,k}$, $I_{i+1;j,k}$, $I_{j;i,k}$, $I_{j+1;i,k}$, $I_{k;i,j}$ and $I_{k+1;i,j}$ that are multiplied by six different residues. There is a 6-term identity relating them

$$\begin{aligned} & [i, j, j+1, k, k+1] + [i+1, j, j+1, k, k+1] + [j, i, i+1, k, k+1] \\ & + [j+1, i, i+1, k, k+1] + [k, i, i+1, j, j+1] + [k+1, i, i+1, j, j+1] = 0 \end{aligned}$$

which can only possibly be of help in canceling spurious cuts if the integrands they multiply have support on the same Schubert problems, with unit leading singularities.

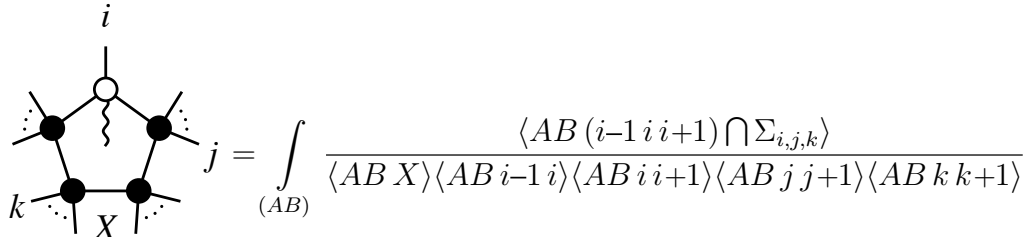
There is one final guiding principle for determining the structure of the numerator $N(i, j, k)$. The topologies occurring in (5.6.94) are the same as for the MHV amplitude, while the second class of integrals is “purely” NMHV-like. Since IR-divergences are universal, it would be nice if the IR-divergences could be completely isolated in the MHV-like topology. We should then try to choose the numerator $N(i, j, k)$ to be strictly finite. It would be nice if these integrals could be chosen to be manifestly finite. The only divergence in (5.6.96) can come from the Z_i -corner, *i.e.* the region when (AB) crosses point Z_i and lies in the plane $(i-1 i i+1)$. In order to control this region the numerator should be of the form $N = \langle AB (i-1 i i+1) \cap (\dots) \rangle$. Combined with the unit leading singularity constraint, the form of the numerator is fixed completely:

$$N(i, j, k) \equiv \langle AB (i-1 i i+1) \cap \Sigma_{i,j,k} \rangle \quad (5.6.97)$$

with $\Sigma_{i,j,k}$ a special plane defined according to

$$\Sigma_{i,j,k} \equiv \frac{1}{2} [(j j+1 (i k k+1) \cap X) - (k k+1 (i j j+1) \cap X)] \quad (5.6.98)$$

This is in fact the only choice we could have made consistent with little group weights and the desire to treat the j, k indices symmetrically. We will denote this by,



$$\int_{(AB)} \frac{\langle AB (i-1 i i+1) \cap \Sigma_{i,j,k} \rangle}{\langle AB X \rangle \langle AB i-1 i \rangle \langle AB i i+1 \rangle \langle AB j j+1 \rangle \langle AB k k+1 \rangle}$$

With these objects in hand, we once again brazenly sum over all ranges of indices, including “boundary” terms with $j = i \pm 1$ not directly associated with colored graphs for leading singularities. The same magic happens as we saw in the MHV case—this sum agrees with the 1-loop NMHV amplitude as computed by BCFW recursion, and we find,

$$\mathcal{A}_{\text{NMHV}}^{1\text{-loop}} = \sum_{i < j < k < i} \left\{ \begin{array}{c} \text{Diagram 1} \\ j \times [i, j, j+1, k, k+1] \end{array} \right\} + \sum_{i < j < i} \left\{ \begin{array}{c} \text{Diagram 2} \\ \times \mathcal{A}_{\text{NMHV}}^{\text{tree}}(j, j+1, \dots, i-1, i) \end{array} \right\}. \quad (5.6.99)$$

Note also that as in the MHV case, the only IR-divergent integrals are in the boundary terms. The (generically) finite integrals for $I_{i,j,k}$ are given by

$$I_{i,j,k} = -\text{Li}_2(1 - u_1) - \text{Li}_2(1 - u_2) + \text{Li}_2(1 - u_3) + \log(u_4) \log(u_5)$$

where the cross ratios are defined as:

$$u_1 \equiv \frac{\langle i i+1 j j+1 \rangle \langle X i-1 i \rangle}{\langle i i+1 X \rangle \langle j j+1 i-1 i \rangle}, \quad u_2 \equiv \frac{\langle i i+1 X \rangle \langle k k+1 i-1 i \rangle}{\langle i i+1 k k+1 \rangle \langle X i-1 i \rangle}, \quad u_3 \equiv \frac{\langle i i+1 j j+1 \rangle \langle k k+1 i-1 i \rangle}{\langle i i+1 k k+1 \rangle \langle j j+1 i-1 i \rangle},$$

$$u_4 \equiv \frac{\langle X k k+1 \rangle \langle i-1 i j j+1 \rangle}{\langle X i-1 i \rangle \langle k k+1 j j+1 \rangle}, \quad u_5 \equiv \frac{\langle j j+1 X \rangle \langle k k+1 i i+1 \rangle}{\langle j j+1 k k+1 \rangle \langle X i i+1 \rangle},$$

Finally, let us examine the 1-loop NMHV ratio function

$$\mathcal{R}_{\text{NMHV}}^{1\text{-loop}} = \mathcal{A}_{\text{NMHV}}^{1\text{-loop}} - \mathcal{A}_{\text{MHV}}^{1\text{-loop}} \cdot \mathcal{A}_{\text{NMHV}}^{\text{tree}} \quad (5.6.100)$$

Comparing the expressions 5.6.88 and 5.6.99 we can see that the ratio function has the same form as NMHV amplitude, except that in the first sum we have $\mathcal{A}_{\text{NMHV}}^{\text{tree}}(i, i+1, \dots, j-1, j) - \mathcal{A}_{\text{NMHV}}^{\text{tree}}$ instead of just $\mathcal{A}_{\text{NMHV}}^{\text{tree}}(i, i+1, \dots, j-1, j)$. The manifest finiteness is obvious. The only divergent integrals are in the boundary term $j = i - 1$, but their coefficient is given by $\mathcal{A}_{\text{NMHV}}^{\text{tree}}(i, i+1, \dots, j-1, j) - \mathcal{A}_{\text{NMHV}}^{\text{tree}}(1, \dots, n) = \mathcal{A}_{\text{NMHV}}^{\text{tree}}(i, i+1, \dots, i-2, i-1) - \mathcal{A}_{\text{NMHV}}^{\text{tree}}(1, \dots, n) = 0$. Therefore, the ratio function can be written only using manifestly finite integrals.

$\langle ABCD \rangle$. That allows us to write two numerator factors exactly as we need. Therefore, we consider,

$$= \left\{ \frac{\langle AB(i-1\ i\ i+1) \cap (j-1\ j\ j+1) \rangle \langle i\ j\ k\ l \rangle}{\langle AB\ i-1 \rangle \langle AB\ i\ i+1 \rangle \langle AB\ j-1\ j \rangle \langle AB\ j\ j+1 \rangle \langle ABCD \rangle} \right. \\ \left. \times \frac{\langle CD(k-1\ k\ k+1) \cap (l-1\ l\ l+1) \rangle}{\langle CD\ k-1\ k \rangle \langle CD\ k\ k+1 \rangle \langle CD\ l-1\ l \rangle \langle CD\ l\ l+1 \rangle} \right\}$$

Of course, this integral has also many other cuts—both composite and non-composite—that involve the propagator $\langle ABCD \rangle$, and we have to match other colored graphs in (5.6.101) as well. However, just as in our 1-loop examples, simply summing over all indices with a planar ordering reproduces the full amplitude as a cyclic sum over just one integral topology:

$$\mathcal{A}_{\text{MHV}}^{2\text{-loop}} = \frac{1}{2} \sum_{i < j < k < l < i} \text{Diagram} \quad (5.6.102)$$

The “boundary terms” in this case occur for for $j = i+1$ and/or $l = k+1$. In these cases the numerator exactly cancels one of the propagators, leaving us with:¹³

$$(5.6.103)$$

Log of the Amplitude

Finally, we give an interesting new expression for the logarithm of the amplitude, using a non-planar sum of the same set of objects. At 2-loops, the log of the amplitude is

$$[\log \mathcal{A}]_{\text{MHV}}^{2\text{-loop}} = \left[\mathcal{A}_{\text{MHV}}^{2\text{-loop}} - \frac{1}{2} \left(\mathcal{A}_{\text{MHV}}^{1\text{-loop}} \right)^2 \right] \quad (5.6.104)$$

¹³This simplification was missed in Chapter [15], and the 2-loop MHV integrand was presented as a sum over three terms. We would like to thank Johannes Henn for pointing the simplification out to us.

A beautiful expression for the log of the amplitude is made possible by the existence of a simple relation between the sum of 1-loop square and 2-loop diagrams:

$$\sum_{i < j} \text{Diagram 1} \times \sum_{k < l} \text{Diagram 2} = \sum_{i < j, k < l} \text{Diagram 3} \quad (5.6.105)$$

The left-hand side is just $(\mathcal{A}_{\text{MHV}}^{1\text{-loop}})^2$ while the right-hand side contains not only the planar diagrams present in $\mathcal{A}_{\text{MHV}}^{2\text{-loop}}$ but also non-planar graphs when for example $i < k < j < l$. In fact, all planar graphs are equal to $2\mathcal{A}_{\text{MHV}}^{2\text{-loop}}$ while all non-planar graphs give us the log of the amplitude in the form

$$[\log \mathcal{A}]_{\text{MHV}}^{2\text{-loop}} = - \sum_{i < k < j < l < i} \text{Diagram 3} \quad (5.6.106)$$

The formula found in [127] is the 4pt version of this expression.

Note that naïvely, all these integrals are IR finite because each individual 1-loop sub-integral is just a finite pentagon(which can not shrink to a box due to the restriction $j \neq i + 1$ and $l \neq k + 1$). However, the criteria for finiteness we described in section 4 applies to planar integrals, while the log contains non-planar terms which can be IR-divergent.

Let us focus on the piece of the integrand of the form

$$\frac{\langle ABX \rangle}{\langle AB i-1i \rangle \langle AB i i+1 \rangle} \cdot \frac{1}{\langle ABCD \rangle} \cdot \frac{\langle CDY \rangle}{\langle CD j-1j \rangle \langle CD j j+1 \rangle} \quad (5.6.107)$$

Here X controls the IR-divergence of the region where the line (AB) intersects point Z_i and lies in the plane $(Z_{i-1}Z_iZ_{i+1})$, just as Y does for (CD) sector. However, if $i = j$ then (AB) and (CD) intersect in the point i and the propagator $\langle ABCD \rangle$ vanishes. Therefore, finiteness of the 1-loop sub-integrals is not enough. We need an extra condition that regulates this joint divergence. It is not hard to see that unless $\langle XY \rangle = 0$, a (mild) IR-divergence remains.

As a result, we can find that almost all integrals in (5.6.106) are finite except for the class of diagrams:

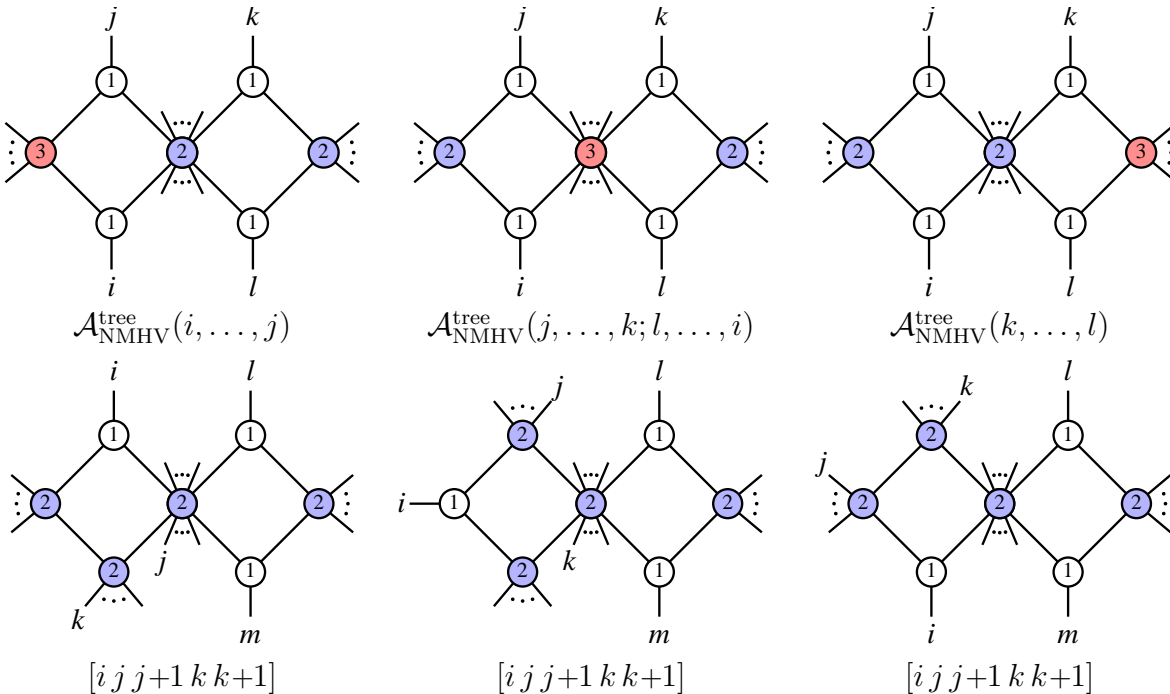
(5.6.108)

In this case $X = (i-2 i-1 i) \cap (i i+1 i+2)$ and $Y = (i-1 i i+1) \cap (j-1 j j+1)$, so $\langle XY \rangle \neq 0$. However the divergence is mild, as observed in the 4-point result of [127].

IV. All 2-Loop NMHV Amplitudes

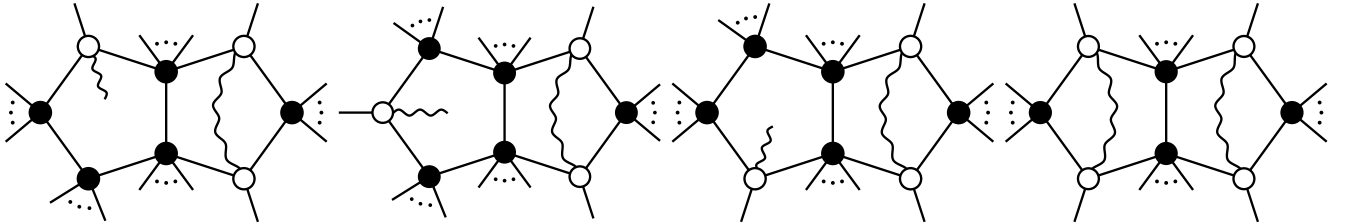
We move on to present the integrand for all 2-loop NMHV amplitudes. The 6- and 7- point integrands were presented in Chapter 4, by expanding the BCFW result into a basis of pure integrals. The parity-even part of the 6- point integrand was presented using standard (dual) space-time variables in [96]. Here, instead of a brute-force expansion into a basis of integrals, we follow the same strategy outlined above, obtaining results vastly simpler than those presented to date, which also generalize to all n . Now

Let us first start by drawing the colored-graphs that contribute for general 2-loop NMHV amplitude that do not cut the internal propagator $\langle(ABCD)\rangle$.



Below each colored graph, we have indicated the leading singularity below each. Notice that the coefficient $\mathcal{A}_{\text{NMHV}}^{\text{tree}}(j, \dots, k; l, \dots, i)$ is the *same* function as an ordinary tree amplitude with particles labelled $(j, \dots, k; l, \dots, i)$ where k, l and i, j are both treated as if they were adjacently-labelled.

The idea is again to find a set of integrals that each individually have the same leading singularities as the amplitude on a given set of octa-cuts. The first step is to realize that the octa-cuts on the first line of 5.6.109 respectively looks like the product of NMHV 1-loop quad-cut \times MHV 1-loop quad-cut and MHV 1-loop quad-cuts \times MHV 1-loop quad-cuts. Therefore, one might think that the right integrals to start with look like the product of pentagons that appear in MHV and NMHV 1-loop amplitudes. This strategy worked perfectly in the MHV 2-loop case, where the amplitude was literary made from double-pentagons whose origin was in the product of two MHV-like pentagons. So the natural objects to consider here are the same double-pentagons as in MHV 2-loop case and also other double-pentagons that look like NMHV 1-loop \times MHV 1-loop:



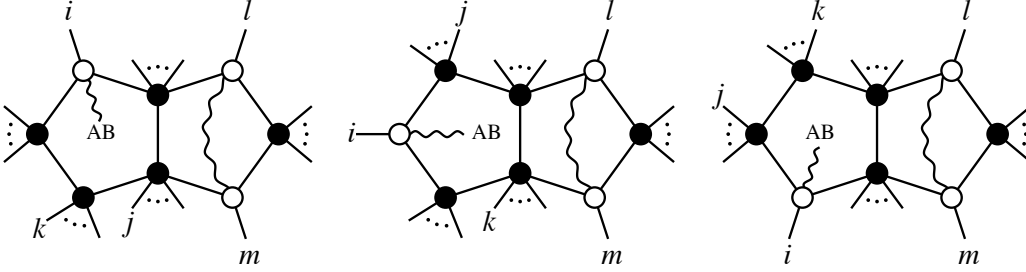
The numerators of the first three graphs have the same structure as the ones that appear in the NMHV 1-loop integrand. We provide the complete expressions in appendix F.

Note that first three diagrams are really represented just by single diagram with permuted indices. For instance, the second one can be obtained from the first one if we require $k > i$. So, it is non-planar version of the first graph in the same sense as we saw in the last subsection in the case of the log of MHV amplitude. We see that these four graphs are in one-to-one correspondence with the first four colored graphs in 5.6.109. If we cut all propagators except $\langle ABCD \rangle$ we get not only the same cuts as are in these colored graphs, but also the support on the correct Schubert problems. These integrals are definitely the right ones to start with. In order to get the correct field theory answer we have to multiply them by the leading singularities of corresponding octa-cuts which are

Now summing over all allowed indices we get,

$$\begin{aligned}
& \sum_{\substack{\text{all allowed} \\ i,j,k,l,m}} \text{Diagram 1} + \frac{1}{2} \sum_{i < j < k < l < i} \text{Diagram 2} \quad (5.6.109) \\
& \times [i, j, j+1, k, k+1] \times \left\{ \begin{aligned} & \mathcal{A}_{\text{NMHV}}^{\text{tree}}(j, \dots, k; l, \dots, i) \\ & + \mathcal{A}_{\text{NMHV}}^{\text{tree}}(i, \dots, j) \\ & + \mathcal{A}_{\text{NMHV}}^{\text{tree}}(k, \dots, l) \end{aligned} \right\}
\end{aligned}$$

where the first diagram really represents three as we mentioned earlier, namely, the complete set of cyclically ordered figures



The rest of the story proceeds in the by now familiar way. Simply carrying out the sum over the range of indices corresponding to the colored graphs does not give the right answer, however, a judicious choice for the range of summation adds the correct “boundary terms” to give exactly the right answer, and we finally obtain:

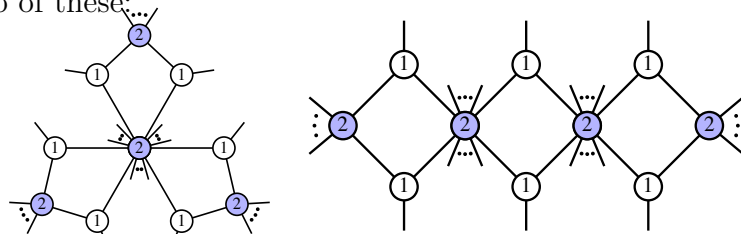
$$\begin{aligned}
\mathcal{A}_{\text{NMHV}}^{2\text{-loop}} = & \sum_{\substack{i < j < l < m \leq k < i \\ i < j < k < l < m \leq i \\ i \leq l < m \leq j < k < i}} \text{Diagram 1} + \frac{1}{2} \sum_{i < j < k < l < i} \text{Diagram 2} \\
& \times [i, j, j+1, k, k+1] \times \left\{ \begin{aligned} & \mathcal{A}_{\text{NMHV}}^{\text{tree}}(j, \dots, k; l, \dots, i) \\ & + \mathcal{A}_{\text{NMHV}}^{\text{tree}}(i, \dots, j) \\ & + \mathcal{A}_{\text{NMHV}}^{\text{tree}}(k, \dots, l) \end{aligned} \right\} \quad (5.6.110)
\end{aligned}$$

These two terms represent the general 2-loop NMHV amplitude for any number of external particles. The explicit forms of the integrals in term of momentum-twistors are presented in appendix F.

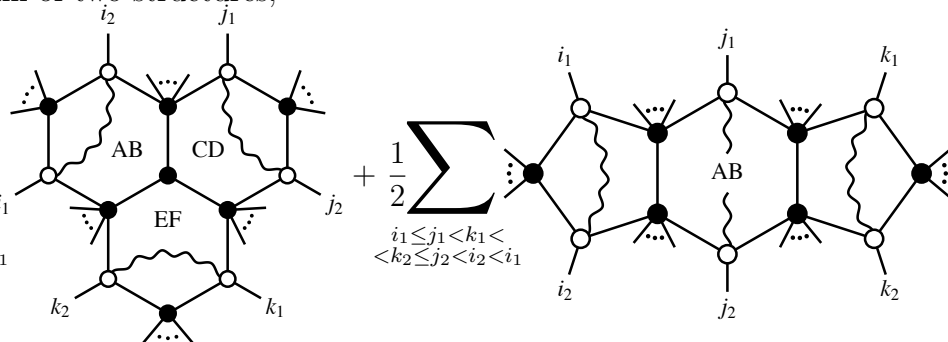
V. All 3-Loop MHV Amplitudes

Finally, we present the integrand for all 3-loop MHV amplitudes. These amplitudes were studied in the past, the 4pt formula for the integrand was given in [101] and the 5pt in [99]. The 4pt and 5pt amplitudes were also determined using BCFW recursion and translated into pure momentum-twistor integrals in Chapter 4. However once again our new strategy will both yield vastly simpler expressions for these integrands and also generalize to all n .

We begin as always by drawing the colored graphs that contribute to general 3-loop amplitude. While there are a large number of them, our experience with the 2-loop NMHV calculation tells us that for the purpose of “translating” the graphs into the integrals, one needs to focus on the colored graphs without internal propagators. There are just two of these:


(5.6.111)

The colored graphs suggest that the correct 3-loop integral must correspond to “gluing” together three 1-loop MHV integrals. But these can not be just pentagons because of number of internal propagators, we would also need hexagons. Fortunately, in the “polytope picture” of Chapter 6, the most natural form of MHV amplitude *is* written using hexagons. We leave the detailed exploration of this gluing procedure to future work. It suffices to say that we can indeed find objects which have support on the correct leading dodecacuts (5.6.111). Having identified them, the magic happens again: to get the full 3-loop amplitude, we need only to identify the correct ranges for the summations involved. As a result, we can write the general 3-loop MHV amplitude for any number of external particles as a sum of two structures,

$$\mathcal{A}_{\text{MHV}}^{3\text{-loop}} = \frac{1}{3} \sum_{\substack{i_1 \leq i_2 < j_1 \leq \\ \leq j_2 < k_1 \leq k_2 < i_1}} \text{[Graph 1]} + \frac{1}{2} \sum_{\substack{i_1 \leq j_1 < k_1 < \\ < k_2 \leq j_2 < i_2 < i_1}} \text{[Graph 2]}$$


The explicit formulas for these graphs with all numerator factors are given in the appendix [G](#).

Chapter 6 *Scattering Amplitudes and the Geometry of Polytopes*

6.1 Towards a Geometry of Scattering Amplitudes

Recent months have seen significant advances in our understanding of perturbative scattering amplitudes in gauge theories, especially for $\mathcal{N} = 4$ SYM in the planar limit. A generalization of the BCFW recursion relations [7, 31] to all loops has been given to determine the planar integrand described in Chapter 4 of the theory, naturally formulated in momentum-twistor space [20], making the Yangian symmetry [49] manifest, and extending the Grassmannian duality for leading singularities [10] to the full theory. The integrand has also been beautifully interpreted [116, 117] as a supersymmetric generalization of the null-polygonal Wilson-Loop [40], making dual-superconformal invariance [8, 9, 40, 47] manifest and providing a general proof [116, 132] of the Wilson-Loop/Amplitude duality [40].

Despite these advances, our understanding of the integrand still leaves something to be desired. The definition in terms of either scattering amplitudes or the Wilson-Loop only manifests half of the superconformal symmetries of the theory, obscuring the infinite-dimensional Yangian symmetry; it also invokes gauge redundancies that are made necessary by any local Lagrangian description. The BCFW representation of the amplitude is more compact, and gives a complete definition of the theory making no direct reference to space-time notions. However it is not manifestly cyclically invariant: there are many different BCFW forms, depending on the choice of legs for BCFW deformation. All of this suggests that the various formulations for scattering amplitudes that have been uncovered so far are different representations of a single underlying object, which awaits a deeper, more intrinsic and invariant characterization.

In this brief Chapter we take some preliminary steps towards uncovering this underlying structure. We will study the simplest non-trivial amplitudes in the theory—the

tree-level NMHV amplitudes, and the integrand for the 1-loop MHV amplitudes. Following and generalizing the observations of [20], we will interpret these amplitudes as the volumes of polytopes in certain extensions of momentum-twistor space. To actually evaluate the volume, we need to triangulate the polytope into elementary simplicies, and one natural choice of triangulation leads directly to BCFW (and CSW) representations of these amplitudes. However we also find even simpler triangulations of the polytopes that yield completely new expressions for these familiar old friends.

The BCFW representation of the NMHV tree amplitude, written in momentum-twistor space, is

$$M_n^{\text{NMHV}} = \frac{1}{2} \sum_{i,j} [1\ i\ i+1\ j\ j+1] \quad (6.1.1)$$

where

$$[abcde] = \frac{\delta^4(\eta_a \langle bcde \rangle + \dots + \eta_e \langle abc d \rangle)}{\langle bcde \rangle \langle cdea \rangle \langle deab \rangle \langle eabc \rangle \langle abcd \rangle} \quad (6.1.2)$$

is the basic “ R -invariant” [8] written in momentum-twistor space [19]. Similarly, the 1-loop integrand for MHV amplitudes is [15]

$$M_{1\text{-loop},n}^{\text{MHV}} = \frac{1}{2} \sum_{i,j} [1\ i\ i+1; 1\ j\ j+1] \quad (6.1.3)$$

where we have introduced objects $[abc; xyz]$ via

$$[abc; xyz] = \frac{(\langle Aabc \rangle \langle Bxyz \rangle - \langle Axyz \rangle \langle Babc \rangle)^2}{\langle ABab \rangle \langle ABbc \rangle \langle ABca \rangle \langle ABxy \rangle \langle AByz \rangle \langle ABzx \rangle}. \quad (6.1.4)$$

Note the presence, in both of these formulas, of the special point “1”. The CSW representation [51, 132] of the same amplitude is obtained by replacing “1” in this formula with a general momentum twistor, $Z_1 \rightarrow Z_*$.

The BCFW/CSW expressions for the amplitudes are not manifestly cyclically invariant/independent of the auxiliary twistor Z_* , nor are they manifestly free of spurious poles. All these properties only emerge after the summation is performed. There is a nice algebraic way of seeing this. The basic objects appearing in the formulas satisfy identities that allow us to express them in different ways. In general, such identities follow from Grassmannian residue theorems [10]. We can also understand them in the following simple way. Take any Yangian invariant object $Y_{n,k}(Z_1, \dots, Z_n)$, which is a residue of the

Grassmannian integral. Consider its BCFW deformation under $Z_n \rightarrow Z_n + zZ_{n-1}$. It is easy to show that the residues of all the poles in the complex z plane are *also* Grassmannian residues, and are therefore Yangian invariant. Thus, an application of Cauchy’s theorem on the BCFW deformed function of z yields a relation between Yangian invariants.

Starting with the basic NMHV R -invariant $[abcde]$, we can slightly generalize this procedure and consider a general deformation $Z_a \rightarrow Z_a + zZ_f$. Then, Cauchy’s theorem yields the familiar 6-term identity

$$[abcde] + [bcdef] + [cdefa] + [defab] + [efabc] + [fabcd] = 0. \quad (6.1.5)$$

We can also apply this to the basic objects $[abc; xyz]$. It is interesting to note here that that while the $[1\ i\ i+1; 1\ j\ j+1]$ are indeed Yangian invariant, the general $[abc; xyz]$ are not. Nonetheless under the deforming $Z_a \rightarrow Z_a + zZ_d$, or $Z_x \rightarrow Z_x + zZ_w$, Cauchy’s theorem yields 4-term identities

$$\begin{aligned} [abc; xyz] + [bcd; xyz] + [cda; xyz] + [dab; xyz] &= 0, \\ [abc; xyz] + [abc; yzw] + [abc; zwx] + [abc; wxy] &= 0. \end{aligned} \quad (6.1.6)$$

Suppose we are given some linear combination of the $[abcde]$ ’s. Given these identities, we can have two different linear combinations representing the same function. How then can we determine if two expressions are equal? More formally, how can we characterize the equivalence class of linear combinations of R -invariants, which differ by these identities?

The key is to note that the R -invariant identity can formally be written using a “boundary” operation. Imagine what is (for now) a completely formal object, a “5-simplex” $[abcdef]$, which is completely antisymmetric in its indices. Then, the linear combination of R -invariants entering the 6-term identity is just the “boundary” of this simplex, and the identity becomes

$$\partial [abcdef] = 0. \quad (6.1.7)$$

Now suppose that α and β are two linear combinations of R -invariants. We wish to determine if $\alpha = \beta$ up to 6-term identities; that is we want to determine whether there exists some simplex σ such that

$$\alpha = \beta + \partial\sigma. \quad (6.1.8)$$

Since $\partial^2 = 0$, it suffices to check that

$$\partial\alpha = \partial\beta. \tag{6.1.9}$$

Thus we have learned that while any given representation of an amplitude in terms of a sum of R -invariants is not unique, the “boundary” of the amplitude *is* invariant. Using the standard definition of the boundary operation on simplicies, the “boundary” of one of the R -invariants is

$$\partial[abcde] = [abcd] + [bcde] + [cdea] + [deab] + [eabc]. \tag{6.1.10}$$

Note that the boundary is also a list of the poles occurring in the definition of the R -invariant—this is not an accident, as will become clear in the polytope picture of the next sections.

We can now easily compute the boundary of the BCFW/CSW forms of the NMHV tree amplitude:

$$\partial \sum_{i,j} [*i\ i+1\ j\ j+1] = \sum_{i,j} [i\ i+1\ j\ j+1] \tag{6.1.11}$$

which is a beautifully cyclic object, independent of the point Z_* , in one-to-one correspondence with the democratic sum over all the physical poles of the NMHV amplitude! This is enough to prove that the BCFW/CSW forms of the NMHV amplitude define a cyclic object free of spurious poles. It is possible to prove something stronger: the *only* combination of R -invariants that is free of spurious poles is the NMHV tree amplitude! This is because if the amplitude is free of spurious poles, its boundary must only contain “physical” 3-simplicies of the form $[i\ i+1\ j\ j+1]$. Since this is supposed to be a boundary, *its* boundary must vanish. It is easy to see that the only combination of physical 3-simplicies that its boundary is free is $\sum_{i,j} [i\ i+1\ j\ j+1]$.

We can do exactly the same exercise for the MHV 1-loop amplitude. The 4-term identities can be interpreted as

$$[\partial(abcd), xyx] = 0, \quad [abc, \partial(xyzw)] = 0. \tag{6.1.12}$$

This makes it natural to define a boundary operation on $[\sigma_1; \sigma_2]$ as acting separately on the two simplicies σ_1, σ_2 ,

$$\partial[\sigma_1; \sigma_2] = [\partial\sigma_1; \partial\sigma_2]. \tag{6.1.13}$$

The boundary of the individual terms in eqn. (6.1.3) are again in one-to-one correspondence with their poles. The boundary of the BCFW/CSW form of the 1-loop amplitude is

$$\partial \sum_{i,j} [*i i+1; *j j+1] = \sum_{i,j} [i i+1; j j+1]. \quad (6.1.14)$$

Again this is a beautifully cyclic object, independent of the point Z_* , in one-to-one correspondence with all the physical poles of the integrand. We can in fact give a slightly more general expression for the MHV integrand using *two* reference twistors $Z_*, Z_{*'}$, which has the same boundary, as

$$M_{1\text{-loop},n}^{\text{MHV}} = \frac{1}{2} \sum_{i,j} [*i i+1; *'j j+1]. \quad (6.1.15)$$

There are of course many other representations of these amplitudes; again, only the “boundary” is invariant.

We have gone through this discussion in some detail because these sorts of algebraic arguments—reflecting Grassmannian residue theorems—generalize readily to more complicated amplitudes [35]. In the rest of this chapter, however, we will pursue a different line of thought. Taking our cue from [20], we will see that the appearance of “simplicies” and “boundaries” is not an accident, but has a deeper geometric origin. As we have mentioned already, the amplitudes will be interpreted as the volumes of certain polytopes. Certain triangulations of these polytopes give a very pretty and direct geometric interpretation of the BCFW/CSW representations of the amplitudes. But the picture does more than simply re-organize algebraic manipulations in geometric terms: a different triangulation of the polytopes leads to entirely new representations of the amplitudes, which are both strikingly simple and manifestly cyclic and *local*.

We will begin our discussions with an extremely simple warm-up exercise familiar from elementary plane geometry. We then move on to discussing the MHV 1-loop and NMHV tree amplitudes.

6.2 Warm-Up: The Area of Polygons in \mathbb{CP}^2

Consider a simple set of functions

$$[abc] = \frac{1}{2} \frac{\langle abc \rangle^2}{\langle Aab \rangle \langle Abc \rangle \langle Aca \rangle}. \quad (6.2.16)$$

Here $Z_{a,b,c}$ and Z_A are in \mathbb{C}^3 . Since $[abc]$ has weight zero under rescaling a, b, c we can also think of $Z_{a,b,c}$ as points in \mathbb{CP}^2 , corresponding to twistors for our “external particles”, while Z_A is a reference twistor.

Clearly the $[abc]$'s are analogous to (a particular Grassmann component of) the R -invariants $[abcde]$ we are familiar with, and are also very closely related to the $[abc; xyz]$ objects appearing in the 1-loop MHV amplitude. Let us define an analog of the “amplitude”, A_n , via a “BCFW/CSW” formula of the form

$$A_n = \sum_i [* i i+1]. \tag{6.2.17}$$

This expression is manifestly cyclic invariant but term-by-term has “unphysical poles” (where “physical poles” are only of the form $\langle A j j+1 \rangle$). However, we can easily see that the sum is in fact cyclic and only has physical poles. Following our earlier discussion, we can derive identities satisfied by $[abc]$ by deforming $Z_a \rightarrow Z_a + zZ_d$, to find a 4-term identity

$$[abc] + [bcd] + [cda] + [dab] = 0. \tag{6.2.18}$$

We can think of this formally as

$$\partial[abcd] = 0. \tag{6.2.19}$$

Following our earlier logic, we can define the “boundary” of $[abc]$ itself as

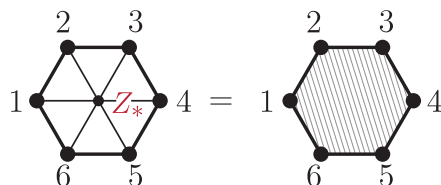
$$\partial[abc] = [ab] + [bc] + [ca] \tag{6.2.20}$$

which is in one-to-one correspondence with the poles in $[abc]$. Finally, we can compute the “boundary” of the “amplitude” to find

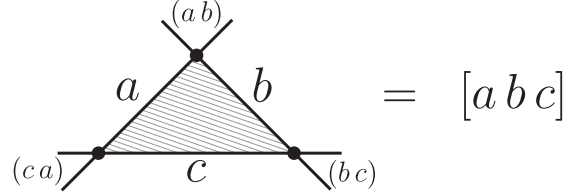
$$\partial A_n = \sum_i [i i+1] \tag{6.2.21}$$

which is just the democratic sum over all “physical” boundaries.

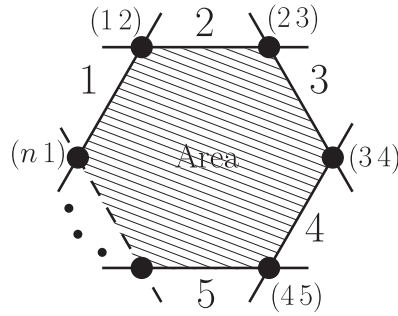
These observations make it natural to associate $[abc]$ with a triangle in \mathbb{CP}^2 whose vertices are Z_a, Z_b, Z_c , and the amplitude itself with the interior of the polygon L_n with vertices Z_i and edges (Z_i, Z_{i+1}) , as in the figure below for the case of six particles:



Now the $[abc]$ certainly have the same additive structure as the simplicies defined by the triangles (abc) . We should therefore be able to give a formula for $[abc]$ as a function of the triangle (abc) , in a way that preserves this additive structure. This is very easy to do. The function $[abc]$ is the *area* of the *geometric dual* triangle to $[abc]$ in \mathbb{CP}^2 , whose *edges* are the dual lines to Z_a, Z_b, Z_c :



The amplitude is then simply the area of the geometric dual \tilde{L}_n of the polygon L_n :



Let us see how this works explicitly by doing some very elementary plane geometry. Let the twistors $Z_{a,b,c,\dots}^I$ and the reference twistor Z_A^I have an upstairs SL_3 index. We are interested in the dual space whose co-ordinates W_I have a lower SL_3 index. Now, suppose we are given three points W_1^I, W_2^I, W_3^I . As is standard in projective geometry, the point Z_A^I breaks SL_3 but leaves an SL_2 invariant, and defines a projection direction. Putting

$$Z_A^I = \begin{pmatrix} 0 \\ 0 \\ 1 \end{pmatrix}, \quad W_I = \begin{pmatrix} x \\ y \\ 1 \end{pmatrix} \quad (6.2.22)$$

we can think of the points (x, y) as lying in a two-dimensional plane, on which the unbroken SL_2 acts. The area of the triangle associated with W^1, W^2, W^3 is the SL_2 invariant given by

$$\text{Area}(W^1, W^2, W^3) = \frac{1}{2} \begin{vmatrix} x^1 & x^2 & x^3 \\ y^1 & y^2 & y^3 \\ 1 & 1 & 1 \end{vmatrix} \quad (6.2.23)$$

which we can write in a projectively invariant way as

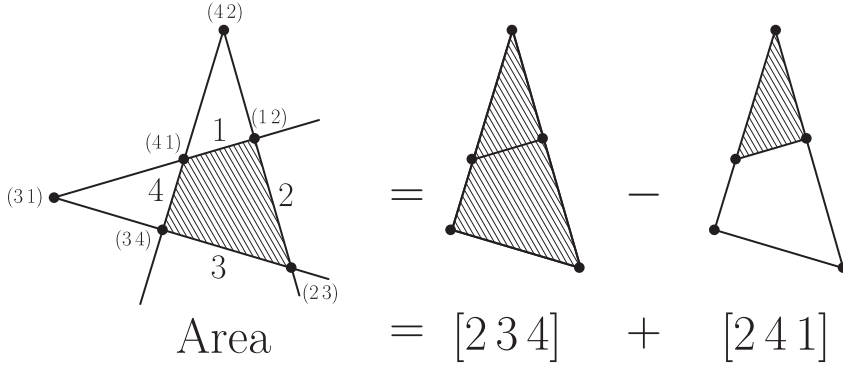
$$\text{Area}(W^1W^2W^3) = \frac{1}{2} \frac{\langle W^1W^2W^3 \rangle}{(Z_A \cdot W^1)(Z_A \cdot W^2)(Z_A \cdot W^3)}. \quad (6.2.24)$$

Note that this is *not* invariant under rescaling the reference twistor Z_A , which is appropriate, since Z_A defines the plane in which the area is defined and the area is not dimensionless.

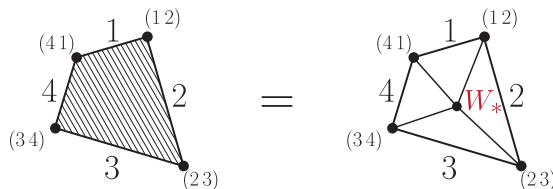
Now, suppose we are given instead three points in the original space, Z_a^I, Z_b^I, Z_c^I . Each of these points is associated with a line in the W space, with e.g. the point a defining the line $Z_a^I W_I = 0$. The lines a and b intersect at the point (ab) in W space, with co-ordinate $W_I^{(ab)} = \epsilon_{IJK} Z_a^J Z_b^K$. Thus, the area of this dual triangle is

$$\text{Area}(\widetilde{[abc]}) = \frac{1}{2} \frac{\langle (ab)(bc)(ca) \rangle}{\langle Aab \rangle \langle Abc \rangle \langle Aca \rangle} = \frac{1}{2} \frac{\langle abc \rangle^2}{\langle Aab \rangle \langle Abc \rangle \langle Aca \rangle} = [abc]. \quad (6.2.25)$$

With these elementary facts in hand, it is easy to identify the triangulations of the polygon associated with the BCFW/CSW representations of the amplitude, which correspond to triangulating \widetilde{L}_n , with the dual triangles $[\ast i i+1]$. An example of a BCFW triangulation for the 4-particle amplitude is shown below:



Note that the BCFW triangulation is characterized by not introducing any new *lines*, but certainly introduces new vertices. However, we have an even more obvious triangulation of the same object, introducing a dual reference point W_* , and triangulating directly using the vertices as



For a general polygon, the area can be triangulated using the triangles with vertices $(W_*, (i-1 i), (i i+1))$. We can compute the area of this triangle using equation (6.2.24), giving an n -term expression for the amplitude

$$A_n = \frac{1}{2} \sum_i \frac{\langle W_* (i-1 i) (i i+1) \rangle}{Z_A \cdot W_* \langle A i-1 i \rangle \langle A i i+1 \rangle} = \sum_i \frac{(Z_i \cdot W_*) \langle i-1 i i+1 \rangle}{(Z_A \cdot W_*) \langle A i-1 i \rangle \langle A i i+1 \rangle}. \quad (6.2.26)$$

Note that in this form, *all* the poles involving the Z_i are manifestly “physical”. This is obvious, since we have triangulated the polygon only using its vertices, and the divergences of the amplitude can only occur if some vertex $(k k+1)$ moves off to infinity, making the area diverge. By contrast, the BCFW/CSW representations introduce new points in W space, with associated spurious pole which cancel in the sum. Note also that this triangulation involved a natural reference point W_* , analogous to the reference point Z_* in the CSW representation of the amplitude. The result is independent of W_* , but term-by-term has a “spurious pole” $(Z_A \cdot W_*)$. We can choose W_* to coincide with one of the external points, say $W_* = (k k+1)$, giving an $(n-2)$ term expression with manifestly physical poles which is however no longer manifestly cyclic invariant.

We close this warm-up section with a few comments. We have drawn pictures of our polygons on a real 2-dimensional plane, but of course the functions are all holomorphic and defined on \mathbb{CP}^2 . The complex areas have a very nice interpretation in terms of contour integrals in \mathbb{CP}^2 with boundaries on the polygon \tilde{L}_n [20]. It is perhaps easiest to get a feeling for such contour integrals with boundary by considering the simplest case of a standard integral over one complex variable z , thought of as a projective integral over \mathbb{CP}^1 . Let’s introduce a variable $w_I = (x, y)$ in \mathbb{C}^2 . Consider an integral with boundaries on $z_a^I w_I = 0, z_b^I w_I = 0$:

$$\int \frac{Dw}{(z_c \cdot w)^2} \quad (6.2.27)$$

$$z_a \cdot w = 0$$

$$z_b \cdot w = 0$$

here, we use

$$D^{n-1}w \equiv \frac{d^n w}{\text{vol}(GL_1)} \quad (6.2.28)$$

to denote the measure on \mathbb{CP}^{n-1} . Using inhomogeneous co-ordinates $w = (1, z)$, the boundaries are at $w = -x_a/y_a$ and $w = -x_b/y_b$. The integrand is simply $\frac{1}{(x_c + y_c z)^2}$, and

can be trivially integrated on any contour between the two end-points. The result is

$$\int_{\substack{z_a \cdot w = 0 \\ z_b \cdot w = 0}} \frac{Dw}{(z_c \cdot w)^2} = \frac{\langle ab \rangle}{\langle ac \rangle \langle cb \rangle}. \quad (6.2.29)$$

This simple result generalizes readily to \mathbb{CP}^n ; for instance our elementary triangle $[abc]$ is given by

$$[abc] = \int_{\substack{Z_a \cdot W = 0 \\ Z_b \cdot W = 0 \\ Z_c \cdot W = 0}} \frac{D^2W}{(Z_A \cdot W)^3}. \quad (6.2.30)$$

This representation of the $[abc]$'s as a contour integral makes the additive properties and the 4-term identities manifest, since Z_a, Z_b, Z_c define the boundaries of the integration region. The full amplitude A_n is expressed as a contour integral with boundaries given on the dual polygon \tilde{L}_n :

$$A_n = \int_{\tilde{L}_n} \frac{D^2W}{(Z_A \cdot W)^3}. \quad (6.2.31)$$

In the following sections, we will need the generalization of the simple formula for the area of triangles in \mathbb{CP}^2 to the general volume of $(n-1)$ -simplicies in \mathbb{CP}^{n-1} , again projected along some specific direction Z_A . Specifying the vertices W_I^1, \dots, W_I^n , the volume is obviously

$$\text{Vol} [W_I^1, \dots, W_I^n] = \frac{1}{(n-1)!} \frac{\langle W^1 \dots W^n \rangle}{(Z_A \cdot W^1) \dots (Z_A \cdot W^n)}. \quad (6.2.32)$$

If instead we specify the $(n-1)$ -simplex by giving its faces Z_1^I, \dots, Z_n^I , the volume is

$$\text{Vol} [Z_1^I, \dots, Z_n^I] = \frac{1}{(n-1)!} \frac{\langle Z_1 \dots Z_n \rangle^n}{\langle Z_A Z_1 \dots Z_{n-1} \rangle \langle Z_A Z_2 \dots Z_n \rangle \dots \langle Z_A Z_n \dots Z_{n-2} \rangle}. \quad (6.2.33)$$

Finally, in our discussion of MHV 1-loop amplitudes, we will encounter plane polygons defined by twistors in \mathbb{CP}^3 . Suppose we are given two reference twistors, Z_A^I, Z_B^I . The Z_B^I define a plane and thus a \mathbb{CP}^2 inside the \mathbb{CP}^3 . Restricting all the twistors to this plane, we can then project along the direction Z_A to define the area as we did above. Thus,

given three twistors Z_a^I, Z_b^I, Z_c^I in \mathbb{CP}^3 , there is an associated area we can label $[abc]_{B;A}$, where the subscript reminds us that we are in the plane defined by Z_B and projecting along Z_A . This area is given by

$$[abc]_{B;A} = \frac{\langle Babc \rangle^2}{\langle BAab \rangle \langle BAbc \rangle \langle BAca \rangle}. \quad (6.2.34)$$

The area of the corresponding n -gon is

$$A_{nB;A} = \sum_i [*ii+1]_{B;A}. \quad (6.2.35)$$

We can also interpret this as a contour integral as

$$A_{nB;A} = \int \frac{D^3W}{(Z_B \cdot W)(Z_A \cdot W)^3} \quad (6.2.36)$$

where the contour of integration is “ $S^1 \times \text{Polygon}$ ”, where the S^1 is evaluated around the pole $Z_B \cdot W = 0$, restricting the integral to the appropriate \mathbb{CP}^2 , leaving us with the remaining boundary on the polygon \tilde{L}_n .

We can also give a “local” triangulation of $A_{nB;A}$ analogous to equation(6.2.26). The reference point W_* in \mathbb{CP}^2 can be obtained by restricting a general reference bi-twistor X to the Z_B plane, via $W_{*I} = \epsilon_{IJKL} Z_B^J X^{KL}$. This gives us

$$A_{nB;A} = \sum_i \frac{\langle BXi \rangle \langle Bi-1ii+1 \rangle}{\langle BAX \rangle \langle BAi-1i \rangle \langle B A ii+1 \rangle}. \quad (6.2.37)$$

There are obviously n terms in this sum. Note again that all the poles involving the Z_i are manifestly local. Each term does have a spurious pole $\langle BAX \rangle$, but of course these poles all cancel as the result is independent of X . We could make a special choice where $X = (kk+1)$ co-incides with one of the vertices of the polygon. This gives us an expression with only $(n-2)$ terms and no spurious poles of any kind, which is however not manifestly cyclically invariant.

6.3 1-Loop MHV Amplitude Integrands

We now give a simple polytope interpretation of the 1-loop MHV integrand. Almost all the results we need were already discussed in our warm-up. Let us again examine the 1-loop MHV integrand in BCFW/CSW form

$$\sum_{i,j} \frac{(\langle A * ii+1 \rangle \langle B * jj+1 \rangle - \langle A * jj+1 \rangle \langle B * ii+1 \rangle)^2}{\langle AB * i \rangle \langle AB ii+1 \rangle \langle AB i+1 * \rangle \langle AB * j \rangle \langle AB jj+1 \rangle \langle AB j+1 * \rangle}. \quad (6.3.38)$$

We will expand the square in the numerator. The first term is given by the sum

$$\sum_i \frac{\langle A * ii+1 \rangle^2}{\langle AB * i \rangle \langle AB ii+1 \rangle \langle AB i+1 * \rangle} \times \sum_j \frac{\langle B * jj+1 \rangle^2}{\langle BA * j \rangle \langle BA jj+1 \rangle \langle BA j+1 * \rangle}. \quad (6.3.39)$$

We can recognize these expressions as computing the area $A_{nB;A}$ discussed in the warm-up section, corresponding to the area of the polygon restricted to the \mathbb{CP}^2 defined by Z_B and projected along Z_A . The above sum becomes

$$\begin{aligned} \sum_i [*ii+1]_{A;B} &\times \sum_j [*jj+1]_{B;A} \\ &= A_{nA;B} \times A_{nB;A}. \end{aligned} \quad (6.3.40)$$

Let's now look at the cross-term, which has the form

$$-2 \sum_{i,j} \frac{\langle A * ii+1 \rangle \langle B * ii+1 \rangle}{\langle AB * i \rangle \langle AB ii+1 \rangle \langle AB i+1 * \rangle} \times \frac{\langle B * jj+1 \rangle \langle A * jj+1 \rangle}{\langle BA * j \rangle \langle BA jj+1 \rangle \langle BA j+1 * \rangle}. \quad (6.3.41)$$

We can also relate this to a polygon areas by using a differential operator

$$\frac{\langle A * ii+1 \rangle \langle B * ii+1 \rangle}{\langle AB * i \rangle \langle AB ii+1 \rangle \langle AB i+1 * \rangle} = \frac{1}{2} \left(Z_B \cdot \frac{\partial}{\partial Z_A} \right) \frac{\langle A * ii+1 \rangle^2}{\langle AB * i \rangle \langle AB ii+1 \rangle \langle AB i+1 * \rangle}. \quad (6.3.42)$$

The cross-term becomes

$$\begin{aligned} -\frac{1}{2} \left(Z_B \cdot \frac{\partial}{\partial Z_A} \right) \sum_i [*ii+1] &\times \left(Z_A \cdot \frac{\partial}{\partial Z_B} \right) \sum_j [*jj+1] \\ &= -\frac{1}{2} \left(Z_B \cdot \frac{\partial}{\partial Z_A} \right) A_{nA;B} \times \left(Z_A \cdot \frac{\partial}{\partial Z_B} \right) A_{nB;A}. \end{aligned} \quad (6.3.43)$$

We finally have

$$M_{1\text{-loop},n}^{\text{MHV}} = A_{nA;B} + A_{nB;A} - \frac{1}{2} \left(Z_B \cdot \frac{\partial}{\partial Z_A} \right) A_{nA;B} \times \left(Z_A \cdot \frac{\partial}{\partial Z_B} \right) A_{nB;A}. \quad (6.3.44)$$

This expression of course makes the cyclic invariance of the integrand completely manifest.

We can interpret the MHV 1-loop integrand as a contour integral in a number of ways. The direct transcription of the expressions we have given is a contour integral of the form

$$\int K(U, V, A, B) D^3 U D^3 V \quad (6.3.45)$$

where

$$K(U, V, A, B) = \frac{1}{(B \cdot U)^3(A \cdot V)} - \frac{2}{(B \cdot U)^2(A \cdot V)^2} + \frac{1}{(B \cdot U)(A \cdot V)^3}. \quad (6.3.46)$$

The contour of integration is “Polygon $\times S^1 \times S^1 \times$ Polygon” in the obvious way. This integral representation can be directly derived from a Fourier transformation of the Grassmannian formula for the MHV 1-loop integrand given in Chapter 4, but we won’t pursue this interpretation further in this chapter.

Note that this form does not make it completely obvious that the integral depends on A, B only through the line (AB) , though we can note that $Z_A \cdot \partial/\partial Z_B K = Z_B \cdot \partial/\partial Z_A K = 0$. There is a more elegant representation as a contour integral, which makes the dependence on the line (AB) more explicit:

$$\int \frac{D^3 U D^3 V}{\langle UVAB \rangle^4} \quad (6.3.47)$$

where the contour is “Polygon $\times S^2 \times$ Polygon”. Note that the integrand is not only explicitly only a function of the line (AB) , it is also only a function of the line (UV) ; the integral over the S^2 leaves us with an integral over the Grassmannian $G(2, 4)$.

Finally, returning to eqn. (6.3.44), we can obtain a local form of the MHV 1-loop integrand using the “local triangulation” of $A_{nA;B}$ given in equation (6.2.37). It is natural to use two different reference bi-twistors X, Y for triangulating $A_{nA;B}$ and $A_{nB;A}$. A short computation yields

$$M_{1\text{-loop},n}^{\text{MHV}} = \sum_{i,j} \frac{\langle AB(i) \cap (Yj) \rangle \langle AB(i-1 \ i \ i+1) \cap (j-1 \ j \ j+1) \rangle}{\langle ABX \rangle \langle ABY \rangle \langle ABi-1 \ i \rangle \langle ABi \ i+1 \rangle \langle ABj-1 \ j \rangle \langle ABj \ j+1 \rangle}. \quad (6.3.48)$$

Here

$$\begin{aligned} \langle AB(Xi) \cap (Yj) \rangle &= \langle AXi \rangle \langle BYj \rangle - (A \leftrightarrow B), \\ \langle AB(i-1 \ i \ i+1) \cap (j-1 \ j \ j+1) \rangle &= \langle Ai-1 \ i \ i+1 \rangle \langle Bj-1 \ j \ j+1 \rangle - (A \leftrightarrow B). \end{aligned} \quad (6.3.49)$$

This expression for the amplitude is also manifestly cyclic. Note that, in complete parallel with the discussion around equation (6.2.37), all the poles involving the Z_i twistors are manifestly local. Each term has a dependence on the X, Y bi-twistors, but these cancel in the sum which is independent of X, Y . There are a number of obvious special cases of interests for this new form of the integrand. For instance we can take the two bi-twistors X and Y to be equal, yielding the form

$$\sum_{i,j} \frac{\langle Xi \ j \rangle \langle AB(i-1 \ i \ i+1) \cap (j-1 \ j \ j+1) \rangle}{\langle ABX \rangle \langle ABi-1 \ i \rangle \langle ABi \ i+1 \rangle \langle ABj-1 \ j \rangle \langle ABj \ j+1 \rangle}. \quad (6.3.50)$$

We can further take X to be a simple bi-twistor corresponding to one of the external points, for instance $X = (n1)$. With this choice there are no spurious poles of any sort, but the result is not manifestly cyclic invariant. Averaging over all cyclic images yields the local form of the integrand given in Chapter 4.

The equality between the local form equation (6.3.48) and the BCFW form of equation (6.1.3) is a highly non-trivial identity between rational functions that we have now understood geometrically. As stressed in Chapter 4, the loop integrand is a well-defined object in the planar limit of any theory, and should manifest all symmetries. While the BCFW form on the integrand exhibits the Yangian invariance of the theory, the local form is also crucially needed [15] for a physical IR regularization [92–94] of the theory. It is therefore very pleasing to see the two forms related in such a direct way.

6.4 NMHV Tree Amplitudes

We now turn to the NMHV tree amplitude, which has been given a polytope volume interpretation in [20]. In [20], the description of the polytope was closely associated with the BCFW representation of the amplitude. We will begin by describing the polytope in a slightly more invariant way.

As a consequence of the 6-term identity equation (6.1.5) for R -invariants, we can observe that the $[abcde]$'s have exactly the same additive properties as 4-simplices in \mathbb{CP}^4 . In our warm-up example, we associated the $[abc]$'s with the area of a dual triangle in \mathbb{CP}^2 . We would like to do the same for the R -invariants $[abcde]$, but there is a small difference: each particle i is labeled by a supertwistor (Z_i^I, η_i^α) , where $\alpha = 1, \dots, 4$ is the $SU(4)$ R-symmetry index. In order to proceed we have to associate a point in \mathbb{CP}^4 with this super-twistor. Fortunately this is easy to do. Let's introduce an auxiliary set of four Grassmann variables ϕ_α , and define an “extended twistor” in \mathbb{CP}^4 by

$$\mathcal{Z}_i^{\mathcal{I}} = \left(\begin{array}{c} Z_i^I \\ \phi \cdot \eta_i \end{array} \right). \quad (6.4.51)$$

We also introduce the reference twistor

$$\mathcal{Z}_0^I = \begin{pmatrix} 0 \\ 0 \\ 0 \\ 0 \\ 1 \end{pmatrix} \quad (6.4.52)$$

which preserves the SL_4 symmetry acting on the bosonic Z^I . It is natural to consider the (bosonic) volume of the 4-simplex whose faces are $\mathcal{Z}_a, \mathcal{Z}_b, \mathcal{Z}_c, \mathcal{Z}_d, \mathcal{Z}_e$:

$$\mathcal{V}[\mathcal{Z}_a, \dots, \mathcal{Z}_e] = \frac{1}{4!} \frac{\langle\langle \mathcal{Z}_a \mathcal{Z}_b \mathcal{Z}_c \mathcal{Z}_d \mathcal{Z}_e \rangle\rangle^4}{\langle\langle \mathcal{Z}_0 \mathcal{Z}_a \mathcal{Z}_b \mathcal{Z}_c \mathcal{Z}_d \rangle\rangle \langle\langle \mathcal{Z}_0 \mathcal{Z}_b \mathcal{Z}_c \mathcal{Z}_d \mathcal{Z}_e \rangle\rangle \dots \langle\langle \mathcal{Z}_0 \mathcal{Z}_e \mathcal{Z}_a \mathcal{Z}_b \mathcal{Z}_c \rangle\rangle}. \quad (6.4.53)$$

We use the notation $\langle\langle \mathcal{Z}_a \mathcal{Z}_b \dots \mathcal{Z}_e \rangle\rangle$ to denote the contraction of the extended twistors with the 5-index $\epsilon_{\mathcal{I}\mathcal{J}\mathcal{K}\mathcal{L}\mathcal{M}}$ tensor, to distinguish it from the 4-brackets $\langle abcd \rangle$ used with the usual bosonic Z_a^I twistors in \mathbb{CP}^3 . We find trivially that

$$\mathcal{V}[\mathcal{Z}_a, \dots, \mathcal{Z}_e] = \frac{1}{4!} \frac{(\phi \cdot \eta_a \langle bcde \rangle + \text{cyclic})^4}{\langle abcd \rangle \langle bcde \rangle \dots \langle eabc \rangle}. \quad (6.4.54)$$

This depends on ϕ ; to get a function of the (Z_i, η_i) alone we simply integrate over the ϕ_α . This directly yields the R -invariant

$$[abcde] = \int d^4 \phi \mathcal{V}[\mathcal{Z}_a, \dots, \mathcal{Z}_e]. \quad (6.4.55)$$

Thus, in complete analogy with our warm-up example, we have associated the $[abcde]$ with (the ϕ integral of) the volume of a simplex in the $\mathcal{W}_{\mathcal{I}}$ space geometrically dual to $\mathcal{Z}^{\mathcal{I}}$ space, whose faces are $\mathcal{Z}_a, \dots, \mathcal{Z}_e$. The algebraic properties of the R -invariants we have already discussed then precisely reflect the geometry of these simplicies.

We can now give a nice definition for the NMHV amplitude polytope. Let us return to the BCFW/CSW expression

$$M_n^{\text{NMHV}} = \frac{1}{2} \sum_{i,j} [* i i+1 j j+1]. \quad (6.4.56)$$

Mirroring our algebraic arguments from the introductory section, we can think of the R -invariants $[* i i+1 j j+1]$ as defining a 4-simplex in a (\mathcal{Z} -space) \mathbb{CP}^4 ; the sum over all these tetrahedra defines a polytope P_n . P_n is completely characterized by giving its boundary, which is $\partial P_n = \sum_{i,j} [i i+1 j j+1]$, showing that P_n is actually independent of the point $*$.

We can think of P_n as the “square” of the Wilson-polygon L_n in a natural way. Speaking slightly more generally, suppose we are given two ordered sets of points $X = (x_1, x_2, \dots, x_n)$ and $Y = (y_1, y_2, \dots, y_n)$, each of which defines an (in general non-planar) polygon loop in \mathbb{CP}^4 . We can form a 3-simplex $[x_i x_{i+1} y_j y_{j+1}]$ in \mathbb{CP}^4 , by taking pairs of edges in X and Y . Summing over all these 3-simplicies defines a polyhedron Q_n , and it is easy to check that $\partial Q_n = 0$ so Q_n is a closed 3-volume. As such, we can write $Q_n = \partial(X \otimes Y)$, where $(X \otimes Y)$ is a 4-Polytope in \mathbb{CP}^4 , one triangulation of which can be given as $(X \otimes Y) = \sum_{i,j} [* i i+1 j j+1]$. Note that we have used the \mathbb{CP}^4 structure in an essential way here, in going from Q_n being closed to being expressed as the boundary of a unique 4-dimensional object. Note also that the \otimes operation behaves as an algebraic direct product in that it is linear in its two factors. It is also interesting to note that, while the X, Y polygons are in general non-planar, they nonetheless behave as plane polygons in this product, as reflected in the fact that $X \otimes Y$ satisfies 4-term tetrahedral identities separately in X and Y .

With this definition, the polytope P_n associated with the NMHV tree amplitude is related to the Wilson-Loop Polygon L_n as

$$P_n = \frac{1}{2} L_n \otimes L_n. \quad (6.4.57)$$

The NMHV amplitude is $\int d^4\phi$ of the volume of the polytope \tilde{P}_n geometrically dual to P_n , which we can represent as a contour integral via

$$M_n^{\text{NMHV}} = 4! \int d^4\phi \int_{\tilde{P}_n} \frac{D^4\mathcal{W}}{(\mathcal{Z}_0 \cdot \mathcal{W})^5}. \quad (6.4.58)$$

In order to actually compute this volume, we need a triangulation of \tilde{P}_n in terms of elementary 4-simplicies. We may triangulate the polytope in any way we like. The BCFW representation of the amplitude is one particular choice, which yields the shortest expressions for the amplitude but has spurious poles. The BCFW triangulation adds no new planes, but does add new vertices, and the spurious poles are associated with these “spurious” vertices. The geometrically dual choice—adding no new vertices but adding spurious planes—will yield expressions for the amplitude that allow us to expose manifest cyclicity and locality in a new way.

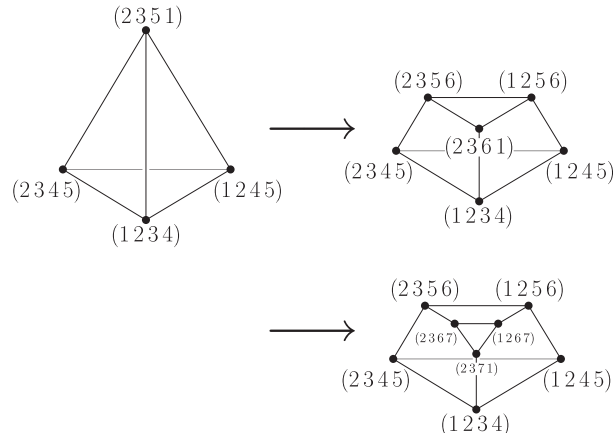
We do this by first triangulating each of the *faces* of \tilde{P}_n . All the boundaries of \tilde{P}_n lie in the planes dual to the \mathcal{Z}_j ; we denote the face contained in this plane by $F_{j,n}$.

Conveniently, the faces are 3-polytopes, which will allow us to visualize them easily. We can triangulate $F_{j,n} = \sum_{\gamma} T_{j,n}^{\gamma}$, where each of the $T_{j,n}^{\gamma}$ is a tetrahedron with 4 vertices. In order to triangulate \tilde{P}_n , we introduce a reference “suspension point” \mathcal{W}_* . With each tetrahedron $T_{j,n}^{\gamma}$, we associate a 4-simplex $\mathcal{T}_{j,n}^{\gamma}$ just by adding the point \mathcal{W}_* to the 4 vertices of $T_{j,n}^{\gamma}$. The sum over all these 4-simplicies then gives a triangulation of \tilde{P}_n given by $\tilde{P}_n = \sum_{j,\gamma} \mathcal{T}_{j,n}^{\gamma}$.

We have a natural choice for the “suspension point” \mathcal{W}_* . Given that our choice of \mathcal{Z}_0 leaves the SL_4 acting on the usual bosonic momentum-twistors invariant, it is natural to choose \mathcal{W}_* to also preserve this SL_4 . Explicitly, we can choose $\mathcal{W}_* = (0, 0, 0, 0, 1)$. Finally, for a “local” triangulation, we will choose to triangulate the faces only using the given “physical” vertices $(i\ i+1\ j\ j+1)$.

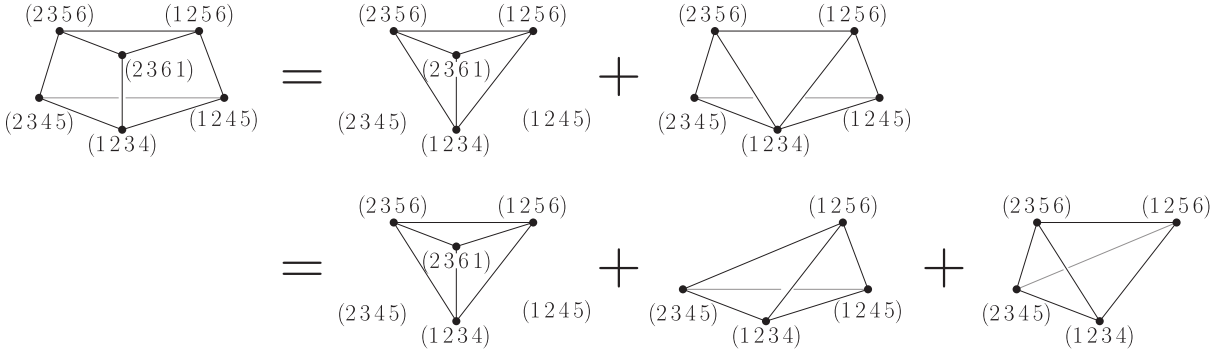
Following [20], let us get acquainted with the faces of \tilde{P}_n by looking at $F_{2,n}$. The vertices of $F_{2,n}$ are all the points of the form $(1\ 2\ k\ k+1)$ and $(2\ 3\ l\ l+1)$. Two vertices $(2abc), (2xyz)$ are connected by an edge if the triples $(abc), (xyz)$ share two indices in common. In the simplest case $n = 5$, the face $F_{2,5}$ is just a tetrahedron with vertices $(1234), (1245), (2345), (2351)$. For 6 particles, $F_{2,6}$ has six vertices, and while e.g. (2356) is connected by an edge to (2345) , there is no edge connecting (2356) to (1234) .

It is very easy to recursively build $F_{2,n}$ systematically, starting from the tetrahedron for $F_{2,5}$. While the vertices $(1234), (1245), (2345)$ occur in both $F_{2,5}$ and $F_{2,6}$, the vertex (2351) occurring in $F_{2,5}$ is absent in $F_{2,6}$; conversely there are three new vertices $(2356), (1256)$ and (2361) in $F_{2,6}$ not contained in $F_{2,5}$. Thus we can obtain $F_{2,6}$ by starting with $F_{2,5}$, “chopping off” the vertex (2351) and replacing it with the three new vertices, as shown below:



Similarly, we can go from the $F_{2,6}$ to $F_{2,7}$ by “chopping off” the vertex (2361), and continue in this way to define all the $F_{2,n}$.

We now wish to give a local triangulation of the $F_{2,n}$. Let’s illustrate this in pictures with one local triangulation for the first non-trivial case of $F_{2,6}$:

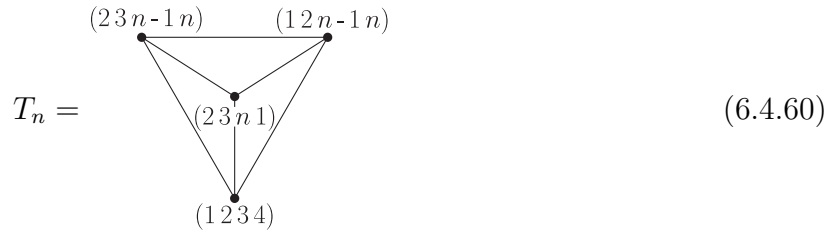


This “local” triangulation is to be contrasted with a “BCFW” triangulation, which would adds back the “spurious” point (2351), and represent the prism for $F_{3,6}$ as $F_{2,5}$ with the “chopped off” tetrahedron subtracted.

For general n , we can build $F_{2,n}$ from $F_{2,n-1}$ by “chopping off” the vertex (23n-11) and adding the three vertices (23n1), (23n-1n), (12n-1n). This makes it natural to define

$$F_{2,n} = G_n + T_n \tag{6.4.59}$$

where T_n is the tetrahedron



In going from $F_{2,n-1}$ to $F_{2,n}$, we just chop off the vertex (23n-11) from T_{n-1} , thus we can write

$$F_{2,n} = G_{n-1} + \begin{array}{c} (23n-2n-1) \quad (12n-2n-1) \\ \bullet \quad \bullet \\ (23n-1n) \quad (12n-1n) \\ \bullet \quad \bullet \\ (23n1) \\ \bullet \\ (1234) \end{array} = G_{n-1} + T_n + \begin{array}{c} (23n-2n-1) \quad (12n-2n-1) \\ \bullet \quad \bullet \\ (23n-1n) \quad (12n-1n) \\ \bullet \quad \bullet \\ (1234) \end{array} \tag{6.4.61}$$

Since $F_{2,n} = G_n + T_n$, this gives us a recursive formula for the G_n :

$$G_n = G_{n-1} + \begin{array}{c} (23n-2n-1) \quad (12n-2n-1) \\ \bullet \quad \bullet \\ \diagdown \quad \diagup \\ (23n-1n) \quad (12n-1n) \\ \bullet \quad \bullet \\ \diagdown \quad \diagup \\ (1234) \end{array} = G_{n-1} + \begin{array}{c} (12n-2n-1) \\ \bullet \\ \diagdown \quad \diagup \\ (23n-1n) \quad (12n-1n) \\ \bullet \quad \bullet \\ \diagdown \quad \diagup \\ (1234) \end{array} + \begin{array}{c} (23n-2n-1) \quad (12n-2n-1) \\ \bullet \quad \bullet \\ \diagdown \quad \diagup \\ (23n-1n) \\ \bullet \\ \diagdown \quad \diagup \\ (1234) \end{array}$$

Note that in the last step we chose one of two possible triangulations of the prism occurring in the first term. This is not fundamental, we have made this choice because it will lead to the a slightly simpler final form for the amplitude.

We can trivially solve for all the G_n . Doing this and adding T_n we find for $F_{2,n}$

$$F_{2,n} = \sum_i \left(\begin{array}{c} (23i-1i) \quad (12i-1i) \\ \bullet \quad \bullet \\ \diagdown \quad \diagup \\ (23ii+1) \\ \bullet \\ \diagdown \quad \diagup \\ (1234) \end{array} + \begin{array}{c} (12i-1i) \\ \bullet \\ \diagdown \quad \diagup \\ (23ii+1) \quad (12ii+1) \\ \bullet \quad \bullet \\ \diagdown \quad \diagup \\ (1234) \end{array} \right) \quad (6.4.62)$$

note that the T_n contribution is nicely represented by the term with $i = n$ in the first sum. Note also that we sum over all i without worrying about any limits since any degenerate configurations have vanishing volume. Actually it is easy to see that the number of non-degenerate terms is $2n - 9$ since we start with one tetrahedron when $n = 5$, and then each increase in n needs one more chopping which generates two more terms.

Obviously this procedure works for any face $F_{j,n}$ just by cycling labels, and the final result for $F_{j,n}$ is

$$F_{j,n} = \sum_i \left(\begin{array}{c} (jj+1i-1i) \quad (j-1ji-1i) \\ \bullet \quad \bullet \\ \diagdown \quad \diagup \\ (jj+1ii+1) \\ \bullet \\ \diagdown \quad \diagup \\ (j-1jj+1j+2) \end{array} + \begin{array}{c} (j-1ji-1i) \\ \bullet \\ \diagdown \quad \diagup \\ (jj+1ii+1) \quad (j-1jii+1) \\ \bullet \quad \bullet \\ \diagdown \quad \diagup \\ (j-1jj+1j+2) \end{array} \right) = \sum_{i;s=\pm 1} \begin{array}{c} (jj+1ii+1) \quad (j-1ji-1i) \\ \bullet \quad \bullet \\ \diagdown \quad \diagup \\ (jj+s i-s i) \\ \bullet \\ \diagdown \quad \diagup \\ (j-1jj+1j+2) \end{array} \quad (6.4.63)$$

Now that we have the triangulation of the faces, we can easily compute the volume of the triangulations of the polytope itself, involving the addition of our suspension point $\mathcal{W}_* = (0, 0, 0, 0, 1)$. The volume associated with the tetrahedra appearing in equation (6.4.63) for the face $F_{j,n}$, is

$$\frac{\langle\langle \mathcal{W}_* (j-1jj+1j+2) (j-1ji-1i) (jj+1ii+1) (jj+si-si) \rangle\rangle}{\langle j-1jj+1j+2 \rangle \langle j-1ji-1i \rangle \langle jj+1ii+1 \rangle \langle jj+si-si \rangle} \quad (6.4.64)$$

which can easily be computed. There are 16 $\mathcal{Z}^{\mathcal{I}}$'s in the numerator and a single dual twistor $\mathcal{W}_{*\mathcal{I}}$. Thus the 5-bracket expands to a sum of terms where one of the \mathcal{Z} 's is contracted with \mathcal{W}_* , and the remaining 15 are grouped into the product of three 5-brackets. Since \mathcal{Z}_j occurs four times, for a non-zero result one of these \mathcal{Z}_j must be contracted with \mathcal{W}_* . There is only one non-vanishing way of grouping the remaining \mathcal{Z} 's into 5-brackets, and we find this volume to be

$$\frac{\phi \cdot \eta_j \langle \langle j-1 j j+1 j+2 i \rangle \rangle \langle \langle j-1 j j+1 i-s i \rangle \rangle \langle \langle j j+s i-1 i i+1 \rangle \rangle}{\langle j-1 j j+1 j+2 \rangle \langle j-1 j i-1 i \rangle \langle j j+1 i i+1 \rangle \langle j j+s i-s i \rangle} \quad (6.4.65)$$

the $\int d^4\phi$ integration is trivially done to yield

$$\frac{\langle \eta_j, \{j-1 j j+1 j+2 i\}, \{j-1 j j+1 i-s i\}, \{j j+s i-1 i i+1\} \rangle}{\langle j-1 j j+1 j+2 \rangle \langle j-1 j i-1 i \rangle \langle j j+1 i i+1 \rangle \langle j j+s i-s i \rangle}. \quad (6.4.66)$$

Here, we have defined the Grassmann object

$$\{abcde\} = \eta_a \langle bcde \rangle + \dots + \eta_e \langle abcd \rangle \quad (6.4.67)$$

and the four-bracket in the numerator represents the contraction of $SU(4)_R$ indices of the η 's.

We have thus found a manifestly cyclic and local formula for the NMHV tree amplitude

$$M_n^{\text{NMHV}} = \sum_{i,j;s=\pm 1} \frac{\langle \eta_j, \{j-1 j j+1 j+2 i\}, \{j-1 j j+1 i-s i\}, \{j j+s i-1 i i+1\} \rangle}{\langle j-1 j j+1 j+2 \rangle \langle j-1 j i-1 i \rangle \langle j j+1 i i+1 \rangle \langle j j+s i-s i \rangle}. \quad (6.4.68)$$

This expression is amazingly simple, with $n(2n-9)$ non-vanishing terms. Here $(2n-9)$ is simply the number of tetrahedra in each face we already encountered in equation (6.4.63).

It also has another striking property: despite naturally being written as a function of the supersymmetric Grassmann η variables, the individual terms in the sum are *not* invariant under supersymmetry transformation (to speak nothing of the Yangian symmetry). Indeed, the SUSY variation cancels only in a telescopic sum over all the terms.

There are other possible local triangulations of this polytope. For instance, we can choose the ‘‘suspension point’’ to be one of the vertices of the polytope $(k k+1 j j+1)$. This is analogous to the choice ‘‘ $X = (n1)$ ’’ for the reference bitwistor in the local form of the MHV 1-loop integrand, and gives a shorter formula with $(n-4)(2n-9)$ terms, but at the cost of losing manifest cyclic symmetry. These local forms can finally be compared

with the BCFW expressions with $\frac{1}{2}(n-3)(n-4)$ terms, which contain $\sim \frac{1}{4}$ as many terms at large n , but don't make cyclicity or locality manifest.

It is also amusing to give a formula for standard helicity amplitudes; this only requires computing simple determinants as explained in e.g. [51]. Consider in particular gluon amplitudes $A_n(1^- i^- j^-)$ where particles $1, i, j$ have negative helicity and the rest have positive helicity. Up to the Parke-Taylor pre-factor, the result is precisely given by the above formula for M_n^{NMHV} , with the η_k replaced by a particular function of the spinor-helicity variables. Explicitly, we find that

$$A_n(1^- i^- j^-) = \frac{1}{\langle 12 \rangle \langle 23 \rangle \cdots \langle n1 \rangle} M_n^{\text{NMHV}} \left(\eta_k \rightarrow \begin{array}{ll} \langle ij \rangle \langle k1 \rangle & 1 < k \leq i \\ \langle kj \rangle \langle i1 \rangle & i < k \leq j \\ 0 & \text{otherwise} \end{array} \right). \quad (6.4.69)$$

The split helicity amplitudes are particularly easy to extract for all n :

$$A_n(1^- 2^- 3^-) = \frac{\langle 12 \rangle^4 \langle 23 \rangle^4}{\langle 12 \rangle \langle 23 \rangle \cdots \langle n1 \rangle} \sum_{i,s=\pm 1} \frac{\langle 134i \rangle \langle 13i-si \rangle \langle 2+s i-1 i i+i \rangle}{\langle 1234 \rangle \langle 12i-1 i \rangle \langle 23i i+1 \rangle \langle 22+s i-s i \rangle}. \quad (6.4.70)$$

Using $\langle i-1 i j j+1 \rangle = \langle i-1 i \rangle \langle j j+1 \rangle (p_i + \cdots + p_j)^2$, the poles are directly functions of spinor-helicity variables and take the usual form of Feynman propagators. For $n=6$, this expression is equivalent to a form derived long ago using the Berends-Giele recursion relations [3]; we now see that this formula and all its variant forms flow from the single formula, equation (6.4.69), which also generalizes to all helicity configurations and all n .

We conclude our discussion of NMHV amplitudes by remarking that the use of a bosonic \mathbb{CP}^4 space to describe supersymmetric amplitudes is quite striking. One might have expected supersymmetric amplitudes to be expressed as an integral over $\mathbb{CP}^{3|4}$, and indeed the R -invariants have a beautiful interpretation as the super-volume of a super-polytope [20] in $\mathbb{CP}^{3|4}$. This form is also very closely related to the momentum-twistor Grassmannian formula [19]. The non-linear way in which $\mathcal{Z}_i, \mathcal{Z}_0$ package the supersymmetric information of the theory into only a single extra dimension is more novel and interesting, and made the local triangulation leading to equation (6.4.68) possible. We expect that further generalizations of this idea are needed for higher $N^k\text{MHV}$ amplitudes.

6.5 Discussion

Many of the advances in our understanding of perturbative scattering amplitudes in the last five years were driven by the discovery of the CSW and BCFW recursion relations for tree amplitudes. The ability to analytically compute all tree amplitudes enabled the generation of a huge amount of “data” about the theory, which exposed a number of new, remarkable and deeply interwoven mathematical structures underlying the physics. Amongst other things, these insights stimulated the generalization of the early methods to all loop orders, making a more incisive exploration of the structure of the theory possible. In this chapter we have continued the exploration of one of the beautiful structures uncovered in this period.

The polytope picture is clearly intimately related to the Grassmannian formula in momentum twistor space, giving a lovely geometric understanding of the additive structures appearing in the amplitudes, which are understood more algebraically as a consequence of residue theorems in the Grassmannian formalism.

The Grassmannian picture extends to all amplitudes and loop orders, giving expressions that are term-by-term manifestly Yangian-invariant. There is clearly a beautiful algebraic structure at work in governing the properties of Grassmannian residues and residue theorems, guaranteeing the emergence of physical properties such as cyclic invariance, locality and unitarity. While we have not yet extended the polytope picture to these more general amplitudes, there are strong reasons to suspect this must be possible, and we expect that such an extension would give a more geometric understanding of these algebraic structures.

However, even in the baby examples we have studied in this chapter, it is clear that the polytope picture does much more than simply geometrize the understanding of relations between Yangian invariants! While one simple class of polytope triangulations do indeed provide such an understanding, the even more natural class of triangulations we examined here have opened the door to a completely new set of objects and ideas, far removed from their BCFW/CSW origins. The existence of such strikingly simple and manifestly local forms for the scattering amplitudes is a real surprise. Indeed the tremendous complexity of standard Feynman diagram calculations is directly related to making locality manifest, while the tremendous advantages of BCFW seemed inexorably tied to the appearance of

spurious poles!

This strongly suggests a new set of principles at play. It is tempting to speculate that these principles will be closely connected to a more physical “spin-chain” picture for scattering amplitudes. Superficially, the new expressions for the amplitudes we have found certainly *look* more closely related to an underlying spin-chain, not only on account of their manifest cyclicity, but also because of the suggestive way some of the symmetries are realized. It is also refreshing to move somewhat away from dealing with objects that are manifestly supersymmetric/Yangian invariant, particularly keeping in mind the eventual goal of understanding non-supersymmetric theories!

There is clearly some remarkable geometry behind these polytope formulas. It is particularly striking that in both of the examples we studied, the Wilson-Loop behaves as if it were a plane polygon, with additive identities like those of the triangles in \mathbb{CP}^2 explained in our warm-up example.

Finally, the polytope picture also strongly inspired the search for and discovery of the amazingly simple local expressions for multi-loop integrands described in Chapter 5. These expressions are far simpler than their BCFW counterparts, and clearly beg for a much deeper understanding. We hope to see significant progress on these questions in the near future.

Appendix A *Vernacular of the S-Matrix: Kinematics and Computational Tools*

A.1 Introduction

The on-shell recursion relations for scattering amplitudes described by Britto, Cachazo, Feng and Witten (BCFW) [7,31] are very well known and have been widely used to compute scattering amplitudes for both purely-theoretical and extremely practical purposes in a wide variety of theories [134]. They represent one of the major new tools in the study of quantum field theory. Theoretically, the power and simplicity of the recursive definitions of scattering amplitudes has allowed for the development of an arguably ‘phenomenological’ approach to the advancement of our understanding of quantum field theory: by making once intractable problems essentially effortless, many new questions can be asked—and answered. And practically, tree-amplitudes for processes involving many external particles are of importance for the accurate prediction of backgrounds for new physics at the LHC, for example; BCFW—along with a variety of other computational frameworks such as those based on the powerful Berends-Giele recursion relations [3]—has greatly aided this effort. Considering for example that colour-stripped tree-amplitudes in $\mathcal{N} = 4$ encode all the data of scattering amplitudes in ordinary, non-supersymmetric massless QCD [135], it is clear that understanding $\mathcal{N} = 4$ is an important step along the way to understanding QFT in general, and as it is observed in the Standard Model as backgrounds for new physics at the LHC.

Partly because of the existence and incredible simplicity of recursive definitions of the S-Matrix, tree-amplitudes in $\mathcal{N} = 4$ have been largely understood in the literature for some time now. Indeed, there exists today a large number of independent presentations of all perturbative tree-amplitudes in $\mathcal{N} = 4$, including those based on the BCFW recursion relations [15, 50, 72], twistor string theory [4, 14, 39, 63, 103], contour integrals in the Grassmannian [10, 22], and the CSW recursion relations [5, 51, 132], for example. Many of these results were made possible in part through the existence of privately-developed, powerful computational tools which have proven themselves essential for gaining intuition

and necessary for checking results. Recently, some of these tools have become publicly available through the release of the MATHEMATICA package **Gluon-Gluino-Trees (GGT)**, [135], which is capable of analytically computing all N^k MHV tree-amplitudes involving combinations of external gluons and gluinos, and can compute these numerically using the package ‘**SOM**,’ [136].

With this chapter, we extend the reach of these resources to include *all* N^k MHV tree-amplitudes—including those involving squarks—by making available the MATHEMATICA package **bcfw**, included in [137]. In addition to its complete generality, there are two principle features of **bcfw** that should make it particularly useful to those who are interested in gaining intuition about or evaluating tree-amplitudes in $\mathcal{N} = 4$. First, the analytic formulae generated by **bcfw** are often dramatically more compact and easier to evaluate than any existing formulae obtained using BCFW. These gains in efficiency can be traced directly to **bcfw**’s: 1. use of momentum-twistor variables, and 2. representation of all tree-amplitudes in a fully-supersymmetric way (realized as contour integrals over the Grassmannian), making any n -point N^k MHV helicity-amplitude easily obtained from any other. Another feature of **bcfw** that should make it useful to researchers is its ability to solve the BCFW-recursions using a wide variety of different recursive ‘schemes,’ leading to a large number of independent analytic formulae for any particular amplitude.¹ And it may be worth mentioning that the **bcfw** package has been designed with hopes of being intuitive-enough to be useful even to those with very little experience with MATHEMATICA.

One of the functions defined by **bcfw** is ‘**Amp**,’ which can generate analytic formulae for any helicity-amplitude in $\mathcal{N} = 4$. An example of how **Amp** can be used is given in Figure A.1.² Using ‘**m**’ and ‘**p**’ to denote each minus-helicity and plus-helicity gluon, respectively, **Amp** will generate any purely gluonic N^k MHV amplitude. For amplitudes involving 2 gluinos together with any number of gluons, a similar, simplified notation can be used,³ where ‘**m/2**’ and ‘**p/2**’ indicate the two gluinos; an example of this is given in

¹For example, we have included as a worked example in the demonstration file included with the **bcfw** package the construction of all 74 linearly-independent, 20-term formulae for the 8-point N^2 MHV tree-amplitude, involving a total of 176 different Yangian-invariant objects.

²Also used in these examples is the function ‘**nice**’ which formats formulae generated by **bcfw** to be more readable—for example, by converting ‘**ab[1,2]**’ \mapsto ‘**<1 2>**’.

³An overall sign for these amplitudes has been implicitly fixed by the convention that the particle

Figure A.1: $\mathcal{A}_6^{(3)}(-, -, -, +, +, +)$. The split-helicity 6-point NMHV amplitude.

```

[1]:= Amp[m,m,m,p,p,p]//nice
[2]:= Amp[m,m,m,p,p,p]//toSpinorHelicity[6]//nice
t[1]:=  $\frac{\langle 12 \rangle^3 \langle 23 \rangle^3 \langle 3451 \rangle^3}{\langle 34 \rangle \langle 45 \rangle \langle 56 \rangle \langle 61 \rangle \langle 1234 \rangle \langle 2345 \rangle \langle 4512 \rangle \langle 5123 \rangle} + \frac{\langle 12 \rangle^3 \langle 23 \rangle^3 \langle 3561 \rangle^3}{\langle 34 \rangle \langle 45 \rangle \langle 56 \rangle \langle 61 \rangle \langle 1235 \rangle \langle 2356 \rangle \langle 5612 \rangle \langle 6123 \rangle}$ 
t[2]:=  $-\frac{\langle 23 \rangle^2 \langle 34 \rangle \langle 1|x_{63}x_{34}|5 \rangle^3}{\langle 45 \rangle^3 \langle 56 \rangle \langle 61 \rangle \langle 5|x_{41}x_{12}|3 \rangle s_{23}s_{34}s_{234}} - \frac{\langle 12 \rangle \langle 23 \rangle \langle 3|x_{25}x_{56}|1 \rangle^3}{\langle 34 \rangle \langle 45 \rangle \langle 61 \rangle^2 \langle 5|x_{41}x_{12}|3 \rangle s_{61}s_{12}s_{612}}$ 

```

Figure A.2: $\mathcal{A}_6^{(3)}(-, -, \psi_{-1/2}^{(123)}, +, +, \psi_{+1/2}^{(4)})$. A 6-point NMHV amplitude involving two gluinos and four gluons.

```

In[1]:= Amp[m,m,m/2,p,p,p/2]//nice
Out[1]:=  $\frac{\langle 12 \rangle^3 \langle 23 \rangle^2 \langle 3451 \rangle^2}{\langle 34 \rangle \langle 45 \rangle \langle 56 \rangle \langle 1234 \rangle \langle 5123 \rangle \langle 4512 \rangle} + \frac{\langle 12 \rangle^3 \langle 23 \rangle^2 \langle 3561 \rangle^2}{\langle 34 \rangle \langle 45 \rangle \langle 56 \rangle \langle 1235 \rangle \langle 5612 \rangle \langle 6123 \rangle}$ 

```

Figure A.2. (The reader will notice that—unless ‘toSpinorHelicity[n]’ is used—the only two kinematical invariants used by `bcfw` are the momentum-twistor ‘four-bracket’ $\langle \cdot \cdot \cdot \cdot \rangle$ and its associated ‘two-bracket’ $\langle \cdot \cdot \rangle$; these will be reviewed along with the spinor-helicity invariants in section A.2.)

field	SU_4 R -charge	short-notation
g_+	$\{\}$	\mathbf{p}
$\psi_{+1/2}^{(i)}$	$\{\mathbf{i}\}$	$\mathbf{p}/2(\iff \{4\})$
$s_0^{(ij)}$	$\{\mathbf{i}, \mathbf{j}\}$	—
$\psi_{-1/2}^{(ijk)}$	$\{\mathbf{i}, \mathbf{j}, \mathbf{k}\}$	$\mathbf{m}/2(\iff \{1, 2, 3\})$
g_-	$\{\mathbf{1}, \mathbf{2}, \mathbf{3}, \mathbf{4}\}$	\mathbf{m}

Table A.1: Conventions for the arguments of the functions `Amp`, `nAmp`, `nAmpTerms`, etc.

For amplitudes involving more than two gluinos (or any number of squarks), simple labels such as ‘ \mathbf{m} ’ or ‘ $\mathbf{p}/2$ ’ are not sufficiently precise. This is remedied by choosing instead to label each external particle by its SU_4 R -charge, where each of the external superfields are decomposed according to

$$\Phi^+ = g_+ + \tilde{\eta}_i \psi_{+1/2}^{(i)} + \tilde{\eta}_i \tilde{\eta}_j \phi^{(ij)} + \tilde{\eta}_i \tilde{\eta}_j \tilde{\eta}_k \psi_{-1/2}^{(ijk)} + \tilde{\eta}_1 \tilde{\eta}_2 \tilde{\eta}_3 \tilde{\eta}_4 g_- . \quad (\text{A.1.1})$$

The syntactical rules which follow from these conventions are summarized in Table A.1,

labelled ‘ $\mathbf{m}/2$ ’ has SU_4 R -charge (123); refer to Table A.1.

Figure A.3: $\mathcal{A}_8^{(4)} \left(\psi_{+1/2}^{(1)}, \psi_{+1/2}^{(1)}, \psi_{+1/2}^{(1)}, \phi_0^{(13)}, \psi_{-1/2}^{(234)}, \psi_{-1/2}^{(234)}, \psi_{-1/2}^{(234)}, \phi_0^{(24)} \right)$.

An example 8-point N^2 MHV helicity-amplitude involving 6 gluinos and 2 squarks.

```
In[1]:= Amp[{1},{1},{1},{1,3},{2,3,4},{2,3,4},{2,3,4},{24}];
        %//twistorSimplify//nice
Out[1]:= 
$$\frac{\langle 56 \rangle^2 \langle 67 \rangle^2 \langle 1236 \rangle \langle 2345 \rangle}{\langle 81 \rangle \langle 1267 \rangle \langle 2356 \rangle \langle 2367 \rangle \langle 3456 \rangle}$$

```

Figure A.4: $\mathcal{A}_{10}^{(5)} \left(\psi_{+1/2}^{(1)}, \psi_{+1/2}^{(1)}, \psi_{+1/2}^{(1)}, \psi_{+1/2}^{(1)}, \psi_{-1/2}^{(123)}, \psi_{-1/2}^{(234)}, \psi_{-1/2}^{(234)}, \psi_{-1/2}^{(234)}, \psi_{-1/2}^{(234)}, \psi_{+1/2}^{(4)} \right)$.

An example 10-point N^3 MHV helicity-amplitude involving only gluinos.

```
In[1]:= Amp[{1},{1},{1},{1},{1,2,3},{2,3,4},{2,3,4},{2,3,4},{2,3,4},{4}];
        %//twistorSimplify//nice
Out[1]:= 
$$\frac{\langle 56 \rangle \langle 67 \rangle^2 \langle 78 \rangle^2 \langle 89 \rangle^2 \langle 1239 \rangle \langle 2348 \rangle \langle 3457 \rangle}{\langle 101 \rangle \langle 1289 \rangle \langle 2378 \rangle \langle 2389 \rangle \langle 3467 \rangle \langle 3478 \rangle \langle 4567 \rangle}$$

```

but we hope they are sufficiently intuitive to be clear by example. Examples of how these more general helicity-component amplitudes can be specified are given in Figure A.3, which shows an 8-point N^2 MHV helicity-amplitude involving 6 gluinos and 2 squarks, and Figure A.4, which shows a 10-point N^3 MHV amplitude involving 10 gluinos. These examples also illustrate the general-purpose function ‘twistorSimplify,’ which can often greatly simplify momentum-twistor formulae.

This Chapter is outlined as follows. In the next section we will review the kinematics of momentum-twistors and their connection to ordinary four-momenta and spinor-helicity variables. In section A.3, we review the tree-level BCFW recursion-relations as a statement about contour integrals in the momentum-twistor Grassmannian, [18, 19], and describe a three-parameter family of recursive ‘schemes’ in which the BCFW recursion relations can be implemented. In section A.4 we describe the basic use of the `bcfw` package along with its principle functions. (A more thorough walk-through, containing numerous example computations, can be found in the MATHEMATICA notebook `bcfw-v0-walk-through.nb` distributed alongside the `bcfw` package—attached to the submission file to the arXiv for [137].)

A.2 Kinematics: Momenta to Momentum-Twistors (and Back)

By default, all tree-amplitudes generated by the `bcfw` package are handled internally as purely-holomorphic functions of the momentum-twistor variables $\{Z_a\}$ introduced by Andrew Hodges in [20], together with an overall MHV-amplitude pre-factor which also depends on what is known as the ‘infinity (bi-)twistor,’ I_∞ , which associates with each momentum-twistor Z_a a Lorentz spinor $\lambda_a^{\alpha=1,2}$ in the fundamental representation of $SL_2(\mathbb{C})$. In addition to the many theoretical advantages of working with momentum-twistors, there are many indications that tree amplitudes are most compactly-written and most efficiently-evaluated in terms of momentum-twistors. But before we review this relatively novel formalism, we should reiterate that `bcfw` is fully-equipped to work with kinematics specified in terms of four-momenta or spinor-helicity variables (or momentum-twistors, of course), and can convert momentum-twistor formulae into those involving spinor-helicity variables and dual coordinates (but at a substantial cost in efficiency). Because of this, `bcfw` should be relatively easy to incorporate into other computational frameworks.

The connection between ordinary four-momenta p^μ and momentum-twistors starts with the association of a (Hermitian) matrix $p^{\alpha\dot{\alpha}}$ with each (real) four-momentum p^μ ,

$$p^\mu \mapsto p^{\alpha\dot{\alpha}} \equiv p^\mu \sigma_\mu^{\alpha\dot{\alpha}} = \begin{pmatrix} p_0 + p_3 & p_1 - ip_2 \\ p_1 + ip_2 & p_0 - p_3 \end{pmatrix}. \quad (\text{A.2.2})$$

Noticing that $p^\mu p_\mu = \det(p^{\alpha\dot{\alpha}})$, it follows that light-like momenta are represented by matrices with vanishing determinant. Any such matrix can be written as an outer-product,

$$\det(p^{\alpha\dot{\alpha}}) = 0 \iff p^{\alpha\dot{\alpha}} \equiv \lambda^\alpha \tilde{\lambda}^{\dot{\alpha}}, \quad (\text{A.2.3})$$

where λ and $\tilde{\lambda}$ are the famous *spinor-helicity* variables. For real momenta, it is easy to see that $\tilde{\lambda}^{\dot{\alpha}} = \pm (\lambda^\alpha)^*$, where the sign is determined by whether p^μ has positive or negative energy, respectively. Of course, this identification is only defined up-to an arbitrary phase: $\lambda \mapsto e^{i\theta} \lambda, \tilde{\lambda} \mapsto e^{-i\theta} \tilde{\lambda}$. Such re-phasing is induced by the action of little-group for massless particles in four-dimensions.

One of the principle advantages to working with spinor-helicity variables is that any function built out of the $SL_2(\mathbb{C})$ -invariants

$$\begin{aligned} \langle \lambda_a \lambda_b \rangle &\equiv \langle ab \rangle \equiv \det(\lambda_a \lambda_b) = \begin{vmatrix} \lambda_a^1 & \lambda_b^1 \\ \lambda_a^2 & \lambda_b^2 \end{vmatrix}, \\ \text{and} \quad [\tilde{\lambda}_a \tilde{\lambda}_b] &\equiv [ab] \equiv \det(\tilde{\lambda}_a \tilde{\lambda}_b) = \begin{vmatrix} \tilde{\lambda}_a^1 & \tilde{\lambda}_b^1 \\ \tilde{\lambda}_a^2 & \tilde{\lambda}_b^2 \end{vmatrix}, \end{aligned} \tag{A.2.4}$$

will automatically be Lorentz-invariant up to little-group re-phasing. Amplitudes involving massless particles, therefore, when written in terms of spinor-helicity variables, will be functions with uniform weight under $\lambda_a \mapsto u\lambda_a$ (with weight equal to minus twice the helicity of particle a).

The next step along the road from momenta to momentum-twistors are *dual coordinates* $x_a^{\alpha\dot{\alpha}}$ (also known as *region momenta*) defined (implicitly) through the identification

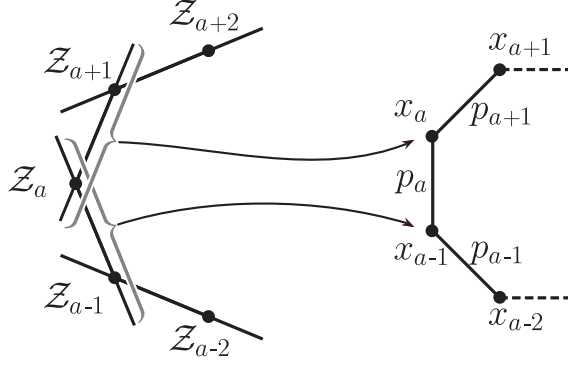
$$p_a \equiv x_a - x_{a-1}. \tag{A.2.5}$$

(Whenever it is necessary to fix a convention, we will choose x_1 to be the origin of dual coordinate space.) One of the most important recent discoveries regarding scattering amplitudes in $\mathcal{N} = 4$ SYM is that, after dividing by the n -point MHV tree-amplitude, scattering amplitudes in $\mathcal{N} = 4$ are not just superconformally-invariant in ordinary spacetime, but are also superconformally-invariant with respect to these dual-coordinates, [8, 9], and this is made manifest term-by-term in BCFW, [50]. The existence of a conformal symmetry on this dual space led Andrew Hodges to propose in [20] that amplitudes be described in the twistor-space associated with these dual coordinates; the twistor space of dual-coordinates is known as *momentum twistor* space.

Because each pair of *consecutive* dual coordinates are null-separated (the momenta being on-shell), the null-line joining them corresponds to a single momentum-twistor. And because the pair of dual coordinates (x_a, x_{a-1}) encode the null-momentum p_a , it is natural to call the momentum-twistor associated with this null-line ‘ Z_a ’. Making this identification will associate the line (Z_a, Z_{a-1}) in momentum-twistor space with the point x_{a-1} , and the line (Z_{a+1}, Z_a) with the point x_a ; that these two lines intersect at the twistor Z_a reflects the fact that the points x_a and x_{a-1} are null-separated.

Using the conventions just established, we canonically associate a momentum-twistor

Figure A.5: The map connecting momentum-twistor variables and dual-coordinates.



Z_a to each momentum p_a according to the rule,

$$p_a = \lambda_a \tilde{\lambda}_a = x_a - x_{a-1} \quad \Longleftrightarrow \quad Z_a \equiv \begin{pmatrix} \lambda_a^\alpha \\ x_a \underline{\dot{\alpha}} \lambda_a^\alpha \end{pmatrix} \equiv \begin{pmatrix} \lambda_a^\alpha \\ \mu_a^{\dot{\alpha}} \end{pmatrix}. \quad (\text{A.2.6})$$

Notice that our convention of choosing x_1 as the origin of dual-coordinate space trivially fixes $\mu_1 = \begin{pmatrix} 0 \\ 0 \end{pmatrix}$. Moreover, because this implies that $p_2 = \lambda_2 \tilde{\lambda}_2 = x_2 - x_1 = x_2$, we see that $\mu_2 = x_2 \underline{\dot{\alpha}} \lambda_2^\alpha (\propto \langle \lambda_2 \lambda_2 \rangle) = \begin{pmatrix} 0 \\ 0 \end{pmatrix}$ as well. Working out the rest of this map explicitly—as was described in Chapter 1—we find that we may write

$$\mu_a = (\mathbb{Q}_F^{-1})_{ab} \tilde{\lambda}_b, \quad \text{where} \quad (\mathbb{Q}_F^{-1})_{ab} = \begin{pmatrix} 0 & 0 & 0 & \cdots & \cdots & \cdots & 0 \\ 0 & 0 & 0 & 0 & \cdots & \cdots & 0 \\ 0 & \langle 23 \rangle & 0 & 0 & \ddots & \ddots & 0 \\ 0 & \langle 24 \rangle & \langle 34 \rangle & 0 & 0 & \ddots & 0 \\ 0 & \langle 25 \rangle & \langle 35 \rangle & \langle 45 \rangle & 0 & \ddots & 0 \\ \vdots & \vdots & \vdots & \vdots & \ddots & \ddots & 0 \\ 0 & \langle 2n \rangle & \langle 3n \rangle & \langle 4n \rangle & \cdots & \langle n-1n \rangle & 0 \end{pmatrix}. \quad (\text{A.2.7})$$

$(\mathbb{Q}_F^{-1})_{ab}$ is so-named because it is a ‘Formal-inverse’ of the (singular) map \mathbb{Q}_{ab} which relates the μ ’s to the $\tilde{\lambda}$ ’s according to $\tilde{\lambda}_a = \mathbb{Q}_{ab} \mu_b$ where

$$\mathbb{Q}_{ab} = \begin{pmatrix} \frac{\langle 2n \rangle}{\langle n1 \rangle \langle 12 \rangle} & \frac{1}{\langle 12 \rangle} & 0 & \cdots & \cdots & \cdots & \frac{1}{\langle n1 \rangle} \\ \frac{1}{\langle 12 \rangle} & \frac{\langle 31 \rangle}{\langle 12 \rangle \langle 23 \rangle} & \frac{1}{\langle 23 \rangle} & 0 & \cdots & \cdots & 0 \\ 0 & \frac{1}{\langle 23 \rangle} & \frac{\langle 42 \rangle}{\langle 23 \rangle \langle 34 \rangle} & \frac{1}{\langle 34 \rangle} & 0 & \ddots & \vdots \\ \vdots & 0 & \frac{1}{\langle 34 \rangle} & \frac{\langle 53 \rangle}{\langle 34 \rangle \langle 45 \rangle} & \frac{1}{\langle 45 \rangle} & \ddots & 0 \\ 0 & \vdots & \ddots & \ddots & \ddots & \ddots & \frac{1}{\langle n-1n \rangle} \\ \frac{1}{\langle n1 \rangle} & 0 & \cdots & \cdots & 0 & \frac{1}{\langle n-1n \rangle} & \frac{\langle 1n-1 \rangle}{\langle n-1n \rangle \langle n1 \rangle} \end{pmatrix}. \quad (\text{A.2.8})$$

It is worth emphasizing that although Q_{ab} is singular, our conventions ensure that $\mu_a = (Q_F^{-1})_{ab} Q_{bc} \mu_c$, and $\tilde{\lambda}_a = Q_{ab} (Q_F^{-1})_{bc} \tilde{\lambda}_c$, which justifies calling $(Q_F^{-1})_{ab}$ the ‘inverse’ of Q_{ab} .

What we have described so far have been ordinary (Bosonic) momentum twistors; these have a natural extension to momentum-*supertwistors* defined by

$$\mathcal{Z}_a \equiv \begin{pmatrix} Z_a \\ \eta_a \end{pmatrix} \equiv \begin{pmatrix} \lambda_a \\ \mu_a \\ \eta_a \end{pmatrix}, \quad (\text{A.2.9})$$

where the Fermionic η -components of the supertwistors are related to the ordinary Fermionic parameters $\tilde{\eta}$ which define each superfield (A.1.1) in precisely the same way that the μ variables are related to the $\tilde{\lambda}$ variables. To summarize, the components of the momentum-supertwistors are related to the ordinary spinor-helicity variables via

$$\lambda_a^{\alpha=1,2} = Z_a^{1,2}, \quad \text{and} \quad \mu_a^{\dot{\alpha}=1,2} = Z_a^{3,4}, \quad (\text{A.2.10})$$

$$\tilde{\lambda}_a = Q_{ab} \mu_b, \quad \text{and} \quad \mu_a = (Q_F^{-1})_{ab} \tilde{\lambda}_b, \quad (\text{A.2.11})$$

$$\tilde{\eta}_a = Q_{ab} \eta_b, \quad \text{and} \quad \eta_a = (Q_F^{-1})_{ab} \tilde{\eta}_b. \quad (\text{A.2.12})$$

Just as spinor-helicity variables went a long way toward trivializing Lorentz-invariance, momentum-twistors essentially trivialize momentum conservation and dual conformal invariance. Momentum conservation is trivial because *any* set of n (ordered) momentum twistors will define n null-separated region momenta through the maps given above. Furthermore, up to little-group rescaling, dual-conformal transformations act on momentum-twistors as $SL_4(\mathbb{C})$ transformations, meaning that any function of the (only) natural $SL_4(\mathbb{C})$ -invariant product—namely, ‘det’—will automatically be dual-conformally invariant if it has appropriate little-group weights. This suggests the natural generalization of the ‘angle-bracket’ $\langle ab \rangle$ defined for 2-spinors above would be the momentum-twistor four-bracket $\langle \cdot \cdot \cdot \cdot \rangle$ defined according to

$$\text{ab}[a, b, c, d] \iff \langle a b c d \rangle \equiv \begin{vmatrix} Z_a^1 & Z_b^1 & Z_c^1 & Z_d^1 \\ Z_a^2 & Z_b^2 & Z_c^2 & Z_d^2 \\ Z_a^3 & Z_b^3 & Z_c^3 & Z_d^3 \\ Z_a^4 & Z_b^4 & Z_c^4 & Z_d^4 \end{vmatrix} \iff \text{Det}[\text{Zs}[\{\{a, b, c, d\}\}]]; \quad (\text{A.2.13})$$

So it would appear that, including also the MHV-amplitude pre-factor, all amplitudes can be written in terms of four-brackets $\langle \cdot \cdot \cdot \cdot \rangle$ and two-brackets $\langle \cdot \cdot \rangle$; but it is easy to see that the latter is just a special-case of the former. Notice that the map connecting a momentum-twistor Z_a and ordinary spinor-helicity variables, equation (A.2.6), is a *component-wise* definition. Because any such definition is manifestly *not* $SL_4(\mathbb{C})$ -invariant, this map breaks dual-conformal invariance. We can make this clear by choosing to write I_∞ explicitly, defining two-brackets via,

$$\text{ab}[\mathbf{a}, \mathbf{b}] \iff \langle a b \rangle \equiv \langle a b I_\infty \rangle \equiv \begin{vmatrix} Z_a^1 & Z_b^1 & 0 & 0 \\ Z_a^2 & Z_b^2 & 0 & 0 \\ Z_a^3 & Z_b^3 & 1 & 0 \\ Z_a^4 & Z_b^4 & 0 & 1 \end{vmatrix} \iff \text{Det}[\text{Zs}[[\{\mathbf{a}, \mathbf{b}\}, 1; ; 2]]]. \quad (\text{A.2.14})$$

Because momentum twistors are still somewhat unfamiliar to many researchers, we should mention that there is a completely canonical map between four-brackets and ordinary spinor-helicity variables which follows directly from definition (A.2.6). Rather than giving this map for a completely general four-bracket, we will see in the next section that tree-level BCFW only generates formulae involving four-brackets which involve at least one pair of adjacent momentum-twistors—that is, tree amplitudes involve only four-brackets of the form $\langle a j j+1 b \rangle$. Using (A.2.6), it is easy to see that

$$\langle a j j+1 b \rangle = \langle j+1 j \rangle \langle a | x_{a j} x_{j b} | b \rangle, \quad (\text{A.2.15})$$

where we have used the notation $x_{a b} \equiv x_b - x_a$.⁴ This further simplifies in the special case of a four-bracket involving two pairs of adjacent momentum-twistors,

$$\begin{aligned} \langle a-1 a b b+1 \rangle &= \langle a-1 a \rangle \langle b b+1 \rangle (p_a + p_{a+1} + \dots + p_{b-1} + p_b)^2 \\ &\equiv \langle a-1 a \rangle \langle b b+1 \rangle s_{a\dots b} \equiv \langle a-1 a \rangle \langle b b+1 \rangle x_{a-1 b}^2. \end{aligned} \quad (\text{A.2.16})$$

It is worth mentioning that the fact that tree-level BCFW involves only four-brackets of the form $\langle a j j+1 b \rangle$ means that in general, every superamplitude in $\mathcal{N} = 4$ involves strictly fewer than $\binom{n}{4}$ kinematical invariants.

A.3 Trees as Contour Integrals in the Grassmannian

The `bcfw` package describes each n -point N^k MHV tree-amplitude as a contour integral in the Grassmannian $G(k, n)$ of k -planes in n -dimensions (see [10, 12, 15, 18]),

⁴This notation (and sign-convention) becomes clearer if $x_{a b}$ is viewed as the vector from x_a to x_b .

$$\begin{aligned}
\mathcal{A}_n^{(m=k+2)} &= \frac{1}{\text{vol}(GL_k)} \oint_{\Gamma_{n,m}} \frac{d^{n \times k} D_{\alpha a} \prod_{\alpha=1}^k \delta^{4|4}(D_{\alpha a} \mathcal{Z}_a)}{(1 \cdots k)(2 \cdots k+1) \cdots (n \cdots k-1)}, \\
&= \sum_{\gamma \in \Gamma_{n,m}} \left\{ \frac{1}{\text{vol}(GL_k)} \oint_{|D_{\alpha a} - (\text{dMatrix}_\gamma)| = \epsilon} \frac{d^{n \times k} D_{\alpha a} \prod_{\alpha=1}^k \delta^{4|4}(D_{\alpha a} \mathcal{Z}_a)}{(1 \cdots k)(2 \cdots k+1) \cdots (n \cdots k-1)} \right\}, \quad (\text{A.3.17}) \\
&= \sum_{\gamma \in \Gamma_{n,m}} \left\{ (\text{residue}_\gamma) \prod_{\alpha=1}^k \delta^{0|4} \left((\text{dMatrix}_\gamma)_{\alpha a} \eta_a \right) \right\},
\end{aligned}$$

where we have used the scripted ‘ $\mathcal{A}_n^{(m)}$ ’, to indicate that this is the tree-amplitude *divided by the (supersymmetric) n -point MHV-amplitude*⁵,

$$\mathcal{A}_n^{(2)} = \frac{\prod_{\alpha=1}^2 \delta^{0|4}(\lambda_{\tilde{a}}^\alpha \tilde{\eta}_a)}{\langle 1 2 \rangle \langle 2 3 \rangle \cdots \langle n-1 n \rangle \langle n 1 \rangle}. \quad (\text{A.3.18})$$

As all the terms generated by the BCFW recursion relations are Yangian-invariant [49], they are each residues of the integral (A.3.17), [11, 68]—computed for contours which ‘encircle’ isolated poles in the Grassmannian. Therefore, each term can be described as a part of the complete ‘tree-contour’ $\Gamma_{n,m}$. This helps to explain the nomenclature of `bcfw`, where each superamplitude stored as a function called ‘`treeContour.`’ Notice that the coefficients appearing in the Fermionic δ -functions of (A.3.17), `dMatrix $_\gamma$` , directly represent the isolated *points* in $G(k, n)$ where the integral (A.3.17) develops a pole (of the appropriate co-dimension) which is to be ‘encircled’ by the contour $\Gamma_{n,m}$, each giving rise to a particular residue of the integral. Of course, knowing the poles—that is, knowing *just* the list of points in $G(k, n)$ (and the orientation of the contour about each)—is sufficient to calculate each residue using the contour integral (A.3.17); but it turns out that this is in fact unnecessary for our purposes: the BCFW recursion relations directly calculate the *residues* themselves in a canonical way.

As described in Chapter 4, when expressed in terms of momentum-twistor variables, the tree-level BCFW recursion relations become the following.

$$\begin{aligned}
\mathcal{A}_n^{(m=k+2)} &= \mathcal{A}_{n-1}^{(m)} \\
&+ \sum_{\substack{n_L, m_L \\ n_R, m_R}} \mathcal{A}_{n_L}^{(m_L)}(1, \dots, j, \widehat{j+1}) R[n-1 \ n \ 1 \ j \ j+1] \mathcal{A}_{n_R}^{(m_R)}(\widehat{j}, j+1, \dots, n-1, \widehat{n}),
\end{aligned} \quad (\text{A.3.19})$$

⁵Here, we are not including the ordinary momentum-conserving δ -function, $\delta^4(\lambda_a \tilde{\lambda}_a)$, because all momentum-twistor amplitudes are automatically on its support.

where,⁶

$$\begin{aligned}
\widehat{\mathcal{Z}}_{j+1} &= (j+1 j) \cap (n-1 n 1) \equiv \mathcal{Z}_{j+1} + \mathcal{Z}_j \frac{\langle j+1 n-1 n 1 \rangle}{\langle n-1 n 1 j \rangle}, \\
\widehat{\mathcal{Z}}_j &= (j j+1) \cap (n-1 n 1) \equiv \mathcal{Z}_j + \mathcal{Z}_{j+1} \frac{\langle j n-1 n 1 \rangle}{\langle n-1 n 1 j+1 \rangle}, \\
\widehat{\mathcal{Z}}_n &= (n n-1) \cap (1 j j+1) \equiv \mathcal{Z}_n + \mathcal{Z}_{n-1} \frac{\langle n 1 j j+1 \rangle}{\langle 1 j j+1 n-1 \rangle},
\end{aligned} \tag{A.3.20}$$

and

$$R[abcde] \equiv \frac{\delta^{0|4} \left(\eta_a \langle bcde \rangle + \eta_b \langle cdea \rangle + \eta_c \langle deab \rangle + \eta_d \langle eabc \rangle + \eta_e \langle abcd \rangle \right)}{\langle abcd \rangle \langle bcde \rangle \langle cdea \rangle \langle deab \rangle \langle eabc \rangle}. \tag{A.3.21}$$

This tree-level BCFW-bridge is illustrated in Figure A.6.

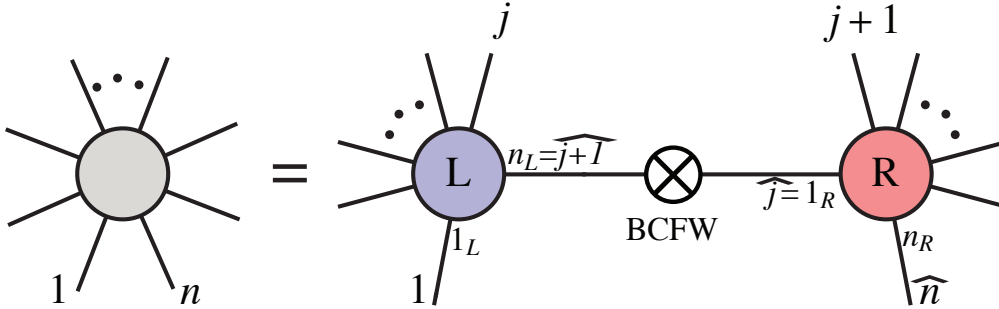


Figure A.6: The momentum-twistor BCFW-bridge (without any rotations).

The shifted momentum-twistors in (A.3.20) should be understood supersymmetrically, and the shifted Fermionic η -variables result in a shifted matrix of coefficients. Specifically, for terms bridged in the recursion, the residues (evaluated with shifted arguments) are simply multiplied, and the supersymmetric $\delta^{0|4}$'s combine according to:

⁶It is worth noting that $\widehat{\mathcal{Z}}_{j+1}$ and $\widehat{\mathcal{Z}}_j$ are projectively equivalent; the reason for distinguishing them as in (A.3.20) is to preserve canonical little-group assignments.

$$\underbrace{\begin{pmatrix} d_{1,1}^L & \cdots & \cdots & \cdots & d_{1,n_L}^L \\ \vdots & \vdots & L & \vdots & \vdots \\ d_{k_L,1}^L & \cdots & \cdots & \cdots & d_{k_L,n_L}^L \end{pmatrix} \otimes_{\text{BCFW}} \begin{pmatrix} d_{1,1}^R & \cdots & \cdots & \cdots & d_{1,n_R}^R \\ \vdots & \vdots & R & \vdots & \vdots \\ d_{k_R,1}^R & \cdots & \cdots & \cdots & d_{k_R,n_R}^R \end{pmatrix}}$$

$$\left(\begin{array}{cccccc} \begin{pmatrix} d_{1,1}^L & d_{1,2}^L \cdots d_{1,j-1}^L & (d_{1,j}^L + \zeta_{j+1}^L d_{1,j+1}^L) & d_{1,j+1}^L \\ \vdots & \vdots & L & \vdots \\ d_{k_L,1}^L & d_{k_L,2}^L \cdots d_{k_L,j-1}^L & (d_{k_L,j}^L + \zeta_{j+1}^L d_{k_L,j+1}^L) & d_{k_L,j+1}^L \end{pmatrix} & 0 & \cdots & 0 & 0 & 0 \\ \langle j j+1 n-1 n \rangle & 0 & \cdots & 0 & \langle j+1 n-1 n 1 \rangle & \langle n-1 n 1 j \rangle & 0 & \cdots & 0 & \langle n 1 j j+1 \rangle & \langle 1 j j+1 n-1 \rangle \\ 0 & 0 & \cdots & 0 & \begin{pmatrix} d_{1,j}^R & (d_{1,j+1}^R + \zeta_j^R d_{1,j}^R) & d_{1,j+2}^R & \cdots & d_{1,n-2}^R & (d_{1,n-1}^R + \zeta_n^R d_{1,n}^R) & d_{1,n}^R \\ \vdots & \vdots & \vdots & R & \vdots & \vdots & \vdots \\ d_{k_R,j}^R & (d_{k_R,j+1}^R + \zeta_j^R d_{k_R,j}^R) & d_{k_R,j+2}^R & \cdots & d_{k_R,n-2}^R & (d_{k_R,n-1}^R + \zeta_n^R d_{k_R,n}^R) & d_{k_R,n}^R \end{pmatrix} \\ \vdots & \vdots & \ddots & \vdots & \vdots & \vdots & \vdots \\ 0 & 0 & \cdots & 0 & \vdots & \vdots & \vdots \end{array} \right)$$

with

$$\zeta_{j+1}^L \equiv \frac{\langle j+1 n-1 n 1 \rangle}{\langle n-1 n 1 j \rangle}, \quad \zeta_j^R \equiv \frac{\langle j n-1 n 1 \rangle}{\langle n-1 n 1 j+1 \rangle}, \quad \text{and} \quad \zeta_n^R \equiv \frac{\langle n 1 j j+1 \rangle}{\langle 1 j j+1 n-1 \rangle}. \quad (\text{A.3.22})$$

Thus, the tree-level BCFW recursion relations amount to little more than cutting-and-pasting (and re-labeling) matrices, allowing most amplitudes of interest to be recursed in essentially real-time.

I. Generalized BCFW Recursion Schemes

Although the recursive BCFW formula (A.3.19) fixes $\mathcal{A}_n^{(m)}$ given all amplitudes with strictly fewer particles, (A.3.19) by itself does not uniquely identify any *particular* sum of residues. The reason for this is simple (and completely trivial): the lower-point amplitudes appearing in the recursion (A.3.19) can be written in any way whatsoever—with many choices corresponding to all the representatives $\Gamma_{n,m}$ of each tree-contours' homology-class. Said another way, in order to use (A.3.19) to obtain *a particular* contour for the n -point amplitude, it is necessary to know the *particular, representative* contours for all lower-point amplitudes; but these lower-point contours need-not have been recursed in any particular way. In order to obtain *an explicit, representative contour* through the use of the BCFW recursion relations—i.e. using (A.3.19)—it is necessary to give a prescription for how *all* lower-point amplitudes are also to be recursed.

One especially natural prescription would be to recurse *all* lower-point amplitudes *exactly* according to equation (A.3.19)—with each n -point amplitude having ordered-

arguments $(1, \dots, n)$. This is the default recursive scheme used by `bcfw` and is obtained with the function `treeContour[n,m]=generalTreeContour[0,0,0][n,m]`. This scheme follows from Figure A.6 where each lower-point amplitude is recursed precisely according to Figure A.6.

Among the many recursive prescriptions one could imagine, a remarkable degree of complexity results from simply allowing for arbitrary (and separate) ‘rotations’ of the amplitudes appearing on the left- and right-hand sides of the BCFW bridge,⁷ and also allowing for an over-all rotation of the the n -point amplitude being recursed—or equivalently, which legs are deformed in the recursion. Specifically, letting g denote a cyclic-rotation of (an explicit formula) of an amplitude $g : \mathcal{A}_n(1, \dots, n) \mapsto \mathcal{A}_n(2, \dots, n, 1)$; then the class of generalized BCFW recursion schemes implemented in `bcfw` is given by,

$$\text{generalTreeContour}[\mathbf{a}, \mathbf{b}, \mathbf{c}][\mathbf{n}, \mathbf{m}] : g^{-\mathbf{c}}[\mathcal{A}_n^{(m)}]_{\{\mathbf{a}, \mathbf{b}, \mathbf{c}\}} = g^{\mathbf{a}}[\mathcal{A}_{n-1}^{(m)}] + \sum_{\substack{n_L, m_L \\ n_R, m_R}} g^{\mathbf{a}}[\mathcal{A}_{n_L}^{(m_L)}] \otimes_{\text{BCFW}} g^{\mathbf{b}}[\mathcal{A}_{n_R}^{(m_R)}],$$

where, as with the default contour prescription, *this same recursive rule is used for every lower-point amplitude*. This is illustrated in Figure A.7. By varying the parameters

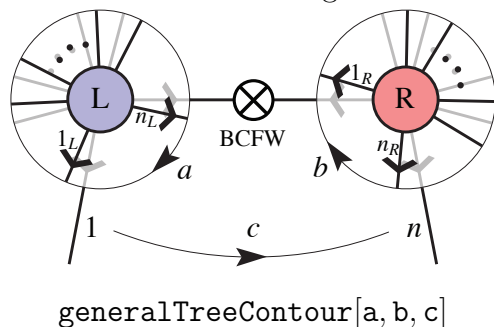


Figure A.7: An illustration of the generalized BCFW recursion-schemes used by `bcfw`’s function `generalTreeContour`[$\mathbf{a}, \mathbf{b}, \mathbf{c}$]. Here, the legs being deformed in the left-hand amplitude, for example, should be thought-of as being actively ‘rotated’ clockwise by an amount ‘ \mathbf{a} ’ relative to the default recursive scheme.

{ $\mathbf{a}, \mathbf{b}, \mathbf{c}$ }, one can obtain a very wide-array of analytic formulae for any particular helicity amplitude. It could be that more general recursion-schemes will eventually prove useful,⁸

⁷When making these rotations, the homogeneous term in the recursion, $\mathcal{A}_{n-1}^{(m)}$, must be considered an amplitude occurring on the *left*.

⁸For example, one could consider recursive schemes which make use of the parity-conjugate version of the BCFW-bridge, which make use of reflected (as well as rotated) lower-point amplitudes, or which allow for rotations of lower-point amplitudes to vary as a function of recursive depth. None of these generalizations are necessary for $n \leq 9$, and we suspect that this is true generally.

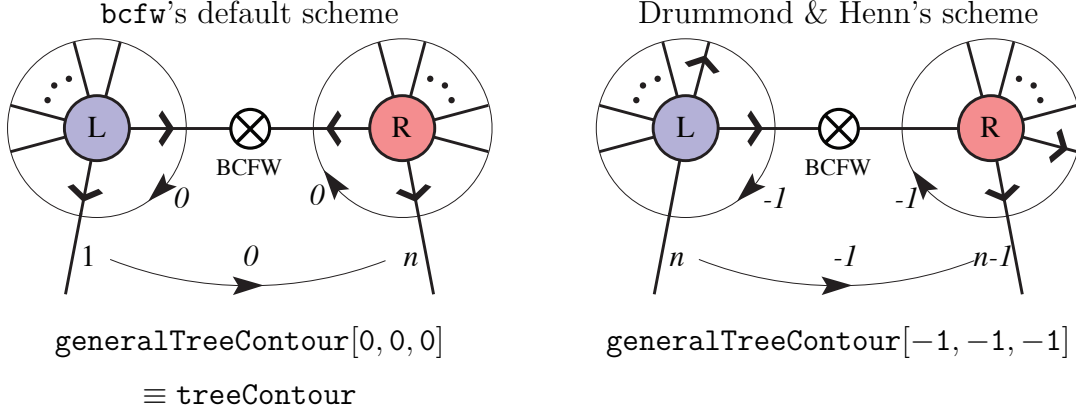
but as far as we have been able to check, this class of recursion schemes has proven in some sense exhaustive. Specifically, we have checked that for up to 9-particles, this three-parameter family is sufficient to generate *all* linearly independent representations of superamplitudes. For example, there turn out to be 74 linearly-independent formulae for the 8-point N^2 MHV tree amplitude, involving 176 Yangian-invariants. All of these formulae are worked-out explicitly as part of the demonstration file for the `bcfw` package.

There are three principle reasons why researchers may find this broad-class of tree-amplitude formulae useful. First, knowing the range of possible tree-amplitude formulae helps one build intuition about amplitudes in general, and allows one to separate general properties about amplitudes from the peculiarities of particular formulae. Secondly, having many different representations available frees one from using unnecessarily inefficient representations of particular helicity amplitudes. For example, it is sometimes heard that “the” BCFW-formula (with the default scheme implicit) for the split-helicity amplitude is maximally-concise⁹ (meaning that a maximal number of terms in the tree-contour vanish); however, fixing a recursive scheme, this is true for at most *one particular* split-helicity amplitude—the other split-helicity amplitudes including some for which almost none of the BCFW terms vanish. And so, it should be possible to use the variety of representations that can be generated by `bcfw` to find a ‘best-case’ formula for any particular helicity amplitude of interest. And finally, because the BCFW formulae obtained using different recursive schemes often have very few spurious poles in common, it may be possible to combine a variety of BCFW formulae to avoid encountering spurious poles while generating Monte-Carlo events for phase-space integration, for example.

It may be helpful to know that the particular recursive-scheme used by Drummond and Henn to solve the BCFW recursion relations in [50], corresponds to `generalTreeContour[-1,-1,-1]`; this scheme is illustrated in Figure A.8.

⁹This observation is true for the default recursion-scheme used by `bcfw`; in particular, the helicity component $\mathcal{A}_n^{(m)}(-, \dots, -, +, \dots, +)$ of `generalTreeContour[0,0,0][n,m]` is the gluonic amplitude with the fewest number of non-vanishing BCFW terms; but this feature is observed for very few of the more general recursive schemes.

Figure A.8: Examples of particular recursion schemes, highlighting how the lower-point amplitudes are rotated.



II. Extracting Helicity Component-Amplitudes from Tree-Contours

To compute a particular helicity amplitude from the supersymmetric contour integral, one need only project-out the desired Grassmann components, as dictated by the definition of the external superfields Φ_a^+ given in equation (A.1.1). Of course, the component fields of Φ_a^+ are given in terms of $\tilde{\eta}$ -variables, which, as described in section A.2, are related to the momentum-supertwistor Grassmann parameters η_a via

$$\tilde{\eta}_a = (\mathbf{Q}_F^{-1})_{ab} \eta_b. \quad (\text{A.3.23})$$

Because the matrix of coefficients of the Grassmann η 's for each `residue` is nothing but its corresponding `dMatrix`, we have that

$$D_{\alpha a} \eta_a = D_{\alpha b} (\mathbf{Q}_F^{-1})_{ba} \tilde{\eta}_a \equiv \hat{C}_{\alpha a} \tilde{\eta}_a. \quad (\text{A.3.24})$$

In terms of the Grassmannian integral (A.3.17), this means that we may write

$$\begin{aligned} (\text{residue}) \prod_{\alpha=1}^k \delta^{0|4} ((\mathbf{dMatrix})_{\alpha a} \eta_a) &= (\text{residue}) \prod_{\alpha=1}^k \delta^{0|4} ((\mathbf{dMatrix})_{\alpha b} (\mathbf{QabInverse}[\mathbf{n}])_{ba} \tilde{\eta}_a) \\ &\equiv (\text{residue}) \prod_{\alpha=1}^k \delta^{0|4} ((\mathbf{cHatMatrix})_{\alpha a} \tilde{\eta}_a). \end{aligned} \quad (\text{A.3.25})$$

Upon explicitly including the full MHV super-amplitude we obtain,

$$\begin{aligned} &\Rightarrow \frac{(\text{residue})}{\langle 12 \rangle \cdots \langle n1 \rangle} \prod_{\alpha=1}^2 \delta^{0|4} (\lambda_a^\alpha \tilde{\eta}_a) \prod_{\alpha=1}^k \delta^{0|4} ((\mathbf{cHatMatrix})_{\alpha a} \tilde{\eta}_a) \\ &\equiv \frac{(\text{residue})}{\langle 12 \rangle \cdots \langle n1 \rangle} \prod_{\hat{\alpha}=1}^{k+2} \delta^{0|4} (\mathbf{cMatrix}_{\hat{\alpha} a} \tilde{\eta}_a), \end{aligned} \quad (\text{A.3.26})$$

where we have defined the matrix $C_{\hat{\alpha}a}$ according to

$$C_{\hat{\alpha}a} \equiv \begin{pmatrix} \hat{C}_{11} & \hat{C}_{12} & \cdots & \hat{C}_{1n-1} & \hat{C}_{1n} \\ \vdots & \vdots & \ddots & \vdots & \vdots \\ \hat{C}_{k1} & \hat{C}_{k2} & \cdots & \hat{C}_{kn-1} & \hat{C}_{kn} \\ \hline \lambda_1^1 & \lambda_2^1 & \cdots & \lambda_{n-1}^1 & \lambda_n^1 \\ \lambda_1^2 & \lambda_2^2 & \cdots & \lambda_{n-1}^2 & \lambda_n^2 \end{pmatrix} \equiv \left(\frac{\hat{C}_{\alpha a}}{\lambda_a^\alpha} \right). \quad (\text{A.3.27})$$

It is worth noting that just as each **dMatrix** represents an isolated *point* in the Grassmannian of k -planes in n -dimensions, each **cMatrix** gives an isolated *point* in the Grassmannian of $m(=k+2)$ -planes in n -dimensions. Indeed, these are the isolated poles ‘encircled’ by the (original) twistor-space Grassmannian contour-integral of [10],

$$\mathcal{A}_n^{(m=k+2)} = \frac{1}{\text{vol}(GL_m)} \oint_{\Gamma_{n,m}} \frac{d^{n \times m} C_{\hat{\alpha}a} \prod_{\hat{\alpha}=1}^m \delta^{4|4}(C_{\hat{\alpha}a} \mathcal{W}_a)}{(1 \cdots m)(2 \cdots m+1) \cdots (n \cdots m-1)}. \quad (\text{A.3.28})$$

The momentum-twistor Grassmannian integral (A.3.17) was derived from the original twistor-space integral (A.3.28) in [18], where it was shown how the MHV-prefactor arises naturally as *the Jacobian of the change-of-variables* in going from the (space-time) twistor-space variables \mathcal{W}_a to the momentum-twistor-space variables \mathcal{Z}_a .

Now, having the matrix of coefficients of the $\tilde{\eta}$ -variables, it is particularly simple to extract any helicity component amplitude. For example, pure-gluon amplitudes are given by

$$\begin{aligned} \mathcal{A}_n^{(m)}(\dots, j_1^-, \dots, j_m^-, \dots) &= \int d^{0|4} \tilde{\eta}_{j_1} \cdots d^{0|4} \tilde{\eta}_{j_m} \left[\mathcal{A}_n^{(m)} \right]; \\ &= \sum_{\gamma \in \Gamma_{n,m}} \frac{(\text{residue}_\gamma)}{\langle 12 \rangle \cdots \langle n1 \rangle} \left(\text{Det}[\text{cMatrix}_\gamma[[\text{All}, \{j_1, \dots, j_m\}]]] \right)^4. \end{aligned} \quad (\text{A.3.29})$$

More generally, each helicity amplitude can be ‘projected-out’ of the superamplitude by multiplying each residue in the tree-contour by the appropriate set of four $(m \times m)$ -minors of its corresponding matrix $C_{\hat{\alpha}a}$. The list of minors which project-out a particular helicity component-amplitude is given by the function `parseInput []`.

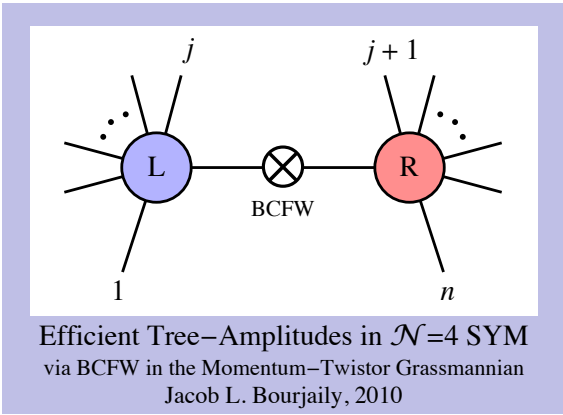
A.4 The bcfw MATHEMATICA Package

A separate MATHEMATICA notebook—distributed along with `bcfw.m`—has been prepared to introduce the reader to the many functions of `bcfw` and their primary usage. We hope that the demonstration notebook is sufficiently self-contained for most users. In this section, we briefly describe the basic algorithmic structures which underly the `bcfw` package, with an emphasis on the features that are likely to prove useful beyond the limited framework of MATHEMATICA.

I. Setup and Initialization

Initialization of the package is simple: so long as the file being used has been saved to the same directory as the package's source `bcfw.m`, one need only call the following:

```
In[1]:= SetDirectory[NotebookDirectory[]];
        <<bcfw.m

Out[1]:= 
```

II. Getting Started with Analytic Tree Amplitudes

To start gaining intuition for how helicity-amplitudes can be specified in `bcfw`, consider a very simple example: the 8-point MHV amplitude $\mathcal{A}_8^{(2)}(+, +, -, +, +, -, +, +)$. This amplitude can easily be found using `bcfw` through the command,

```
In[1]:= Amp[p, p, m, p, p, m, p, p]
Out[1]:= 
$$\frac{ab[3, 6]^4}{ab[1, 2]ab[2, 3]ab[3, 4]ab[4, 5]ab[5, 6]ab[6, 7]ab[7, 8]ab[8, 1]}$$

```

To make the result more aesthetically appealing, any output of `bcfw` can be wrapped by the function `nice[]` which formats the result so that it is more “human-readable.” For example, using `nice`, the above command would return:

```
In[1]:= Amp[p,p,m,p,p,m,p,p]//nice
Out[1]:= 
$$\frac{\langle 36 \rangle^4}{\langle 12 \rangle \langle 23 \rangle \langle 34 \rangle \langle 45 \rangle \langle 56 \rangle \langle 67 \rangle \langle 78 \rangle \langle 81 \rangle}$$

```

We have chosen to make `nice` formatting an `opt-in` option for users, so that the underlying structure is transparent at all times—and in order to avoid the pitfalls of conditional formatting in MATHEMATICA while maximizing the ease of symbolic manipulation.

Although the analytic formulae for tree amplitudes quickly become too long and complex for visual comprehension, `bcfw`'s function `Amp` will in fact write-out any amplitude. As one further example, consider the 6-point NMHV alternating helicity amplitude.

```
In[1]:= Amp[m,p,m,p,m,p]//nice
Out[1]:= 
$$\frac{\langle 15 \rangle^4 (\langle 35 \rangle \langle 1234 \rangle - \langle 34 \rangle \langle 1235 \rangle)^4}{\langle 12 \rangle \langle 23 \rangle \langle 34 \rangle \langle 45 \rangle \langle 56 \rangle \langle 61 \rangle \langle 1234 \rangle \langle 1235 \rangle \langle 1245 \rangle \langle 1345 \rangle \langle 2345 \rangle (\langle 13 \rangle \langle 56 \rangle \langle 1235 \rangle - \langle 15 \rangle (\langle 36 \rangle \langle 1235 \rangle + \langle 35 \rangle \langle 2361 \rangle))^4}$$


$$- \frac{\langle 12 \rangle \langle 23 \rangle \langle 34 \rangle \langle 45 \rangle \langle 56 \rangle \langle 61 \rangle \langle 1235 \rangle \langle 1256 \rangle \langle 1356 \rangle \langle 2356 \rangle \langle 2361 \rangle}{(\langle 13 \rangle \langle 56 \rangle \langle 1345 \rangle - \langle 15 \rangle (\langle 36 \rangle \langle 1345 \rangle + \langle 34 \rangle \langle 1356 \rangle + \langle 35 \rangle \langle 3461 \rangle))^4}$$


$$+ \frac{\langle 12 \rangle \langle 23 \rangle \langle 34 \rangle \langle 45 \rangle \langle 56 \rangle \langle 61 \rangle \langle 1345 \rangle \langle 1356 \rangle \langle 3456 \rangle \langle 3461 \rangle \langle 4561 \rangle}{(\langle 13 \rangle \langle 56 \rangle \langle 1345 \rangle - \langle 15 \rangle (\langle 36 \rangle \langle 1345 \rangle + \langle 34 \rangle \langle 1356 \rangle + \langle 35 \rangle \langle 3461 \rangle))^4}$$

```

We should emphasize, however, that direct evaluation of the formulae generated by `Amp` (or `AmpTerms`) are often *dramatically* less efficient than what can be obtained using `nAmp` (or `nAmpTerms`).¹⁰ This directly reflects the efficiency gained by the momentum-twistor Grassmannian representation of superamplitudes.¹¹

As described in the previous section, each superamplitude is represented by `bcfw` as a contour integral in the momentum-twistor Grassmannian (A.3.17). The particular representation of the n -particle $N^{(m-2)}$ MHV superamplitude derived via the BCFW recursion scheme with rotations `{a, b, c}` is obtained with the function `generalTreeContour[a, b, c][n, m]`

¹⁰This is true even with fairly intelligent caching. Because of this, researchers interested in transferring the formulae generated by `bcfw` to other frameworks should seriously consider using the *superamplitudes* directly.

¹¹To better understand this, observe that each `cMatrix` includes as its first k -rows the matrix `cHatMatrix=dMatrix.QabInverse[n]`; this introduces many new kinematical invariants into each term—the two-brackets—while simultaneously duplicating each column of `dMatrix` many times, greatly obfuscating an underlying simplicity with fundamentally redundant information.

Table A.2: 6-point NMHV superamplitude $\mathcal{A}_6^{(3)}$, given by `treeContour[6,3]`.

Name	residue	dMatrix
$R[1\ 2\ 3\ 4\ 5]$	$\frac{1}{\langle 1\ 2\ 3\ 4 \rangle \langle 2\ 3\ 4\ 5 \rangle \langle 3\ 4\ 5\ 1 \rangle \langle 4\ 5\ 1\ 2 \rangle \langle 5\ 1\ 2\ 3 \rangle \langle 1\ 2\ 3\ 4 \rangle}$	$(\langle 2\ 3\ 4\ 5 \rangle \langle 3\ 4\ 5\ 1 \rangle \langle 4\ 5\ 1\ 2 \rangle \langle 5\ 1\ 2\ 3 \rangle \langle 1\ 2\ 3\ 4 \rangle 0)$
$R[1\ 3\ 4\ 5\ 6]$	$\frac{1}{\langle 1\ 3\ 4\ 5 \rangle \langle 3\ 4\ 5\ 6 \rangle \langle 4\ 5\ 6\ 1 \rangle \langle 5\ 6\ 1\ 3 \rangle \langle 6\ 1\ 3\ 4 \rangle \langle 1\ 3\ 4\ 5 \rangle}$	$(\langle 3\ 4\ 5\ 6 \rangle 0 \langle 4\ 5\ 6\ 1 \rangle \langle 5\ 6\ 1\ 3 \rangle \langle 6\ 1\ 3\ 4 \rangle \langle 1\ 3\ 4\ 5 \rangle)$
$R[1\ 2\ 3\ 5\ 6]$	$\frac{1}{\langle 1\ 2\ 3\ 5 \rangle \langle 2\ 3\ 5\ 6 \rangle \langle 3\ 5\ 6\ 1 \rangle \langle 5\ 6\ 1\ 2 \rangle \langle 6\ 1\ 2\ 3 \rangle \langle 1\ 2\ 3\ 5 \rangle}$	$(\langle 2\ 3\ 5\ 6 \rangle \langle 3\ 5\ 6\ 1 \rangle \langle 5\ 6\ 1\ 2 \rangle 0 \langle 6\ 1\ 2\ 3 \rangle \langle 1\ 2\ 3\ 5 \rangle)$

(see section I). The default representation—obtained using the default recursion scheme, with $\{\mathbf{a}, \mathbf{b}, \mathbf{c}\} = \{0, 0, 0\}$, is obtained with `treeContour[n,m]`. For example, the default representation of the 6-point NMHV superamplitude is given in Table A.2.

III. Referencing, Generating, or Specifying Kinematical Data

In order to evaluate amplitudes numerically using `bcfw`, kinematical data must first be defined. This can be done by calling upon a list of reference momentum-twistors, freshly-generating random kinematics, or by specifying kinematical data explicitly:

1. `useReferences[n]`: use a standard set of reference momentum-twistors; these reference twistors were carefully selected so that
 - all components are integer-valued (and small);
 - there are no physical or spurious singularities;
 - all kinematical invariants are uniformly *positive* (that is, $s_{a\dots b} > 0$ for all ranges $a \dots b$), and that these invariants are numerically given by ratios of relatively small integers—leading to amplitudes that are ratios of integers that are ‘not-too-horrendously-long’;

In Table A.3 we give a sample of the reference momentum-twistors. Because an arbitrary set of momentum-twistors define on-shell, momentum-conserving kinematics, there are no constraints from momentum conservation. Therefore, choosing

Table A.3: Reference momentum-twistors used in `bcfw`'s function `useReferences[n]`.

	Z_1	Z_2	Z_3	Z_4	Z_5	Z_6	Z_7	Z_8	Z_9	Z_{10}	Z_{11}	Z_{12}	Z_{13}	Z_{14}	Z_{15}
Z_a^1	-3	2	-2	3	0	-1	2	2	4	-2	-5	-1	5	6	4
Z_a^2	5	6	5	3	-5	2	0	1	-1	-5	2	6	-5	4	6
Z_a^3	3	-1	-1	5	6	-5	-6	-5	-6	4	6	1	-5	-5	-3
Z_a^4	-3	-3	5	-2	0	-5	-1	-3	1	4	-1	-4	3	-3	-4

Figure A.9: Evaluation of 10-point N^3 MHV helicity amplitudes to infinite precision using *reference momentum-twistors*. The timing reflects the fact that the first computation determined the full superamplitude *and* projected-out a particular helicity component, while the second only needed to perform the projection.

```

useReferences[10];
In[1]:= nAmp[m,m,m,m,m,p,p,p,p,p]//withTiming
      Evaluation of the 10-point  $N^3$ MHV amplitude required 46.7. ms to complete.
Out[1]:= 17886892256634020134576330754470391777
         280278666971743564282064966167680000
In[2]:= nAmp[m,p,m,p,m,p,m,p,m,p]//withTiming
      Evaluation of the 10-point  $N^3$ MHV amplitude required 8.6. ms to complete.
Out[2]:= 5007045380847632725336670465304701314367799201604575059832902148541
         213450466354689126392301641566350924968168379805192061706240000

```

simply the first n twistors from the list in Table A.3 will suffice. It is worth mentioning, however, that these reference momentum-twistors are neither canonically normalized¹², nor do they map to *real* four-momenta in $\mathbb{R}^{3,1}$.

Nonetheless, reference twistors are extremely well-suited for debugging, checking identities, and finding relations to infinite precision. As one can see in Figure A.9, using `bcfw`'s built-in reference momentum-twistors can quickly lead to scattering amplitudes that are known to infinite-precision. Notice that in Figure A.9, once the *superamplitude* has been computed for any helicity-component, all subsequent

¹²By not having canonical normalization, we mean that there are non-trivial, Lorentz-frame (and hence also little-group)-dependent kinematical scale-factors in the spinors; however, this tends to only cause a problem when combining/comparing multiple helicity component-amplitudes.

Figure A.10: Evaluation of 12-point N^4 MHV helicity amplitudes with random kinematics.

```

useRandomKinematics[12];
In[1]:= nAmp[m,p,m,p,m,p,m,p,m,p,m,p,m,p]//withTiming
          Evaluation of the 12-point  $N^4$ MHV amplitude required 596. ms to complete.
Out[1]:= -274.127 - 5171.81 I
In[2]:= nAmp[p,m,p,m,p,m,p,m,p,m,p,m,p,m]//withTiming
          Evaluation of the 12-point  $N^4$ MHV amplitude required 71.4. ms to complete.
Out[2]:= -274.127 + 5171.81 I

```

components are obtained quite rapidly.

2. `useRandomKinematics[n]`: use randomly-generated kinematics in $\mathbb{R}^{3,1}$. This function chooses a random set of (optionally rational or arbitrary-precision) on-shell four-momenta in $\mathbb{R}^{3,1}$, and sets up essentially all the kinematical variables of potential interest, including

- momentum-twistors $\{\vec{Z}\} \equiv Zs$, given as an $(n \times 4)$ matrix—the n rows listing the four homogeneous components of each momentum-twistor; `useRandomKinematics[n]` also defines the ‘dual’ momentum-twistors $\{\vec{W}\} \equiv Ws$, which, although not used by `bcfw`, may be found useful by some researchers;
- spinor-helicity variables $\{\vec{\lambda}\} \equiv Ls$ and $\{\vec{\tilde{\lambda}}\} \equiv Lbs$, each an $(n \times 2)$ matrix of components; these have been normalized so that $\tilde{\lambda}_a = \pm (\lambda_a)^*$, as described in section A.2;
- `fourMomenta`, an $(n \times 4)$ matrix of the components (p^0, p^x, p^y, p^z) of each four-momentum;
- `regionMomenta`, the dual-coordinates (described in section A.2), given as a n -length list of 2×2 Hermitian matrices;

An example of using random kinematics is shown in Figure A.10, where the two alternating-helicity 12-point N^4 MHV amplitudes were evaluated. Notice as before that once the superamplitude has been evaluated, subsequent helicity components are quickly extracted. Also, observe that the randomly-generated spinors and momentum-twistors have been appropriately normalized so that parity-conjugation results in complex-conjugation of the amplitude.

3. using user-defined kinematics, given in terms of:
 - (a) `setupUsingFourMomenta[fourMomentaList]`: generates momentum-twistors and spinor-helicity variables for the input list of four-momenta, `fourMomentaList`, which must be given as an n -tuple of four-vectors listing the components of each four-momentum; the list of four-momenta must conserve momentum;
 - (b) `setupUsingSpinors[Ls,Lbs]`: generates momentum-twistors given the spinor-helicity variables $Ls \equiv \{ \vec{\lambda} \}$ and $Lbs \equiv \{ \vec{\lambda} \}$ each given as an $(n \times 2)$ matrix of components;
 - (c) `setupUsingTwistors[twistorList]`: establishes the necessary kinematical functions given the (unconstrained) list of user-generated momentum-twistors.

Examples of how each of these functions can be used can be found in the demonstration file included with the `bcfw` package.

IV. Numerical Evaluation of Tree Amplitudes

As has been emphasized throughout this chapter, the principle sources of `bcfw`'s efficiency are manifest supersymmetry and the use of momentum-twistor variables, which are both made manifest in the momentum-twistor Grassmannian integral (A.3.17). Because these ingredients—or at least their implementation—are quite novel in `bcfw`, it is worth describing in some detail how amplitudes are evaluated numerically by the `bcfw` package.

The basic evaluation strategy is outlined in Table A.4, where we give the basic eval-

uation times for each step in the evaluation of the 10-point N^3 MHV alternating-helicity tree-amplitude.

Because of the central role played by momentum-twistors, the first step of any numerical evaluation is the establishment of momentum-twistor variables which can then be used to compute the kinematical invariants that determine any scattering amplitude. This can be done in a number of different ways—as described in the previous subsection. Although this should be completely clear from the discussions above, this step is not very computationally-intensive (and indeed, can be discounted entirely by choosing to randomly-generate momentum-twistors instead of four-momenta).

Because of the ubiquity of the MHV-amplitude pre-factor, $1/(\langle 12 \rangle \cdots \langle n1 \rangle)$, and the map $(Q_F^{-1})_{ab}$ used to relate the momentum-twistors’ η -variables to the $\tilde{\eta}$ variables of the external superfields, `bcfw` evaluates these two objects and stores them globally whenever new kinematical data is defined.

The first step in the evaluation of any particular helicity amplitude is actually the evaluation of the *full superamplitude*—represented as the list of BCFW-terms, where each is described by the pair `{residue, dMatrix}` (which is stored in memory as the function `nContour[a,b,c][n,m]`). Because particular helicity amplitudes are usually specified with respect to the $\tilde{\eta}$ -variables of the external superfields, the `dMatrix` of each `residue` is then converted to the corresponding `cMatrix` as described in section A.2.

Once each BCFW-term has been evaluated numerically and stored as the pair `{residue,cMatrix}`, it is relatively easy to extract any particular helicity component amplitude—by multiplying each `residue` by the appropriate four ($m \times m$) minors of its corresponding `cMatrix`. This last step is nothing exotic: it is merely the evaluation of the Grassmann integrals $\int \prod_{i=1}^m d^{0|4}\tilde{\eta}_i$ which project-out a helicity-component amplitude from the superamplitude.

V. Example Applications

In the demonstration file which accompanies the `bcfw` package, several examples are given which illustrate how `bcfw` can be used as a tool to verify results, find identities, or learn about scattering amplitudes more generally. In particular, these examples emphasize how using integer-valued reference momentum-twistors to compute amplitudes (and

Table A.4: The general evaluation strategy used by `bcfw`, with a break-down of evaluation-time requirements for each step in the case of the alternating-helicity 10-point N^3 MHV tree-amplitude, $\mathcal{A}_{10}^{(5)}(-, +, -, +, -, +, -, +, -, +)$ (for random kinematics).

1. <code>setupUsingRandomKinematics</code> [10]	
(a) generate random (on-shell, rational, momentum-conserving) four-momenta in $\mathbb{R}^{3,1}$; define spinors and momentum-twistors	3.61 ms
(b) evaluate the universal objects <code>nMHVprefactor</code> and <code>nQinverse</code>	1.34 ms
2. <code>nAmp</code> [m,p,m,p,m,p,m,p,m,p]	
(a) evaluate the full-superamplitude, which is stored as the function <code>nContour</code> [0,0,0] [10,5] (for possible future use)	23.2 ms
(b) convert each <code>dMatrix</code> to its corresponding <code>cMatrix</code>	3.03 ms
(c) project-out the desired helicity component-amplitude	4.01 ms
Total Time:	35.2 ms

individual BCFW-terms) to infinite-precision can prove quite useful theoretically. The examples include:

- a verification of supersymmetric Ward identities; in particular, we check one of the ‘cyclic’ identities described in [138] for the 10-point N^3 MHV amplitude—

$$\begin{aligned}
0 = & \mathcal{A}_{10}^{(5)} \left(\psi_{-1/2}^{(123)}, \psi_{+1/2}^{(3)}, \psi_{+1/2}^{(1)}, \psi_{+1/2}^{(4)}, \psi_{+1/2}^{(3)}, \phi_0^{(24)}, \phi_0^{(14)}, \phi_0^{(12)}, \psi_{-1/2}^{(234)}, g_{-}^{(1234)} \right) \\
& + \mathcal{A}_{10}^{(5)} \left(\psi_{-1/2}^{(123)}, \psi_{+1/2}^{(4)}, \psi_{+1/2}^{(1)}, \psi_{+1/2}^{(4)}, \psi_{+1/2}^{(3)}, \phi_0^{(24)}, \phi_0^{(13)}, \phi_0^{(12)}, \psi_{-1/2}^{(234)}, g_{-}^{(1234)} \right) \\
& + \mathcal{A}_{10}^{(5)} \left(\psi_{-1/2}^{(123)}, \psi_{+1/2}^{(4)}, \psi_{+1/2}^{(1)}, \psi_{+1/2}^{(4)}, \psi_{+1/2}^{(3)}, \phi_0^{(23)}, \phi_0^{(14)}, \phi_0^{(12)}, \psi_{-1/2}^{(234)}, g_{-}^{(1234)} \right) \\
& + \mathcal{A}_{10}^{(5)} \left(\psi_{-1/2}^{(123)}, \psi_{+1/2}^{(4)}, \psi_{+1/2}^{(1)}, \psi_{+1/2}^{(3)}, \psi_{+1/2}^{(3)}, \phi_0^{(24)}, \phi_0^{(14)}, \phi_0^{(12)}, \psi_{-1/2}^{(234)}, g_{-}^{(1234)} \right)
\end{aligned} \tag{A.4.30}$$

—the verification of which is illustrated in Figure A.11, highlighting the power of knowing amplitudes to infinite precision;

- an explicit verification of the U_1 -decoupling identity for the 10-point N^3 MHV tree-amplitude (which, although a trivial consequence of any Lagrangian field theory, is a highly non-trivial check of numerical code!¹³);

¹³We thank Freddy Cachazo for this suggestion.

- a complete classification of the linearly-independent BCFW-generated formulae for the 8-point N^2 MHV supersymmetric tree-amplitude.

Figure A.11: Verifying a SUSY Ward identity of the 10-point N^3 MHV amplitude.

```

useReferences[10]
In[1]:= List[nAmp[{1, 2, 3}, {3}, {1}, {4}, {3}, {2, 4}, {1, 4}, {1, 2}, {2, 3, 4}, {1, 2, 3, 4}],
            nAmp[{1, 2, 3}, {4}, {1}, {4}, {3}, {2, 4}, {1, 3}, {1, 2}, {2, 3, 4}, {1, 2, 3, 4}],
            nAmp[{1, 2, 3}, {4}, {1}, {4}, {3}, {2, 3}, {1, 4}, {1, 2}, {2, 3, 4}, {1, 2, 3, 4}],
            nAmp[{1, 2, 3}, {4}, {1}, {3}, {3}, {2, 4}, {1, 4}, {1, 2}, {2, 3, 4}, {1, 2, 3, 4}]]
Out[1]:= {
  79370862801471295255
  28753113503920775424',
  1275513453387873135869428633786428491
  77923676342112832490222204964602880',
  40428898488502522106856665437052838463
  10951273590541549612279689882333035520',
  16319258699414773847825256760953737 }
  1057119835135513498965174929610240 }
In[2]:= Total[Out[1]]
Out[2]:= 0

```

A.5 Conclusions

We have described a general, versatile, and efficient implementation of the tree-level BCFW recursion relations within the framework of MATHEMATICA which has been realized by the `bcfw` package which is included with the submission of this posting on the [arXiv](#).¹⁴

Having access to an efficient, reliable, flexible, and robust toolbox for computing scattering amplitudes in $\mathcal{N} = 4$ has proven an essential resource, and an important source

¹⁴From the abstract page on the [arXiv](#) for the `bcfw` package [137], choose the link to download “other formats” (below the option for PDF) and you will find the `bcfw` package and its associated walk-through file with many examples included in the ‘source’ for this chapter. Also, you can download `bcfw` at the project’s page on <http://hepforge.org>, where it will be generally maintained by the author.

of theoretical ‘data.’ It is hard to overlook the exciting recent advances that have been made in our understanding of scattering amplitudes, and many of these results have relied heavily on being able to decisively rule-out or quickly confirm a wide-array of new ideas and proposals, leading to many new insights, and helping to establish what has a chance to become a fundamentally new descriptions of quantum field theory.

We hope that the `bcfw` package proves itself useful to a wide range of researchers—both as a reliable and efficient black-box for computing amplitudes, and as an educational resource for gaining intuition about the still somewhat unfamiliar, but extremely powerful new tools available to describe amplitude such as the momentum-twistor Grassmannian that have played an important role in the recent development of our understanding of scattering amplitudes in $\mathcal{N} = 4$.

Appendix B

The Nine-Point N^2 MHV Tree Amplitude

Residue	Geometry Problem:						Residue	Geometry Problem:					
	f_7^1	f_7^2	f_8^1	f_8^2	f_9^1	f_9^2		f_7^1	f_7^2	f_8^1	f_8^2	f_9^1	f_9^2
(2)(3) ² (4) ² (5) ₄₅₆ ⁹¹	(4567)(5671)(5678)(1346)(2367)(1347)	(2)(4)(5) ² (6)(9) ₆₇	(4567)(5671)(5678)(6781)(6789)(9123)										
(4)(5) ² (6) ² (7) ₆₇₈ ²³	(4567)(5671)(5678)(6781)(6789)(7891)	(2)(4)(5)[(8)(9)] ₁₆	(4567)(5671)(5678)(1238)(9126)(9123)										
(6)(7) ² (8) ² (9) ₈₉₁ ⁴⁵	(1247)(1237)(1258)(6781)(9126)(9123)	[(2)(3)](4)(6)(7) ₄ ⁹	(4567)(3451)(2356)(6781)(6789)(7891)										
(2)(3) ² (4)(7) ₄₅ ⁹	(4567)(3451)(2356)(1346)(2367)(7891)	[(2)(3)](4)(8)(9) ₄ ⁹	(4567)(3451)(2356)(1238)(2367)(9123)										
(2)(3) ² (4)(9) ₄₅ ⁹	(4567)(3451)(2356)(1346)(9126)(9123)	[(4)(5)](6)(8)(9) ₆ ²	(4567)(5671)(5678)(1238)(6789)(9123)										
(4)(5) ² (6)(9) ₆₇ ²	(4567)(5671)(5678)(6781)(6789)(9123)	(2)[(5)(6)](7)(9) ₇ ³	(2345)(5671)(5678)(6781)(6789)(9123)										
(2)(5)(6) ² (7) ₇₈ ³	(2345)(5671)(5678)(6781)(6789)(7891)	(2)(3)(5)[(6)(7)] ₈ ³	(2345)(5671)(5678)(6781)(6789)(7891)										
(2)(7)(8) ² (9) ₉₁ ⁵	(2345)(1237)(1258)(1238)(9126)(9123)	(2)(3)(7)[(8)(9)] ₁ ⁵	(2345)(1237)(2356)(1238)(9126)(9123)										
(4)(7)(8) ² (9) ₉₁ ⁵	(4567)(1237)(1258)(1238)(9126)(9123)	(2)(5)(7)[(8)(9)] ₁ ⁵	(2345)(1237)(5678)(1238)(9126)(9123)										
[(2)(3)][(6)(7)] ₄₈	(2345)(3451)(2356)(6781)(6789)(7891)	(4)(5)(7)[(8)(9)] ₁ ⁵	(4567)(1237)(5678)(1238)(9126)(9123)										
[(2)(3)][(8)(9)] ₁₄	(2345)(3451)(2356)(1238)(9126)(9123)	[(2)(3)](6)(7)(9) ₄	(2345)(3451)(2356)(6781)(6789)(9123)										
[(4)(5)][(8)(9)] ₁₆	(4567)(5671)(5678)(1238)(9126)(9123)	[(2)(3)](6)(8)(9) ₄	(2345)(3451)(2356)(1238)(6789)(9123)										
(2)(3) ² (4)(6)(7) ₄₅₈	(4567)(3451)(2356)(1346)(6789)(7891)	(2)(3)(5)(6)(8)(9) ₁₄₇	(2345)(3451)(5678)(6781)(9126)(9123)										
(2)(3) ² (4)(8)(9) ₄₅₁	(4567)(3451)(2356)(1346)(9126)(9123)	(2)(3)(4)(5)(6)(7) ₆ ³⁹	(4567)(5671)(5678)(6781)(6789)(7891)										
(2)(3)(5)(6) ² (7) ₄₇₈	(2345)(3451)(5678)(6781)(6789)(7891)	(4)(5)(6)(7)(8)(9) ₈ ²⁵	(4567)(1237)(5678)(1238)(6789)(9123)										
(2)(3)(7)(8) ² (9) ₄₉₁	(2345)(3451)(1258)(1238)(9126)(9123)	(1)(2)(3)(5)(6)(9) ₂ ⁸	(2345)(3451)(5678)(1346)(6789)(9123)										
(4)(5) ² (6)(8)(9) ₆₇₁	(4567)(5671)(5678)(6781)(9126)(9123)	(2)(3)(4)(5)(8)(9) ₆ ⁹	(4567)(5671)(5678)(1238)(2367)(9123)										
(4)(5)(7)(8) ² (9) ₆₉₁	(4567)(5671)(5678)(1238)(9126)(9123)	(2)(3)(6)(7)(8)(9) ₈ ⁵	(2345)(1237)(2356)(1238)(6789)(9123)										
(1)(2) ² (3)(6)(9) ₂₄ ⁸	(2345)(3451)(2356)(1346)(6789)(9123)	(2)(5)(6)(7)(8)(9) ₈ ⁵	(2345)(1237)(5678)(1238)(6789)(9123)										
(9)(1) ² (2)(5)(8) ₁₂ ⁷	(2345)(3451)(5678)(1238)(9126)(9123)	(2)(5)(6)(7)(8)(9) ₉ ³	(2345)(5671)(5678)(6781)(6789)(9123)										
(1)(2)[(5)(6)](9) ₂₇	(2345)(3451)(5678)(6781)(6789)(9123)	(1)(2)(5)(6)(8)(9) ₂	(2345)(3451)(5678)(1238)(6789)(9123)										
(2)(3) ² (4)(6)(9) ₄₅	(4567)(3451)(2356)(1346)(9126)(9123)	(2)(3)(5)(6)(8)(9) ₄	(2345)(3451)(5678)(1238)(6789)(9123)										
[(2)(3)](5)(6)(9) ₄₇	(2345)(3451)(5678)(6781)(6789)(9123)	(2)(4)(5)(6)(8)(9) ₆	(4567)(5671)(5678)(1238)(6789)(9123)										
(2)(3)[(5)(6)](9) ₄₇	(2345)(3451)(5678)(6781)(6789)(9123)	(2)(3)(4)(7)(8)(9) ₅₉	(2345)(1237)(2356)(1238)(2367)(7891)										
(2)(3)(5)[(8)(9)] ₁₄	(2345)(3451)(5678)(1238)(9126)(9123)	(2)(3)(5)(6)(7)(9) ₃	(2345)(5671)(5678)(6781)(6789)(7891)										

Appendix C *The BCFW-Form of the 1-Loop 6-Point NMHV Integrand*

In this appendix we present the BCFW form of the 1-loop 6-particle NMHV amplitude. The result is,

$$\begin{aligned}
& \frac{\delta^{0|4} \left(0 + \eta_2 \langle 3456 \rangle + \eta_3 \langle 4562 \rangle + \eta_4 \langle 5623 \rangle + \eta_5 \langle 6234 \rangle + \eta_6 \langle 2345 \rangle \right) \langle AB(561) \cap (123) \rangle^2}{\langle 2345 \rangle \langle 2356 \rangle \langle 3456 \rangle \langle AB12 \rangle \langle AB23 \rangle \langle AB56 \rangle \langle AB61 \rangle \langle AB1(234) \cap (56) \rangle \langle AB1(23) \cap (456) \rangle} \\
& + \frac{\delta^{0|4} \left(\eta_1 \langle 3456 \rangle + 0 + \eta_3 \langle 4561 \rangle + \eta_4 \langle 5613 \rangle + \eta_5 \langle 6134 \rangle + \eta_6 \langle 1345 \rangle \right) \langle AB15 \rangle^2}{\langle AB45 \rangle \langle AB56 \rangle \langle AB61 \rangle \langle AB(345) \cap (561) \rangle \langle 3451 \rangle \langle AB13 \rangle \langle AB1(34) \cap (561) \rangle} \\
& + \frac{\delta^{0|4} \left(\eta_1 \langle 3456 \rangle + 0 + \eta_3 \langle 4561 \rangle + \eta_4 \langle 5613 \rangle + \eta_5 \langle 6134 \rangle + \eta_6 \langle 1345 \rangle \right)}{\langle 3456 \rangle \langle 4561 \rangle \langle AB34 \rangle \langle AB61 \rangle \langle AB(345) \cap (561) \rangle \langle AB31 \rangle} \\
& + \frac{\delta^{0|4} \left(\eta_1 \langle 3456 \rangle + 0 + \eta_3 \langle 4561 \rangle + \eta_4 \langle 5613 \rangle + \eta_5 \langle 6134 \rangle + \eta_6 \langle 1345 \rangle \right) \langle 1234 \rangle^2}{\langle 3456 \rangle \langle 4561 \rangle \langle 6134 \rangle \langle AB12 \rangle \langle AB23 \rangle \langle AB34 \rangle \langle 1345 \rangle \langle AB1(34) \cap (561) \rangle} \\
& + \frac{\delta^{0|4} \left(\eta_1 \langle 3456 \rangle + 0 + \eta_3 \langle 4561 \rangle + \eta_4 \langle 5613 \rangle + \eta_5 \langle 6134 \rangle + \eta_6 \langle 1345 \rangle \right)}{\langle 6134 \rangle \langle AB34 \rangle \langle AB45 \rangle \langle AB56 \rangle \langle 5613 \rangle \langle AB1(34) \cap (561) \rangle} \\
& + \frac{\delta^{0|4} \left(\eta_1 \langle 2356 \rangle + \eta_2 \langle 3561 \rangle + \eta_3 \langle 5612 \rangle + 0 + \eta_5 \langle 6123 \rangle + \eta_6 \langle 1235 \rangle \right) \langle 4561 \rangle^2}{\langle 5612 \rangle \langle 6123 \rangle \langle AB45 \rangle \langle AB56 \rangle \langle AB(561) \cap (123) \rangle \langle 3561 \rangle \langle AB4(23) \cap (561) \rangle} \\
& + \frac{\delta^{0|4} \left(\eta_1 \langle 2356 \rangle + \eta_2 \langle 3561 \rangle + \eta_3 \langle 5612 \rangle + 0 + \eta_5 \langle 6123 \rangle + \eta_6 \langle 1235 \rangle \right) \langle AB(234) \cap (561) \rangle^2}{\langle 5612 \rangle \langle 6123 \rangle \langle AB23 \rangle \langle AB34 \rangle \langle AB56 \rangle \langle AB(561) \cap (123) \rangle \langle AB4(23) \cap (561) \rangle \langle AB5(561) \cap (23) \rangle} \\
& + \frac{\delta^{0|4} \left(\eta_1 \langle 2356 \rangle + \eta_2 \langle 3561 \rangle + \eta_3 \langle 5612 \rangle + 0 + \eta_5 \langle 6123 \rangle + \eta_6 \langle 1235 \rangle \right) \langle 2345 \rangle^2}{\langle 2356 \rangle \langle 5612 \rangle \langle 6123 \rangle \langle AB23 \rangle \langle AB34 \rangle \langle AB45 \rangle \langle 1235 \rangle \langle AB5(561) \cap (23) \rangle} \\
& + \frac{\delta^{0|4} \left(\eta_1 \langle 2345 \rangle + \eta_2 \langle 3451 \rangle + \eta_3 \langle 4512 \rangle + \eta_4 \langle 5123 \rangle + \eta_5 \langle 1234 \rangle + 0 \right) \langle 4561 \rangle^2}{\langle 1234 \rangle \langle 1245 \rangle \langle 2345 \rangle \langle AB45 \rangle \langle AB56 \rangle \langle AB61 \rangle \langle 3451 \rangle \langle AB1(123) \cap (45) \rangle} \\
& + \frac{\delta^{0|4} \left(\eta_1 \langle 2345 \rangle + \eta_2 \langle 3451 \rangle + \eta_3 \langle 4512 \rangle + \eta_4 \langle 5123 \rangle + \eta_5 \langle 1234 \rangle + 0 \right) \langle AB14 \rangle^2}{\langle 1234 \rangle \langle AB12 \rangle \langle AB34 \rangle \langle AB45 \rangle \langle AB15 \rangle \langle AB1(123) \cap (45) \rangle \langle AB4(234) \cap (51) \rangle} \\
& + \frac{\delta^{0|4} \left(\eta_1 \langle 2345 \rangle + \eta_2 \langle 3451 \rangle + \eta_3 \langle 4512 \rangle + \eta_4 \langle 5123 \rangle + \eta_5 \langle 1234 \rangle + 0 \right)}{\langle 2345 \rangle \langle AB12 \rangle \langle AB23 \rangle \langle 3451 \rangle \langle AB15 \rangle \langle AB4(234) \cap (51) \rangle} \\
& + \frac{\delta^{0|4} \left(\eta_1 \langle 2345 \rangle + \eta_2 \langle 3451 \rangle + \eta_3 \langle 4512 \rangle + \eta_4 \langle 5123 \rangle + \eta_5 \langle 1234 \rangle + 0 \right)}{\langle 1245 \rangle \langle AB23 \rangle \langle AB34 \rangle \langle AB45 \rangle \langle 5123 \rangle \langle AB1(123) \cap (45) \rangle} \\
& + \frac{\delta^{0|4} \left(\begin{array}{l} \eta_1 \langle AB(23) \cap (456)1 \rangle + \eta_2 \langle 4561 \rangle \langle AB13 \rangle + \eta_3 \langle 1456 \rangle \langle AB12 \rangle \\ + \eta_4 \langle AB(123) \cap (561) \rangle + \eta_5 \langle AB(123) \cap (46)1 \rangle + \eta_6 \langle AB1(123) \cap (45) \rangle \end{array} \right) \langle AB15 \rangle^2}{\langle AB12 \rangle \langle AB45 \rangle \langle AB56 \rangle \langle AB61 \rangle \langle AB(561) \cap (123) \rangle \langle AB13 \rangle \langle AB14 \rangle \langle AB1(123) \cap (45) \rangle \langle (AB1) \cap (45) \rangle \langle AB \rangle \cap (561)23} \\
& + \frac{\delta^{0|4} \left(\begin{array}{l} \eta_1 \langle AB(23) \cap (456)1 \rangle + \eta_2 \langle 4561 \rangle \langle AB13 \rangle + \eta_3 \langle 1456 \rangle \langle AB12 \rangle \\ + \eta_4 \langle AB(123) \cap (561) \rangle + \eta_5 \langle AB(123) \cap (46)1 \rangle + \eta_6 \langle AB1(123) \cap (45) \rangle \end{array} \right)}{\langle 4561 \rangle \langle AB12 \rangle \langle AB23 \rangle \langle AB61 \rangle \langle AB13 \rangle \langle AB14 \rangle \langle AB1(23) \cap (456) \rangle \langle (AB1) \cap (45) \rangle \langle AB \rangle \cap (561)23} \\
& + \frac{\delta^{0|4} \left(\begin{array}{l} \eta_1 \langle AB1(234) \cap (56) \rangle + \eta_2 \langle AB(34) \cap (561)1 \rangle + \eta_3 \langle AB1(24) \cap (561) \rangle \\ + \eta_4 \langle AB(561) \cap (123) \rangle + \eta_5 \langle 1234 \rangle \langle AB61 \rangle + \eta_6 \langle 1234 \rangle \langle AB15 \rangle \end{array} \right)}{\langle 1234 \rangle \langle AB12 \rangle \langle AB34 \rangle \langle AB56 \rangle \langle AB61 \rangle \langle AB(234) \cap (561) \rangle \langle AB(561) \cap (123) \rangle \langle AB14 \rangle \langle AB15 \rangle} \\
& + \frac{\delta^{0|4} \left(\begin{array}{l} \eta_1 \langle AB1(234) \cap (56) \rangle + \eta_2 \langle AB(34) \cap (561)1 \rangle + \eta_3 \langle AB1(24) \cap (561) \rangle \\ + \eta_4 \langle AB(561) \cap (123) \rangle + \eta_5 \langle 1234 \rangle \langle AB61 \rangle + \eta_6 \langle 1234 \rangle \langle AB15 \rangle \end{array} \right)}{\langle AB12 \rangle \langle AB23 \rangle \langle AB61 \rangle \langle AB(234) \cap (561) \rangle \langle AB14 \rangle \langle AB15 \rangle \langle AB1(234) \cap (56) \rangle \langle AB1(34) \cap (561) \rangle}
\end{aligned}$$

A note on notation: the expression $\langle AB1(56) \cap (234) \rangle$ refers to $\langle AB1X \rangle$ where $X = (56) \cap (234)$ is the point where the line (56) intersects the plane (234), namely, $Z_5 \langle 6234 \rangle + Z_6 \langle 2345 \rangle = -(Z_2 \langle 3456 \rangle + Z_3 \langle 4562 \rangle + Z_4 \langle 5623 \rangle)$; similarly, ‘ $(123) \cap (456)$ ’ is $Z_{12} \langle 3456 \rangle + Z_{23} \langle 1456 \rangle + Z_{31} \langle 2456 \rangle$.

Appendix D *The Full 2-Loop Integrand for the 7-Point NMHV Amplitude*

Here we give the explicit formula for the 2-loop 7-particle NMHV amplitude. We find it most convenient to give a formula for $M_{\text{NMHV}}^{2\text{loop}} - M^{\text{tree}}M_{\text{MHV}}^{2\text{loop}}$. We can expand this in three cyclic classes as $[(7)(1)C_{7,1}] + [(7)(2)C_{7,2}] + [(7)(3)C_{7,3}] + \text{cyclic}$. We give the expression for the coefficients $C_{7,1}, C_{7,2}, C_{7,3}$ in the tables below. Here “ g ” refers to the operation $i \mapsto i + 1$, and P is a parity flip, that exchanges wavy- and dashed-lines (together with their corresponding normalization), and r is the reflection operation $i \mapsto (8 - i)$.

Table D.1: Coefficients of residue $(7)(1) = [2\ 3\ 4\ 5\ 6]$.

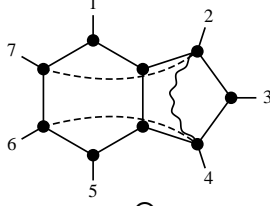
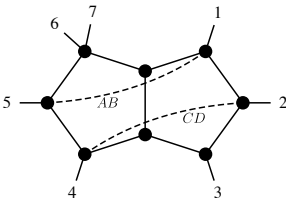
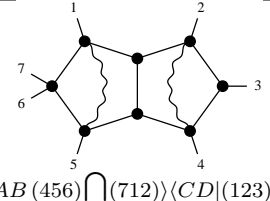
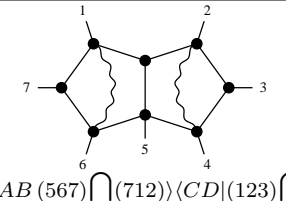
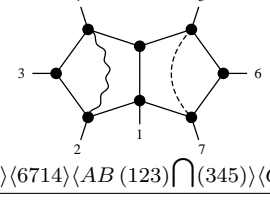
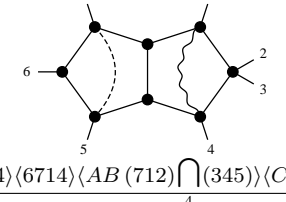
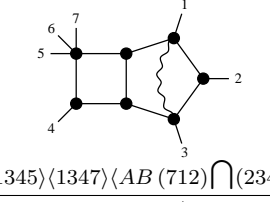
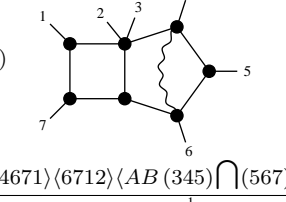
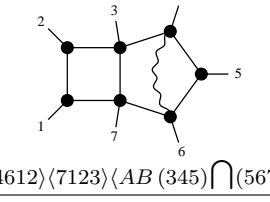
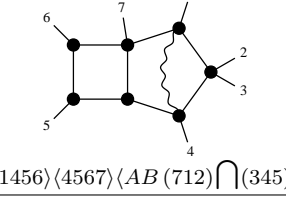
1		$-(1 - g)$	
	$\langle 4512 \rangle \langle 5671 \rangle \langle AB(123) \cap (345) \rangle \langle CD64 \rangle \langle CD72 \rangle$		$\langle 4563 \rangle \langle 4713 \rangle \langle 7123 \rangle \langle AB51 \rangle \langle CD24 \rangle$
1		$-(1 + g^2 + g^4)$	
	$\langle 5124 \rangle \langle AB(456) \cap (712) \rangle \langle CD \mid (123) \cap (345) \rangle$		$\langle 2461 \rangle \langle AB(567) \cap (712) \rangle \langle CD \mid (123) \cap (345) \rangle$
$-(1 + g^4 r)$		1	
	$\langle 5624 \rangle \langle 6714 \rangle \langle AB(123) \cap (345) \rangle \langle CD57 \rangle$		$\langle 5614 \rangle \langle 6714 \rangle \langle AB(712) \cap (345) \rangle \langle CD57 \rangle$
$-(1 - g)$		$(1 + g^2)(1 - g^2 r) + g^2 P(1 - g^4 r)$	
	$\langle 1345 \rangle \langle 1347 \rangle \langle AB(712) \cap (234) \rangle$		$\langle 4671 \rangle \langle 6712 \rangle \langle AB(345) \cap (567) \rangle$
$-(1 + g^2 - gP)$		$1 - g^4 r$	
	$\langle 4612 \rangle \langle 7123 \rangle \langle AB(345) \cap (567) \rangle$		$\langle 1456 \rangle \langle 4567 \rangle \langle AB(712) \cap (345) \rangle$

Table D.2: Coefficients of residue (7)(1) = [2 3 4 5 6], continued

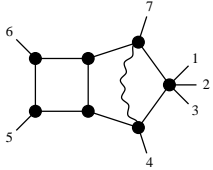
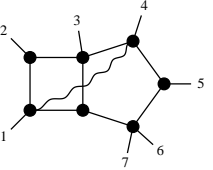
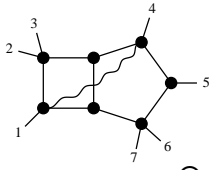
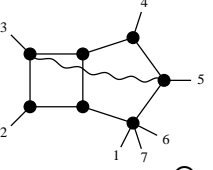
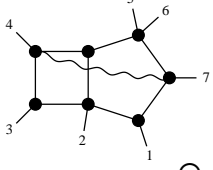
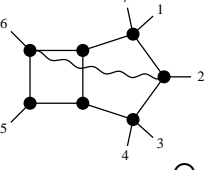
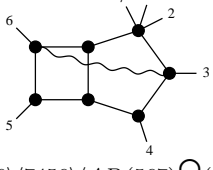
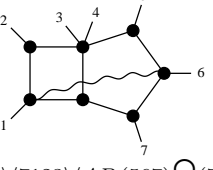
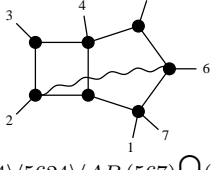
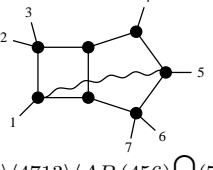
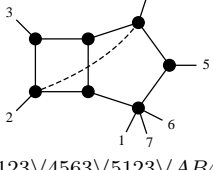
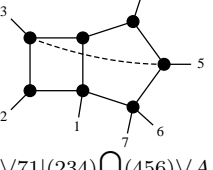
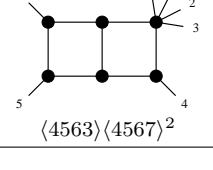
$1 + g^2$  $\langle 7456 \rangle^2 \langle AB(671) \cap (345) \rangle$	$(1 + gP)(1 + g^4r)$  $\langle 4561 \rangle \langle 7123 \rangle \langle AB(345) \cap (712) \rangle$
$-(1 - g)(1 + P)$  $\langle 4561 \rangle \langle 4713 \rangle \langle AB(345) \cap (712) \rangle$	$1 - g^3 - gr$  $\langle 4123 \rangle \langle 5123 \rangle \langle AB(234) \cap (456) \rangle$
-1  $\langle 5234 \rangle \langle 7124 \rangle \langle AB(345) \cap (671) \rangle$	$-(1 - g^2r)$  $\langle 2456 \rangle \langle 7456 \rangle \langle AB(567) \cap (123) \rangle$
$-(1 + g^2)$  $\langle 3456 \rangle \langle 7456 \rangle \langle AB(567) \cap (234) \rangle$	$1 - g$  $\langle 5614 \rangle \langle 7123 \rangle \langle AB(567) \cap (712) \rangle$
1  $\langle 1234 \rangle \langle 5624 \rangle \langle AB(567) \cap (123) \rangle$	$-(1 - g)$  $\langle 4513 \rangle \langle 4713 \rangle \langle AB(456) \cap (712) \rangle$
$1 + g^4r$  $\langle 4123 \rangle \langle 4563 \rangle \langle 5123 \rangle \langle AB42 \rangle$	$1 + g^4r$  $\langle 4123 \rangle \langle 71 \mid (234) \cap (456) \rangle \langle AB53 \rangle$
$-(1 + g^2)$  $\langle 4563 \rangle \langle 4567 \rangle^2$	

Table D.3: Coefficients of residue $(7)(2) = [1\ 3\ 4\ 5\ 6]$

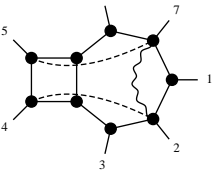
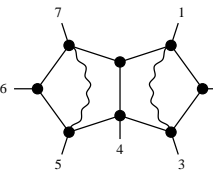
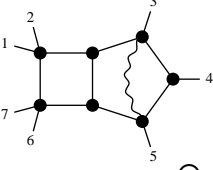
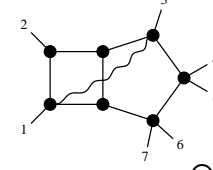
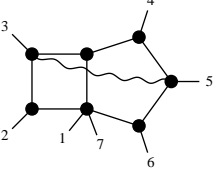
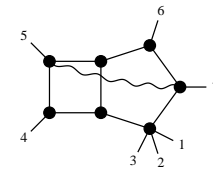
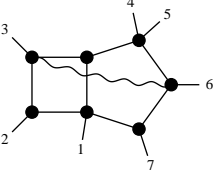
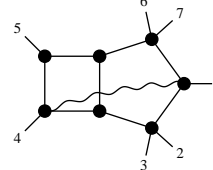
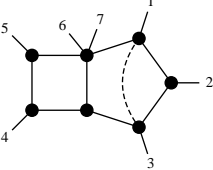
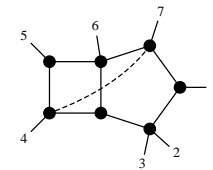
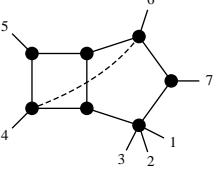
<p>1</p>  <p>$\langle 3456 \rangle^2 \langle AB24 \rangle \langle AB57 \rangle \langle AB(671) \cap (123) \rangle$</p>	<p>-1</p>  <p>$\langle 1357 \rangle \langle AB(712) \cap (234) \rangle \langle CD \mid (456) \cap (671) \rangle$</p>
<p>-1</p>  <p>$\langle 3562 \rangle \langle 3571 \rangle \langle AB(234) \cap (456) \rangle$</p>	<p>$-(1 - g^3)$</p>  <p>$\langle 3561 \rangle \langle 3712 \rangle \langle AB(234) \cap (712) \rangle$</p>
<p>$1 - g^6 r$</p>  <p>$\langle 4123 \rangle \langle 5673 \rangle \langle AB(234) \cap (456) \rangle$</p>	<p>1</p>  <p>$\langle 6345 \rangle \langle 7345 \rangle \langle AB(456) \cap (671) \rangle$</p>
<p>$-(1 - g^6 r)$</p>  <p>$\langle 4123 \rangle \langle 6713 \rangle \langle AB(234) \cap (567) \rangle$</p>	<p>$-(1 - grP)$</p>  <p>$\langle 6145 \rangle \langle 6345 \rangle \langle AB(712) \cap (345) \rangle$</p>
<p>$-(1 - gr)$</p>  <p>$\langle 1247 \rangle \langle 2345 \rangle \langle 3456 \rangle \langle AB13 \rangle$</p>	<p>$1 - gr$</p>  <p>$\langle 1345 \rangle \langle 3456 \rangle \langle 7126 \rangle \langle AB74 \rangle$</p>
<p>$1 + gr$</p>  <p>$\langle 6345 \rangle \langle 6715 \rangle \langle 7345 \rangle \langle AB64 \rangle$</p>	

Table D.4: Coefficients of residue $(7)(3) = [1\ 2\ 4\ 5\ 6]$

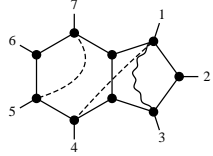
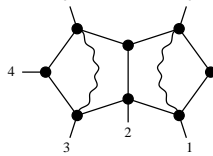
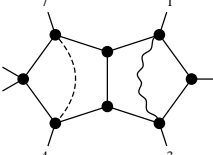
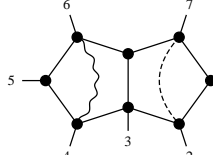
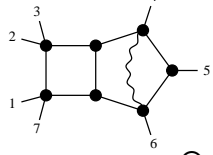
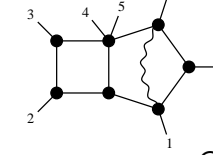
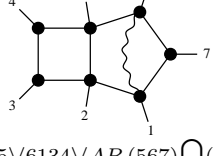
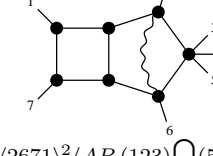
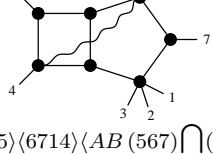
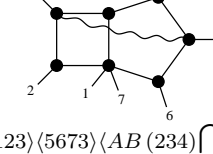
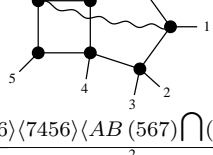
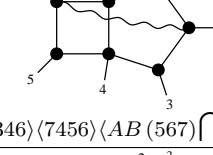
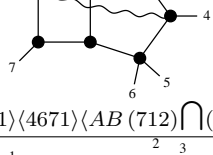
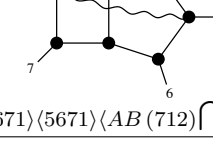
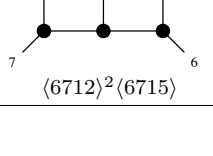
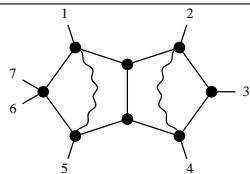
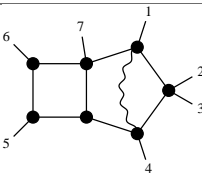
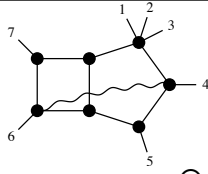
$1 + g^6 r$  $\langle 3456 \rangle \langle 6371 \rangle \langle AB(712) \cap (234) \rangle \langle CD41 \rangle \langle CD57 \rangle$	-1  $\langle 6135 \rangle \langle AB(567) \cap (712) \rangle \langle CD(234) \cap (456) \rangle$
$-(1 + g^3)$  $\langle 4513 \rangle \langle 6713 \rangle \langle AB(712) \cap (234) \rangle \langle CD47 \rangle$	$-(1 + g^2 Pr)$  $\langle 1236 \rangle \langle 7146 \rangle \langle AB(345) \cap (567) \rangle \langle CD72 \rangle$
1  $\langle 4612 \rangle \langle 4673 \rangle \langle AB(345) \cap (567) \rangle$	$-(1 - g^6 r)$  $\langle 1234 \rangle \langle 6123 \rangle \langle AB(567) \cap (712) \rangle$
-1  $\langle 2345 \rangle \langle 6134 \rangle \langle AB(567) \cap (712) \rangle$	$1 + g^2$  $\langle 2671 \rangle^2 \langle AB(123) \cap (567) \rangle$
$1 + g^6 r$  $\langle 6345 \rangle \langle 6714 \rangle \langle AB(567) \cap (345) \rangle$	$-(1 - g^3)$  $\langle 4123 \rangle \langle 5673 \rangle \langle AB(234) \cap (456) \rangle$
$1 + g^6 r$  $\langle 1346 \rangle \langle 7456 \rangle \langle AB(567) \cap (712) \rangle$	$-(1 - g^2 r)$  $\langle 2346 \rangle \langle 7456 \rangle \langle AB(567) \cap (123) \rangle$
$-(1 - g^4 r)$  $\langle 2671 \rangle \langle 4671 \rangle \langle AB(712) \cap (345) \rangle$	$-(1 + g^2)$  $\langle 2671 \rangle \langle 5671 \rangle \langle AB(712) \cap (456) \rangle$
$-(1 + g^2)$  $\langle 6712 \rangle^2 \langle 6715 \rangle$	

Table D.5: Coefficients of A_{tree} (in addition to the 2-loop MHV amplitude)

<p>-1</p>  <p>$\langle 5124 \rangle \langle AB(456) \cap (712) \rangle \langle CD(123) \cap (345) \rangle$</p>	<p>$-(1 - g^4 r)$</p>  <p>$\langle 1456 \rangle \langle 4567 \rangle \langle AB(712) \cap (345) \rangle$</p>
<p>1</p>  <p>$\langle 1467 \rangle \langle 1567 \rangle \langle AB(345) \cap (567) \rangle$</p>	

Appendix E *Residue Computations in Momentum-Twistor Space*

We gave a heuristic argument for the form of the Jacobian in the computation of the residue of a pentagon integral. The actual computation is essentially trivial but it might serve as yet one more way to get used to momentum twistors. This is why we carry it out in detail in this appendix.

Recall that the non-vanishing residue of the pentagon integral for a contour which ‘encircles’ the isolated pole $(AB) = (24)$ is computed using

$$\oint_{|(AB)-(24)|=\epsilon} \frac{\langle AB 13 \rangle \langle 12 45 \rangle \langle 23 45 \rangle}{\langle AB 12 \rangle \langle AB 23 \rangle \langle AB 34 \rangle \langle AB 45 \rangle \langle AB 51 \rangle}, \quad (\text{E.0.1})$$

As with all multidimensional residues, the entire computation amounts to Jacobians. Let us choose to expand Z_A and Z_B using the twistors $\{Z_5, Z_1, Z_2, Z_4\}$ as a basis; this parameterization introduces a Jacobian $J_{AB \rightarrow (5124)} = \langle 5124 \rangle^{-2}$. Exploiting the GL_2 -redundancy of the integrand, may therefore parameterize Z_A and Z_B according to

$$\begin{aligned} Z_A &\equiv \alpha_1 Z_5 + \alpha_2 Z_1 + Z_2; \\ Z_B &\equiv \beta_1 Z_5 + \beta_2 Z_1 + Z_4; \end{aligned} \quad (\text{E.0.2})$$

Of course, the contour being evaluated corresponds to the choice of maps f_i given by $\vec{f} \equiv \{\langle AB 12 \rangle, \langle AB 23 \rangle, \langle AB 34 \rangle, \langle AB 45 \rangle\}$; using these coordinates for Z_A, Z_B , the contour will be evaluated around the pole at the origin: $\alpha_i = \beta_i = 0$.

With this, the integral in question has become fully gauge-fixed and concrete:

$$\oint_{|\alpha_i|, |\beta_i|=\epsilon} d^2 \alpha_i d^2 \beta_i \frac{\langle AB 13 \rangle \langle 12 45 \rangle^3 \langle 23 45 \rangle}{\langle AB 12 \rangle \langle AB 23 \rangle \langle AB 34 \rangle \langle AB 45 \rangle \langle AB 51 \rangle}. \quad (\text{E.0.3})$$

Because the contour encircles the origin, the Jacobian appearing the definition of a multidimensional residue will be evaluated at the origin. This means that for our purposes, we need only compute the maps \vec{f} to linear-order in (α_i, β_i) to compute the residue.

Doing this in complete detail, we see that

$$\begin{aligned}
f_1 &= \langle AB 12 \rangle = \alpha_1 \langle 5 4 1 2 \rangle && + \dots \\
f_2 &= \langle AB 23 \rangle = \alpha_1 \langle 5 4 1 3 \rangle + \alpha_2 \langle 1 4 2 3 \rangle && + \dots \\
f_3 &= \langle AB 34 \rangle = && \beta_1 \langle 2 5 3 4 \rangle + \beta_2 \langle 2 1 3 4 \rangle + \dots \\
f_4 &= \langle AB 45 \rangle = && \beta_2 \langle 2 1 4 5 \rangle + \dots
\end{aligned}$$

where ‘...’ stands for terms quadratic in α_i, β_i . From this, it is trivial to read-off the Jacobian:

$$J \Big|_{(AB)=(24)} = \langle 5 4 1 2 \rangle \langle 1 4 2 3 \rangle \langle 2 5 3 4 \rangle \langle 2 1 4 5 \rangle = \langle 1 2 4 5 \rangle^2 \langle 1 2 3 4 \rangle \langle 2 3 4 5 \rangle; \quad (\text{E.0.4})$$

combining this with the rest of the integrand—e.g. $\langle AB 13 \rangle / \langle AB 51 \rangle$ evaluated on $(AB) = (24)$ —we find that

$$\oint_{|(AB)-(24)|=\epsilon} \frac{\langle AB 13 \rangle \langle 12 45 \rangle \langle 23 45 \rangle}{\langle AB 12 \rangle \langle AB 23 \rangle \langle AB 34 \rangle \langle AB 45 \rangle \langle AB 51 \rangle} = - \frac{\langle 2 4 1 3 \rangle \langle 1 2 4 5 \rangle^3 \langle 2 3 4 5 \rangle}{\langle 1 2 4 5 \rangle^3 \langle 1 2 3 4 \rangle \langle 2 3 4 5 \rangle} = 1.$$

Appendix F

All 2-Loop NMHV Amplitude Integrands

In this appendix, we will provide all the details that go into the formula for the n -point 2-loop NMHV amplitude, which can be graphically represented as follows:

$$\begin{aligned}
 \mathcal{A}_{\text{NMHV}}^{2\text{-loop}} = & \sum_{\substack{i < j < l < m \leq k < i \\ i < j < k < l < m \leq i \\ i \leq l < m \leq j < k < i}} \text{Diagram 1} + \frac{1}{2} \sum_{i < j < k < l < i} \text{Diagram 2} \\
 & \times [i, j, j+1, k, k+1] \times \left\{ \begin{aligned} & \mathcal{A}_{\text{NMHV}}^{\text{tree}}(j, \dots, k; l, \dots, i) \\ & + \mathcal{A}_{\text{NMHV}}^{\text{tree}}(i, \dots, j) \\ & + \mathcal{A}_{\text{NMHV}}^{\text{tree}}(k, \dots, l) \end{aligned} \right\} \quad (\text{F.0.1})
 \end{aligned}$$

Of these two terms, only the first requires any comment, because the second summand involves only the familiar double-pentagons which generate the MHV two-loop amplitude's integrand.

As indicated by the ranges of the summation, the first sum actually represents a sum over three distinct cyclic orderings of the labels (i, j, k, l, m) , corresponding to each of the following cyclically-ordered integrands,

Integrand:			
Range:	$i < j < l < m \leq k < i$	$i \leq l < m \leq j < k < i$	$i < j < k < l < m \leq i$
Boundary terms :	$\left\{ \begin{array}{l} \text{A } i+1 = j \\ \text{B } i-1 = k+1 \end{array} \right\}$	$\left\{ \begin{array}{l} \text{A } i = l \\ \text{B } i-1 = k+1 \end{array} \right\}$	$\left\{ \begin{array}{l} \text{A } i+1 = j \\ \text{B } i = m \end{array} \right\}$

For each range of indices, there are *boundary-terms* for which the general integrand's numerator must change slightly; these have been indicated in the table above. Given the ranges and boundaries indicated above, the numerators for these contributions to the 2-loop NMHV amplitude are given by,

term	numerator	
non-boundary	$\langle AB (i-1 i i+1) \cap (\Sigma_{i,j,k}) \rangle$	
A boundary	$\langle AB i+1(i-1 i) \cap (\Sigma_{i,j,k}) \rangle$	(F.0.2)
B boundary	$\langle AB i-1(i i+1) \cap (\Sigma_{i,j,k}) \rangle$	
A&B boundary	$\langle AB i+1 i-1 \rangle \langle i \Sigma_{i,j,k} \rangle$	

where in all these cases the special plane $\Sigma_{i,j,k}$ is given by the same object encountered at one-loop, but with the arbitrary bitwistor X replaced by (lm) ,

$$\Sigma_{i,j,k} \equiv \frac{1}{2} \left[(j j+1) \left((i k k+1) \cap (lm) \right) - (k k+1) \left((i j j+1) \cap (lm) \right) \right]. \quad (\text{F.0.3})$$

Appendix G

All 3-Loop MHV Amplitude Integrands

In this appendix, we present the explicit form of the n -point 3-loop MHV amplitude, which we represent graphically graphically represented as follows:

$$\mathcal{A}_{\text{MHV}}^{3\text{-loop}} = \frac{1}{3} \sum_{\substack{i_1 \leq i_2 < j_1 \leq \\ \leq j_2 < k_1 \leq k_2 < i_1}} \text{Diagram 1} + \frac{1}{2} \sum_{\substack{i_1 \leq j_1 < k_1 < \\ < k_2 \leq j_2 < i_2 < i_1}} \text{Diagram 2}$$

As described in the body of this Chapter, the ‘boundary terms’ of the summands above require some comment. We will discuss the two topologies separately, starting with with the first summand in the equation above. Because when any two of the indices become identified in the first graph the wavy-line numerators become ill-defined, special consideration must be made for each of the degenerations allowed in the range of the summand—that is, all the cases where two or more of the indices are identified. Separating each type of such degeneration that is allowed in the first summand,

$$\frac{1}{3} \sum_{\substack{i_1 \leq i_2 < j_1 \leq \\ \leq j_2 < k_1 \leq k_2 < i_1}} \text{Diagram 1} = \left\{ \begin{array}{l} 1 \times \frac{1}{3} \sum_{\substack{i_1 < i_2 < j_1 < \\ < j_2 < k_1 < k_2 < i_1}} \mathcal{I}_1^A(i_1, i_2, j_1, j_2, k_1, k_2) \left(\begin{array}{l} \text{all indices} \\ \text{distinct} \end{array} \right) \\ 3 \times \frac{1}{3} \sum_{\substack{i_1 < i_2 < j_1 < \\ < j_2 < k < i_1}} \mathcal{I}_2^A(i_1, i_2, j_1, j_2, k) \quad (k_1 = k_2 \equiv k) \\ 3 \times \frac{1}{3} \sum_{i_1 < i_2 < j < k < i_1} \mathcal{I}_3^A(i_1, i_2, j, k) \quad \left(\begin{array}{l} k_1 = k_2 \equiv k \\ j_1 = j_2 \equiv j \end{array} \right) \\ 1 \times \frac{1}{3} \sum_{i < j < k < i} \mathcal{I}_4^A(i, j, k) \quad \left(\begin{array}{l} k_1 = k_2 \equiv k \\ j_1 = j_2 \equiv j \\ i_1 = i_2 \equiv i \end{array} \right) \end{array} \right.$$

Here, the overall factor of $\frac{1}{3}$ reflects the \mathbb{Z}_3 -symmetry of the loop integrand (recall that every term in the sum is understood to be fully-symmetrized with respect to the 3! permutations of the loop-variable labels); although every term in the summand has the

same factor of $\frac{1}{3}$, the boundary terms for which *e.g.* $k_1 = k_2$ in the sum are equivalent to those where $j_1 = j_2$ or $i_1 = i_2$, allowing us to represent all three degenerations with a single integrand— \mathcal{I}_2^A in this case, and similarly for \mathcal{I}_3^A .

Let us now carefully define the contributions to this class of graph each in turn. First, we have the generic integrand:

$$\bullet \mathcal{I}_1^A(i_1, i_2, j_1, j_2, k_1, k_2) \iff \text{Diagram} \quad \text{Numerator} \quad \text{Tr}[(i_1 | AB | i_2)(j_1 | CD | j_2)(k_1 | EF | k_2)]$$

Here, we have left implicit the twelve propagators shown in the figure by solid lines, and the three ‘wavy-line’ numerators $\langle AB (i_1-1 i_1 i_1+1) \cap (i_2-1 i_2 i_2+1) \rangle$ etc. Observe that we have introduced a new notation for remaining tensor components of the numerator for this integrand. Letting ‘ \bullet ’ denote an arbitrary bitwistor, we may define a ‘trace’ over a pair of such auxiliary bitwistors: $\text{Tr}[(ab \bullet)(\bullet cd)] \equiv \langle abcd \rangle$; that is, the trace is nothing but the completely-antisymmetric contraction of bitwistors which are dual to a pair of auxiliary bitwistors, which are indicated by ‘ \bullet ’ in the corresponding formula.¹

It may be helpful to illustrate the meaning of this numerator using the familiar notation of Wick contraction; in this notation, the tensor numerator of $\mathcal{I}_1^A(i_1, i_2, j_1, j_2, k_1, k_2)$ corresponds to:

$$\text{Tr}[(i_1 | AB | i_2)(j_1 | CD | j_2)(k_1 | EF | k_2)] \equiv \langle AB (i_1 \bullet) \overline{\cap (i_2 \bullet)} \rangle \langle CD (j_1 \bullet) \overline{\cap (j_2 \bullet)} \rangle \langle EF (k_1 \bullet) \overline{\cap (k_2 \bullet)} \rangle;$$

alternatively, the numerator can be written in any one of the following equivalent forms (the equality of which offering further justification for calling this a ‘trace’):

$$\begin{aligned} & \text{Tr}[(i_1 | AB | i_2)(j_1 | CD | j_2)(k_1 | EF | k_2)] \\ & \equiv \langle i_2 j_1 \left[\left(j_2 k_1 \left((k_2 i_1 A) \cap (FE) \right) \right) \cap (DC) \right] B \rangle - (A \leftrightarrow B); \\ & = \langle j_2 k_1 \left[\left(k_2 i_1 \left((i_2 j_1 C) \cap (BA) \right) \right) \cap (FE) \right] D \rangle - (C \leftrightarrow D); \\ & = \langle k_2 i_1 \left[\left(i_2 j_1 \left((j_2 k_1 E) \cap (DC) \right) \right) \cap (BA) \right] F \rangle - (E \leftrightarrow F). \end{aligned}$$

¹The idea of ‘tracing’ over auxiliary bitwistors turns out to be a very powerful generalization of the four-bracket. Indeed, all the four-brackets in this chapter could be translated directly into traces, and often with considerable simplification.

As we will see presently, this numerator will change only very slightly for the boundary terms in the summand. Always leaving the propagators and wavy-line implicit from the the corresponding figures, the remaining integrands are defined according to the following:

$$\begin{aligned}
 & \bullet \mathcal{I}_2^A(i_1, i_2, j_1, j_2, k) \iff \text{Diagram 1} \quad \text{Numerator} \\
 & \quad \text{for } i_1 < i_2 < j_1 < j_2 < k < i_1 \quad \text{Tr} [(i_1 | AB | i_2)(j_1 | CD | j_2)(k | k-1 \ k+1 | k)] \\
 & \bullet \mathcal{I}_3^A(i_1, i_2, j, k) \iff \text{Diagram 2} \quad \text{Numerator} \\
 & \quad \text{for } i_1 < i_2 < j < k < i_1 \quad \text{Tr} [(i_1 | AB | i_2)(j | j-1 \ j+1 | j)(k | k-1 \ k+1 | k)] \\
 & \bullet \mathcal{I}_4^A(i, j, k) \iff \text{Diagram 3} \quad \text{Numerator} \\
 & \quad \text{for } i < j < k < i \quad \text{Tr} [(i | i-1 \ i+1 | i)(j | j-1 \ j+1 | j)(k | k-1 \ k+1 | k)]
 \end{aligned}$$

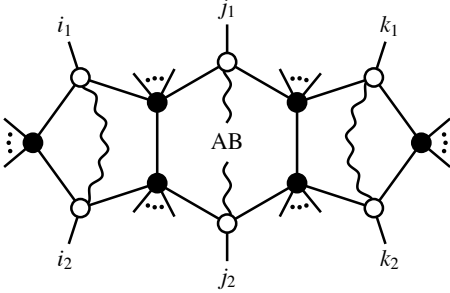
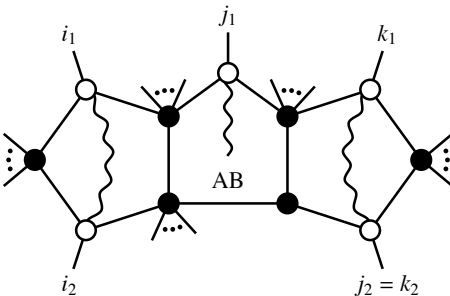
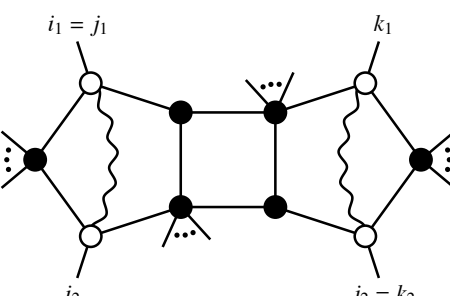
For the second topology, the boundary terms in the summand lead to just three separate contributions that must be specifically addressed.

$$\frac{1}{2} \sum_{\substack{i_1 \leq j_1 < k_1 < \\ < k_2 \leq j_2 < i_2 < i_1}} \text{Diagram 4} = \begin{cases} 1 \times \frac{1}{2} \sum_{\substack{i_1 < j_1 < k_1 < \\ < k_2 < j_2 < i_2 < i_1}} \mathcal{I}_1^B(i_1, j_1, k_1, k_2, j_2, i_2) & \begin{pmatrix} \text{all indices} \\ \text{distinct} \end{pmatrix} \\ 2 \times \frac{1}{2} \sum_{\substack{i_1 < j_1 < k_1 < \\ < k_2 < i_2 < i_1}} \mathcal{I}_2^B(i_1, j_1, k_1, k_2, i_2) & (k_2 = j_2 \equiv k_2) \\ 1 \times \frac{1}{2} \sum_{\substack{i_1 < k_1 < \\ < k_2 < i_2 < i_1}} \mathcal{I}_3^B(i_1, k_1, k_2, i_2) & \begin{pmatrix} i_1 = j_1 \equiv i_1 \\ k_2 = j_2 \equiv k_2 \end{pmatrix} \end{cases}$$

As above, the overall factor of ‘ $\frac{1}{2}$ ’ reflects the \mathbb{Z}_2 -symmetry of the integrand (we remind the reader that each term in the summand is to be fully-symmetrized with respect to the 3! permutations of the loop variables). As before, we have exploited the symmetry of

the integrand to identify various boundary terms: the degenerations $i_1 = j_1$ and $k_2 = j_2$, being equivalent in the cyclic sum, they can be combined into the single summand \mathcal{I}_2^B — which explains its relative factor of 2.

With this, we can directly present the three classes of integrands of the second topology which contribute to the 3-loop MHV amplitude:

$\bullet \mathcal{I}_1^B(i_1, j_1, k_1, k_2, j_2, i_2)$ for $i_1 < j_1 < k_1 < k_2 < j_2 < i_2 < i_1$	\iff 	<p style="text-align: center;">Numerator</p> $\langle AB(i_2 i_1 j_2) \cap (j_1 - 1 j_1 j_1 + 1) \rangle$ $\times \langle AB(j_2 - 1 j_2 j_2 + 1) \cap (j_1 k_1 k_2) \rangle$
$\bullet \mathcal{I}_2^B(i_1, j_1, k_1, k_2, i_2)$ for $i_1 < j_1 < k_1 < k_2 < i_2 < i_1$	\iff 	<p style="text-align: center;">Numerator</p> $\langle AB(i_2 i_1 k_2) \cap (j_1 - 1 j_1 j_1 + 1) \rangle$ $\times \langle k_2 + 1 j_1 k_1 k_2 \rangle$
$\bullet \mathcal{I}_3^B(i_1, k_1, k_2, i_2)$ for $i_1 < k_1 < k_2 < i_2 < i_1$	\iff 	<p style="text-align: center;">Numerator</p> $\langle k_2 i_2 i_1 i_1 + 1 \rangle$ $\times \langle k_2 + 1 i_1 k_1 k_2 \rangle$

Bibliography

- [1] S. J. Parke and T. R. Taylor, “Gluonic Two Goes To Four,” *Nucl. Phys.* **B269** (1986) 410. 1
- [2] S. J. Parke and T. R. Taylor, “An Amplitude for n Gluon Scattering,” *Phys. Rev. Lett.* **56** (1986) 2459. 1, 99
- [3] F. A. Berends and W. T. Giele, “Recursive Calculations for Processes with n Gluons,” *Nucl. Phys.* **B306** (1988) 759. 2, 99, 235, 238
- [4] E. Witten, “Perturbative Gauge Theory as a String Theory in Twistor Space,” *Commun. Math. Phys.* **252** (2004) 189–258, [arXiv:hep-th/0312171](#). 2, 17, 26, 29, 38, 41, 81, 99, 106, 238
- [5] F. Cachazo, P. Svrcek, and E. Witten, “MHV Vertices and Tree Amplitudes in Gauge Theory,” *JHEP* **09** (2004) 006, [arXiv:hep-th/0403047](#). 2, 11, 28, 99, 238
- [6] K. Risager, “A Direct Proof of the CSW Rules,” *JHEP* **12** (2005) 003, [arXiv:hep-th/0508206](#). 2, 11, 12, 15, 28
- [7] R. Britto, F. Cachazo, B. Feng, and E. Witten, “Direct Proof of Tree-Level Recursion Relation in Yang- Mills Theory,” *Phys. Rev. Lett.* **94** (2005) 181602, [arXiv:hep-th/0501052](#). 2, 12, 28, 81, 99, 143, 215, 238
- [8] J. M. Drummond, J. Henn, G. P. Korchemsky, and E. Sokatchev, “Dual Superconformal Symmetry of Scattering Amplitudes in $\mathcal{N} = 4$ Super-Yang-Mills Theory,” *Nucl. Phys.* **B828** (2010) 317–374, [arXiv:0807.1095 \[hep-th\]](#). 3, 8, 9, 28, 99, 107, 147, 189, 215, 216, 243
- [9] N. Berkovits and J. Maldacena, “Fermionic T-Duality, Dual Superconformal Symmetry, and the Amplitude/Wilson Loop Connection,” *JHEP* **09** (2008) 062, [arXiv:0807.3196 \[hep-th\]](#). 3, 215, 243
- [10] N. Arkani-Hamed, F. Cachazo, C. Cheung, and J. Kaplan, “A Duality For The S-Matrix,” *JHEP* **03** (2010) 020, [arXiv:0907.5418 \[hep-th\]](#). 3, 6, 7, 9, 10, 27, 28, 31, 32, 51, 52, 56, 59, 61, 67, 76, 78, 80, 87, 100, 101, 110, 143, 164, 168, 215, 216, 238, 246, 253

- [11] J. M. Drummond and L. Ferro, “The Yangian Origin of the Grassmannian Integral,” *JHEP* **12** (2010) 010, [arXiv:1002.4622 \[hep-th\]](#). 3, 80, 101, 169, 247
- [12] N. Arkani-Hamed, J. Bourjaily, F. Cachazo, and J. Trnka, “Unification of Residues and Grassmannian Dualities,” *JHEP* **01** (2011) 049, [arXiv:0912.4912 \[hep-th\]](#). 4, 80, 81, 82, 84, 85, 86, 87, 94, 101, 106, 246
- [13] N. Arkani-Hamed, J. L. Bourjaily, F. Cachazo, A. Hodges, and J. Trnka, “A Note on Polytopes for Scattering Amplitudes,” [arXiv:1012.6030 \[hep-th\]](#). 4, 5, 146
- [14] J. L. Bourjaily, J. Trnka, A. Volovich, and C. Wen, “The Grassmannian and the Twistor String: Connecting All Trees in $\mathcal{N} = 4$ SYM,” *JHEP* **01** (2011) 038, [arXiv:1006.1899 \[hep-th\]](#). 4, 101, 106, 238
- [15] N. Arkani-Hamed, J. L. Bourjaily, F. Cachazo, S. Caron-Huot, and J. Trnka, “The All-Loop Integrand For Scattering Amplitudes in Planar $\mathcal{N} = 4$ SYM,” *JHEP* **01** (2011) 041, [arXiv:1008.2958 \[hep-th\]](#). 4, 5, 143, 157, 159, 202, 207, 208, 216, 228, 238, 246
- [16] C. Vergu, “The Two-Loop MHV Amplitudes in $\mathcal{N} = 4$ Supersymmetric Yang-Mills Theory,” [arXiv:0908.2394 \[hep-th\]](#). 4, 104, 132
- [17] N. Arkani-Hamed, F. Cachazo, C. Cheung, and J. Kaplan, “The S-Matrix in Twistor Space,” *JHEP* **03** (2010) 110, [arXiv:0903.2110 \[hep-th\]](#). 7, 27, 110, 138, 168
- [18] N. Arkani-Hamed, F. Cachazo, and C. Cheung, “The Grassmannian Origin Of Dual Superconformal Invariance,” *JHEP* **03** (2010) 036, [arXiv:0909.0483 \[hep-th\]](#). 7, 28, 80, 100, 101, 169, 241, 246, 253
- [19] L. Mason and D. Skinner, “Dual Superconformal Invariance, Momentum Twistors and Grassmannians,” *JHEP* **11** (2009) 045, [arXiv:0909.0250 \[hep-th\]](#). 7, 8, 28, 80, 100, 101, 169, 216, 235, 241
- [20] A. Hodges, “Eliminating Spurious Poles from Gauge-Theoretic Amplitudes,” [arXiv:0905.1473 \[hep-th\]](#). 8, 28, 100, 101, 146, 149, 151, 215, 216, 219, 223, 228, 231, 235, 242, 243

- [21] A. Brandhuber, P. Heslop, and G. Travaglini, “A Note on Dual Superconformal Symmetry of the $\mathcal{N} = 4$ Super Yang-Mills S-Matrix,” *Phys. Rev.* **D78** (2008) 125005, [arXiv:0807.4097 \[hep-th\]](#). 8, 28, 99, 110
- [22] J. Kaplan, “Unraveling $\mathcal{L}_{n,k}$: Grassmannian Kinematics,” *JHEP* **03** (2010) 025, [arXiv:0912.0957 \[hep-th\]](#). 9, 28, 38, 80, 81, 109, 238
- [23] M. Bullimore, L. J. Mason, and D. Skinner, “Twistor-Strings, Grassmannians and Leading Singularities,” *JHEP* **03** (2010) 070, [arXiv:0912.0539 \[hep-th\]](#). 9, 28, 38, 80, 81, 109
- [24] N. Arkani-Hamed, J. L. Bourjaily, F. Cachazo, C. Cheung, J. Kaplan, and J. Trnka, “Notes on Inverse Soft Factors.” unpublished. 9, 34, 61, 66, 67, 68, 70, 76, 80, 81, 94, 106
- [25] F. Cachazo, P. Svrcek, and E. Witten, “Gauge Theory Amplitudes in Twistor Space and Holomorphic Anomaly,” *JHEP* **10** (2004) 077, [arXiv:hep-th/0409245](#). 11, 28
- [26] F. Cachazo, P. Svrcek, and E. Witten, “Twistor Space Structure of One-Loop Amplitudes in Gauge Theory,” *JHEP* **10** (2004) 074, [arXiv:hep-th/0406177](#). 11, 28
- [27] K. Risager, “Unitarity and On-Shell Recursion Methods for Scattering Amplitudes,” [arXiv:0804.3310 \[hep-th\]](#). 11, 28
- [28] P. Mansfield, “The Lagrangian Origin of MHV rules,” *JHEP* **03** (2006) 037, [arXiv:hep-th/0511264](#). 11
- [29] A. Gorsky and A. Rosly, “From Yang-Mills Lagrangian to MHV Diagrams,” *JHEP* **01** (2006) 101, [arXiv:hep-th/0510111](#). 11
- [30] R. Boels, L. Mason, and D. Skinner, “From Twistor Actions to MHV Diagrams,” *Phys. Lett.* **B648** (2007) 90–96, [arXiv:hep-th/0702035](#). 11
- [31] R. Britto, F. Cachazo, and B. Feng, “New Recursion Relations for Tree Amplitudes of Gluons,” *Nucl. Phys.* **B715** (2005) 499–522, [arXiv:hep-th/0412308](#). 12, 28, 76, 81, 99, 143, 215, 238

- [32] C. Cheung, “On-Shell Recursion Relations for Generic Theories,” *JHEP* **03** (2010) 098, [arXiv:0808.0504 \[hep-th\]](#). 12
- [33] L. J. Mason and D. Skinner, “Scattering Amplitudes and BCFW Recursion in Twistor Space,” *JHEP* **01** (2010) 064, [arXiv:0903.2083 \[hep-th\]](#). 12, 41, 110
- [34] N. Arkani-Hamed and J. Kaplan, “On Tree Amplitudes in Gauge Theory and Gravity,” *JHEP* **04** (2008) 076, [arXiv:0801.2385 \[hep-th\]](#). 12, 110, 112
- [35] N. Arkani-Hamed, J. Bourjaily, F. Cachazo, S. Caron-Huot, and J. Trnka. In preparation, 2010. 18, 25, 104, 105, 111, 120, 124, 125, 129, 130, 131, 219
- [36] R. Roiban, M. Spradlin, and A. Volovich, “A Googly Amplitude from the B-Model in Twistor Space,” *JHEP* **04** (2004) 012, [arXiv:hep-th/0402016](#). 26, 94
- [37] L. Dolan and P. Goddard, “Gluon Tree Amplitudes in Open Twistor String Theory,” *JHEP* **12** (2009) 032, [arXiv:0909.0499 \[hep-th\]](#). 26, 29, 43, 44, 45, 46, 49, 57
- [38] N. Berkovits, “An Alternative String Theory in Twistor Space for $\mathcal{N} = 4$ Super-Yang-Mills,” *Phys. Rev. Lett.* **93** (2004) 011601, [arXiv:hep-th/0402045](#). 26, 29
- [39] M. Spradlin and A. Volovich, “From Twistor String Theory To Recursion Relations,” *Phys. Rev.* **D80** (2009) 085022, [arXiv:0909.0229 \[hep-th\]](#). 26, 29, 43, 44, 46, 49, 77, 80, 81, 86, 87, 94, 106, 238
- [40] L. F. Alday and J. M. Maldacena, “Gluon Scattering Amplitudes at Strong Coupling,” *JHEP* **06** (2007) 064, [arXiv:0705.0303 \[hep-th\]](#). 26, 28, 99, 215
- [41] A. Gorsky and A. Zhiboedov, “Aspects of the $\mathcal{N} = 4$ SYM Amplitude – Wilson Polygon Duality,” *Nucl. Phys.* **B835** (2010) 343–363, [arXiv:0911.3626 \[hep-th\]](#). 26
- [42] J. M. Drummond, G. P. Korchemsky, and E. Sokatchev, “Conformal Properties of Four-Gluon Planar Amplitudes and Wilson loops,” *Nucl. Phys.* **B795** (2008) 385–408, [arXiv:0707.0243 \[hep-th\]](#). 26, 99

- [43] J. M. Drummond, J. Henn, G. P. Korchemsky, and E. Sokatchev, “On Planar Gluon Amplitudes/Wilson Loops Duality,” *Nucl. Phys.* **B795** (2008) 52–68, [arXiv:0709.2368 \[hep-th\]](#). 26, 99
- [44] J. M. Drummond, J. Henn, G. P. Korchemsky, and E. Sokatchev, “Conformal Ward Identities for Wilson Loops and a Test of the Duality with Gluon Amplitudes,” *Nucl. Phys.* **B826** (2010) 337–364, [arXiv:0712.1223 \[hep-th\]](#). 26, 99
- [45] J. M. Drummond, J. Henn, G. P. Korchemsky, and E. Sokatchev, “The Hexagon Wilson Loop and the BDS Ansatz for the Six- Gluon Amplitude,” *Phys. Lett.* **B662** (2008) 456–460, [arXiv:0712.4138 \[hep-th\]](#). 26, 99
- [46] J. M. Drummond, J. Henn, G. P. Korchemsky, and E. Sokatchev, “Hexagon Wilson Loop = Six-Gluon MHV Amplitude,” *Nucl. Phys.* **B815** (2009) 142–173, [arXiv:0803.1466 \[hep-th\]](#). 26, 99
- [47] J. M. Drummond, J. Henn, V. A. Smirnov, and E. Sokatchev, “Magic Identities for Conformal Four-Point Integrals,” *JHEP* **01** (2007) 064, [arXiv:hep-th/0607160](#). 28, 99, 102, 148, 152, 215
- [48] H. Elvang, D. Z. Freedman, and M. Kiermaier, “Dual Conformal Symmetry of 1-Loop NMHV Amplitudes in $\mathcal{N} = 4$ SYM Theory,” [arXiv:0905.4379 \[hep-th\]](#). 28, 99, 189
- [49] J. M. Drummond, J. M. Henn, and J. Plefka, “Yangian Symmetry of Scattering Amplitudes in $\mathcal{N} = 4$ Super Yang-Mills Theory,” *JHEP* **05** (2009) 046, [arXiv:0902.2987 \[hep-th\]](#). 28, 78, 99, 215, 247
- [50] J. M. Drummond and J. M. Henn, “All Tree-Level Amplitudes in $\mathcal{N} = 4$ SYM,” *JHEP* **04** (2009) 018, [arXiv:0808.2475 \[hep-th\]](#). 28, 81, 101, 138, 238, 243, 251
- [51] N. Arkani-Hamed, J. Bourjaily, F. Cachazo, and J. Trnka, “Local Spacetime Physics from the Grassmannian,” *JHEP* **01** (2011) 108, [arXiv:0912.3249 \[hep-th\]](#). 42, 80, 85, 101, 216, 235, 238

- [52] R. Roiban, M. Spradlin, and A. Volovich, “On the Tree-Level S-Matrix of Yang-Mills Theory,” *Phys. Rev.* **D70** (2004) 026009, [arXiv:hep-th/0403190](#). 29, 38, 41, 81, 106
- [53] R. Roiban, M. Spradlin, and A. Volovich, “All Googly Amplitudes from the B-Model in Twistor Space,” *JHEP* **04** (2004) 012, [arXiv:hep-th/0402016](#). 29, 81, 94
- [54] E. Witten, “Parity Invariance for Strings in Twistor Space,” *Adv. Theor. Math. Phys.* **8** (2004) 779–796, [arXiv:hep-th/0403199](#). 29
- [55] C. Vergu, “On the Factorisation of the Connected Prescription for Yang-Mills Amplitudes,” *Phys. Rev.* **D75** (2007) 025028, [arXiv:hep-th/0612250](#). 29
- [56] S. Gukov, L. Motl, and A. Neitzke, “Equivalence of Twistor Prescriptions for Super Yang- Mills,” *Adv. Theor. Math. Phys.* **11** (2007) 199–231, [arXiv:hep-th/0404085](#). 29
- [57] L. J. Dixon, “Twistor String Theory and QCD,” *PoS HEP2005* (2006) 405, [arXiv:hep-ph/0512111](#). 29
- [58] L. J. Mason, “Twistor Actions for Non-Self-Dual Fields: A Derivation of Twistor-String Theory,” *JHEP* **10** (2005) 009, [arXiv:hep-th/0507269](#). 29
- [59] N. Berkovits and E. Witten, “Conformal Supergravity in Twistor-String Theory,” *JHEP* **08** (2004) 009, [arXiv:hep-th/0406051](#). 29
- [60] L. Dolan and J. N. Ihry, “Conformal Supergravity Tree Amplitudes from Open Twistor String Theory,” *Nucl. Phys.* **B819** (2009) 375–399, [arXiv:0811.1341 \[hep-th\]](#). 29
- [61] J. Bedford, “On Perturbative Field Theory and Twistor String Theory,” [arXiv:0709.3478 \[hep-th\]](#). 29
- [62] L. Mason and D. Skinner, “Heterotic Twistor-String Theory,” *Nucl. Phys.* **B795** (2008) 105–137, [arXiv:0708.2276 \[hep-th\]](#). 29

- [63] L. Dolan and P. Goddard, “Tree and Loop Amplitudes in Open Twistor String Theory,” *JHEP* **06** (2007) 005, [arXiv:hep-th/0703054](#). 29, 80, 81, 82, 86, 87, 94, 95, 97, 98, 106, 238
- [64] F. Cachazo and P. Svrcek, “Lectures on Twistor Strings and Perturbative Yang-Mills Theory,” *PoS RTN2005* (2005) 004, [arXiv:hep-th/0504194](#). 29
- [65] P. Griffiths and J. Harris, *Principles of Algebraic Geometry*. Wiley, New York, 1978. 29, 81, 101, 113, 163, 166
- [66] D. Nandan, A. Volovich, and C. Wen, “A Grassmannian Etude in NMHV Minors,” *JHEP* **07** (2010) 061, [arXiv:0912.3705 \[hep-th\]](#). 29, 43, 44, 80, 81, 82, 84, 86, 87, 94, 95, 101, 106
- [67] H. White, “Seven Points on a Twisted Cubic Curve,” *Proc. Natl. Acad. Sci.* **1** (1915) 464. 46
- [68] J. M. Drummond and L. Ferro, “Yangians, Grassmannians and T-duality,” *JHEP* **07** (2010) 027, [arXiv:1001.3348 \[hep-th\]](#). 80, 101, 247
- [69] G. P. Korchemsky and E. Sokatchev, “Superconformal Invariants for Scattering Amplitudes in $\mathcal{N} = 4$ SYM Theory,” *Nucl. Phys.* **B839** (2010) 377–419, [arXiv:1002.4625 \[hep-th\]](#). 80, 101
- [70] L. Dolan and P. Goddard, “General Split Helicity Gluon Tree Amplitudes in Open Twistor String Theory,” *JHEP* **05** (2010) 044, [arXiv:1002.4852 \[hep-th\]](#). 80, 81, 94
- [71] J. Brödel and S. He, “Dual Conformal Constraints and Infrared Equations from Global Residue Theorems in $\mathcal{N} = 4$ SYM Theory,” *JHEP* **06** (2010) 054, [arXiv:1004.2400 \[hep-th\]](#). 80
- [72] N. Arkani-Hamed, F. Cachazo, and J. Kaplan, “What is the Simplest Quantum Field Theory?,” *JHEP* **09** (2010) 016, [arXiv:0808.1446 \[hep-th\]](#). 99, 162, 238
- [73] Z. Bern, L. J. Dixon, and D. A. Kosower, “On-Shell Methods in Perturbative QCD,” *Annals Phys.* **322** (2007) 1587–1634, [arXiv:0704.2798 \[hep-ph\]](#). 99

- [74] C. F. Berger *et al.*, “An Automated Implementation of On-Shell Methods for One-Loop Amplitudes,” *Phys. Rev.* **D78** (2008) 036003, [arXiv:0803.4180 \[hep-ph\]](#). 99
- [75] Z. Bern, L. J. Dixon, D. C. Dunbar, and D. A. Kosower, “One-Loop n -Point Gauge Theory Amplitudes, Unitarity and Collinear Limits,” *Nucl. Phys.* **B425** (1994) 217–260, [arXiv:hep-ph/9403226](#). 99, 156, 185
- [76] Z. Bern, L. J. Dixon, D. C. Dunbar, and D. A. Kosower, “Fusing Gauge Theory Tree Amplitudes into Loop Amplitudes,” *Nucl. Phys.* **B435** (1995) 59–101, [arXiv:hep-ph/9409265](#). 99
- [77] Z. Bern, L. J. Dixon, and D. A. Kosower, “Progress in One-Loop QCD Computations,” *Ann. Rev. Nucl. Part. Sci.* **46** (1996) 109–148, [arXiv:hep-ph/9602280](#). 99
- [78] Z. Bern, L. J. Dixon, and D. A. Kosower, “Two-Loop $g \rightarrow gg$ Splitting Amplitudes in QCD,” *JHEP* **08** (2004) 012, [arXiv:hep-ph/0404293](#). 99
- [79] Z. Bern, J. J. M. Carrasco, H. Johansson, and D. A. Kosower, “Maximally Supersymmetric Planar Yang-Mills Amplitudes at Five Loops,” *Phys. Rev.* **D76** (2007) 125020, [arXiv:0705.1864 \[hep-th\]](#). 99, 104
- [80] J. L. Bourjaily, J. M. Henn, and M. Spradlin. Work in progress, 2010. 99
- [81] L. F. Alday and J. Maldacena, “Comments on Gluon Scattering Amplitudes via AdS/CFT,” *JHEP* **11** (2007) 068, [arXiv:0710.1060 \[hep-th\]](#). 99, 129
- [82] A. Brandhuber, P. Heslop, and G. Travaglini, “MHV Amplitudes in $\mathcal{N} = 4$ Super Yang-Mills and Wilson Loops,” *Nucl. Phys.* **B794** (2008) 231–243, [arXiv:0707.1153 \[hep-th\]](#). 99
- [83] Z. Bern *et al.*, “The Two-Loop Six-Gluon MHV Amplitude in Maximally Supersymmetric Yang-Mills Theory,” *Phys. Rev.* **D78** (2008) 045007, [arXiv:0803.1465 \[hep-th\]](#). 99, 104
- [84] L. F. Alday and J. Maldacena, “Null Polygonal Wilson Loops and Minimal Surfaces in Anti- de-Sitter Space,” *JHEP* **11** (2009) 082, [arXiv:0904.0663 \[hep-th\]](#). 99

- [85] A. Brandhuber, P. Heslop, and G. Travaglini, “One-Loop Amplitudes in $\mathcal{N} = 4$ Super Yang-Mills and Anomalous Dual Conformal Symmetry,” *JHEP* **08** (2009) 095, [arXiv:0905.4377 \[hep-th\]](#). 99
- [86] A. Brandhuber, P. Heslop, and G. Travaglini, “Proof of the Dual Conformal Anomaly of One-Loop Amplitudes in $\mathcal{N} = 4$ SYM,” *JHEP* **10** (2009) 063, [arXiv:0906.3552 \[hep-th\]](#). 99, 189
- [87] N. Arkani-Hamed, J. L. Bourjaily, F. Cachazo, S. Caron-Huot, J. M. Drummond, J. M. Henn, and J. Trnka. Work in progress. 100, 141
- [88] N. Beisert, J. Henn, T. McLoughlin, and J. Plefka, “One-Loop Superconformal and Yangian Symmetries of Scattering Amplitudes in $\mathcal{N} = 4$ Super Yang-Mills,” *JHEP* **04** (2010) 085, [arXiv:1002.1733 \[hep-th\]](#). 101
- [89] T. Bargheer, N. Beisert, W. Galleas, F. Loebbert, and T. McLoughlin, “Exacting $\mathcal{N} = 4$ Superconformal Symmetry,” *JHEP* **11** (2009) 056, [arXiv:0905.3738 \[hep-th\]](#). 101
- [90] A. Sever and P. Vieira, “Symmetries of the $\mathcal{N} = 4$ SYM S-matrix,” [arXiv:0908.2437 \[hep-th\]](#). 102
- [91] S. Caron-Huot, “Loops and Trees,” [arXiv:1007.3224 \[hep-ph\]](#). 103, 118, 142
- [92] A. Hodges, “The box integrals in momentum-twistor geometry,” [arXiv:1004.3323 \[hep-th\]](#). 103, 104, 151, 155, 228
- [93] L. J. Mason and D. Skinner, “Amplitudes at Weak Coupling as Polytopes in AdS_5 ,” *J. Phys.* **A44** (2011) 135401, [arXiv:1004.3498 \[hep-th\]](#). 103, 104, 155, 228
- [94] L. F. Alday, J. M. Henn, J. Plefka, and T. Schuster, “Scattering into the Fifth Dimension of $\mathcal{N} = 4$ Super Yang-Mills,” *JHEP* **01** (2010) 077, [arXiv:0908.0684 \[hep-th\]](#). 104, 140, 158, 228
- [95] F. Cachazo, M. Spradlin, and A. Volovich, “Leading Singularities of the Two-Loop Six-Particle MHV Amplitude,” *Phys. Rev.* **D78** (2008) 105022, [arXiv:0805.4832 \[hep-th\]](#). 104, 128

- [96] D. A. Kosower, R. Roiban, and C. Vergu, “The Six-Point NMHV Amplitude in Maximally Supersymmetric Yang-Mills Theory,” *Phys. Rev.* **D83** (2011) 065018, [arXiv:1009.1376 \[hep-th\]](#). 104, 210
- [97] F. Cachazo, “Sharpening The Leading Singularity,” [arXiv:0803.1988 \[hep-th\]](#). 104, 128, 163, 164, 191
- [98] E. I. Buchbinder and F. Cachazo, “Two-Loop Amplitudes of Gluons and Octa-Cuts in $\mathcal{N} = 4$ Super Yang-Mills,” *JHEP* **11** (2005) 036, [arXiv:hep-th/0506126](#). 104, 164
- [99] M. Spradlin, A. Volovich, and C. Wen, “Three-Loop Leading Singularities and BDS Ansatz for Five Particles,” *Phys. Rev.* **D78** (2008) 085025, [arXiv:0808.1054 \[hep-th\]](#). 104, 128, 213
- [100] C. Anastasiou, Z. Bern, L. J. Dixon, and D. A. Kosower, “Planar amplitudes in maximally supersymmetric Yang-Mills theory,” *Phys. Rev. Lett.* **91** (2003) 251602, [arXiv:hep-th/0309040](#). 104
- [101] Z. Bern, L. J. Dixon, and V. A. Smirnov, “Iteration of Planar Amplitudes in Maximally Supersymmetric Yang-Mills Theory at Three Loops and Beyond,” *Phys. Rev.* **D72** (2005) 085001, [arXiv:hep-th/0505205](#). 104, 213
- [102] Z. Bern, M. Czakon, L. J. Dixon, D. A. Kosower, and V. A. Smirnov, “The Four-Loop Planar Amplitude and Cusp Anomalous Dimension in Maximally Supersymmetric Yang-Mills Theory,” *Phys. Rev.* **D75** (2007) 085010, [arXiv:hep-th/0610248](#). 104
- [103] D. Skinner, “A Direct Proof of BCFW Recursion for Twistor-Strings,” *JHEP* **01** (2011) 072, [arXiv:1007.0195 \[hep-th\]](#). 110, 238
- [104] Z. Bern and G. Chalmers, “Factorization in One Loop Gauge Theory,” *Nucl. Phys.* **B447** (1995) 465–518, [arXiv:hep-ph/9503236](#). 119
- [105] W. L. van Neerven and J. A. M. Vermaseren, “Large Loop Integrals,” *Phys. Lett.* **B137** (1984) 241. 125, 155

- [106] J. M. Drummond, J. Henn, G. P. Korchemsky, and E. Sokatchev, “Generalized Unitarity for $\mathcal{N} = 4$ Super-Amplitudes,” [arXiv:0808.0491 \[hep-th\]](#). 129, 189
- [107] A. P. Hodges, “Twistor Diagrams for All Tree Amplitudes in Gauge Theory: A Helicity-Independent Formalism,” [arXiv:hep-th/0512336](#). 138
- [108] A. B. Goncharov, M. Spradlin, C. Vergu, and A. Volovich, “Classical Polylogarithms for Amplitudes and Wilson Loops,” *Phys. Rev. Lett.* **105** (2010) 151605, [arXiv:1006.5703 \[hep-th\]](#). 140
- [109] L. F. Alday, D. Gaiotto, and J. Maldacena, “Thermodynamic Bubble Ansatz,” [arXiv:0911.4708 \[hep-th\]](#). 140
- [110] L. F. Alday, J. Maldacena, A. Sever, and P. Vieira, “Y-System for Scattering Amplitudes,” *J. Phys.* **A43** (2010) 485401, [arXiv:1002.2459 \[hep-th\]](#). 140, 146
- [111] L. F. Alday, D. Gaiotto, J. Maldacena, A. Sever, and P. Vieira, “An Operator Product Expansion for Polygonal Null Wilson Loops,” [arXiv:1006.2788 \[hep-th\]](#). 140, 146
- [112] L. F. Alday, B. Eden, G. P. Korchemsky, J. Maldacena, and E. Sokatchev, “From Correlation Functions to Wilson Loops,” [arXiv:1007.3243 \[hep-th\]](#). 140
- [113] B. Eden, G. P. Korchemsky, and E. Sokatchev, “From Correlation Functions to Scattering Amplitudes,” [arXiv:1007.3246 \[hep-th\]](#). 140
- [114] J. M. Henn, S. G. Naculich, H. J. Schnitzer, and M. Spradlin, “Higgs-Regularized Three-Loop Four-Gluon Amplitude in $\mathcal{N} = 4$ SYM: Exponentiation and Regge Limits,” *JHEP* **04** (2010) 038, [arXiv:1001.1358 \[hep-th\]](#). 140
- [115] J. M. Henn, S. G. Naculich, H. J. Schnitzer, and M. Spradlin, “More Loops and Legs in Higgs-Regulated $\mathcal{N} = 4$ SYM Amplitudes,” *JHEP* **08** (2010) 002, [arXiv:1004.5381 \[hep-th\]](#). 140
- [116] S. Caron-Huot, “Notes on the Scattering Amplitude / Wilson Loop Duality,” [arXiv:1010.1167 \[hep-th\]](#). 143, 202, 215

- [117] L. Mason and D. Skinner, “The Complete Planar S-Matrix of $\mathcal{N} = 4$ SYM as a Wilson Loop in Twistor Space,” *JHEP* **12** (2010) 018, [arXiv:1009.2225 \[hep-th\]](#). 143, 215
- [118] L. F. Alday and R. Roiban, “Scattering Amplitudes, Wilson Loops and the String/Gauge Theory Correspondence,” *Phys.Rept.* **468** (2008) 153–211, [arXiv:0807.1889 \[hep-th\]](#). * Temporary entry *. 143
- [119] D. Gaiotto, J. Maldacena, A. Sever, and P. Vieira, “Bootstrapping Null Polygon Wilson Loops,” [arXiv:1010.5009 \[hep-th\]](#). * Temporary entry *. 146
- [120] F. A. Berends, R. Kleiss, P. De Causmaecker, R. Gastmans, and T. T. Wu, “Single Bremsstrahlung Processes in Gauge Theories,” *Phys. Lett.* **B103** (1981) 124. 148
- [121] P. De Causmaecker, R. Gastmans, W. Troost, and T. T. Wu, “Multiple Bremsstrahlung in Gauge Theories at High-Energies. 1. General Formalism for Quantum Electrodynamics,” *Nucl. Phys.* **B206** (1982) 53. 148
- [122] R. Kleiss and W. J. Stirling, “Spinor Techniques for Calculating $p\bar{p} \rightarrow W^\pm Z^0 +$ Jets,” *Nucl. Phys.* **B262** (1985) 235–262. 148
- [123] J. F. Gunion and Z. Kunszt, “Improved Analytic Techniques for Tree Graph Calculations and the $Ggq\bar{q}$ Lepton anti-Lepton Subprocess,” *Phys. Lett.* **B161** (1985) 333. 148
- [124] Z. Xu, D.-H. Zhang, and L. Chang, “Helicity Amplitudes for Multiple Bremsstrahlung in Massless Nonabelian Gauge Theories,” *Nucl. Phys.* **B291** (1987) 392. 148
- [125] R. Penrose, “Twistor Algebra,” *J. Math. Phys.* **8** (1967) 345. 149
- [126] L. J. Dixon, “Calculating Scattering Amplitudes Efficiently,” [arXiv:hep-ph/9601359](#). 154
- [127] J. M. Drummond and J. M. Henn, “Simple Loop Integrals and Amplitudes in $\mathcal{N} = 4$ SYM,” [arXiv:1008.2965 \[hep-th\]](#). 157, 209, 210

- [128] R. J. Eden, P. V. Landshoff, D. I. Olive, and J. C. Polkinghorne, *The Analytic S-Matrix*. Cambridge University Press, 1966. 161
- [129] R. Britto, F. Cachazo, and B. Feng, “Generalized Unitarity and One-Loop Amplitudes in $\mathcal{N} = 4$ Super-Yang-Mills,” *Nucl. Phys.* **B725** (2005) 275–305, [arXiv:hep-th/0412103](#). 161, 166
- [130] H. Schubert, *Kalkül der Abzählenden Geometrie*. Verlag von B. G. Teubner, 1879. 169
- [131] W. Burau and B. Renschuch, *Ergänzungen zur Biographie von Hermann Schubert*. Mitt. Math. Ges. Hamb. 13, pp. 63–65, ISSN 0340-4358, 1993. 169
- [132] M. Bullimore, “MHV Diagrams from an All-Line Recursion Relation,” [arXiv:1010.5921 \[hep-th\]](#). 215, 216, 238
- [133] N. Arkani-Hamed, J. L. Bourjaily, F. Cachazo, and J. Trnka, “Local Integrals for Planar Scattering Amplitudes,” [arXiv:1012.6032 \[hep-th\]](#).
- [134] T. Cohen, H. Elvang, and M. Kiermaier, “On-Shell Constructibility of Tree Amplitudes in General Field Theories,” [arXiv:1010.0257 \[hep-th\]](#). 238
- [135] L. J. Dixon, J. M. Henn, J. Plefka, and T. Schuster, “All Tree-Level Amplitudes in Massless QCD,” *JHEP* **01** (2011) 035, [arXiv:1010.3991 \[hep-ph\]](#). 238, 239
- [136] D. Maitre and P. Mastrolia, “S@M, a Mathematica Implementation of the Spinor-Helicity Formalism,” *Comput. Phys. Commun.* **179** (2008) 501–574, [arXiv:0710.5559 \[hep-ph\]](#). 239
- [137] J. L. Bourjaily, “Efficient Tree-Amplitudes in $\mathcal{N} = 4$: Automatic BCFW Recursion in Mathematica,” [arXiv:1011.2447 \[hep-ph\]](#). 239, 241, 262
- [138] H. Elvang, D. Z. Freedman, and M. Kiermaier, “Solution to the Ward Identities for Superamplitudes,” [arXiv:0911.3169 \[hep-th\]](#). 261